DIRECTIONAL DYNAMIC ANALYSIS OF AN ARTICULATED VEHICLE WITH ARTICULATION DAMPERS AND FORCED-STEERING

Rama Krishna Vallurupalli

A Thesis
in
The Department
of
Mechanical Engineering

Presented in Partial Fulfillment of the Requirements
for
the Degree of Master of Applied Science
at
Concordia University
Montreal, Quebec, Canada

August 1993

ISBN 0-315-87291-8

Canada

Abstract

Directional Dynamic Analysis of an Articulated Vehicle with Articulation Dampers and Forced-Steering

Rama Krishna Vallurupalli

Articulated vehicles are known to exhibit appreciable yaw oscillations during high-speed directional maneuvers. Excessive vehicle off-tracking of multiple axle semitrailers causes rapid tire wear and poor maneuverability at low speeds. The concepts in articulation damping and forced-steering of the semitrailer axles are investigated to achieve improved low speed maneuverability as well as high speed directional control performance of the vehicle. The concept of a damped articulation mechanism is introduced and its potential benefits in limiting the yaw and lateral oscillations of semitrailer are investigated. Different force-steering algorithms are formulated to achieve both improved low- and medium-speed manoeuvrability and high-speed directional control performance. A nonlinear yaw plane model of an articulated vehicle with a multiple axles semitrailer comprising two articulation dampers and forced-steering of a semitrailer axle is formulated. The cornering forces and aligning moments of a radial truck tire are characterized by a nonlinear function in normal load, side-slip angle and pneumatic trail. The damping forces and moments acting on the sprung masses due to the articulation dampers are derived from the kinematic and dynamic analysis of the articulation mechanism. The equations of motion of the vehicle are solved for typical low-speed cornering and high-speed lane-change and evasive maneuvers. A parametric study is performed to establish the influence of articulation damping coefficients on the magnitude of lateral and yaw oscillations of the semitrailer. The result of the study show that the yaw and lateral oscillations encountered during high speed directional maneuvers

can be significantly reduced by the articulation dampers. The low- and medium-speed manoeuvrability and high-speed directional dynamics of the vehicle are further investigated using forced-steering of a semitrailer axle, assuming proportional control and negligible generator dynamics. The results are discussed to highlight the influence of the location of the forced-steering axle, feedback variables and control gains. The study showed that a forced-steering algorithm based on articulation angle and speed sensitive articulation angle offers considerable potentials in realizing both the improved low speed manoeuvrability and high-speed directional control performance.

Acknowledgement

The author wishes to express deep sense of gratitude and appreciation to his supervisor, Dr. S. Rakheja for his continued support, encouragement, guidance during the course of this work.

I would like to thank Alain Piche, inmates of CONCAVE and my friends for their help in developing this work.

The financial support by the Mechanical Engineering Department at Concordia University, is further acknowledged.

Special thanks are due to my family for their moral support.

Contents

List of Figures

List of Tables

Nomenclature

a	Distance between dampers pivot points L and C and the longitudinal axis passing through c.g of tractor (m) (Figure 2.1)
a_1, a_2	Lateral acceleration of tractor and semitrailer, respectively (m/s^2)
b	Longitudinal distance between plane joining the points L and C and c.g. of tractor (m) (Figure 2.3)
c	Distance between dampers pivot points M and B and the longitudinal axis passing through c.g of semitrailer (m) (Figure 2.1)
$c.g$	Centre of gravity
C_s	Longitudinal stiffness coefficient (N/unit slip)
C_{SR}, C_{SL}	Viscous damping constants of dampers BC and LM (Ns/m)
C_{SA}, C_{SB}, C_{SC}	Cornering stiffness coefficients in piece-wise linear describing curve (N/s)
C_{sij}	Longitudinal stiffness of a tire on axle ij (N/unit slip)
C_{ij}	Sum of the cornering stiffness of all tires mounted on axle ij (N/degree)
d	Longitudinal distance between plane joining the pivot points M and B and c.g. of semitrailer (m) (Figure 2.1)
f	Longitudinal distance of articulation point from point O_2 (m) (Figure 2.3)
F_{SL1}, F_{SL2}	Forces developed in damper LM at pivot points L and M, respectively (Ns/m) (Figure 2.3)
F_{SR1}, F_{SR2}	Forces developed in damper BC at pivot points B and C, respectively (Ns/m) (Figure 2.3)
F_{SL}, F_{SR}	Force developed in dampers LM and BC, respectively (Ns/m)
F_{Zij}	Normal load on the tire of j-th axle of i-th element (N)
F_{ij}	Lateral cornering force at the j-th axle of the i-th element (N)

F_{XA}	Longitudinal constraint force at articulation point O of semitrailer (N)
F_{YA}	Lateral constraint force at articulation point O of semitrailer (N)
F_X	Longitudinal constraint force at articulation point O of tractor(N)
F_Y	Lateral constraint force at articulation point O of tractor(N)
g	Distance of articulation point from the point O_1 (m) (Figure 2.3)
g_c	Acceleration due to gravity (m/s^2)
I_i	Yaw moment of inertia of the i-th element (N s^2/m)
K_{1i}	Front wheel steer gain of the i-th axle of semitrailer
K_{2i}	Articulation gain of the i-th axle of semitrailer
K_{3i}	Articulation rate gain of the i-th axle of semitrailer
K_{4i}	Speed sensitive articulation gain of the i-th axle of semitrailer (h/km)
K_{5i}	Speed sensitive articulation rate gain of the i-th axle of semitrailer (h/km)
K_{us}, K_{ust}	Coefficients of understeer of tractor and semitrailer, respectively
L_1	Length of wheel base of tractor (m)
L_2	Length of wheel base of semitrailer (m)
m_i	Mass of the i-th element of the train (N.m^2/s)
M_{ij}	Aligning (yaw) moment from the j-th axle of the i-th element (N-m)
N_{ij}	Sum of the aligning moments/unit slip angle of all the tires mounted on axle ij (N m/degree)
P_CG1	Peak lateral distance traced by tractor's c.g. (m)
P_CG2	Peak lateral distance traced by semitrailer's c.g. (m)
OS_CG1	Peak over-shoot made by tractor's c.g (m)
OS_CG2	Peak over-shoot made by semitrailer's c.g (m)
OT_23L_11R	Off-tracking distance between front right-wheel of tractor and rearmost left-wheel of semitrailer (m)
r_i	Yaw rate of the i-th element of the train (rad/s)
R_1, R_2	Radii traced by tractor and semitrailer, respectively (m)
t_{ij}	Pneumatic trail of the tire (m)

T	Distance between the centre of inner tire of left or right set of dual tires to the centre of the axle. (m)
u_i	Forward velocity at the mass center of the i-th element (m/s)
U	Forward constant velocity (m/s)
v_i	Lateral velocity at the mass center of the i-th element (m/s)
X_L, Y_L, Z_L	Lengths of sides of triangle LMN, LN, MN and ML, respectively (m) (Figure 2.3)
X_R, Y_R, Z_R	Lengths of sides of triangle CC_1B, CC_1, C_1B and BC, respectively (m) (Figure 2.3)
X_{ij}	Distance of axle ij from the mass center of the i-th element (m)
X_{1A}	Distance of tractor fifth wheel from mass center of tractor (m)
X_{2A}	Distance of tractor fifth wheel from mass center of semitrailer (m)
y_{ij}	Spacing distance between the dual tires on axle ij (m)
α_{ij}	Side-slip angle of the j-th axle of the i-th element (rad)
α_a	Rearward amplification of lateral acceleration
α_ω	Rearward amplification of yaw-velocity
β_1, β_2	Angles made by damper BC with longitudinal axis passing through pivot points C and B, respectively (rad)
δ_{FSi}	Forced steering angle made by i-th axle of semitrailer (rad)
δ	Steer angle at the front wheels of the tractor (rad)
γ	Articulation angle (rad)
$\dot{\gamma}$	Articulation rate (rad/s)
ΔV_{SL}	Relative velocity between points L and M (m/s)
ΔV_{SR}	Relative velocity between points C and B (m/s)
ζ_1, ζ_2	Angles made by damper LM with longitudinal axis passing through pivot points L and M, respectively (rad)

Chapter 1

Introduction

1.1 General

For reasons of economy, transport industry has indicated a continuing interest in increasing the sizes and load carrying capacities of freight vehicles. The gross weight and dimensions of these vehicles have been considerably relaxed during the past few years. The use of multiple axle semitrailers has been increasing steadily to carry heavier loads. The population of articulated vehicles with semitrailers with four-, five- or six-axles has grown considerably, specifically in Quebec and Ontario. It has been established that handling and directional control characteristics of articulated freight and passenger vehicles are adversely influenced by the increased weights and dimensions. The increases in weight, dimensions, wheel bases, center of gravity height have contributed to poor yaw and roll stability limits of these vehicles. The lateral and yaw motions associated with side-sway of the articulated vehicles, during a directional maneuver, specifically pose a severe threat to the highway safety due to excessively high inertia of the heavy vehicle.

Articulated vehicles equipped with multiple-axle semitrailer and steering at the tractor's front axle yield excessive swept path and off-tracking during a turning maneuver.

The excessive off-tracking of these vehicles causes rapid tire scrub and wear, poor fuel economy, and increased fatigue of suspension and axle components.

The semitrailers with multiple widespread axles are frequently equipped with either one or two drop axles. The drop axles, when raised during turns, provide reduced off-tracking, tire wear rate and transverse stresses on the chassis and improved maneuverability limits. The increased loads on the remaining axles on the ground, however, cause excessive road damage, which increases exponentially with the increased axle loads. Furthermore, when the axles are raised, the lateral and roll stability limits of the vehicle are affected in an adverse manner.

Alternatively, self-steering axles are increasingly being employed to improve the maneuverability limits of articulated (freight and passenger transport) vehicles. While the self-steering axles provide improved maneuverability and eliminate the excessive road damage caused by drop axle semitrailers, considerably lower lateral cornering forces generated by these axles affect the directional stability and control in an adverse manner. The concerns over highway safety, high tire wear, high suspension and chassis stresses, and poor stability and maneuverability limits of these vehicle have all contributed to a strong desire to seek vehicles configuration, components and sub-system, and safer operating practices that will lead to improved directional control and maneuverability. Concepts in multiple-steerable axles, which are increasingly being used in passenger cars, have been proposed for heavy vehicles to achieve improved manoeuvrability limits and reduced tire scrub.

In this dissertation two different concepts are investigated to explore the potential improvements in yaw and lateral directional control characteristics, and maneuverability limits, respectively. The concept of damped articulated mechanism is introduced and its potential benefits in limiting the yaw and lateral motion of the semitrailer are investigated. The concept of forced-steering at the multiple-axle semitrailer is investigated to achieve

improved maneuverability and stability limits.

1.2 Review of Previous Investigations

The handling, directional control and stability characteristics of heavy trucks and articulated vehicles have been extensively investigated during past two decades. The studies on lateral dynamics of articulated vehicles have been thoroughly reviewed by Vlk [1]. This review concluded that only few investigations have focused on the directional dynamics of such vehicles. In view of the changing weights and dimensions, and safety risks posed by accidents involving such vehicles, numerous analytical and experimental studies have been conducted to demonstrate the influence of weights and dimensions on the stability and control characteristics. The relevant literature on directional dynamics of articulated freight and passenger vehicles is briefly reviewed in the following sections.

1.2.1 Directional Dynamics of Heavy Vehicles

The directional dynamics of heavy vehicles are investigated to establish the handling, directional control and directional stability characteristics of vehicles under steady and transient steering maneuvers. Between the application of steering input and the attainment of steady state motion, the vehicle is in a transient state. The behavior of the vehicle in this period is usually referred to as transient response characteristics. The overall handling qualities of a vehicle depend, to a great extent, on its transient behavior. In analyzing the transient response, the inertia properties of the vehicle must be taken into consideration. During a turning maneuver, the vehicle is in translation as well as in rotation. Steady state handling performance is concerned with the directional behavior of a vehicle during a turn under non-time varying conditions. In the analysis of steady-state handling behaviour, the inertia properties of the vehicle are not considered.

The earliest documented research on directional dynamics of truck-trailer vehicles was performed by Huber and Dietz [2], and Dietz [3,4]. The experimental study was specially concerned with the lateral stability of straight-running vehicle configurations with two-axle towbar trailers equipped with either turnable or Ackerman steering. The investigation involved testing of scale model trailers, constrained laterally, moving on an endless moving belt. The study concluded that the trailer yaw oscillations could be most effectively suppressed by introducing viscous damping within the turntable. While the Coulomb damping within the turntable was observed to be some what undesirable, the Coulomb damping applied at the hitch was considered quite favourable. This experimental study was followed by a complementary theoretical effort by Ziegler [5,6], by considering the tire forces similar to the Coulomb damping. The directional stability of truck-trailer vehicles, investigated by Laurien [7], also concluded that the trailer yaw oscillations could be most effectively suppressed by the introduction of coulomb damping at the hitch and at the trailer steering mechanism. The trailer with Ackerman steering was observed to be more prone to lateral oscillations than the trailer with turntable (dolly) steering.

Paslay and Slibar [8] investigated theoretically the yaw oscillations of a two axle trailer with turntable steering, assuming two degrees-of-freedom motion: yaw angle of drawbar and yaw angle of the trailer body. The study was the first to consider the influence of sideslip on the cornering forces. The characteristic equation was solved to determine the undamped natural frequencies of a two-axle drawbar trailer. The experimental and analytical studies conducted by Zakin [9,10,11] on one- and two-axle towbar trailers concluded that the lateral oscillations of the trailer may be reduced by increasing the wheelbase and the towbar length. An analog computer model of a two-axle turntable trailer incorporating turntable Coulomb friction was developed by Morozov et al. [12] for theoretical investigations of the lateral dynamics. The trailer was modeled as a double pendulum, and the influence of friction moment at the turntable, the position of the center

of gravity, and the lateral play within the hitch on the lateral oscillations was investigated. The influence of tire cornering forces, wheelbase of the trailer, and overall trailer length on the yaw oscillations was further investigated by Meyer [13], using a two-degrees-of-freedom vehicle model. The coupling between the dynamics of truck and the trailer, however, was neglected in all the above studies.

The interdependence between truck and trailer motions was investigated by Schimid [14] and Jindra [15]. From the analog computer simulation of the coupled truck-trailer model, Jindra concluded that the yaw oscillations of the trailers increase with an increase in the yaw moment of inertia of the trailer body. Increased viscous damping at the hitch or the turntable, drawbar length and trailer wheelbase resulted in reduced yaw oscillations. Gerlach [16] analyzed a similar mathematical model incorporating turntable offset, coulomb and/or viscous damping at the hitch and the turntable. The results of the study established that a truck-trailer combination with high cornering stiffness of tires, either coulomb or viscous damping at the hitch, long drawbar and the turntable center located ahead of the dolly axle, lead to good dynamic stability. While the viscous damping at the turntable resulted in lower yaw oscillations, the coulomb damping resulted in continuous undamped yaw oscillations of the trailer.

A vehicle dynamics simulation program was developed by Nordstrom et al. [17] at the National Swedish Road and Traffic Research Institute. Several full-scale field tests were performed to validate the simulation program and to evaluate proposed test methods. The results of the simulation programs correlated quite well with those derived from the tests (Nordstrom and Strandberg [18]).

A comprehensive digital computer program was further developed to simulate for directional dynamics of combinations incorporating vehicles up to three articulations, a maximum of nine axles, driving or braking forces, lateral load transfer, etc. The eight degree-of-freedom analytical model was developed assuming fixed roll axles, linear

springs, negligible interaction between lateral and longitudinal tire forces, negligible pitch and longitudinal load transfer [19]. Based upon the simulation results for a lane change directional maneuver, it was concluded that a satisfactory lane change behaviour can be achieved by long trailer wheel base, low normal load on the tires, short distance between the truck rear axle and the tow pin, and roll understeer on the trailer rear axle. A longer drawbar, however, resulted in large amplitude lateral oscillations.

Bakhmutskii and Gineburg [20] have investigated the directional response characteristics through road tests performed with various vehicle combinations and drivers. The handling characteristics of the vehicle and the driver-vehicle systems were derived from the test data. The tests were performed to step steer and lane-change maneuvers. A linear four degrees-of-freedom mathematical model was used for the theoretical analysis.

Mallikarjunarao and Fancher [21] developed a linear analytical model to study the directional response and stability of tractor-semitrailer combinations with multi-axled and multi-articulated tanker trucks, while neglected the roll dynamics. An eigen value analysis was performed to determine the natural modes of oscillation and the directional stability limits of the vehicle. The study concluded that the lateral acceleration of the pub trailer of the Michigan double tanker is significantly larger when compared to that attained by the tractor, during the obstacle-avoidance maneuver performed at highway speeds. This rearward amplification of lateral acceleration was considerably reduced by increasing the rigidity of the pintle hook connection.

Vlk [1,22] indicated that while many studies have described the development of various computer simulations models to analyze the lateral dynamics of articulated vehicles, there exist relatively few published studies on comparison of these models. Further, the in-plane vehicle models discussed above assume linear tire cornering forces. The influence of size and weight variables on the stability and control of heavy trucks and tractor-trailer combinations was examined by Ervin et al. [23], using computer

simulations. The computer simulation studies were validated through a limited number of field tests. These models clearly predicted the periodic yaw response of the trailer about its equilibrium, but did not yield information about aperiodic trailer swing and jackknife due to lack of a bounded and nonlinear tire model.

The research efforts, in the recent years, have been directed towards development of increasingly sophisticated computer simulation models to handle complex tire models. Since the directional dynamics of a vehicle combination is strongly related to the forces generated at the tire-road interface, nonlinear tire models have been used in the lateral stability analysis of heavy vehicles subject to braking and steering maneuvers [24]. Susemihl and Kranter [25] developed a nonlinear vehicle model allowing the evaluation of current design features, such as fifth wheel reactions and automatic anti-lock system.

A comprehensive three-dimensional vehicle model, referred to as the "Phase IV[1] model", was developed by UMTRI [26], to simulate the directional dynamics of heavy vehicle combinations subject to braking and steering maneuvers. The model is capable of simulating the directional dynamics of trucks, tractor-semitrailers, doubles and triples. The mathematical model incorporates up to 71 degrees-of-freedom depending upon the vehicle configuration. The nonlinear tire forces, and force-deflection characteristics of the suspension are incorporated using a lock-up table. The simulation program may be operated either for an open-loop (known steering input) or a closed loop (known path) steering maneuvers on roads of specified grade or cross-grade.

Gindy and Wong [27] performed a comparative study of different simulation packages of different levels of complexities developed for directional response analysis of commercial articulated vehicles. The study focussed on four simulation models: the

[1]The Phase 4 model is a time-domain mathematical simulation of a truck/tractor, a semitrailer, and up to two full trailers. It represents UMTRI's latest thinking in computer modelling of the braking and steering response of commonly used commercial vehicles. This model incorporates up to 71 degrees of freedom.

linear yaw plane model; the TBS[2] total braking and steering model [28]; the yaw/roll model; and the Phase IV model, developed by UMTRI [26]. The study concluded that more sophisticated simulation model, such as the Phase IV model, does not necessarily yield more accurate predictions in quantitative terms than the simpler models, such as the TBS or the linear yaw plane model. The transient steering response characteristics of a tractor-semitrailer in a lane-change maneuver, analyzed using the four simulation programs, were observed to be qualitatively similar. A comparison of the simulation results with the measured data available revealed that the more sophisticated Phase IV model does not necessarily yield more accurate transient response than the simpler TBS and linear yaw plane models.

1.2.2 Dynamics of Multiple-Axle Semitrailers

Multi-axle trailers are increasingly being used to carry maximum permissible loads. The axles of these trailers are spaced so that they distribute the load evenly on roadways and bridge roads. The directional dynamics of vehicle combinations with multiple axle trailers is strongly influenced by the number and spacing of the axles. Gillespie and Winkler [29] investigated the cornering performance of heavy trucks incorporating multiple non-steering rear axles and dual tires. The cornering performance evaluated in the linear regime was compared to that of a conventional two-axle vehicle. The study concluded that the multiple axles generate a moment that resists turning. These vehicles thus require larger steering angles to negotiate a turn, than the conventional two-axle vehicles. The effective wheelbase of multiple axle vehicles is considerably larger than the geometric wheel base. The curvature gain of a three-axle vehicle was observed to be 10-20 % lower than that of the two-axle vehicle. Vehicles with more axles exhibit much greater reductions in the curvature gain.

[2]TBS is a simplified non-linear mathematical model, originally formulated by Leucht. It is similar to the yaw plane model, but with non-linear tire model and dynamic load transfers.

Fancher [30] investigated the influence of multiple axles and articulation points of heavy truck combinations on the directional dynamics and performance characteristics. The performance characteristics of these vehicles were evaluated in terms of steady turning, directional stability, forced response in obstacle avoidance maneuvers, and handling qualities. A handling equation was derived to analyze the steady turing performance of vehicles with multiple axles. The study revealed that the vehicles with multiple-axle full-trailers yield large rearward amplification, which must be appropriately considered in evaluating the safety qualities of these vehicles.

The multiple-axle vehicles, not only affect the high speed directional dynamics but also the low speed maneuverability. Non-steerable additional axles in a vehicle combination yield increased off-tracking, larger swept path, rapid tire wear, and increased stresses in axle components and the chassis [31]. The maneuverability limits of these vehicles, specifically in tight turns, are adversely influenced by additional axles. The steady-state off-tracking and the swept path of articulated vehicles with multiple and non-steered axles have been investigated by Woodrooffe [32] and Sweatman [33]. The multiple-axle vehicles cause increased side-slip angles at the trailer axles and thus the rapid tire wear during turning maneuvers.

Since the regulations permit higher load limits for vehicles with wide spread multiple axles, the trailers are frequently designed with widespread axles, which lead to reduced manoeuvrability limits. Semitrailers with widespread axles are, therefore, equipped with either one or two drop axles. The drop axles, when raised, make the vehicle combination easier to maneuver during turns, while reducing the transverse stresses on the chassis. The raised axles, however, overload the remaining axles on the ground resulting in excessive road damage. Various studies have established that the road damage increases exponentially with the increased axle loads [34]. Furthermore, the lateral stability of the vehicle is adversely affected, when the axles are raised, due to reduced cornering forces. Self- and forced-steering axles have been proposed to eliminate the overloading of some

of the trailer axles, and to improve the maneuverability limits of multiple-axle articulated vehicles.

1.2.3 Self- and Forced-steering Axles

There is a lack of technical information describing the influence of self-steering on vehicle performance since the self-steering axles have evolved from the principle of "design precedent", that is, it has been developed in the field without the benefit of analytical studies focusing on the detailed mechanics and dynamics of the axle and its effect on vehicle behavior. Self-steering axle may be a fixed axle mounted on a turntable, or a steering axle with a tilted kingpin installed as a supplementary axle without being connected to the steering system. These self-steering axles are equipped with a self-centering mechanism to ensure vehicle stability when unequal forces are applied to two sides of the axle by the road obstacles or by braking on an uneven ground. The influence of self-steering axle design parameters on the steady-state handling behavior of various vehicle configurations is examined, by neglecting the coulomb friction and linearizing the cornering characteristics of the self-steering axle. The principles of self-steering axles and an analysis of the forces developed has been discussed by Leblanc et al. [35]. A study conducted by Woodrooffe et al. [36] concluded that the self-steering system must generate a minimum lateral force of 25% of the rated axle load and a minimum longitudinal force of 10% at the same axle load. The minimum force requirement must be attained within 1 degree of steer. The angular displacement over which the minimum force requirement must be maintained is 15 degrees.

In a study conducted by the Ministry of Transportation of Ontario [37], there was virtually no difference between the regular three-axle configuration and the one with a tandem axle and a self-steering belly-axle. The low acceleration level during the test was probably insufficient to activate the self-steering mechanism. At higher speeds,

it is expected to react with characteristics between those of the two- and three-axle configurations. It was also shown that the self-steering axle in the forward location results in offtracking similar to that of the two-axle configuration. Although the offtracking was observed to be worse than that of the fixed axle vehicle, the tire scrub was virtually eliminated. Billing et al [38] reported that there is little experience with self-steering axles on semitrailers at this time. This was one of the reasons why they were not recommended by the CCMTA/RTAC[3] Vehicle Weights and Dimensions Study. Two self-steering axles would add considerable mechanical and dynamic complexity to these vehicles. While a development and demonstration program of reasonable duration might address concerns for single self-steering axles, two self-steering axles are considered an inappropriate risk at this time.

The self-steering axles, however, provide little or no lateral cornering force leading to poor directional stability and control performance. It is thus necessary to generate sufficient cornering forces for the total vehicle weight. Alternatively, concepts of forced-steering axles have been proposed to achieve improved maneuverability limits of articulated freight and passenger transport vehicles. The forced-steering axles are steered through either the mechanical linkages or hydraulic actuators in certain proportion to the tractor's front axle angle or articulation angle. Forced-steering axles, employing mechanical linkages between the articulation mechanism and the axle, have been used in articulated buses to achieve reduced tire wear and offtracking, and improved maneuverability at low speeds [39].

Vlk [40] proposed the control concepts for forced-steering axles for articulated buses. A linear yaw-plane model was developed to study the directional response of articulated buses with forced -steering axle to a step steer input. The forced-steering was introduced at the trailing axle of second unit, and the steer angle was generated as a proportional function of articulation angle between the front and rear sections of the

[3]Road and Transport Association of Canada

articulated bus. A comprehensive parametric study was carried out to study the influence of various vehicle design parameters, such as masses of the front and rear sections, turntable viscous damping constant, centre of gravity location of front and rear sections, forward speed, etc.

Aurell et al. [41] studied the influence of steered axles on the dynamic stability of different vehicle configurations. The influence of the location of the steered axles and the steering principle on the dynamics stability was investigated. Self- or forced-steered axles were used to apply the steer-angle of the rear axle in the linear and non-linear models. The study concludes that, the steered axles can be located either in front or behind the fixed axle of the trailer. The forced steering did not influence the dynamic stability limits of single trucks. The self-steering axle, when located as the rear most axle, resulted in directional instabilities. Better directional performance was achieved when the self-steering was incorporated to the leading axle of the trailer.

Sankar et al [42] investigated the dynamic characteristics of a self-steering axle integrated to a three-dimensional nonlinear directional dynamic model of the vehicle. They also developed two forced-steering algorithms relating the vehicle speed and response quantities to the angle of the wheels of the steerable axle, and integrated to the non-linear directional dynamic model of the vehicle. Computer simulations were performed to determine the directional response characteristics of a tractor-semitrailer with self-and force-steering axles for low as well as high speed maneuvers. The directional response characteristics of the vehicles with self- and forced-steering axles were discussed in view of the self-steering parameters and forced-steering gains, and compared to those of the vehicle with conventional axles. The study concluded that the low-speed maneuverability and the dynamic directional performance of the vehicle is strongly influenced by the steerable axle location, and its static and dynamic properties.

1.3 Scope and Layout of the Thesis

From the literature review, it is evident that while extensive efforts have been mounted to improve directional stability of articulated vehicles, the directional control and maneuverability characteristics of multiple-axle vehicles remain the subject of concern. Although earlier studies have described the significance of articulation damping in reducing yaw and lateral oscillations of the trailers, the comprehensive vehicle dynamics analysis programs developed during the past decade place very limited emphasis on articulation damping. The primary objectives of this dissertation research are thus formulated to investigated the directional control and manoeuvrability performance potentials of articulation damping and forced-steering axles for articulated vehicles. The detailed objectives of the study are:

1. To develop the analytical models of an articulated vehicle with articulation damping and forced-steering.
2. To formulate the nonlinear tire lateral force model to be integrated to the vehicle model.
3. To formulate different control concepts for forced-steering axles.
4. To investigate the yaw and lateral dynamics of the vehicle, as influenced by the articulation damping and forced-steering axles.

Nonlinear yaw-plane model of an articulated vehicle incorporating nonlinear cornering forces of the tires and kinematics and dynamics of the articulation dampers is developed in chapter 2. The nonlinear lateral forces due to tires are represented as a function of the normal load and side-slip angles. Different control schemes relating the steer angle of the forced-steering axle to the tractor's front wheel steer angle, forward

speed and vehicle response quantities, are formulated. An articulated vehicle with multiple axle semitrailer equipped with forced-steering axle is analytically modeled.

The directional dynamics response characteristics of the articulated vehicle with articulation damping and forced-steering are evaluated for low and medium-speed turning maneuvers, and highway speed lane change maneuvers. The results of the study are presented and discussed in chapter 3 and 4. The directional control characteristics are presented in terms of vehicle path, lateral acceleration, lateral velocity and yaw-response of the vehicle. The manoeuvrability limits of the vehicle are characterized in terms of tire side-slip angles, vehicle off-tracking and vehicle path. The directional response characteristics of the vehicle model with articulated damping and forced-steering axle are compared to those of a conventional vehicle model, and the relative performance benefits are discussed.

The conclusions drawn from the study are summarized in chapter 5, and recommendations for future studies on damping mechanism and control schemes for forced-steering angle generation are proposed.

Chapter 2

Development of Analytical Models

2.1 General

Numerous in-plane and three-dimensional models of varying complexities have been developed and analyzed to determine the yaw, lateral and roll directional dynamics of heavy vehicles. The analytical models vary from simple linear yaw-plane model to the sophisticated 71 degrees-of-freedom Phase IV model [26,44]. Vehicle dynamics simulation programs have been developed to evaluate the directional response characteristics of heavy trucks and truck-trailer combinations subject to steering and braking inputs. A comparative study of some of the simulation programs revealed that more sophisticated models do not necessary yield more precise simulation of vehicle motions. Further more, the complex simulation models, such as yaw/roll and phase IV models require extensive input data and computer time. A simpler yaw-plane model can thus be used to effectively determine the yaw and lateral directional dynamics of heavy vehicles, while neglecting roll dynamics and the influence of suspension forces. Linear yaw-plane models have been extensively used to study the handling and directional control characteristics of heavy vehicles.

While the yaw-plane models, incorporating linear cornering properties of tires, provide a reasonable estimation of periodic yaw response, the aperiodic response characteristics cannot be accurately estimated due to lack of bounded and nonlinear tire forces. Furthermore the lateral forces developed by current designs of radial truck tires are strongly related to normal loads and side-slip angles. The measured tire data, reported in the literature, suggest that the relationship between the tire lateral forces, normal loads and side-slip angles are strongly nonlinear.

A nonlinear yaw-plane model is thus derived in this study to investigate the directional dynamics of articulated vehicles with damped articulation and forced-steering axles. The analytical models are initially derived for conventional vehicles assuming linear tire cornering characteristics. The measured tire data is analyzed to derive a nonlinear function relating the cornering force, normal load and side-slip angle, which is then integrated to the yaw-plane vehicle model.

2.2 Linear Yaw-Plane model of an Articulated Vehicle with Damped Articulation

Linear yaw-plane analysis of a vehicle is performed to determine the lateral and yaw motions of the vehicle, while assuming negligible pitch and roll. The dynamics of the steering mechanism are neglected, since the natural frequency of the wheel masses, constrained by the steering stiffness and aligning stiffness of tires, is considerably higher than the frequency of yaw motion. The dynamics due to the suspension is also neglected in the yaw-plane analysis.

The damping within a conventional fifth wheel coupling is considered negligible in the yaw-plane analysis. Many studies conducted in the 50's and 60's have briefly described the significance of Coulombs and Viscous damping within the hitch and towbar

in reducing the yaw oscillations [2-7]. The study carried out by Rakheja et al.[43] and Sireteanu [47] demonstrated that higher damping is needed at higher velocities to retain lateral stability of the vehicles. The conventional fifth wheel couplings provide damping due to coulomb friction only between the fifth wheel plates. Additional dampers have been recently introduced at the articulation of an articulated bus to reduce the lateral vibrations transmitted to the passengers [39]. While no analysis have been performed, the additional dampers are observed to reduce the transmission of lateral jerk to the passenger's neck [40]. A damping mechanism, similar to the one used in articulation buses, may be employed to realized articulation damping of freight vehicles.

The damping mechanism comprises two dampers installed near the articulation between the tractor and the semitrailer, as shown in Figure 2.1. The damping forces and moments imposed on the tractor and semitrailer units are related to the kinematics of the damper links, damping coefficients, and dynamic response of the two units. The damping forces incorporating geometric nonlinearities due to damper links are derived and integrated to the yaw-plane model of the tractor-semitrailer vehicle incorporating linear cornering properties of tires. The equations of motion for the vehicle model are derived subject to following assumptions [44].

1. The vehicle is assumed to move on a horizontal surface with uniform friction characteristics at constant forward velocity.
2. The variations in longitudinal tire forces are considered negligible.
3. All joints are frictionless and articulation takes place about the vertical axis. The tractor and semitrailer units are free to yaw relative to each other, while the motion of two units are constrained along the lateral and longitudinal directions at the articulation point.

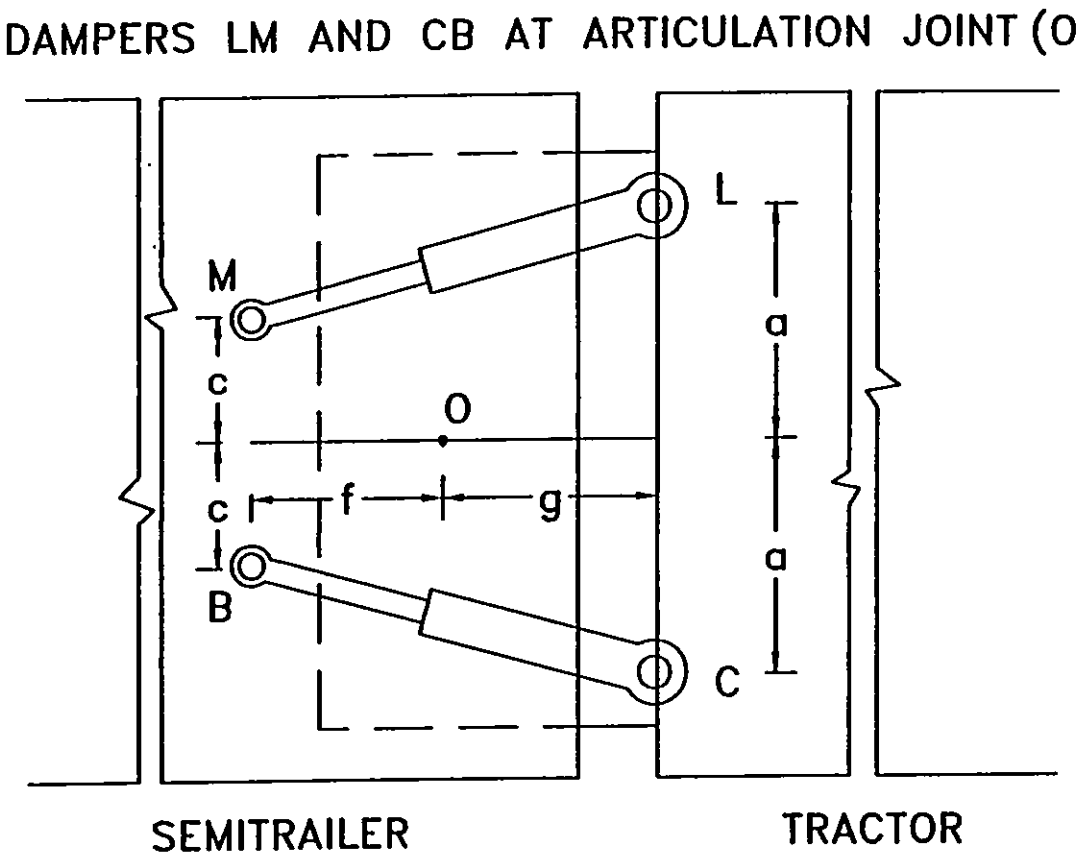

Figure 2.1: Schematic of the articulation damping mechanism

4. The cornering forces and aligning moments generated at the tire-road interface are assumed to be linear functions of the side slip angle at the tire.

5. Articulation angles are assumed to be small, such that sin $\gamma = \gamma$ and cos $\gamma = 1$, where γ is the articulation angle.

6. Each element or unit of the combination is considered as a rigid body and the unsprung masses are assumed to be rigidly attached to their respective sprung masses.

7. Gyroscopic moments due to rotating elements such as wheels and tires are assumed to be small and hence neglected.

8. Steering system dynamics are neglected and steer input is characterized by the front wheel angle, assuming parallel steering.

Figure 2.2 illustrates the yaw-plane model of an articulated vehicle comprising a three-axle tractor (Unit 1) and a three-axle semitrailer (Unit 2). The equation of motion of the vehicle, derived upon considering the longitudinal and lateral forces, and yaw moments, are presented below:

2.2.1 Equations of Motion

Unit 1:

$$m_1 (\dot{u}_1 - v_1 r_1) = -F_{11} \sin\delta + F_{XA} - F_{SL} \cos\zeta_1 - F_{SR} \cos\beta_1 \qquad (2.1)$$

$$\begin{aligned} m_1 (\dot{v}_1 + u_1 r_1) &= F_{11} \cos\delta + F_{12} + F_{13} + F_{YA} \\ &- F_{SR} \sin\beta_1 + F_{SL} \sin\zeta_1 \end{aligned} \qquad (2.2)$$

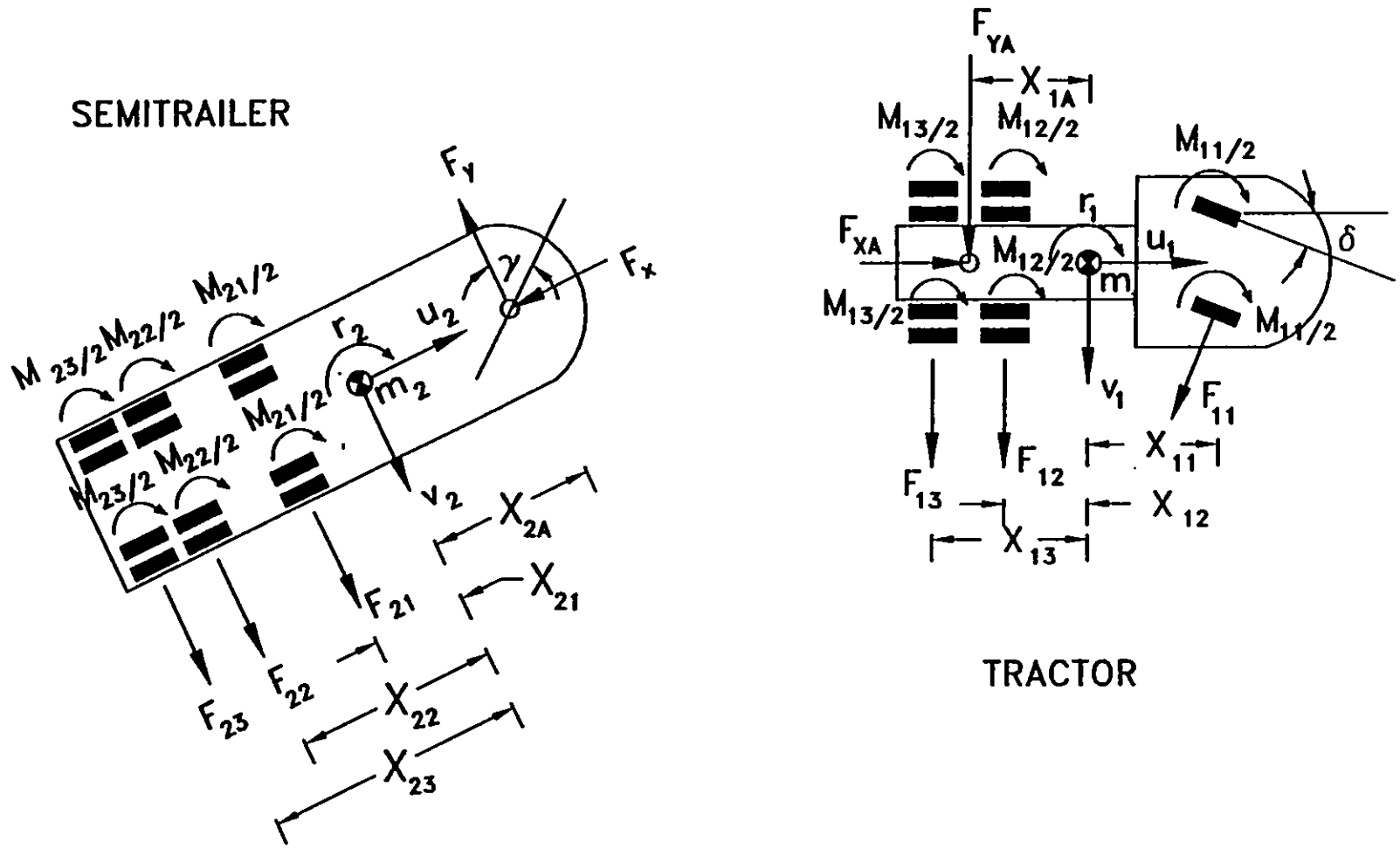

Figure 2.2: Yaw-Plane models of the tractor and semitrailer

$$
\begin{aligned}
I_1\dot{r}_1 &= F_{11}\cos\delta\, X_{11} - F_{12}X_{12} - F_{13}X_{13} \\
&+ M_{11} + M_{12} + M_{13} - F_{YA}\, X_{1A} + a\, F_{SR}\cos\beta_1 \\
&+ b\, F_{SR}\sin\beta_1 - a\, F_{SL}\cos\zeta_1 - b\, F_{SL}\sin\zeta_1
\end{aligned} \tag{2.3}
$$

Unit 2:

$$
\begin{aligned}
m_2\,((\dot{u}_2 - v_2 r_2) &= -F_{XA}\cos\gamma + F_{YA}\sin\gamma \\
&+ F_{SL}\cos\zeta_2 + F_{SR}\cos\beta_2
\end{aligned} \tag{2.4}
$$

$$
\begin{aligned}
m_2\,(\dot{v}_2 + u_2 r_2) &= F_{21} + F_{22} + F_{23} - F_{YA}\cos\gamma - F_{XA}\sin\gamma \\
&- F_{SL}\sin\zeta_2 + F_{SR}\sin\beta_2
\end{aligned} \tag{2.5}
$$

$$
\begin{aligned}
I_2\dot{r}_2 &= -(F_{YA}\cos\gamma + F_{XA}\sin\gamma)\, X_{2A} - F_{21}X_{21} - F_{22}X_{22} \\
&- F_{23}X_{23} + M_{21} + M_{22} + M_{23} + c\, F_{SL}\cos\zeta_2 \\
&- d\, F_{SL}\sin\zeta_2 + d\, F_{SR}\sin\beta_2 - F_{SR}\cos\beta_2
\end{aligned} \tag{2.6}
$$

where m_1 and m_2 are the masses of tractor and semitrailer, respectively. I_1 and I_2 represent the yaw mass moment of inertia of the tractor and semitrailer units. u_i, v_i and r_i are the longitudinal, lateral and yaw velocities of unit i (i = 1,2), respectively. F_{ij} and M_{ij} are the lateral forces and aligning moments, respectively, due to tires on axle j of unit i. δ is the front wheel steer angle and γ is the articulation angle. F_{XA} and F_{YA} are the longitudinal and lateral constraint forces at the articulation point. X_{ij} represents the longitudinal distance between centre of gravity (c.g.) of unit i and axle j attached to the same unit. X_{1A} and X_{2A} are the longitudinal distances between the articulation point (fifth wheel) and the c.g. of units 1 and 2, respectively.

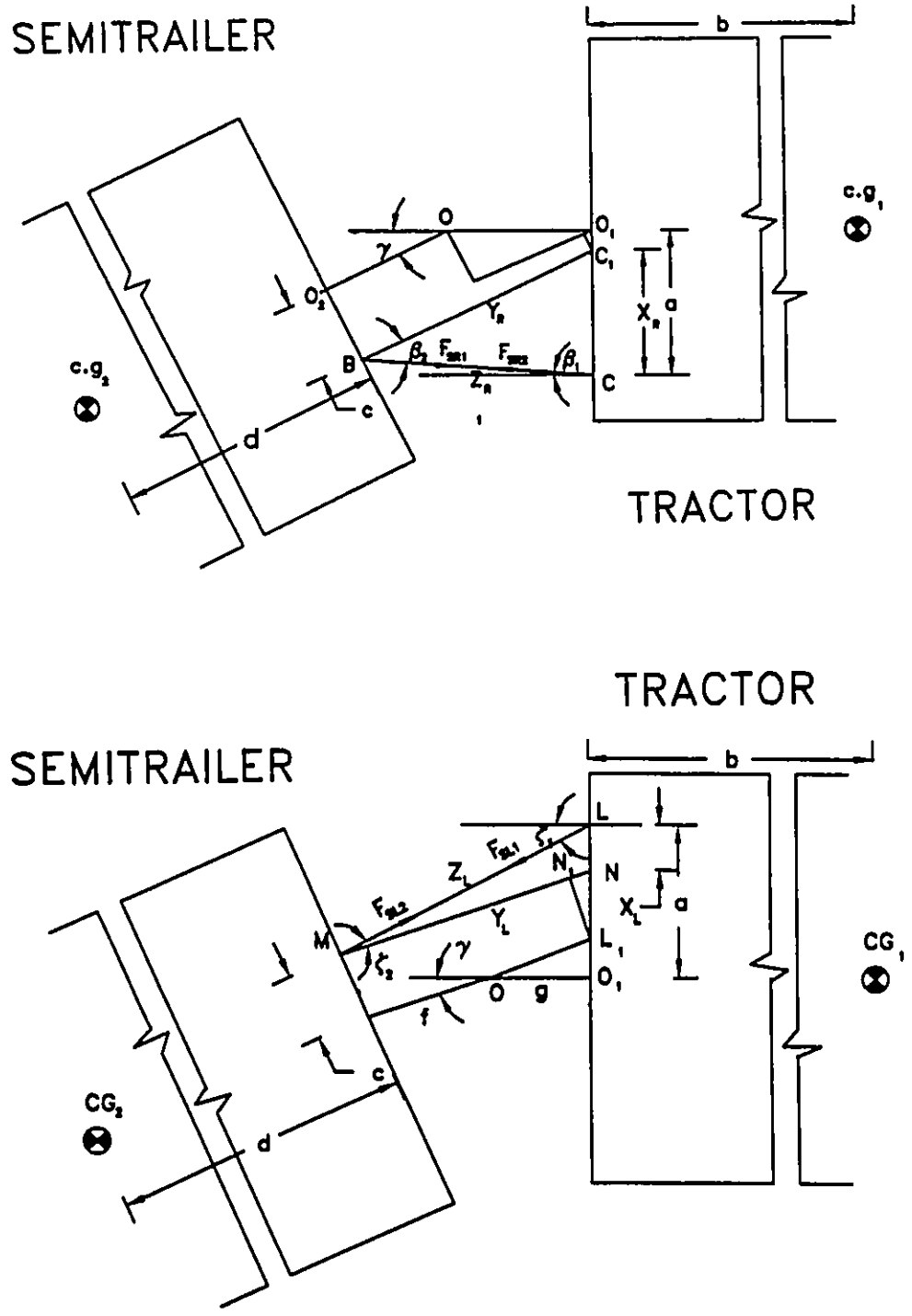

Figure 2.3: Kinematic model of the articulation damper and damper forces acting on the two units

F_{SL} and F_{SR} are the damping forces acting on the two units, generated by the left- and right-dampers, respectively. β_1, β_2, ζ_1 and ζ_2 are the angles derived from kinematic model of the dampers, shown in Figure 2.3. Various forces and moments due to tires, articulation and dampers are derived in the following sub-sections.

2.2.2 Lateral Tire Forces (F_{ij})

Assuming linear cornering characteristics of the tires, the lateral forces generated at the tire-road interface are expressed as:

$$F_{ij} = -C_{ij}\alpha_{ij} \tag{2.7}$$

where α_{ij} is the average side-slip angle developed at the tires mounted on axle j of unit i. C_{ij} is the cornering stiffness of tires, and is equal to C_α, when identical tires are used. The cornering stiffness of a pneumatic tire is derived from the lateral forces F_{yij} developed at the tire road interface:

$$C_\alpha = \frac{\partial F_{yij}}{\partial \alpha_{ij}};\ for\ \alpha_{ij} \approx 0 \tag{2.8}$$

2.2.3 Aligning Moments M_{ij}

The total aligning moment developed at the tire-road interface comprises of two components: an aligning moment due to the dual tire effect and an aligning moment due to the pneumatic trail effect [41]. The aligning moment due to dual tire is computed from

$$(M_{ij})_{DT} = -\left(\frac{y^2_{ij}}{2u_i}C_{xij}\right)r_i \tag{2.9}$$

where y_{ij} is the dual tire spacing, C_{xij} is the longitudinal stiffness of tire on axle j of unit i. The aligning moment due to pneumatic trail is approximated by linear relationship:

$$(M_{ij})_{PT} = N_{ij}\alpha_{ij} \tag{2.10}$$

where N_{ij} is a coefficient, representing the sum of aligning moments per unit side-slip, developed by all the tires on an axle. The total aligning moment of the tires is thus expressed as:

$$M_{ij} = N_{ij}\alpha_{ij} - \left(\frac{y^2{}_{ij}}{u_i}C_{sij}\right)r_i \tag{2.11}$$

2.2.4 Side-Slip Angles α_{ij}

The side-slip angles α_{ij}, developed primarily due to lateral elasticity of the tires, are related to forward and lateral velocities at the contact patch. Figure 2.4 illustrates the longitudinal and lateral velocities, and the side-slip angles developed at contact patch of the front and rear most tires. Assuming small angles, the side-slip angles are derived as

$$\alpha_{11} = \frac{v_1 + x_{11}r_1}{u_1} - \delta$$

and

$$\alpha_{ij} = \frac{v_i - x_{ij}r_i}{u_i}; \quad for \begin{cases} i = 1; & j = 2,3 \\ i = 2; & j = 1,2,3 \end{cases} \tag{2.12}$$

2.2.5 Constraint Forces and Velocities

The two units are free to yaw relative to each other, while in the lateral and longitudinal directions, the two units are constrained to move together at the articulation point. Equal and opposite forces thus act on the leading and trailing units due to the motion constraint posed by the articulation, as shown in Figure 2.5.

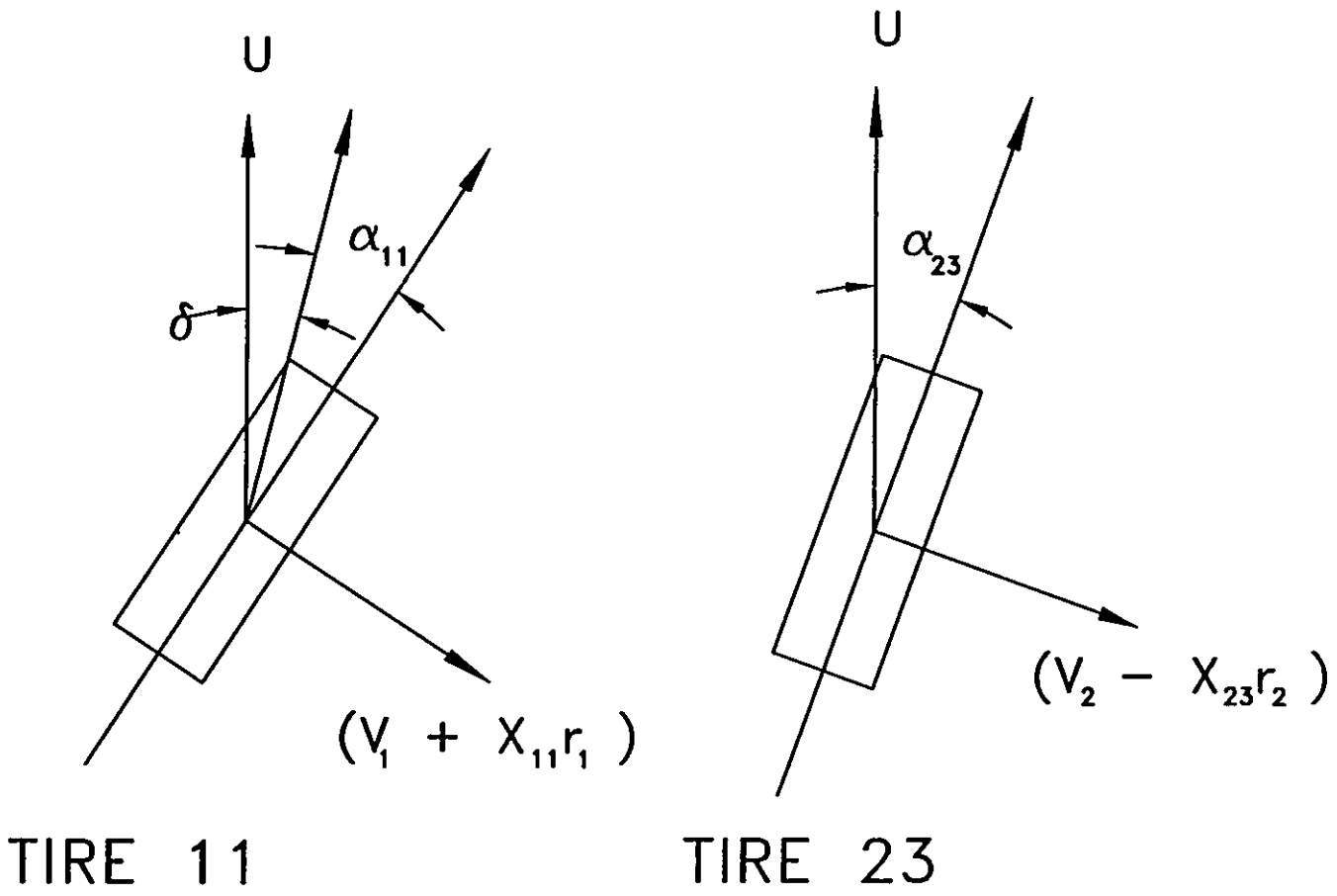

Figure 2.4: Longitudinal and lateral tire velocities, and side-slip angles

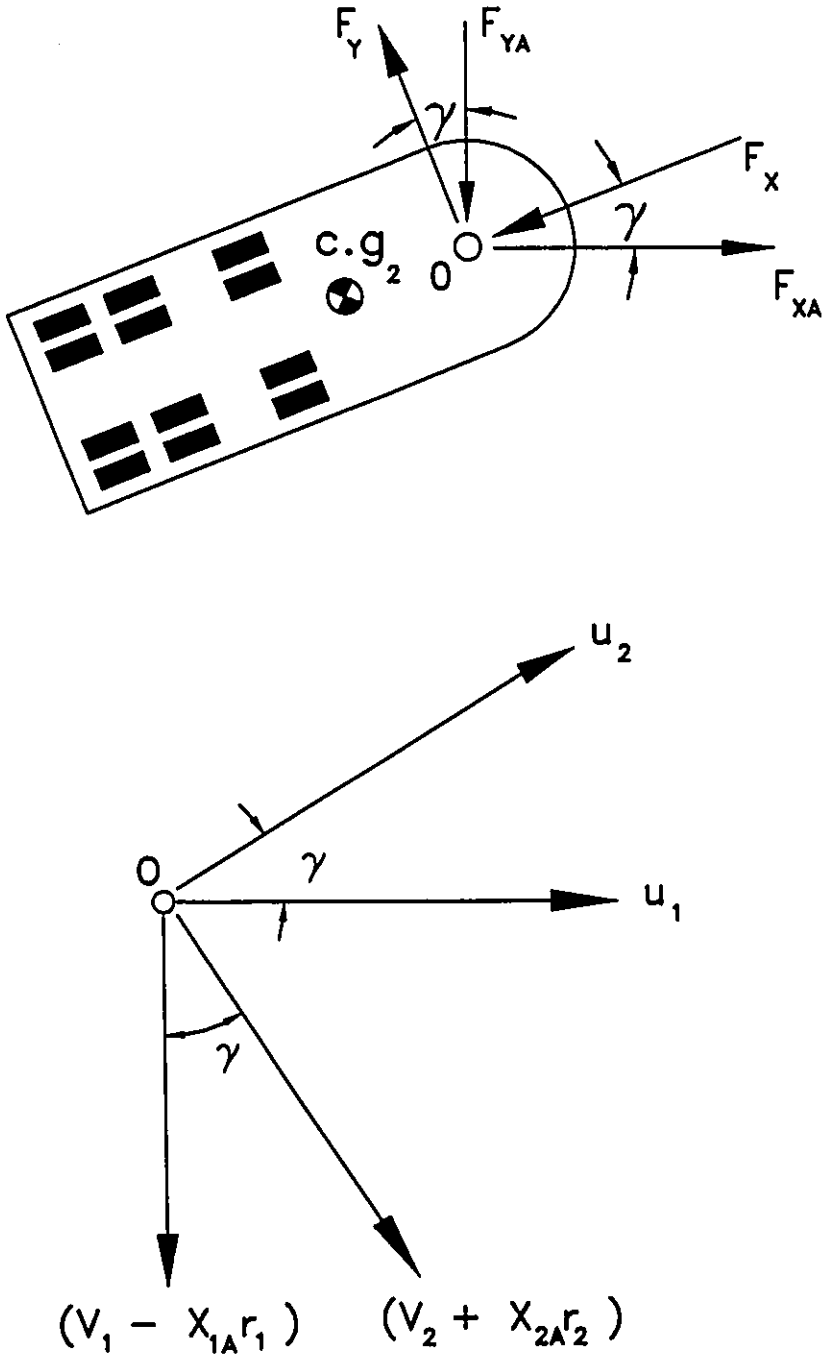

Figure 2.5: Forces and velocities at the articulation joint

The constraint forces acting on the trailing unit can thus be expressed in terms of those acting on the leading unit:

$$F_X = F_{XA} \cos\gamma - F_{YA} \sin\gamma$$

$$F_Y = F_{YA} \cos\gamma + F_{XA} \sin\gamma \tag{2.13}$$

From constraint relationships in the lateral and longitudinal directions (Figure 2.5), assuming small angles, the lateral velocity of the trailing unit can be related to that of the leading unit in the following manner:

$$v_2 = v_1 + U\gamma - X_{1A}\, r_1 - X_{2A}\, r_2$$

and

$$\dot{v}_2 = \dot{v}_1 + U(r_1 - r_2) - X_{1A}\, \dot{r}_1 - X_{2A}\, \dot{r}_2 \tag{2.14}$$

where U = u_1 = u_2, and (r_1 - r_2) is the articulation rate, $\dot{\gamma}$.

2.2.6 Damping forces and Moments

The kinematic representations of the two articulation dampers mounted between the tractor and the semitrailer are illustrated in Figure 2.3. LM and CB represent the left- and right-dampers attached to the tractor at pivot L and C, respectively. The two dampers are attached to the semitrailer at pivot points M and C. The points L and C are located at a distance of 'a' from the longitudinal axis passing through the c.g. of the tractor (O_1). The pivot points M and B are located at a distance of 'c' from the longitudinal axis passing through c.g. of the semitrailer (O_2). The point O represents the articulation point, which is located at a longitudinal distance of 'g' from the pivot points on the tractor, and 'f' is the longitudinal distance between the articulation point O and the pivot points L and C. ζ_1 and ζ_2 are the angles between the axis of the dampers LM and the longitudinal axes

of the tractor and semitrailer, respectively. β_1 and β_2 are the angles between damper CB axis and the longitudinal axes of the tractor and semitrailer, respectively.

From the geometry, shown in Figure 2.3, the angles β_1, β_2 ζ_1 and ζ_2 are derived as:

$$\beta_1 = \beta_2 - \gamma$$

$$\beta_2 = sin^{-1}\left(\frac{X_R \cos\gamma}{Z_R}\right)$$

$$\zeta_1 = \zeta_2 + \gamma$$

$$\zeta_2 = sin^{-1}\left(\frac{X_L \cos\gamma}{Z_L}\right) \tag{2.15}$$

where,

$$X_L = a - \frac{c}{cos\gamma} - g\ tan\ \gamma;$$

$$X_R = a - \left(\frac{c - g\ sin\gamma}{cos\gamma}\right);$$

$$Z_L = \sqrt{(X_L^2 + Y_L^2 - 2\ X_L\ Y_L\ cos\,(90 + \gamma))};$$

$$Y_L = f + \frac{g}{cos\gamma} - c\ tan\ \gamma;$$

$$Y_R = f + g\ cos\gamma - (c - g sin\gamma)\ tan\ \gamma;$$

$$Z_R = \sqrt{(X_R^2 + Y_R^2 - 2\ X_R\ Y_R\ cos\,(90 - \gamma))};$$

The damping forces developed by the articulation dampers, along their respective axis, are derived from the relative velocities across the dampers. The relative velocities

along the axis of the dampers are related to the longitudinal, lateral and yaw velocities of the two units, and the dampers geometry. Figure 2.6 illustrate the velocities at the pivot points of two dampers, derived from kinematic relations.

The damping forces due to left- and right- dampers, F_{SL} and F_{SR}, developed along the axis of the dampers are expressed as a linear function of the relative velocities:

$$F_{SL} = C_{SL} * \Delta V_{SL}$$

and

$$F_{SR} = C_{SR} * \Delta V_{SR} \tag{2.16}$$

where C_{SL} and C_{SR} are the viscous damping coefficients, and ΔV_{SL} and ΔV_{SR} are the relative velocities across the left- and right dampers, respectively. The relative velocities across the dampers, along their axes, derived from Figure 2.6, are expressed as:

$$\begin{aligned} \Delta V_{SL} &= (U + a\, r_1)\, cos\zeta_1 - (v_1 - b\, r_1)\, sin\zeta_1 \\ &- (U + c\, r_2)\, cos\zeta_2 + (v_2 + d\, r_2)\, sin\zeta_2 \end{aligned}$$

$$\begin{aligned} \Delta V_{SR} &= (U - a\, r_1)\, cos\beta_1 + (v_1 - b\, r_1)\, sin\beta_1 \\ &- (U - c\, r_2)\, cos\beta_2 - (v_2 + d\, r_2)\, sin\beta_2 \end{aligned} \tag{2.17}$$

Upon elimination of the constraint forces, using equations (2.13), substituting for semitrailer lateral velocity from (2.14), and assuming constant forward velocity (driving forces balanced by the motion resistances), the yaw-plane dynamics of the vehicle can be represented by the following first-order coupled differential equations of motion.

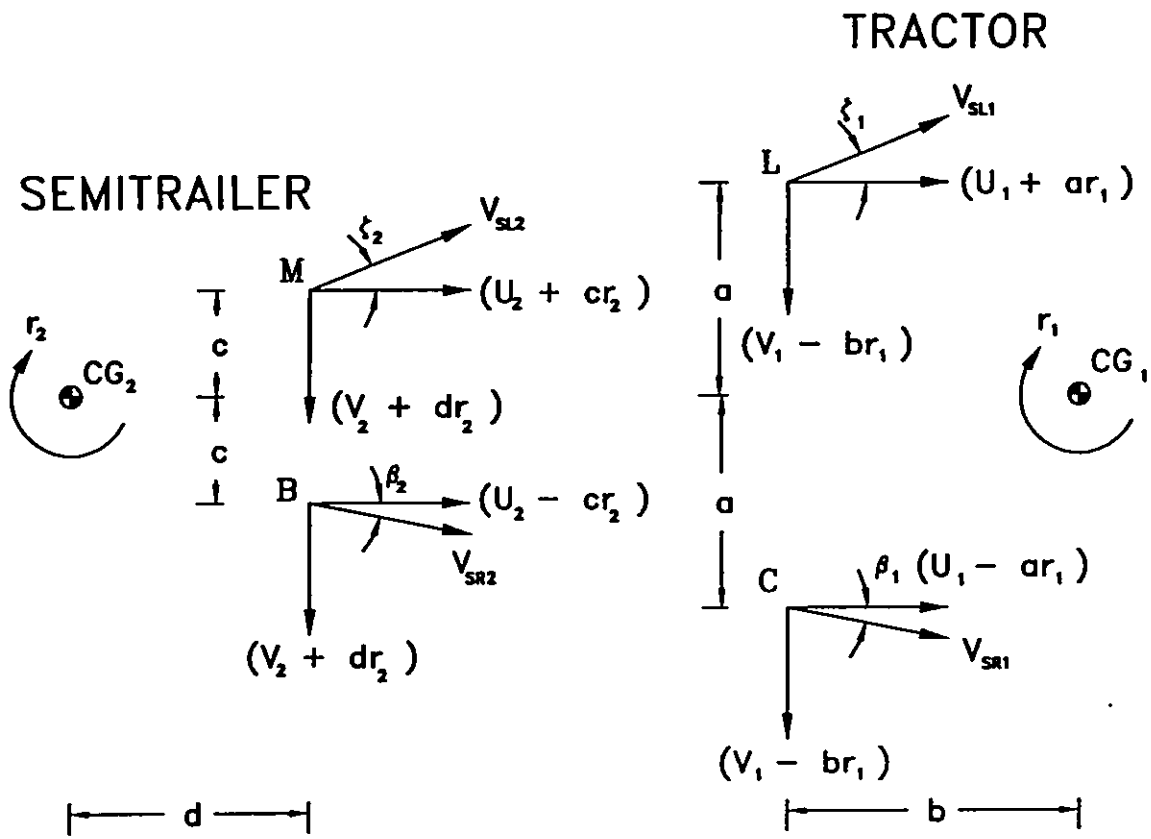

Figure 2.6: Velocities at the pivot points of right- and left-dampers

$$m_1(\dot{v}_1 + u_1 r_1) + m_2(\dot{v}_2 + u_2 r_2) = F_{11} + F_{12} + F_{13} + F_{21} + F_{22} + F_{23}$$
$$+ F_{SR}(\sin\beta_2 - \sin\beta_1) + F_{SL}(\sin\zeta_2 - \sin\zeta_1) \quad (2.18)$$

$$I_1\dot{r}_1 = [m_2(\dot{v}_2 + u_2 r_2) - F_{21} - F_{22} - F_{23}]X_{1A}$$
$$+ F_{11}X_{11} - F_{12}X_{12} - F_{13}X_{13} + M_{11} + M_{12} + M_{13}$$
$$+ F_{SR}(a\cos\beta_1 + b\sin\beta_1 - X_{1A}\sin\beta_2)$$
$$- F_{SL}(a\cos\zeta_1 + b\sin\zeta_1 - X_{1A}\sin\zeta_2) \quad (2.19)$$

$$I_2\dot{r}_2 = [m_2(\dot{v}_2 + u_2 r_2) - F_{21} - F_{22} - F_{23}]X_{2A}$$
$$- F_{21}X_{21} - F_{22}X_{22} - F_{23}X_{23} + M_{21} + M_{22} + M_{23}$$
$$+ F_{SL}(c\cos\zeta_2 - d\sin\zeta_2 + X_{2A}\sin\zeta_2)$$
$$- F_{SR}(d\sin\beta_2 - c\cos\beta_2 - X_{2A}\sin\beta_2) \quad (2.20)$$

The rate of articulation, $\dot{\gamma}$, is derived from the yaw velocities of the two units.

$$\dot{\gamma} = r_1 - r_2 \quad (2.21)$$

Equations (2.18) to (2.21), together with equations (2.7), (2.11), (2.12) and (2.16), describe the yaw plane dynamics of an articulated vehicle with damped articulation. The equation of motion can be expressed in the following matrix form

$$[A]\{\dot{q}\} = [[B] + [BD]]\{q\} + \{\{CD\} + \{C\}\delta\} \quad (2.22)$$

where, $[A]$ is $(4 * 4)$ matrix of mass and inertia properties of the vehicle, $[B]$ and $[BD]$ are $(4 * 4)$ matrices of constant vehicle parameters, and damping forces and moments, respectively. $\{C\}$ is an $(4 * 1)$ vector of vehicle parameter, and $\{CD\}$ is the forcing-damping vector. $\{q\}$ is the vector of generalized coordinates, given by $\{v_1, r_1, r_2, \gamma\}^{-1}$.

2.3 Yaw-Plane model of the Articulated Vehicle with Non-linear Tire Forces

The yaw-plane model, presented in section 2.2, describes the lateral directional dynamics of the vehicle assuming linear cornering characteristics of the tires. Majority of the studies, reported in the literature, have utilized this linear model with zero damping forces to estimate the handling and directional control characteristics of the vehicle. It has been established that while these models provide a reasonable estimate of the periodic yaw response, the aperiodic response characteristics cannot be accurately estimated due to absence of the nonlinear and bounded tire model [23]. Furthermore, the measured data reported for truck tires, clearly illustrates that the cornering forces developed by the tires are strongly dependent upon the normal load and the side-slip angle. Figure 2.7 illustrates the cornering force characteristics of an 11R22.5 radial truck-tire with 1/3 tread, as a function of the normal load and the side-slip angle, for normal inflation pressure [8-12]. From the figure, it is evident that the cornering force increases with an increase in the normal load and side-slip angle in a highly nonlinear manner. The linear cornering force relationship, described in 2.7, can be considered valid only in the vicinity of a given normal load for slip angles below 4 degrees. The normal loads on tires of articulated vehicles vary considerably depending upon the loading of the vehicle. The cornering characteristics of the tires are thus expected to vary with the vehicle loads. A nonlinear model of the tire is thus derived and integrated to the yaw-plane model of the vehicle in order to estimate the directional response characteristics under varying loading and operating conditions.

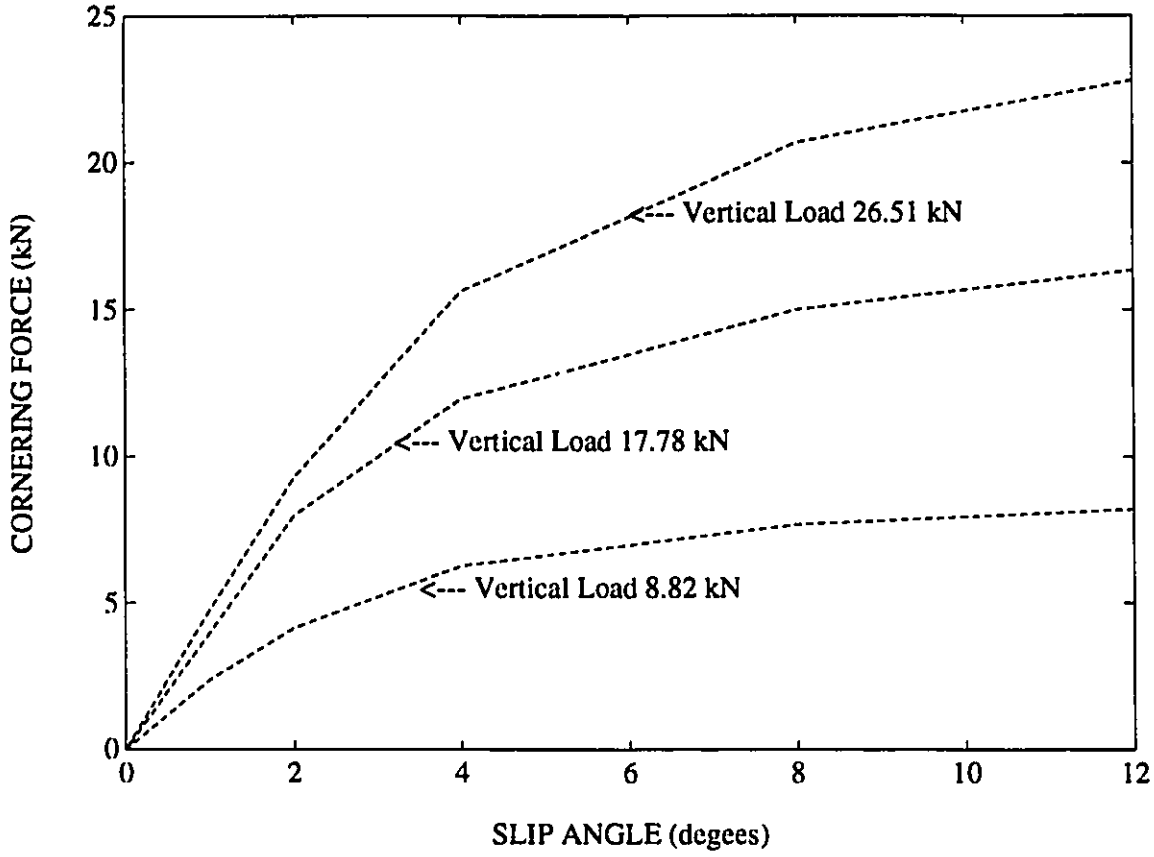

Figure 2.7: Cornering force characteristics of an 11R22.5 Radial tire

2.3.1 Nonlinear Cornering Force Relations of Tires

The cornering characteristics of tires are expressed as nonlinear functions of the normal load and side-slip angles, using two methods:

1. A Piece-wise Linear Describing Function
2. A Continuous Describing Function

Piece-wise Linear Describing Function of Tire Forces

The cornering characteristics of tires, presented in Figure 2.7, reveal that for a given normal load the lateral force can be characterized as a piece wise linear function of the side-slip angle. The cornering force curve is thus divided into three linear segments, and piecewise linear cornering stiffness coefficients are defined in each segment. For a given normal load, the cornering force expressed as a piecewise linear function of the side-slip angles, in the following manner:

$$F_y = \begin{cases} C_{SA}\alpha; & |\alpha| < \alpha_1 \\ C_{SA}\alpha_1 sgn(\alpha) + C_{SB}[\alpha - \alpha_1 sgn(\alpha)]; & \alpha_1 < |\alpha| < \alpha_2 \\ C_{SA}\alpha_1 sgn(\alpha) + C_{SB}(\alpha_2 - \alpha_1)sgn(\alpha) \\ +C_{SC}[\alpha - \alpha_2 sgn(\alpha)]; & |\alpha| > \alpha_2 \end{cases} \tag{2.23}$$

where F_y is the cornering force developed by the tire, and α is its side-slip angle. C_{SA}, C_{SB} and C_{SC} are the cornering stiffness coefficients in the three linear segments. α_1 and α_2 define the limits of the linear segments. The limits selected from the measured data are $\alpha_1 = 4$ degrees; and $\alpha_2 = 8$ degrees. The cornering stiffness coefficients of the tires, however, vary with the normal load, as illustrated in Figure 2.7. The variations in

these coefficients are approximated by a quadratic function in the normal load:

$$C_{SK} = a_K F_Z^2 + b_K F_Z + c_K \quad for\ K = A,B,C \tag{2.24}$$

A curve-fit algorithm is used to determine the constant coefficients a_K b_K and c_K. The piecewise linear cornering stiffness coefficients of tire, formulated using the measured data, are expressed as a function of the normal load, F_Z:

$$C_{SA} = -0.001705\ F_Z^2 + 13.7403305\ F_Z - 1832.07326; \quad for\ |\alpha| < 4^0$$

$$C_{SB} = 0.000397\ F_Z^2 + 1.50445696\ F_Z + 387.12113; \quad for\ 4^0 < |\alpha| < 8^0$$

$$C_{SC} = -0.00004234\ F_Z^2 + 1.441345\ F_Z - 489.357524; \quad for\ |\alpha| > 8^0 \tag{2.25}$$

The cornering forces derived from the piecewise linear model, described by equations (2.23) and (2.24), are compared to the measured data to demonstrate its validity. Figure 2.8 presents a comparison of the measured and estimated cornering forces for three different normal loads. The comparison reveals that the piecewise linear model can accurately represent the cornering force characteristics for the load range considered in this study, except for low slip angles. For light loads, the piecewise linear model provides slightly lower values of cornering forces for slip angles below 4 degrees.

Continuous Describing Function of Tire Forces

Alternatively, the nonlinear cornering forces of a pneumatic tire may be characterized by a continuous polynomial function in the normal load and the side-slip angle. A regression analysis is performed to determine the coefficients and the order of the polynomial that best describes the measured data in the selected ranges of load (8800 N - 42000 N), and side-slip angles (0^0 - 12^0). A statistical package, referred to as 'minitab', was used to carry out the regression analysis based on the least square method [45]. The

analysis revealed that the nonlinear cornering characteristics can be best described by the following fourth order polynomial in normal load and the side-slip angle:

$$\begin{aligned} F_Y &= C_0 + C_1 * F_Z + C_2 * \alpha + C_3 * \alpha^2 + C_4 * \alpha^3 \\ &+ C_5 * F_Z^2 + C_6 * F_Z^3 + C_7 * F_Z * \alpha + C_8 * F_Z^2 * \alpha^2 \\ &+ C_9 * \alpha^4 + C_{10} * F_Z^4 + C_{11} * F_Z * \alpha^2 \\ &+ C_{12} * F_Z^2 * \alpha + C_{13} * F_Z * \alpha^3 + C_{14} * F_Z^3 * \alpha \end{aligned} \tag{2.26}$$

For, $0 \leq |\alpha| \leq 12^0$ and $8800\ N \leq F_Z \leq 42000\ N$. The constants C_0 to C_{14}, derived from the regression analysis, are $C_0 = -283.03$, $C_1 = 0.158761$, $C_2 = 540.50$, $C_3 = -159.348$, $C_4 = 11.4736$, $C_5 = -0.0000197$, $C_7 = 0.168234$, $C_8 = -0.00000008$, $C_{12} = -0.00000383$ and $C_{13} = -0.00070750$.

The cornering force characteristics, computed from equation (2.26), are compared to the measured data, as shown Figure 2.9. The comparison reveals a reasonable correlation between the measured and estimated values, with certain errors at low side-slip angles. A comparison of Figures 2.8 and 2.9 reveals that a piecewise linear model can more accurately describe the nonlinear cornering characteristics of the truck tire. The piecewise linear model, however, may yield errors in the vehicle response near the discontinuities ($\alpha = \alpha_1$, or $\alpha = \alpha_2$). The nonlinear aligning moment component due to pneumatic trail of tires are computed from the nonlinear cornering forces and the pneumatic trail:

$$(M_{ij})_{PT} = F_{y_{ij}} * t_{ij} \tag{2.27}$$

where t_{ij} is the pneumatic trail of the tire. The pneumatic trail of the tire is related to the normal load by the following relation [46]:

$$t_{ij} = [\ 2.10 + 1.25 * 10^{-4}(4.536 * F_{Z_{ij}} - 6040)\ ] * 0.0254 \tag{2.28}$$

In the above relation, $F_{Z_{ij}}$ is the normal load in newtons and t_{ij} is in meters.

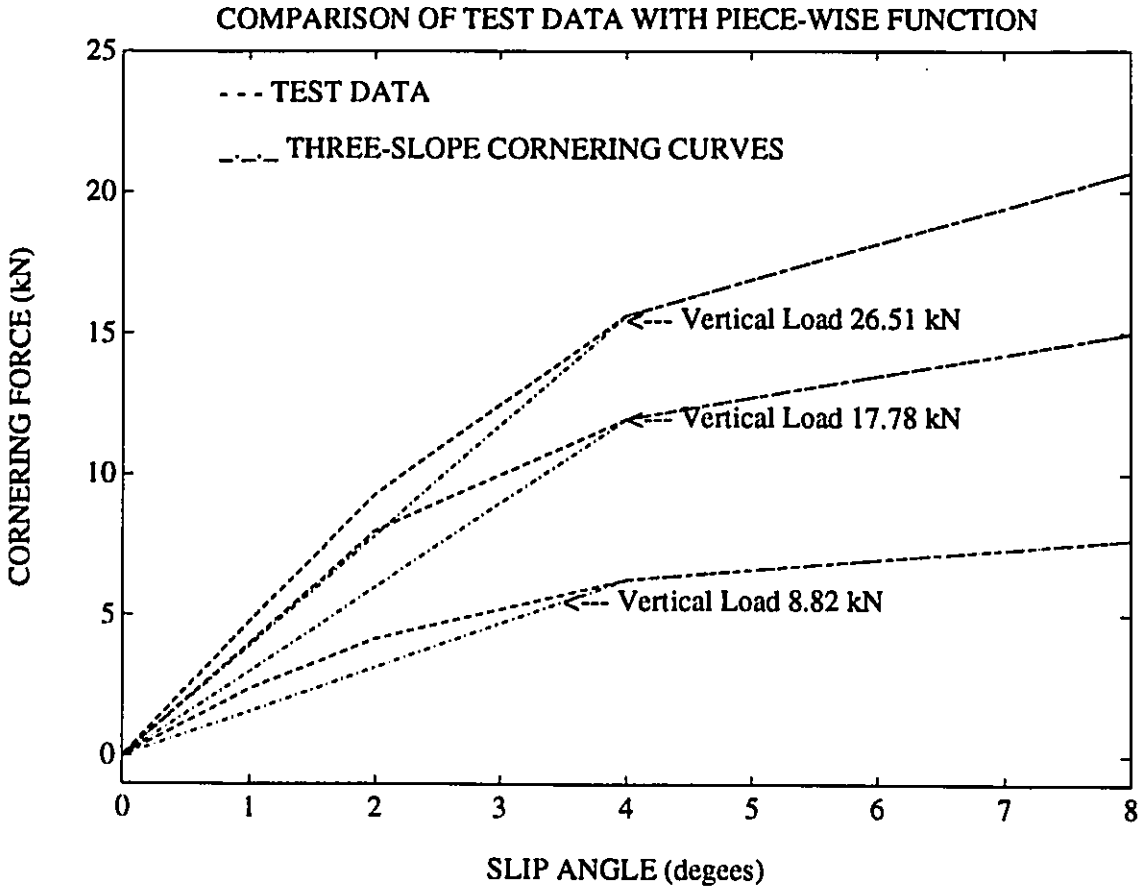

Figure 2.8: Cornering force of tire developed by Piecewise Linear Function

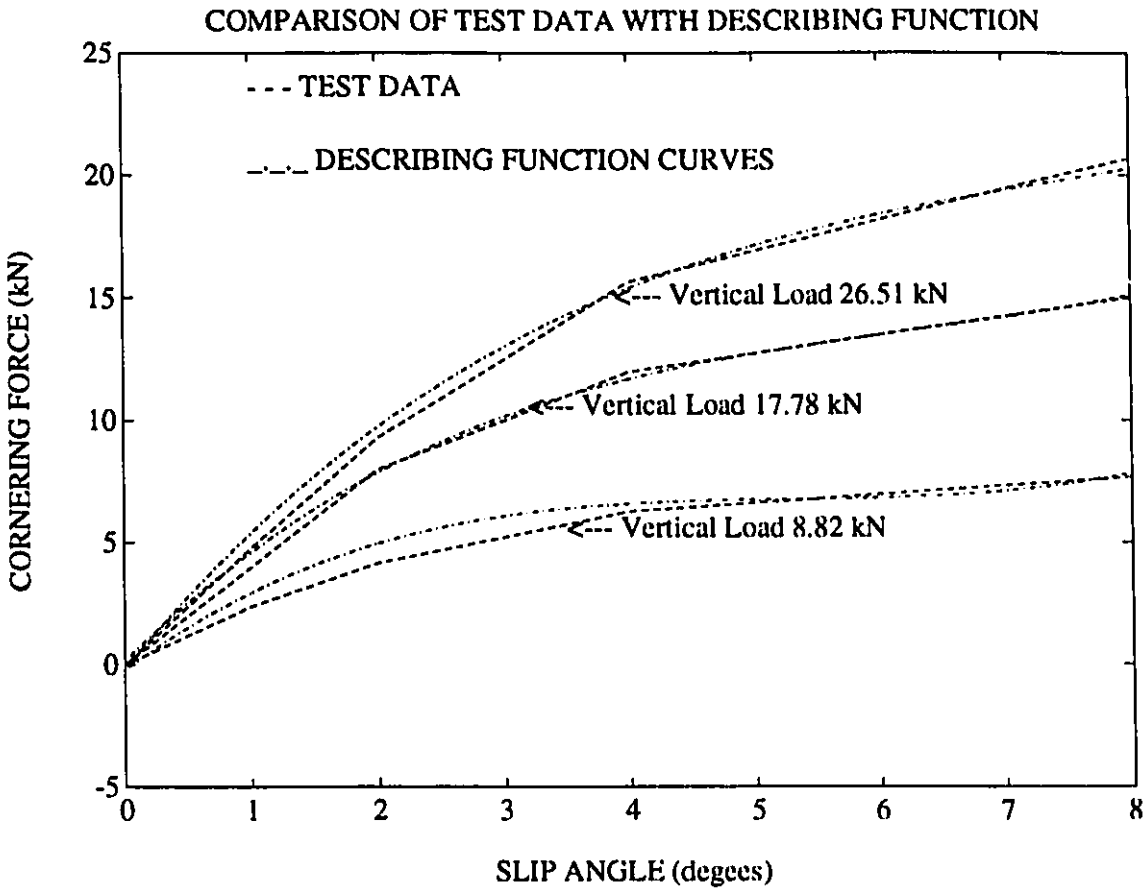

Figure 2.9: Cornering force of tire developed by Continuous Describing Function

2.3.2 Equations of Motion

The equation of motion of the yaw-plane model of articulated vehicle incorporating nonlinear cornering characteristics of the tires and damped articulation are identical to those presented in Equations (2.18) to (2.21). The cornering forces (F_{ij}) are described by either the piecewise linear or nonlinear continuous functions presented in equations (2.23), (2.24) and (2.26). The nonlinear aligning moments of the tires (M_{ij}) are derived from equations (2.9) and (2.27), while the damping forces remain the same as described in equation (2.16). The equations of motion are expressed in the following matrix form:

$$[A]\{\dot{q}\} = [[B] + [BD]]\ \{q\} + \{\{CD\} + \{DD\} + \{C\}\delta\} \qquad (2.29)$$

where [A], [B] and [BD] are (4x4) matrices of mass/inertia properties of the vehicle, vehicle and tire parameters, and damping forces, respectively. $\{CD\}$, $\{DD\}$ and $\{C\}$ are (4x1) vectors.

2.4 Yaw-Plane Model of the Articulated Vehicle with Forced-steering Axles and Damped Articulation

In view of the recently relaxed weights and dimensions regulation, the population of articulated vehicles with multiple axle semitrailers has been increasing rapidly. While either one or two drop axles are currently being used to overcome the poor maneuverability limits of vehicles with multiple axle trailers, the excessive road damage caused by the raised drop axles has raised many concerns among the fleet operators and policy makers. The self-steering axles are increasingly being used to improve the maneuverability and to reduce the rate of tire wear during cornering maneuvers. The tires of the self-steering axles, however, provide limited or no cornering forces, and thus affect the directional stability in an adverse manner. Alternatively forced-steering axles offer considerable performance potentials by varying the steer angle of the trailer axles in response to the

changing speed and dynamic response of the vehicle. Forced steering control schemes relating the vehicle response quantities to the angle of the wheels of the steerable axle are purposed and integrated to the nonlinear yaw plane model of the vehicle to formulate the directional dynamic model of the articulated vehicle with forced-steering axles of the semitrailer.

2.4.1 Forced-Steering Algorithms

The wheel angle of the forced-steering axle is expressed as a function of the selected dynamic response quantities. While only limited number of studies have been reported on the influence of the feedback response quantities, the results of these studies have shown the performance benefits of forced-steering axles, when the angle of the steered-axle is generated in response to the front wheel steer angle (δ), and/or the articulation angle (γ) [40-42]. The results of these studies have also shown that the desired steered wheel angle is strongly related to the vehicle speed [42]. The control scheme is thus formulated as a composite function of the front wheel steer angle (δ), articulation angle (γ), articulation rate ($\dot{\gamma}$), and forward velocity U. Assuming proportional control and negligible dynamics of the force generating mechanism, the wheel angle of the forced-steer axle is expressed as

$$\delta_{FSj} = K_{1j}\delta + K_{2j}\gamma + K_{3j}\dot{\gamma} + K_{4j}U\gamma + K_{5j}U\dot{\gamma}; \quad j = 1,2,3 \tag{2.30}$$

where δ_{FSj} is the angle of the wheels mounted on the force-steered axle j. K_{1j} is the constant front wheel steer gain, K_{2j} is the articulation gain, K_{3j} is the articulation rate gain, and K_{4j} and K_{5j} are the speed sensitive proportional control gains.

2.4.2 Equations of Motion

The equations of motion for the six-axle vehicle combination employing three forced-steered axles at the semitrailer, and articulation damping are derived in a similar manner as described in section 2.3. The angles are not assumed to be small in this analysis. Figure 2.10 illustrates the yaw-plane model of the vehicle incorporating forced-steering of the semitrailer axles. Note that the damping forces due to articulation dampers are not shown in this figure. Assuming constant forward speed, the equation of motion of the vehicle model are derived as:

Unit 1:

$$m_1 (\dot{v}_1 + u_1 r_1) = F_{11} \cos\delta + F_{12} + F_{13} + F_{YA} - F_{SR} \sin\beta_1 + F_{SL} \sin\zeta_1 \qquad (2.31)$$

$$\begin{aligned} I_1 \dot{r}_1 &= F_{11} \cos\delta \, X_{11} - F_{12} \, X_{12} - F_{13} \, X_{13} - F_{YA} \, X_{1A} + \sum_{j=1}^{3} M_{1j} \\ &+ a \, F_{SR} \cos\beta_1 + b \, F_{SR} \sin\beta_1 - a \, F_{SL} \cos\zeta_1 - b \, F_{SL} \sin\zeta_1 \end{aligned} \qquad (2.32)$$

Unit 2:

$$\begin{aligned} m_2(\dot{v}_2 + u_2 r_2) &= \sum_{j=1}^{3} F_{2j} \cos\delta_{FSj} - F_{YA} \cos\gamma - F_{XA} \sin\gamma \\ &- F_{SL} \sin\zeta_2 + F_{SR} \sin\beta_2 \end{aligned} \qquad (2.33)$$

$$\begin{aligned} I_2 \dot{r}_2 &= -(F_{YA} \cos\gamma + F_{XA} \sin\gamma) X_{2A} - \sum_{j=1}^{3} X_{2j} \, F_{2j} \cos\delta_{FSj} + \sum_{j=1}^{3} M_{1j} \\ &+ c \, F_{SL} \cos\zeta_2 - d \, F_{SL} \sin\zeta_1 + d \, F_{SR} \cos\beta_2 - c \, F_{SR} \cos\beta_1 \end{aligned} \qquad (2.34)$$

where F_{ij} and M_{ij} are the nonlinear cornering forces and aligning moments, respectively, described in equations (2.32) to (2.34). The cornering forces and aligning moments developed by the steered-tires of the semitrailer are related to their respective side-slip angles. The side-slip angles of force-steered tire are derived from the longitudinal and lateral velocities of the tire, and steer angle of the wheel. Figure 2.11 illustrates

the velocities, steer angle and side-slip angle of the tires on the rearmost axle. The average side-slip angles of the steered and non-steered tractor and semitrailer tires have been defined in (2.12). The average side-slip angles of the steered-semitrailer tires are expressed as:

$$\alpha_{2j} = tan^{-1}\left(\frac{v_2 - X_{2j}\, r_2}{U}\right) - \delta_{FSj}; \quad for \;\; j = 1,2,3 \tag{2.35}$$

The total aligning moment due to the tires comprises two components: (i) an aligning moment arising from longitudinal forces due to dual tire spacing; and (ii) an aligning moment due to pneumatic trail of the tire. In a dual-tire arrangement, the outer and inner tires are subject to different velocities, as shown in Figure 2.12. The corresponding deformation slip and the longitudinal forces of the steered dual tire set yield an aligning moment $(M_{ij})_{DT}$, which is related to the steer angle of the tires. This component of aligning moment of tires on the steered axles of the semitrailer unit is expressed as:

$$(M_{ij})_{DT} = -\left(\frac{y^2_{ij}\, C_{sij}}{2u_i}\right) r_i \cos \delta_{FSj} \quad for \;\; i = 2, \; j = 1,2,3 \tag{2.36}$$

The component of the aligning moment, arising from pneumatic trail of the tire, is derived form equation (2.38). Upon elimination of constraint forces, using equation (2.13), the equation of motion of the articulated vehicle with forced-steering axles and damped articulation are reduced to:

$$\begin{aligned} m_1(\dot{v}_1 \;+\; u_1 r_1) + m_2(\dot{v}_2 + u_2 r_2) &= F_{11} \cos\gamma \cos\delta + F_{12} \cos\gamma \\ &+ F_{13} \cos\gamma + \sum_{j=1}^{3} F_{2j} \cos\delta_{FSj} + F_{SR}\,(\sin\beta_2 - \sin\beta_1) \\ &+ F_{SL}\,(\sin\zeta_2 - \sin\zeta_1) \end{aligned} \tag{2.37}$$

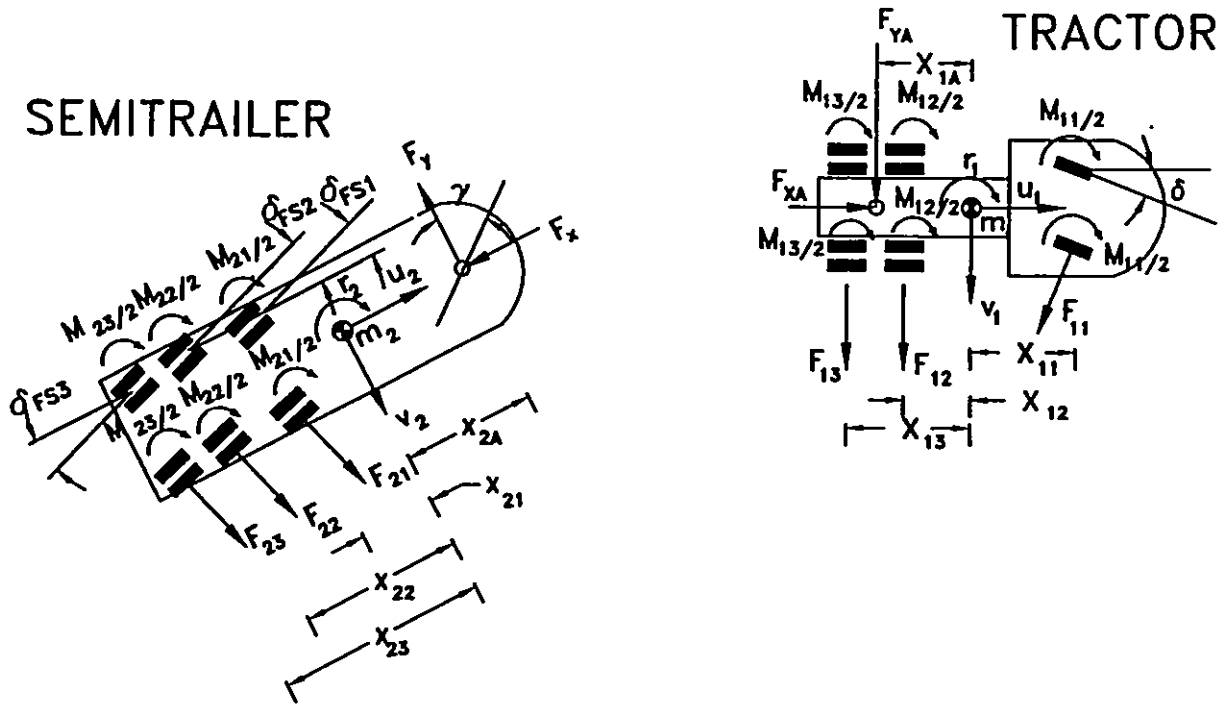

Figure 2.10: Yaw-Plane model of an articulated vehicle with force-steered semitrailer axles

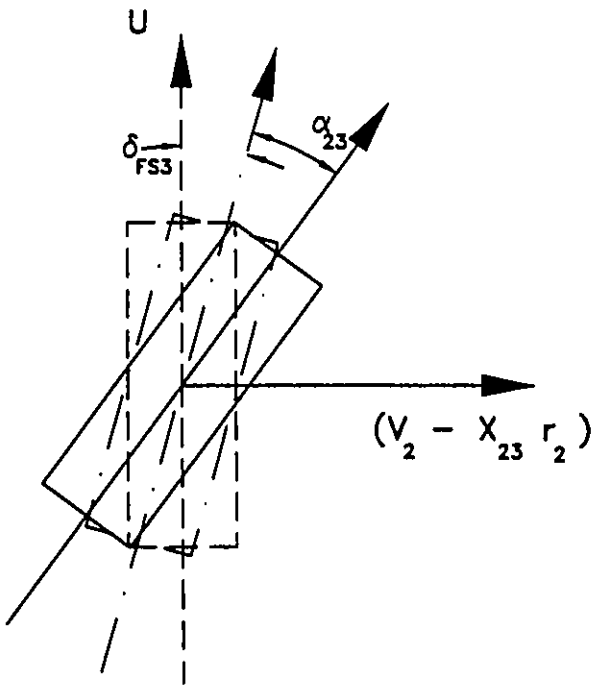

Figure 2.11: Force-steer and slip angles of tire on axle 23

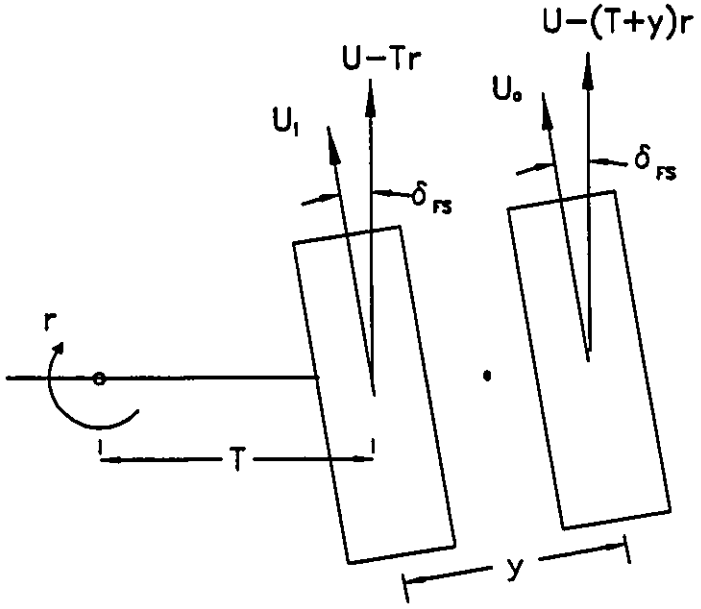

Figure 2.12: The forward velocities of the steered dual tire set

$$I_1 \dot{r}_1 = \left[m_2 (\dot{v}_2 + u_2 r_2) - \sum_{j=1}^{3} F_{2j} \cos \delta_{FSj} \right] \frac{X_{1A}}{\cos \gamma} + F_{11} \cos \gamma X_{11}$$
$$- F_{12} X_{12} - F_{13} X_{13} + \sum_{j=1}^{3} M_{1j} + F_{SR} (a \cos \beta_1 + b \sin \beta_1 - X_{1A} \sin \beta_2)$$
$$- F_{SL} (a \cos \zeta_1 + b \sin \zeta_1 - X_{1A} \sin \zeta_2) \quad (2.38)$$

$$I_2 \dot{r}_2 = \left[m_2 (\dot{v}_2 + u_2 r_2) - \sum_{j=1}^{3} F_{2j} \cos \delta_{FSj} \right] X_{2A} - \sum_{j=1}^{3} X_{2j} F_{2j} \cos \delta_{FSj}$$
$$+ \sum_{j=1}^{3} M_{1j} + F_{SL} (c \cos \zeta_2 - d \sin \zeta_2 + X_{2A} \sin \zeta_2)$$
$$- F_{SR} (d \sin \beta_2 - c \cos \beta_2 - X_{2A} \sin \beta_2) \quad (2.39)$$

and

$$\dot{\gamma} = r_1 - r_2 \quad (2.40)$$

The equations of motion can be expressed in the following matrix form:

$$[A_1]\{\dot{q}\} = [B_1 + BD]\{q\} + \{CD + \{C_1\}\delta\} \quad (2.41)$$

where $[A_1]$, $[B_1]$ and [BD] are (4x4) matrices of mass/inertia properties of the vehicle, vehicle and tire parameters, and damping forces respectively. $\{CD\}$, and $\{C_1\}$ are (4x1) vectors.

2.5 Summary

Nonlinear yaw-plane models of an articulated vehicle incorporating geometric nonlinearities due to damped articulation mechanism, and forced-steering axles of the semitrailer are developed. The nonlinear cornering properties of tires are modeled using piecewise linear and nonlinear continuous describing function. The validity of the describing function is verified by comparing the estimated cornering forces with the measured data for

different normal loads in the side-slip angle range of 0-12 degrees. The comparison revealed that the nonlinear cornering characteristics of the tires can be reasonably estimated using both models.

Chapter 3

Dynamic Response of the Vehicle with Articulation Dampers

3.1 General

The equations of motion describing the yaw and lateral dynamics of the vehicle are solved using numerical integration techniques. The articulated vehicle model incorporating nonlinear cornering characteristics of tires and articulation dampers are solved to investigate the influence of damping on the yaw and lateral dynamic response of the vehicle. The nonlinear cornering characteristics of tires, represented by a continuous describing function of side-slip angles and normal loads, are employed in order to eliminate the influence of discontinuities encountered while using the piecewise linear tire model. The results of the analytical model are first compared to those established from the linear yaw-plane simulation program developed by UMTRI [44]. For comparison purposes, the simulation results of the model, developed in chapter 2, are obtained by setting $C_{SL} = C_{SR} = 0$, and using linear cornering characteristics of the tires. The comparison revealed identical results for both the models. The directional response characteristics of the nonlinear vehicle model are derived for various low-speed and high-speed directional maneuvers using open-loop steering input and closed-loop path input, respectively. The results are

discussed to highlight the influence of articulation damping on the steady-state and transient directional response of the vehicle. The response characteristics are compared to those of the vehicle with conventional articulation ($C_{SL} = C_{SR} = 0$) to derive performance benefits or limitations of the articulation dampers.

3.2 Simulation Vehicle Parameters

The simulation vehicle is a 2.59 m wide tractor-semitrailer comprising of a three-axle tractor, and a 14.63m long three-axle semitrailer with independent air-spring suspension and a conventional fifth wheel. The front axle of the tractor is fitted with a leaf-spring suspension and the tandem axle with a walking-beam leaf-spring suspension. The vehicle dimensions and parameters are given in Table 3.1. The tire model employed in the simulation represents the cornering characteristics of a Michelin XZA 11:00R22.50 Radial dry tire with 1/3 tread. The cornering forces are obtained from the non-linear describing function and the corresponding aligning moment of tires are obtained from the cornering force and the pneumatic trail relation, described in equation (2.28).

3.2.1 Method of Solutions

The directional dynamic model of the articulated vehicle is capable of analyzing the directional response for both open- and closed-loop directional maneuvers. In an open-loop maneuver, the time history of the steer input is provided while the tangent trajectory to be followed by the vehicle is considered in a closed-loop maneuver. In a closed-loop maneuver, the front wheel steer angles required to execute the required maneuvers are computed using a driver model [42].

The equation describing the acceleration vector in terms of various vehicle

Table 3.1: Tractor and semitrailer's dimensions [46]

SIMULATION VEHICLE PARAMETERS

TRACTOR			
Weight of the Sprung mass (kg)		7439	
Sprung mass yaw moment of inertia (kg m/s^2)		1958.6	
Wheelbase (m)		4.826	
	axle 11	axle 12	axle 13
Axle load (kN)	48.898	75.569	75.569
Circumferential Stiffness of tire (kN/unit slip)	13.84	13.84	13.84
Horizontal distance from figure sprung mass c.g. (m)	1.400	-2.670	-4.215
Dual tire spacing (m)	0.000	0.330	0.330
Maximum wheel spread (m)	2.591	2.591	2.591

SEMITRAILER			
Weight of the Sprung mass (kg)		36559	
Sprung mass yaw moment of inertia (kg m/s^2)		80658.382	
Wheelbase (m)		11.735	
	axle 21	axle 22	axle 23
Axle load (kN)	80.015	75.569	75.569
Circumferential Stiffness of tire (kN/unit slip)	13.84	13.84	13.84
Horizontal distance from sprung mass c.g. (m)	-2.959	-4.179	-5.399
Dual tire spacing (m)	0.330	0.330	0.330
Maximum wheel spread (m)	2.591	2.591	2.591

parameters is expressed as

$$\{\dot{q}\} = [A_1]^{-1} \ [B_1 + BD] \ \{q\} + [A_1]^{-1} \ \{\{CD\} + \{C_1\} \ \delta\} \qquad (3.1)$$

Where A_1 is the inertia matrix, C_1 is the force vector, B_1 is the transformation matrix of vehicle dimensions and velocities, BD and CD are the matrices of articulation dampers parameters, and {q} is the velocity vector. A numerical integration algorithm based on trapezoidal method is employed to solve the equations of motion. The tire forces and aligning moments arising due to the side slip angle are computed depending upon the steer input and the sprung mass velocities at each integration step. The directional response simulations are terminated when the simulation time reaches the maximum simulation time specified by the user.

3.2.2 Directional Maneuvers

The yaw and lateral directional response of the vehicle is computed for open-loop constant steer maneuvers at low-speeds and a closed-loop path follower model is used for high-speed lane change and obstacle avoidance maneuvers.

Open-loop Constant Steer Maneuver

A steady or constant steer is defined as a modified step steer where the steer angle initially increases as a ramp function until it reaches a specified value, the steer angle is then held constant during the simulation. Figure 3.1 illustrates the front-wheel angle corresponding to a constant steer input.

Closed-loop Lane Change and Evasive Maneuver

The articulated vehicle combinations experience high rearward amplification and lateral acceleration response during lane change and evasive maneuvers. The directional

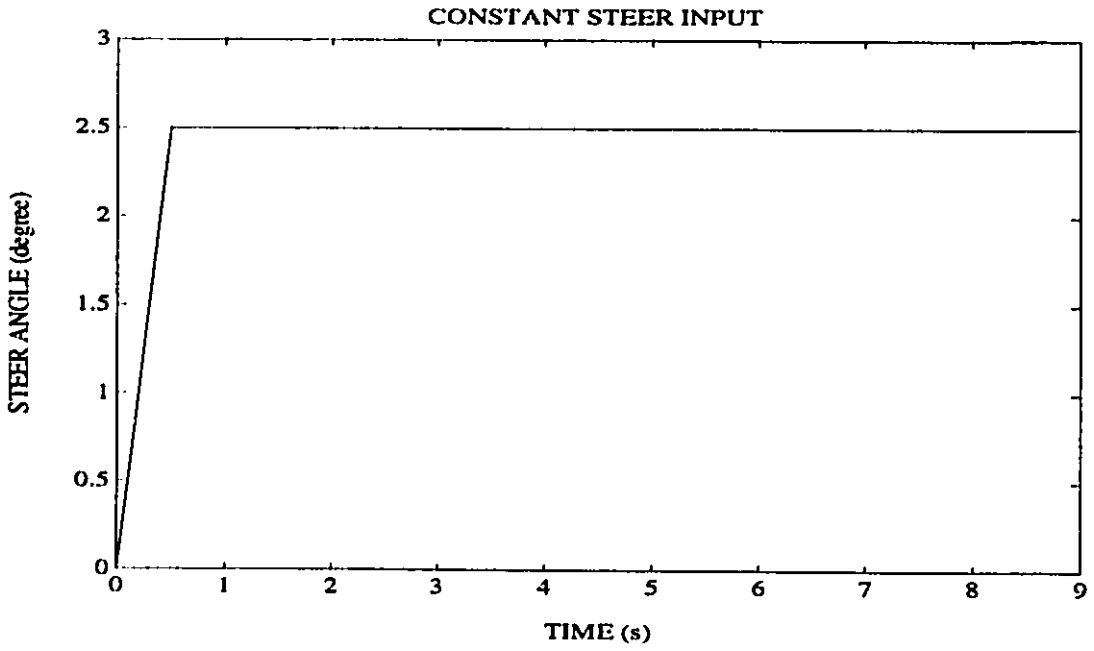

Figure 3.1: Constant Steer Input

dynamics are thus investigated using a closed-loop path-follower model developed to compute the front wheel angle required to follow the prescribed path for lane-change and evasive maneuver as shown in Figure 3.2. For a given path, the front wheel steer angle (δ) is computed in the following manner:

$$\delta = \theta_2 - \theta_1 \tag{3.2}$$

where, θ_2 is the slope of the line joining the center of the front axle and the coordinates of the specified path and θ_1 is the slope of the line joining center of front axle and the future position of the center of the front axle after a small preview time interval, of τ seconds. Figure 3.3 illustrates the front wheel steer angles computed for lane change and evasive maneuvers at a forward speed of 100 km/h.

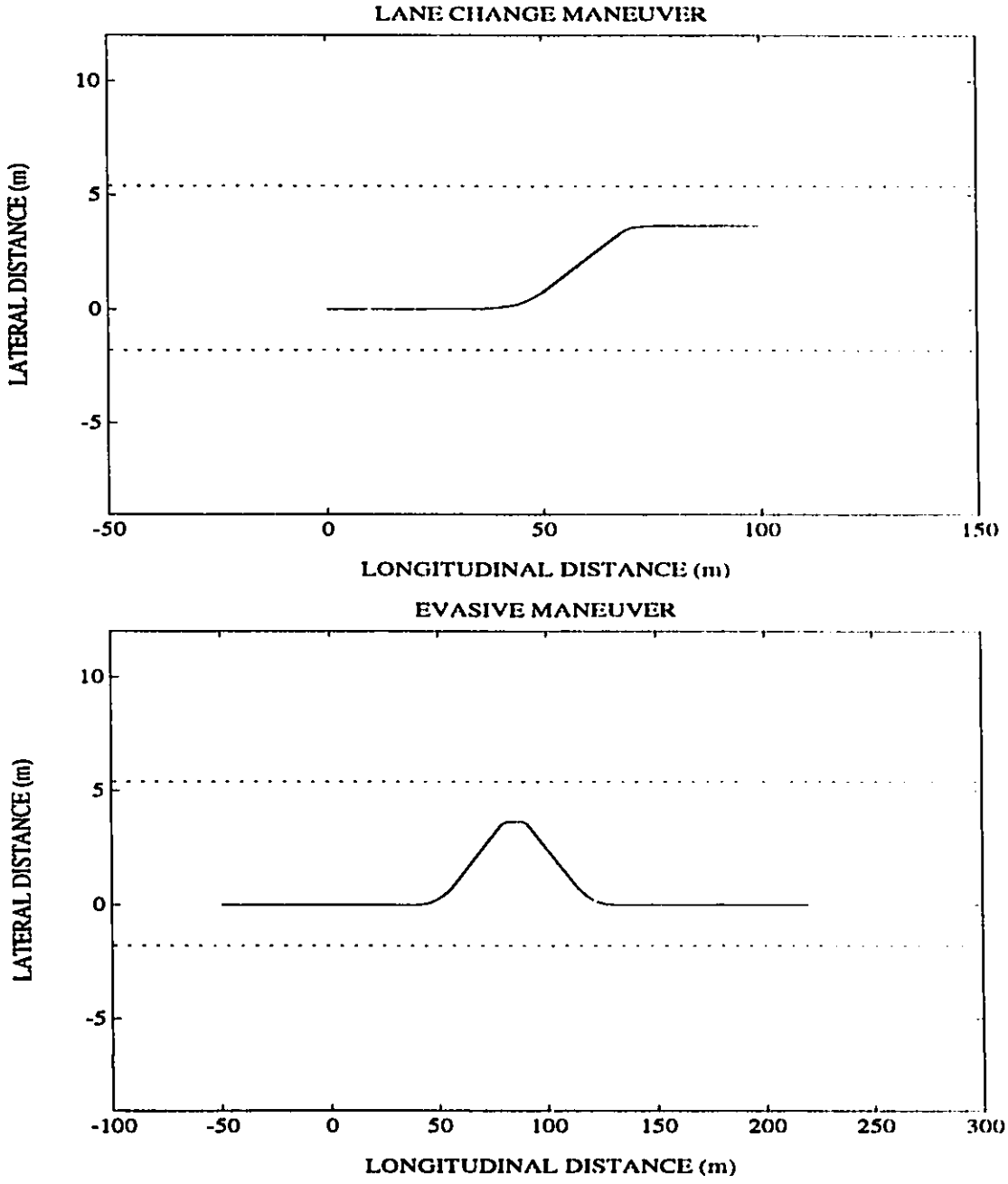

Figure 3.2: Lane-change and Evasive Maneuvers

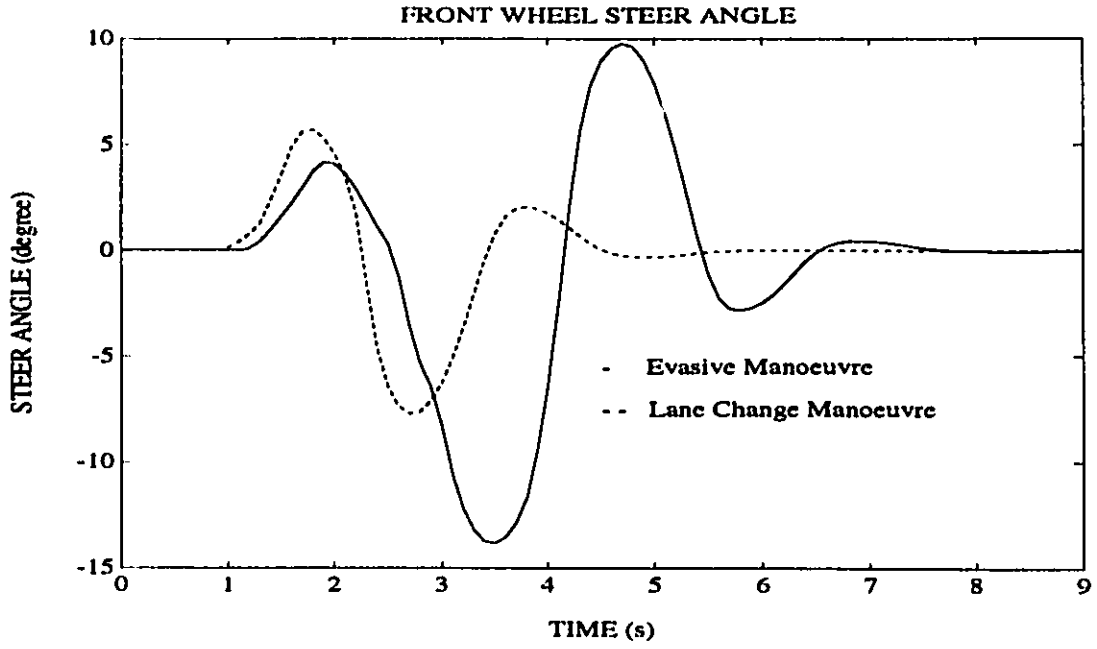

Figure 3.3: Front Wheel Steer Angle for Lane-change and Evasive Maneuvers at 100 km/h

3.2.3 Damping Parameters

The yaw and lateral directional dynamics of the vehicle with articulation dampers are computed for the following combinations of damping coefficients, C_{SL} and C_{SR}:

- **Combination I:** The damping coefficient of left damper C_{SL} is varied from 0 to 1200 Ns/m, while the damping coefficient of right damper C_{SR} is assumed to be 0, to investigate the influence of left damper alone.
- **Combination II:** The damping coefficient of right damper C_{SR} is varied from 0 to 1200 Ns/m, while the damping coefficient of right damper C_{SL} is assumed to be 0, to investigate the influence of right damper alone.
- **Combination III:** The damping coefficient of both left- and right-dampers, C_{SL} and C_{SR} are varied from 0 to 1200 Ns/m to investigate the influence of both

dampers.

The simulation results revealed that the values of damping coefficients greater than 1200 Ns/m yield longer settling time for the directional response of the vehicle. The maximum values of damping coefficients are thus limited to 1200 Ns/m.

3.2.4 Location of Axle 21

The directional dynamics of an articulated vehicle with multiple-axle semitrailer is strongly related to the location of the semitrailer lead axle (axle 21). Computer simulations are performed for different values of X_{21} to determine the optimal axle location. Figure 3.4 illustrates the lateral acceleration and yaw velocity response of the tractor and semitrailers, for different location of axle 21, when subject to 2 degree constant steer input. An examination of the directional response characteristics reveals that the axle 21 located 1.22m ahead of axle 22 ($X_{21} = 2.96\ m$) yields lower values of the response. The further studies are thus carried out using this optimal location of axle 21.

3.3 Response to Constant Steer Maneuvers

The steady-state handling and directional dynamics of the articulated vehicle are investigated for the three combinations of articulation damping. The response characteristics are expressed in terms of lateral and yaw velocities of the semitrailer, turn radius, off-tracking and side-slip angles of the semitrailer axle tires. The steady-state values of the response parameters for three combinations of articulation damping are presented in Tables 3.2 to 3.4, respectively. The semitrailer acceleration, a_2 is computed from:

$$a_2 = \dot{v}_1 + U\, r_1 - X_{1A}\, \dot{r}_1 - X_{2A}\, \dot{r}_2 \tag{3.3}$$

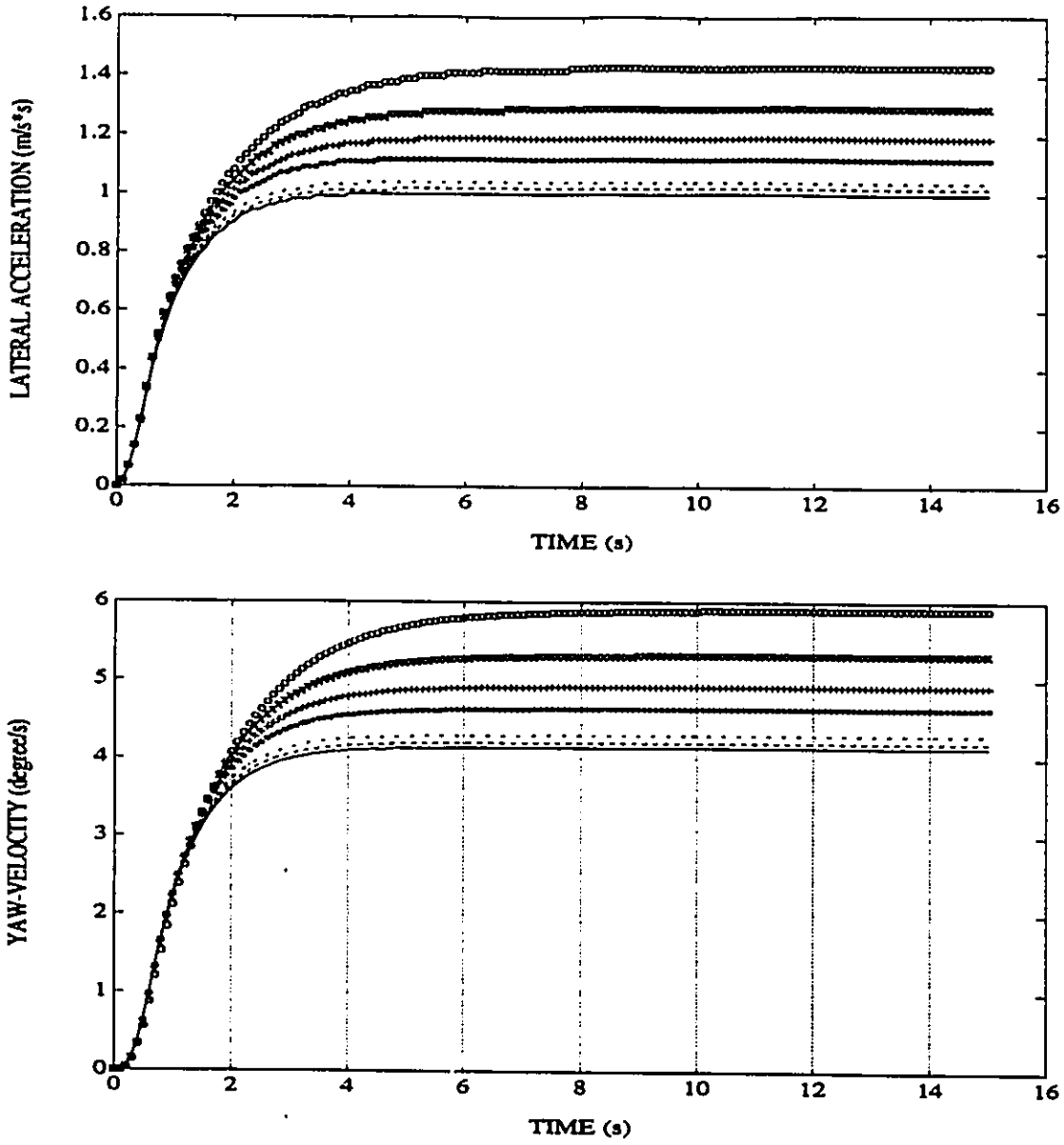

Figure 3.4: Lateral Acceleration and Yaw-Velocity response, for different locations for Axle 21 at 50 km/h
(ooo X_{21} = -3.57 m; xxx X_{21} = -2.47 m; +++ X_{21} = -1.56 m; *** X_{21} = -0.66 m; ... X_{21} = 0.25 m; -.- X_{21} = 1.15 m; - - X_{21} = 2.06 m; — X_{21} = 2.96 m)

Table 3.2: Steady-State Response of the Vehicle with Left-Articulation Damping, Constant Steer Maneuver at 50 km/h

COMBINATION I							
C_{SL} ($\frac{Ns}{m}$) =	0	200	400	600	800	1000	1200
C_{SR} ($\frac{Ns}{m}$) =	0	0	0	0	0	0	0
a_2 (m/s^2)	1.38	1.42	1.47	1.54	1.62	1.73	1.93
v_2 (m/s)	0.29	0.30	0.31	0.32	0.34	0.36	0.40
r_2 $(degrees/s)$	5.69	5.87	6.08	6.34	6.68	7.15	7.97
γ $(degrees)$	4.61	4.78	4.98	5.22	5.53	5.98	6.77
OT-23L-11R (m)	0.81	0.84	0.87	0.91	0.97	1.04	1.20
TURN RADIUS (m)	139.91	135.60	130.84	125.45	119.14	111.27	99.84
α_{11} $(degrees)$	-0.99	-0.97	-0.94	-0.91	-0.86	-0.81	-0.74
α_{12} $(degrees)$	-0.16	-0.19	-0.22	-0.26	-0.32	-0.40	-0.57
α_{13} $(degrees)$	-0.79	-0.84	-0.90	-0.97	-1.06	-1.20	-1.46
α_{21} $(degrees)$	-0.01	-0.01	-0.02	-0.02	-0.02	-0.03	-0.05
α_{22} $(degrees)$	-0.51	-0.53	-0.55	-0.58	-0.61	-0.66	-0.75
α_{23} $(degrees)$	-1.01	-1.04	-1.08	-1.13	-1.20	-1.29	-1.45

Table 3.3: Steady-State Response of the Vehicle with Right-Articulation Damping, Constant Steer Maneuver at 50 km/h

COMBINATION II							
C_{SL} ($\frac{Ns}{m}$) = C_{SR} ($\frac{Ns}{m}$) =	0 000.00	0 200.00	0 400.00	0 600.00	0 800.00	0 1000.0	0 1200.0
a_2 (m/s^2)	1.38	1.37	1.36	1.34	1.33	1.32	1.31
v_2 (m/s)	0.29	0.29	0.29	0.28	0.28	0.28	0.28
r_2 $(degrees/s)$	5.69	5.64	5.59	5.54	5.50	5.45	5.41
γ $(degrees)$	4.61	4.57	4.54	4.50	4.47	4.44	4.40
OT-23L-11R (m)	0.81	0.80	0.80	0.79	0.79	0.78	0.78
TURN RADIUS (m)	139.91	141.14	142.35	143.56	144.75	145.93	147.11
α_{11} $(degrees)$	-0.99	-1.01	-1.03	-1.05	-1.06	-1.08	-1.09
α_{12} $(degrees)$	-0.16	-0.16	-0.17	-0.17	-0.17	-0.17	-0.18
α_{13} $(degrees)$	-0.79	-0.79	-0.79	-0.79	-0.78	-0.78	-0.78
α_{21} $(degrees)$	-0.01	-0.01	-0.01	-0.01	-0.01	-0.01	-0.01
α_{22} $(degrees)$	-0.51	-0.51	-0.50	-0.50	-0.50	-0.49	-0.49
α_{23} $(degrees)$	-1.01	-1.00	-0.99	-0.99	-0.98	-0.97	-0.96

Table 3.4: Steady-State Response of the Vehicle with Left- and Right-Articulation Damping, Constant Steer Maneuver at 50 km/h

COMBINATION III							
C_{SL} ($\frac{Ns}{m}$) =	000.00	200.00	400.00	600.00	800.00	1000.0	1200.0
C_{SR} ($\frac{Ns}{m}$) =	000.00	200.00	400.00	600.00	800.00	1000.0	1200.0
Peak Parametric Values at 50 km/h							
a_2 (m/s^2)	1.38	1.41	1.44	1.53	1.53	1.58	1.65
v_2 (m/s)	0.29	0.30	0.30	0.31	0.32	0.33	0.34
r_2 $(degrees/s)$	5.69	5.81	5.95	6.11	6.30	6.53	6.81
γ $(degrees)$	4.61	4.74	4.88	5.04	5.24	5.48	5.69
OT-23L-11R (m)	0.81	0.83	0.86	0.88	0.92	0.96	1.02
TURN RADIUS (m)	139.91	136.92	133.69	130.15	126.25	121.87	116.89
α_{11} $(degrees)$	-0.99	-0.99	-0.98	-0.98	-0.98	-0.98	-0.99
α_{12} $(degrees)$	-0.16	-0.19	-0.23	-0.27	-0.32	-0.39	-0.48
α_{13} $(degrees)$	-0.79	-0.84	-0.89	-0.95	-1.02	-1.12	-1.24
α_{21} $(degrees)$	-0.01	-0.01	-0.02	-0.02	-0.03	-0.03	-0.04
α_{22} $(degrees)$	-0.51	-0.52	-0.54	-0.56	-0.58	-0.60	-0.64
α_{23} $(degrees)$	-1.01	-1.03	-1.06	-1.09	-1.13	-1.18	-1.23

The steady-state off-tracking of the vehicle is computed from the path prescribed by the front right wheel of the tractor and the rearmost left-wheel of the semitrailer and is represented by OT-23L-11R. The coordinates of the vehicle path are also computed to determine the steady-state turn radius of the vehicle.

For a left-handed constant-steer input, the steady-state values of lateral acceleration, yaw velocity, lateral velocity, articulation angle, side-slip angles and off-tracking tend to increase with an increase in the left-articulation damping, as illustrated in Table 3.2. The lateral force and yaw moment caused by the left-articulation damper, however, yield smaller turn radius of the vehicle. The left-articulation damper thus enables the vehicle to negotiate tighter left-handed turns. The turn radius decreases from 139.9 m for the conventional vehicle to approximately 100 m when C_{SL} = 1200 Ns/m. The influence of right-articulation damper on the steady-state directional response, however, is the opposite, as illustrated in Table 3.3. The lateral acceleration, yaw and lateral ve-

locities, articulation angle, off-tracking and side-slip angles of the semitrailer decrease when right-articulation damping is introduced. The change in these response parameters, however, is not as significant as observed in Table 3.2. The turn radius also increases slightly to approximately 147 m.

The steady-state values of the directional response parameters of the semitrailer also tend to increase when both articulation dampers are employed, as illustrated in Table 3.4. The increase in the steady values, however, is considerably less than that observed for combination I. The turn radius of the vehicle decreases considerably from 139.9 m for the conventional vehicle to approximately 117 m for the vehicle with both articulation dampers. The side-slip angles of the tires of the semitrailer axles, and the vehicle off-tracking increases only slightly. Figure 3.5 illustrates the turn radii of the tractor and semitrailer for different values of the damping coefficients. The figure clearly illustrates that the turning ability of the vehicle improves with increase in articulation damping. The tighter turn radius is primarily achieved by the increased articulation angle, and lateral and yaw velocities of the vehicle. Figure 3.6 illustrates the articulation angle and semitrailer yaw velocity response for different values of damping coefficients. Figure 3.7 shows the lateral acceleration response of the semitrailer. The response characteristics increase linearly with time as the steer angle is increased. The articulation damping does not influence the directional response during the intial period, which may be attributed to low damping forces generated by low relative velocities across the dampers.

The side-slip angles of the tires on the lead and rearmost axles of the tractor and semitrailer are presented in Figures 3.8 and 3.9, respectively, for different values of damping coefficients. The influence of articulation damping on the side-slip angle of the tires on the tractor's front axle (axle 11) is insignificant. The magnitudes of side-slip angles of tires on axles 13, 21 and 23, however, increase with increase in articulation damping. While the tires on all the axles exhibit negative side-slip angles, the tires on axle 21, exhibit positive side-slip angle corresponding to the interval $0 \leq t \leq 0.5s$,

where the steer angle increases. The magnitude of the side-slip angle of tires on this axle is extremely small due to its location near the sprung mass c.g.

The steady-state handling characteristics of the vehicle with articulation dampers are computed and compared to those of the conventional vehicle. The steady-state handling characteristics of the tractor and semitrailer are derived from their respective handling equations.

Tractor:

$$\delta = \frac{L_1}{R_1} + K_{us} \frac{U^2}{g_c R_1}$$

Semitrailer:

$$\gamma = \frac{L_2}{R_2} + K_{ust} \frac{U^2}{g_c R_2} \tag{3.4}$$

where, L_1 and L_2 are the wheel bases of tractor and semitrailer, respectively. R_1 and R_2 are the radii traced by tractor and semitrailer, respectively. K_{us} and K_{ust} are the coefficients of understeer of tractor and semitrailer, respectively. U and g_c are forward speed and acceleration due to gravity of the vehicle.

Assuming steady-state condition, the equations (3.4) are expressed as

$$K_{us}\, a_1 = -\left(\frac{L_1\, r_1}{U} - \delta\right)$$

$$K_{ust}\, a_2 = -\left(\frac{L_2\, r_2}{U} - \gamma\right) \tag{3.5}$$

where a_1 and a_2 are steady-state lateral acceleration of the tractor and semitrailer, respectively in g units. The handling characteristics of the vehicle are directly related to K_{us} and K_{ust}. Further, an understeer vehicle ($K_{us} > 0$; $K_{ust} > 0$) is known to be unconditionally stable. An oversteer tractor ($K_{us} < 0$) may lead to a directional instability, while the oversteer semitrailer may yield poor turning abilities. The handling

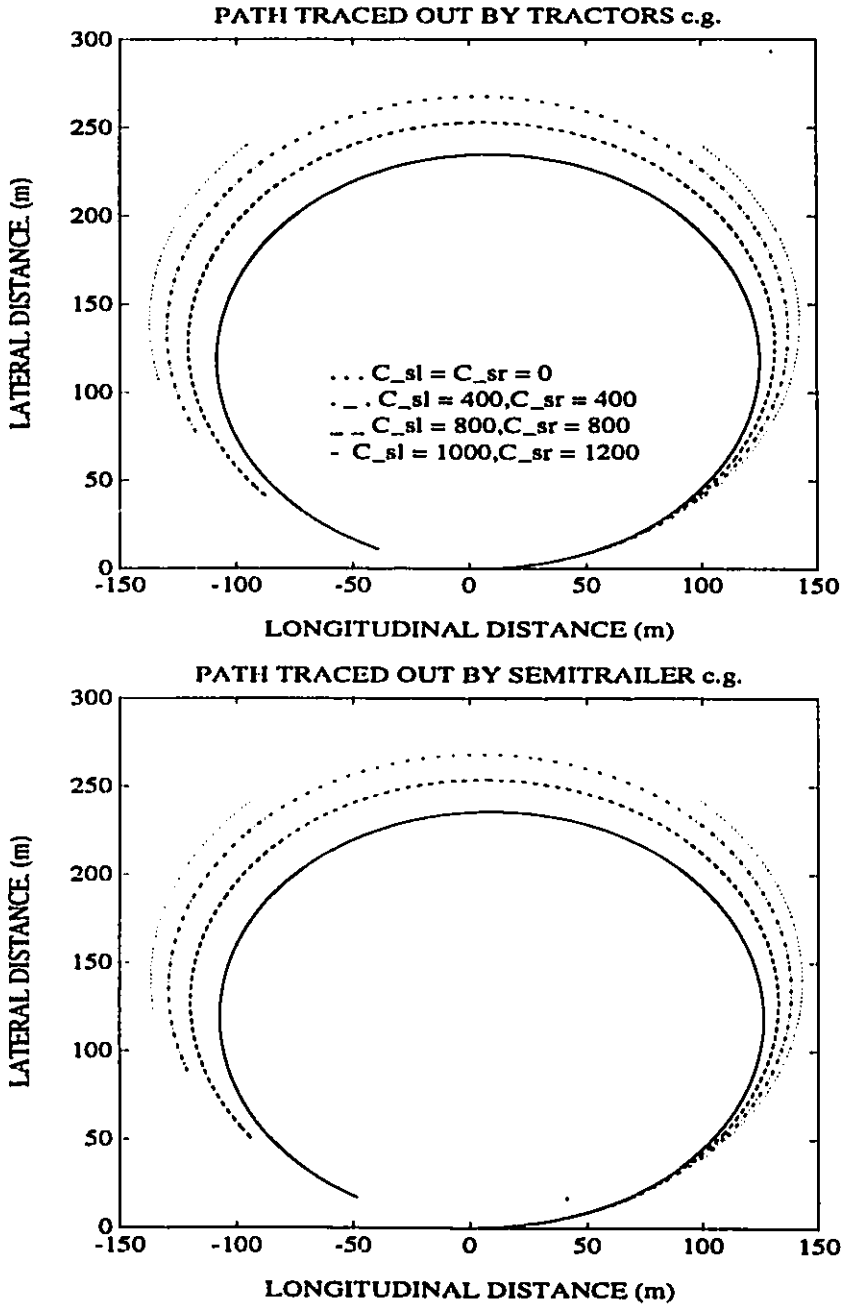

Figure 3.5: Path traced by the Tractor and Semitrailer under a Constant Steer input at 50 km/h

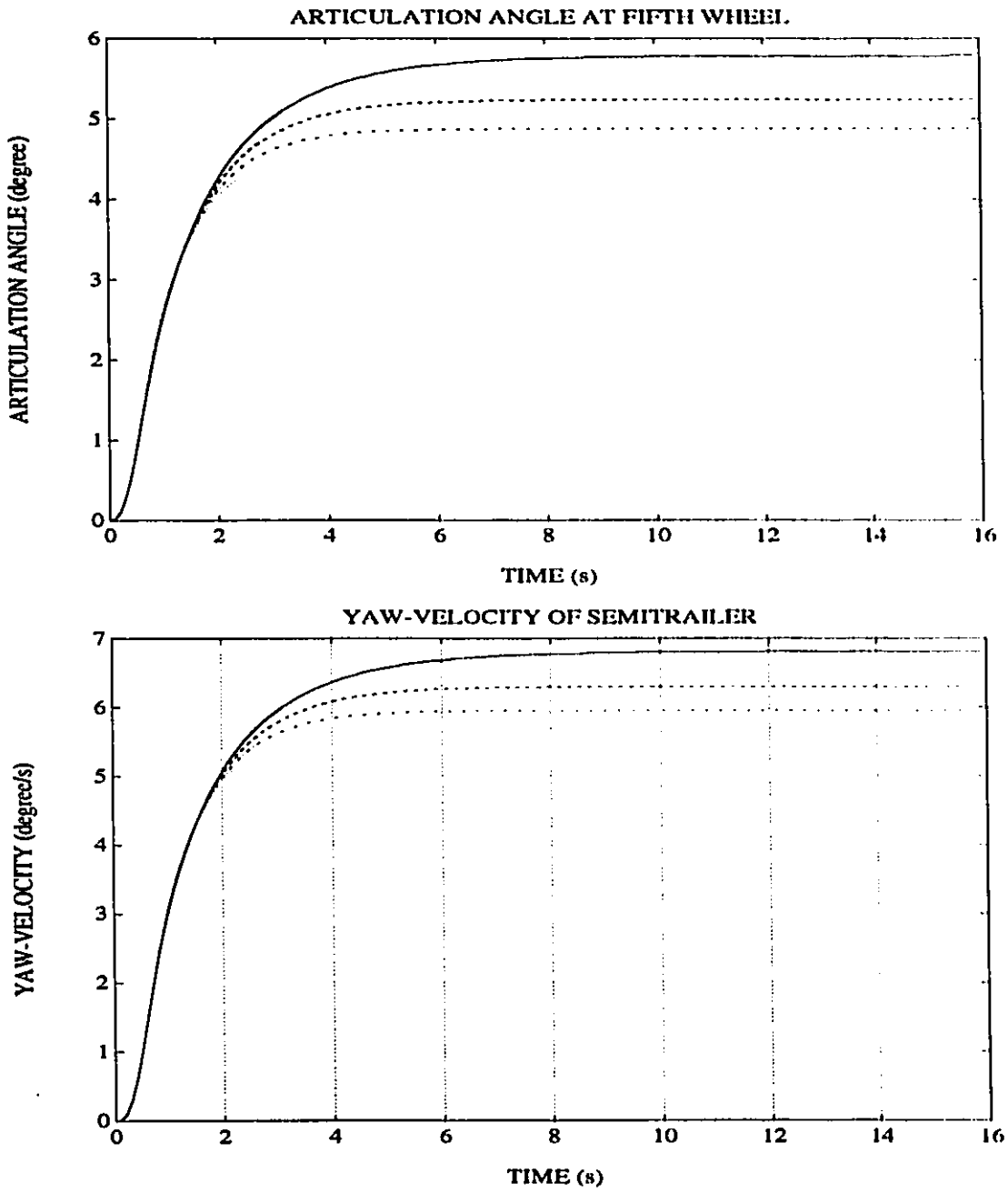

Figure 3.6: Articulation angle and Yaw Velocity response of the semitrailer under a Constant Steer Maneuver at 50 km/h

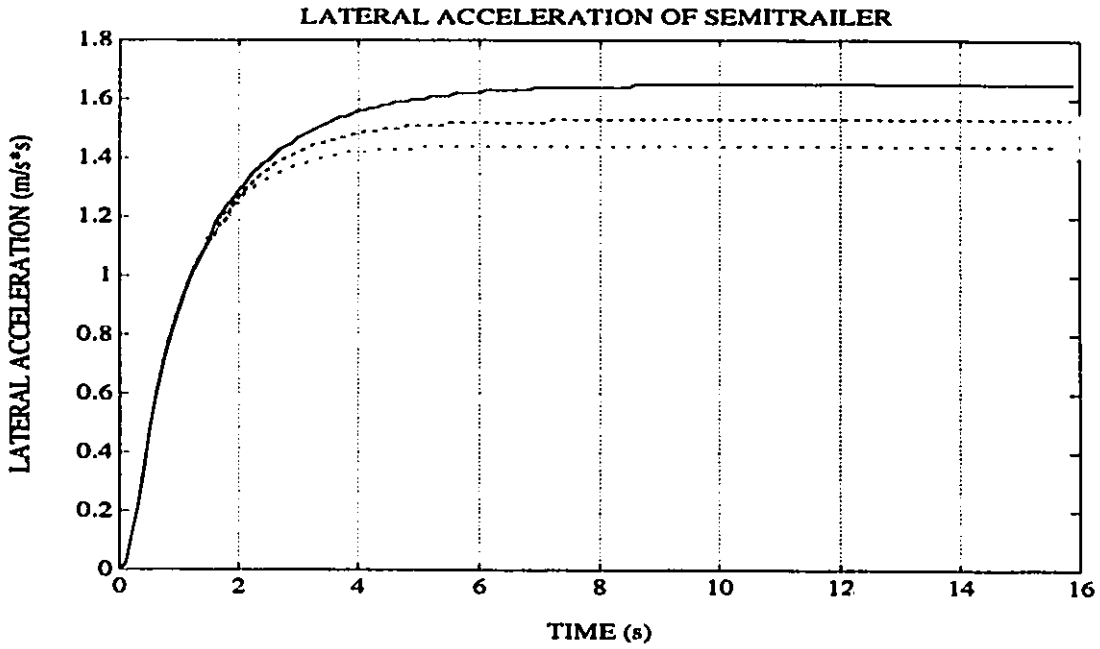

Figure 3.7: Lateral Acceleration Response of the Semitrailer under a Constant Steer Maneuver at 50 km/h

diagrams of the tractor and semitrailer, a plot of lateral acceleration against the handling parameters $\left(\frac{L_1 r_1}{U} - \delta \text{ or } \frac{L_2 r_2}{U} - \gamma\right)$, are obtained from the steady-state response of the vehicle for different values of damping coefficients of 0, 400, 800, and 1200 Ns/m, as shown in Figure 3.10.

3.4 Vehicle Response to a Lane Change Maneuver

The transient directional response characteristics of the vehicle with articulation dampers are computed for lane change maneuvers performed at 80 km/h and 100 km/h, using the path follower model described in section 3.3.1. The response characteristics are compared to those of the conventional vehicle to highlight the influence of articulation dampers on the directional control properties of the vehicle. The directional control properties of an articulated vehicle, subject to highway speed directional maneuvers, are directly related

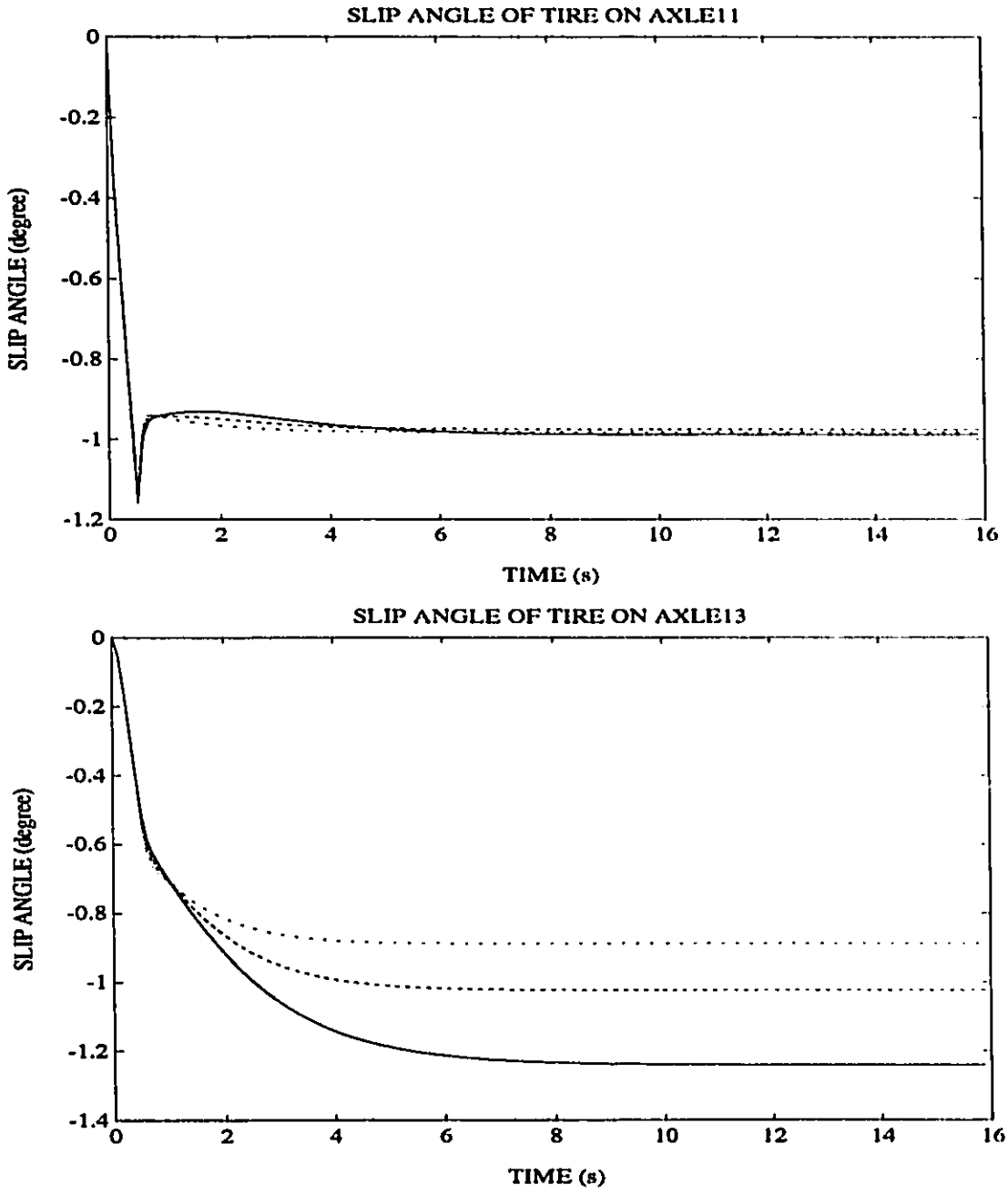

Figure 3.8: Side-Slip Angle response of axle 11 and 13 under a Constant Steer Maneuver at 50 km/h

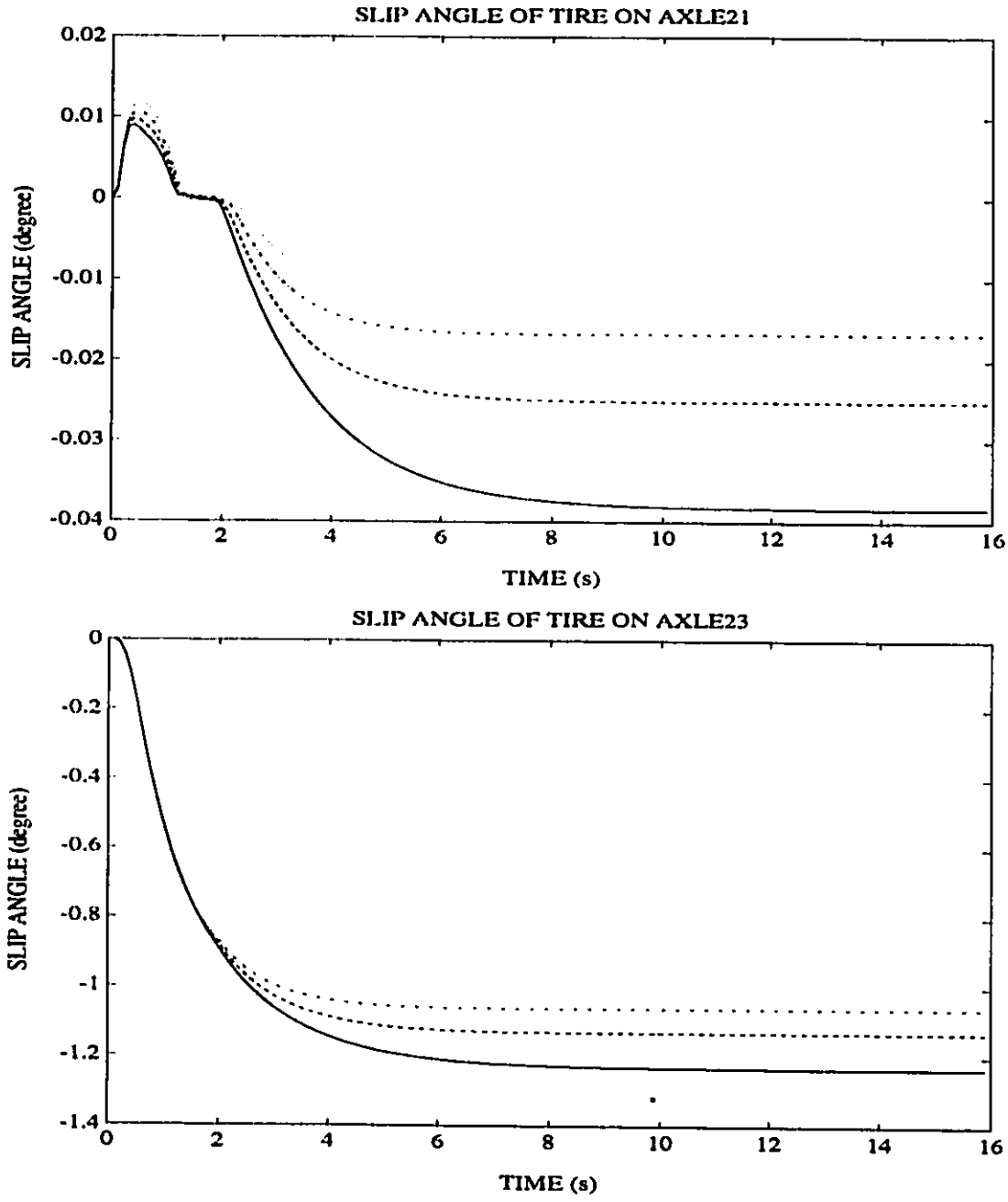

Figure 3.9: Side-Slip Angle response of axle 21 and 23 under a Constant Steer Maneuver at 50 km/h

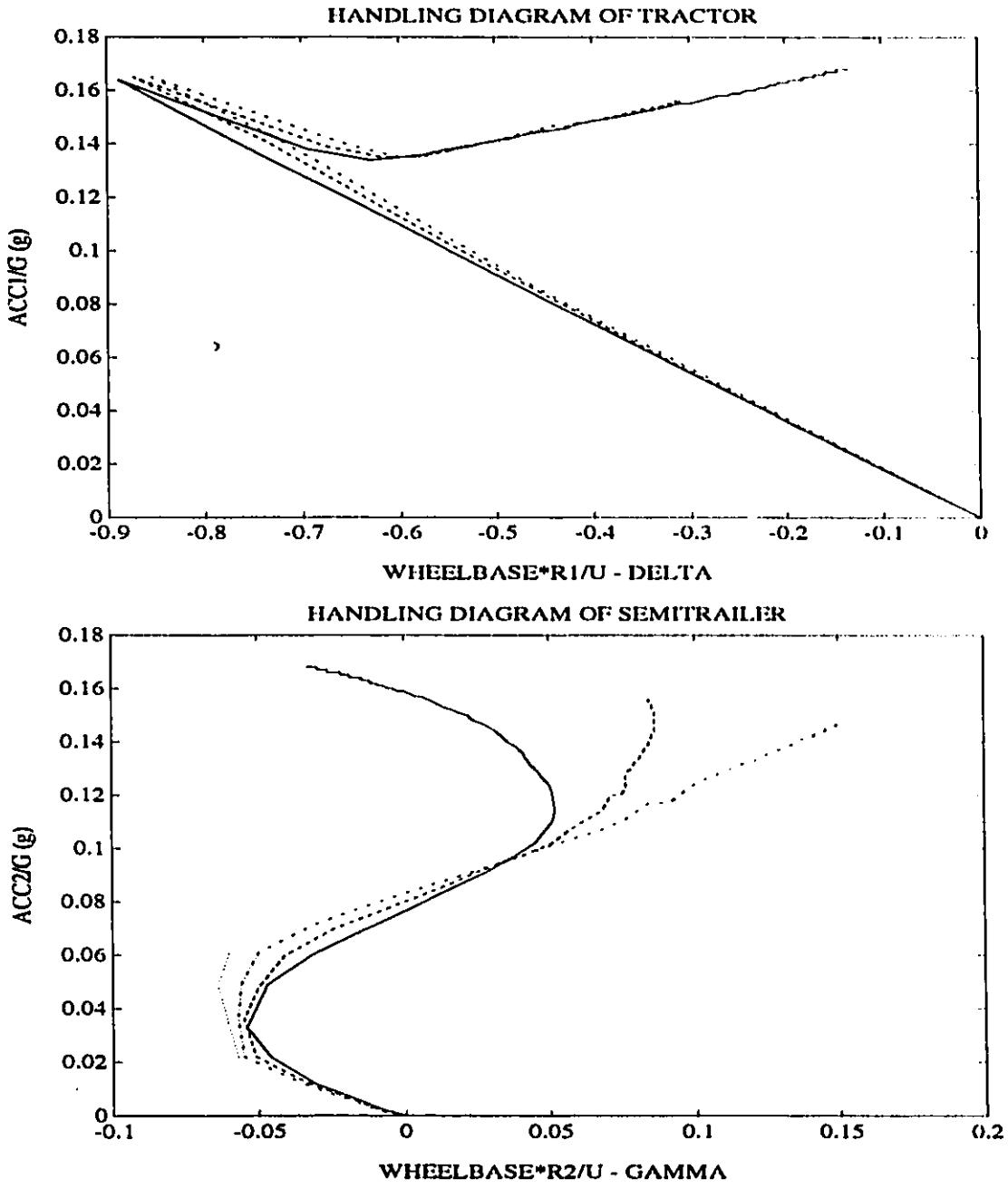

Figure 3.10: Handling Diagrams of Tractor and Semitrailer under a Constant Steer Maneuver at 50 km/h

to its lateral acceleration, yaw velocity and lateral velocity response. The directional response of the articulated vehicle is often expressed by its rearward amplification. The rearward amplification of lateral acceleration, α_a, is computed as the ratio of peak lateral acceleration encountered by the semitrailer to that encountered by the tractor:

$$\alpha_a = \frac{a_2\ )_{peak}}{a_1\ )_{peak}} \tag{3.6}$$

The rearward amplification thus characterizes the amplification or attenuation of the directional response of the articulated units. The rearward amplification of the yaw response α_ω, is expressed in a similar manner

$$\alpha_\omega = \frac{r_2\ )_{peak}}{r_1\ )_{peak}} \tag{3.7}$$

The directional response characteristics and the rearward amplification factors of the vehicle are computed for three combinations of articulation damping described in section 3.2.2. The peak values of the response parameters for lane change maneuver at 100 km/h are summarized in Tables 3.5 to 3.8, respectively. The addition of damping at the articulation joint tends to suppress the oscillatory directional response of the vehicle. The peak values of lateral acceleration, lateral and yaw velocities, and articulation angle response of sprung weights of both the tractor and semitrailer decrease considerably, when only left-articulation damping is increased ($C_{SR} = 0$), as demonstrated in Table 3.5. The average side-slip angles of tires on all the axles also decrease with an increase in the damping coefficient, C_{SL}. The rearward amplification factors α_a and α_ω, also decrease with increase in the left-articulation damping coefficient. The lateral acceleration rearward amplification factor of the vehicle with left-articulation damper ($C_{SL} = 1200Ns/m$) is obtained as 0.844, which is lower than that of the convectional vehicle ($\alpha_a = 0.889$). The yaw velocity rearward amplification of the vehicle with the left-damper ($C_{SL} = 1200Ns/m$) is approximately 14% lower than that of the conventional vehicle. An examination of the peak response values clearly demonstrates that the

directional control and stability limits of the vehicle can be improved considerably by introducing the articulation damping. Further, the rate of tire wear can be reduced as evident through the lower side-slip angles.

The introduction of right-articulation damping (Combination II), however, tends to vary the directional response of the vehicle only slightly, when subject to left-handed lane-change maneuver at 100 km/h, as shown in Table 3.6. The peak lateral acceleration response of the damped vehicle is slightly larger (< 1%) than that of the conventional vehicle. While the yaw velocity response of the sprung weight of the tractor decreases slightly by 5.5% (for C_{SR} = 1200 Ns/m), the peak yaw velocity of the semitrailer remains almost unchanged. The peak lateral velocity response of the damped vehicle is almost identical to that of the conventional vehicle. The rearward amplification factors, α_a and α_ω, thus vary only slightly (< 1%), when C_{SR} is varied from 0 to 1200 Ns/m. The corresponding side-slip angles of the tires on all the axles also exhibit only slight variation. Although, the right-articulation damper exhibits insignificant influence on the directional response to a left-handed lane-change maneuver, its influence on the response to a right-handed directional maneuver is a more significant, as shown in Table 3.7.

Table 3.8 summarizes the peak values of the parameters when both articulation dampers (Combination III) are employed. A comparison of Tables 3.6 and 3.8 clearly reveals that the peak response of the vehicle with both dampers is quite similar to that of the vehicle with left-articulation damper. The directional response characteristics of the vehicle subject to a lane-change maneuver at 80 km/h are evaluated and the peak values are summarized in Tables 3.9 to 3.11 for three combination of articulation damping, respectively. While the peak values are considerably lower than those obtained at a speed of 100 km/h, the influence of articulation damping is identical to that demonstrated in Tables 3.5 to 3.8. The transient response characteristics of the articulated vehicle are thus presented and discussed only for the lane change maneuver performed at a speed of 100 km/h.

Table 3.5: Transient Response of the Vehicle with Left-Articulation Damping, Lane-Change Maneuver at 100 km/h

COMBINATION I: LANE CHANGE WITH DAMPING MECHANISM								
C_{SL} ($\frac{Ns}{m}$) = C_{SR} ($\frac{Ns}{m}$) =		000.00 0	200.00 0	400.00 0	600.00 0	800.00 0	1000.0 0	1200.0 0
Positive and Negative Peak Parameters Values at 100 km/h								
a_1 (m/s^2)	+VE	5.21	5.18	5.16	5.15	5.123	5.12	5.11
	-VE	-5.85	-5.77	-5.71	-5.66	-5.61	-5.56	-5.52
a_2 (m/s^2)	+VE	4.41	4.38	4.34	4.30	4.27	4.23	4.20
	-VE	-5.20	-5.10	-5.00	-4.91	-4.82	-4.74	-4.66
Rearward Amplification		0.889	0.884	0.876	0.867	0.859	0.853	0.844
r_1 ($degrees/s$)	+VE	13.70	13.63	13.58	13.52	13.48	13.43	13.39
	-VE	-17.16	-16.99	-16.82	-16.67	-16.52	-16.60	-16.23
r_2 ($degrees/s$)	+VE	11.53	11.38	11.25	11.11	10.98	10.87	10.75
	-VE	-14.30	-13.90	-13.53	-13.19	-12.89	-12.60	-12.34
Rearward Amplification		0.883	0.818	0.804	0.791	0.780	0.759	0.760
v_1 (m/s)	+VE	0.76	0.71	0.68	0.67	0.66	0.66	0.65
	-VE	-0.85	-0.84	-0.85	-0.84	-0.84	-0.84	-0.84
v_2 (m/s)	+VE	0.84	0.79	0.74	0.69	0.66	0.62	0.59
	-VE	-0.60	-0.59	-0.58	-0.57	-0.55	-0.54	-0.54
γ ($degrees$)	+VE	4.94	4.90	4.86	4.84	4.79	4.75	4.72
	-VE	-6.24	-6.12	-6.00	-5.90	-5.81	-5.72	-5.63
P-CG1 (m)		4.36	4.36	4.36	4.37	4.38	4.38	4.39
OS-CG1 (m)		0.00	0.00	0.00	0.00	0.00	0.00	0.00
P-CG2 (m)		4.35	4.36	4.36	4.37	4.38	4.38	4.39
OS-CG2 (m)		0.00	0.00	0.00	0.00	0.00	0.00	0.00
α_{11} ($degrees$)	+VE	6.96	6.90	6.85	6.80	6.76	6.72	6.69
	-VE	-5.22	-5.24	-5.26	-5.28	-5.30	-5.32	-5.33
α_{12} ($degrees$)	+VE	2.55	2.49	2.44	2.40	2.36	2.33	2.30
	-VE	-2.10	-2.08	-2.06	-2.05	-2.03	-2.02	-2.01
α_{13} ($degrees$)	+VE	3.27	3.20	3.14	3.09	3.04	3.00	2.96
	-VE	-2.75	-2.72	-2.70	-2.68	-2.65	-2.64	-2.62
α_{21} ($degrees$)	+VE	2.76	2.65	2.54	2.45	2.36	2.89	2.21
	-VE	-1.95	-1.92	-1.89	-1.86	-1.84	-1.81	-1.79
α_{22} ($degrees$)	+VE	3.29	3.17	3.05	2.95	2.85	2.77	2.68
	-VE	-2.40	-2.36	-2.33	-2.30	-2.27	-2.24	-2.22
α_{23} ($degrees$)	+VE	3.85	3.72	3.59	3.47	3.36	3.26	3.17
	-VE	-2.87	-2.83	-2.79	-2.76	-2.72	-2.69	-2.66

Table 3.6: Transient Response of the Vehicle with Right-Articulation Damping, Lane-Change Maneuver at 100 km/h

COMBINATION II: LANE CHANGE WITH DAMPING MECHANISM								
C_{SL} ($\frac{N_s}{m}$) = C_{SR} ($\frac{N_s}{m}$) =		0 000.00	0 200.00	0 400.00	0 600.00	0 800.00	0 1000.0	0 1200.0
Positive and Negative Peak Parameters Values at 100 km/h								
a_1 (m/s^2)	+VE	5.21	5.20	5.18	5.17	5.16	5.15	5.14
	-VE	-5.85	-5.85	-5.86	-5.86	-5.87	-5.88	-5.89
a_2 (m/s^2)	+VE	4.41	4.41	4.41	4.41	4.41	4.41	4.41
	-VE	-5.20	-5.21	-5.22	-5.22	-5.23	-5.23	-5.24
Rearward Amplification		0.889	0.890	0.891	0.891	0.891	0.889	0.889
r_1 ($degrees/s$)	+VE	13.70	13.67	13.64	13.61	13.58	13.55	13.52
	-VE	-17.16	-16.99	-16.83	-16.67	-16.52	-16.36	-16.22
r_2 ($degrees/s$)	+VE	11.53	11.52	11.51	11.50	11.49	11.48	11.47
	-VE	-14.30	-14.27	-14.25	-14.23	-14.22	-14.21	-14.20
Rearward Amplification		0.883	0.840	0.847	0.854	0.861	0.869	0.876
v_1 (m/s)	+VE	0.75	0.77	0.79	0.81	0.84	0.85	0.87
	-VE	-0.84	-0.84	-0.84	-0.84	-0.84	-0.84	-0.84
v_2 (m/s)	+VE	0.84	0.84	0.84	0.84	0.84	0.84	0.84
	-VE	-0.60	-0.60	-0.60	-0.60	-0.60	-0.60	-0.60
γ ($degrees$)	+VE	4.94	4.93	4.93	4.92	4.91	4.91	4.90
	-VE	-6.24	-6.24	-6.24	-6.25	-6.25	-6.26	-6.27
P-CG1 (m)		4.36	4.37	4.38	4.38	4.39	4.39	4.40
OS-CG1 (m)		0.00	0.00	0.00	0.00	0.00	0.00	0.00
P-CG2 (m)		4.35	4.35	4.36	4.37	4.37	4.38	4.38
OS-CG2 (m)		0.00	0.00	0.00	0.00	0.00	0.00	0.00
α_{11} ($degrees$)	+VE	6.95	7.01	7.08	7.14	7.20	7.26	7.32
	-VE	-5.22	-5.25	-5.28	-5.30	-5.33	-5.35	-5.38
α_{12} ($degrees$)	+VE	2.55	2.57	2.59	2.62	2.64	2.67	2.69
	-VE	-2.10	-2.10	-2.09	-2.09	-2.09	-2.09	-2.09
α_{13} ($degrees$)	+VE	3.27	3.29	3.31	3.33	3.36	3.38	3.41
	-VE	-2.75	-2.74	-2.74	-2.74	-2.74	-2.74	-2.74
α_{21} ($degrees$)	+VE	2.76	2.75	2.75	2.75	2.75	2.75	2.75
	-VE	-1.95	-1.94	-1.94	-1.94	-1.94	-1.93	-1.93
α_{22} ($degrees$)	+VE	3.29	3.29	3.29	3.29	3.29	3.29	3.29
	-VE	-2.40	-2.39	-2.39	-2.39	-2.38	-2.38	-2.38
α_{23} ($degrees$)	+VE	3.85	3.85	3.85	3.85	3.85	3.85	3.85
	-VE	-2.87	-2.87	-2.87	-2.86	-2.86	-2.86	-2.85

Table 3.7: Transient Response of the Vehicle with both Left- and Right-Articulation Damping, Lane-Change Maneuver at 100 km/h

COMBINATION III: LANE CHANGE WITH DAMPING MECHANISM								
C_{SL} ($\frac{Ns}{m}$) =		000.00	200.00	400.00	600.00	800.00	1000.0	1200.0
C_{SR} ($\frac{Ns}{m}$) =		000.00	200.00	400.00	600.00	800.00	1000.0	1200.0
Positive and Negative Peak Parameters Values at 100 km/h								
a_1 (m/s^2)	+VE	5.21	5.17	5.14	5.11	5.08	5.06	5.03
	-VE	-5.85	-5.77	-5.71	-5.66	-5.62	-5.58	-5.54
a_2 (m/s^2)	+VE	4.41	4.38	4.34	4.30	4.26	4.23	4.19
	-VE	-5.20	-5.11	-5.02	-4.93	-4.85	-4.77	-4.70
Rearward Amplification		0.889	0.886	0.879	0.871	0.863	0.855	0.848
r_1 ($degrees/s$)	+VE	13.70	13.61	13.52	13.44	13.36	13.28	13.21
	-VE	-17.16	-16.83	-16.51	-16.22	-15.96	-15.73	-15.53
r_2 ($degrees/s$)	+VE	11.53	11.37	11.22	11.08	10.94	10.82	10.69
	-VE	-14.30	-13.87	-13.49	-13.14	-12.83	-12.54	-12.28
Rearward Amplification		0.833	0.824	0.817	0.810	0.804	0.797	0.791
γ	+VE	4.94	4.89	4.84	4.80	4.76	4.72	4.68
v_1 (m/s)	+VE	0.75	0.73	0.71	0.71	0.71	0.70	0.70
	-VE	-0.84	-0.84	-0.84	-0.84	-0.84	-0.84	-0.84
v_2 (m/s)	+VE	0.84	0.79	0.74	0.70	0.66	0.63	0.59
	-VE	-0.60	-0.59	-0.58	-0.56	-0.55	-0.54	-0.53
($degrees$)	-VE	-6.24	-6.11	-6.00	-5.90	-5.81	-5.72	-5.64
P-CG1 (m)		4.36	4.37	4.38	4.39	4.39	4.40	4.41
OS-CG1 (m)		0.00	0.00	0.00	0.00	0.00	0.00	0.00
P-CG2 (m)		4.35	4.36	4.37	4.39	4.40	4.41	4.42
OS-CG2 (m)		0.00	0.00	0.00	0.00	0.00	0.00	0.00
α_{11} ($degrees$)	+VE	6.95	6.96	6.96	6.97	6.98	6.99	6.99
	-VE	-5.22	-5.27	-5.31	-5.36	-5.40	-5.45	-5.49
α_{12} ($degrees$)	+VE	2.55	2.51	2.48	2.44	2.42	2.39	2.37
	-VE	-2.10	-2.08	-2.06	-2.04	-2.03	-2.02	-2.00
α_{13} ($degrees$)	+VE	3.27	3.21	3.16	3.12	3.08	3.04	3.01
	-VE	-2.75	-2.72	-2.69	-2.67	-2.65	-2.62	2.60
α_{21} ($degrees$)	+VE	2.76	2.64	2.54	2.45	2.37	2.29	2.22
	-VE	-1.95	-1.91	-1.88	-1.86	-1.83	-1.80	-1.78
α_{22} ($degrees$)	+VE	3.29	3.17	3.05	2.95	2.86	2.77	2.69
	-VE	-2.40	-2.36	-2.32	-2.30	-2.26	-2.23	-2.20
α_{23} ($degrees$)	+VE	3.85	3.72	3.59	3.47	3.37	3.27	3.18
	-VE	-2.87	-2.83	-2.79	-2.75	-2.71	-2.68	-2.65

Table 3.8: Transient Response of the Vehicle with Left-Articulation Damping, Lane-Change Maneuver at 80 km/h

COMBINATION I: LANE CHANGE WITH DAMPING MECHANISM								
C_{SL} ($\frac{Ns}{m}$) = C_{SR} ($\frac{Ns}{m}$) =		000.00 0	200.00 0	400.00 0	600.00 0	800.00 0	1000.0 0	1200.0 0
Positive and Negative Peak Parametric Values at 80 km/h								
a_1 (m/s^2)	+VE	4.27	4.29	4.30	4.32	4.44	4.36	4.38
	-VE	-5.12	-5.12	-5.12	-5.12	-5.12	-5.12	-5.12
a_2 (m/s^2)	+VE	3.15	3.14	3.14	3.14	3.13	3.12	3.12
	-VE	-3.63	-3.62	-3.62	-3.59	-3.57	-3.55	-3.53
Rearward Amplification		0.708	0.707	0.707	0.701	0.697	0.693	0.689
r_1 ($degrees/s$)	+VE	12.48	12.52	12.57	12.61	12.66	12.71	12.76
	-VE	-15.96	-15.97	-15.98	-15.98	-15.98	-15.98	-15.97
r_2 ($degrees/s$)	+VE	9.09	9.07	9.06	9.04	9.02	8.99	8.98
	-VE	-10.92	-10.89	-10.84	-10.80	-10.75	-10.70	-10.64
Rearward Amplification		0.684	0.682	0.678	0.676	0.673	0.669	0.666
v_1 (m/s)	+VE	0.28	0.28	0.28	0.28	0.29	0.29	0.29
	-VE	-0.47	-0.47	-0.48	-0.48	-0.48	-0.49	-0.49
v_2 (m/s)	+VE	0.17	0.17	0.17	0.17	0.17	0.17	0.17
	-VE	-0.24	-0.24	-0.23	-0.23	-0.23	-0.23	-0.23
γ ($degrees$)	+VE	4.73	4.76	4.76	4.78	4.80	4.81	4.83
	-VE	-5.79	-5.79	-5.78	-5.78	-5.77	-5.76	-5.75
P-CG1 (m)		4.02	4.02	4.02	4.02	4.02	4.02	4.02
OS-CG1 (m)		0.00	0.00	0.00	0.00	0.00	0.00	0.00
P-CG2 (m)		3.83	3.84	3.84	3.84	3.85	3.85	3.85
OS-CG2 (m)		0.00	0.00	0.00	0.00	0.00	0.00	0.00
α_{11} ($degrees$)	+VE	5.28	5.31	5.32	5.34	5.35	5.36	5.37
	-VE	-3.66	-3.67	-3.67	-3.67	-3.67	-3.67	-3.67
α_{12} ($degrees$)	+VE	1.66	1.67	1.68	1.68	1.69	1.69	1.69
	-VE	-1.25	-1.26	-1.27	-1.29	-1.29	-1.31	-1.32
α_{13} ($degrees$)	+VE	2.63	2.64	2.64	2.65	2.65	2.65	2.65
	-VE	-2.05	-2.06	-2.06	-2.07	-2.08	-2.09	-2.09
α_{21} ($degrees$)	+VE	1.21	1.21	1.20	1.19	1.19	1.18	1.17
	-VE	-0.96	-0.96	-0.95	-0.95	-0.94	-0.94	-0.94
α_{22} ($degrees$)	+VE	1.76	1.76	1.75	1.75	1.74	1.73	1.71
	-VE	-1.43	-1.43	-1.42	-1.42	-1.42	-1.41	-1.40
α_{23} ($degrees$)	+VE	2.34	2.34	2.33	2.32	2.30	2.29	2.28
	-VE	-1.92	-1.91	-1.91	-1.90	-1.89	-1.89	-1.88

Table 3.9: Transient Response of the Vehicle with Right-Articulation Damping, Lane-Change Maneuver at 80 km/h

COMBINATION II: LANE CHANGE WITH DAMPING MECHANISM								
C_{SL} ($\frac{Ns}{m}$) = C_{SR} ($\frac{Ns}{m}$) =		0 000.00	0 200.00	0 400.00	0 600.00	0 800.00	0 1000.0	0 1200.0
Positive and Negative Peak Parametric Values at 80 km/h								
a_1 (m/s^2)	+VE	4.27	4.26	4.25	4.23	4.22	4.32	4.19
	-VE	-5.12	-5.11	-5.11	-5.11	-5.11	-5.10	-5.10
a_2 (m/s^2)	+VE	3.15	3.15	3.14	3.14	3.14	3.13	3.13
	-VE	-3.63	-3.63	-3.63	-3.63	-3.62	-3.62	-3.62
Rearward Amplification		0.709	0.710	0.710	0.710	0.708	0.710	0.710
r_1 ($degrees/s$)	+VE	12.48	12.45	12.43	12.40	12.37	12.34	12.31
	-VE	-15.96	-15.90	-15.83	-15.77	-15.72	-15.67	-15.63
r_2 ($degrees/s$)	+VE	9.09	9.07	9.06	9.04	9.03	9.02	9.00
	-VE	-10.92	-10.89	-10.86	-10.84	-10.82	-10.79	-10.77
Rearward Amplification		0.684	0.685	0.686	0.687	0.688	0.688	0.689
v_1 (m/s)	+VE	0.28	0.30	0.32	0.34	0.36	0.38	0.40
	-VE	-0.47	-0.47	-0.47	-0.47	-0.47	-0.46	-0.47
v_2 (m/s)	+VE	0.17	0.17	0.17	0.17	0.17	0.17	0.17
	-VE	-0.24	-0.23	-0.24	-0.23	-0.23	-0.23	-0.23
γ ($degrees$)	+VE	4.73	4.72	4.72	4.72	4.71	4.70	4.70
	-VE	-5.79	-5.81	-5.83	-5.84	-5.87	-5.89	-5.91
P-CG1 (m)		4.02	4.02	4.02	4.03	4.03	4.04	4.04
OS-CG1 (m)		0.00	0.00	0.00	0.00	0.00	0.00	0.00
P-CG2 (m)		3.83	3.83	3.84	3.84	3.84	3.85	3.85
OS-CG2 (m)		0.00	0.00	0.00	0.00	0.00	0.00	0.00
α_{11} ($degrees$)	+VE	5.28	5.33	5.38	5.43	5.48	5.53	5.58
	-VE	-3.66	-3.69	-3.71	-3.73	-3.75	-3.78	-3.80
α_{12} ($degrees$)	+VE	1.66	1.66	1.67	1.68	1.70	1.72	1.74
	-VE	-1.25	-1.26	-1.26	-1.26	-1.26	-1.26	-1.26
α_{13} ($degrees$)	+VE	2.63	2.63	2.62	2.63	2.63	2.64	2.65
	-VE	-2.05	-2.04	-2.04	-2.04	-2.04	-2.04	-2.03
α_{21} ($degrees$)	+VE	1.21	1.21	1.20	1.19	1.19	1.19	1.18
	-VE	-0.96	-0.96	-0.96	-0.96	-0.96	-0.96	-0.96
α_{22} ($degrees$)	+VE	1.77	1.76	1.75	1.75	1.75	1.74	1.74
	-VE	-1.43	-1.43	-1.43	-1.43	-1.43	-1.43	-1.43
α_{23} ($degrees$)	+VE	2.34	2.33	2.33	2.32	2.32	2.31	2.31
	-VE	-1.92	-1.92	-1.91	-1.91	-1.91	-1.91	-1.91

Table 3.10: Transient Response of the Vehicle with both Left- and Right-Articulation Damping, Lane-Change Maneuver at 80 km/h

COMBINATION III: LANE CHANGE WITH DAMPING MECHANISM								
C_{SL} ($\frac{Ns}{m}$) =		000.00	200.00	400.00	600.00	800.00	1000.0	1200.0
C_{SR} ($\frac{Ns}{m}$) =		000.00	200.00	400.00	600.00	800.00	1000.0	1200.0
Positive and Negative Peak Parametric Values at 80 km/h								
a_1 (m/s^2)	+VE	4.27	4.27	4.28	4.28	4.28	4.29	4.29
	-VE	-5.12	-5.11	-5.11	-5.11	-5.11	-5.12	-5.13
a_2 (m/s^2)	+VE	3.15	3.14	3.13	3.12	3.11	3.11	3.10
	-VE	-3.63	-3.62	-3.60	-3.58	-3.56	-3.54	-3.51
Rearward Amplification		0.709	0.708	0.705	0.701	0.697	0.691	0.684
r_1 ($degrees/s$)	+VE	12.48	12.49	12.51	12.52	12.54	12.56	12.58
	-VE	-15.96	-15.91	-15.85	-15.81	-15.77	-15.74	-15.72
r_2 ($degrees/s$)	+VE	9.09	9.06	9.03	8.99	8.96	8.93	8.89
	-VE	-10.92	-10.86	-10.79	-10.72	-10.64	-10.57	-10.49
Rearward Amplification		0.684	0.683	0.681	0.678	0.675	0.672	0.667
v_1 (m/s)	+VE	0.28	0.30	0.32	0.34	0.37	0.39	0.40
	-VE	-0.47	-0.47	-0.48	-0.48	-0.48	-0.49	-0.49
v_2 (m/s)	+VE	0.17	0.17	0.17	0.17	0.17	0.17	0.17
	-VE	-0.24	-0.23	-0.23	-0.23	-0.23	-0.22	-0.22
γ ($degrees$)	+VE	4.73	4.74	4.76	4.76	4.77	4.78	4.79
	-VE	-5.79	-5.81	-5.82	-5.83	-5.85	-5.86	-5.87
P-CG1 (m)		4.02	4.02	4.03	4.03	4.04	4.04	4.05
OS-CG1 (m)		0.00	0.00	0.00	0.00	0.00	0.00	0.00
P-CG2 (m)		3.83	3.84	3.85	3.85	3.86	3.87	3.88
OS-CG2 (m)		0.00	0.00	0.00	0.00	0.00	0.00	0.00
α_{11} ($degrees$)	+VE	5.28	5.35	5.42	5.48	5.54	5.60	5.65
	-VE	-3.66	-3.69	-3.71	-3.73	-3.75	-3.77	-3.80
α_{12} ($degrees$)	+VE	1.66	1.67	1.69	1.71	1.73	1.76	1.79
	-VE	-1.25	-1.26	-1.27	-1.29	-1.30	-1.32	-1.33
α_{13} ($degrees$)	+VE	2.63	2.63	2.64	2.65	2.66	2.67	2.68
	-VE	-2.04	-2.05	-2.06	-2.06	-2.07	-2.08	-2.09
α_{21} ($degrees$)	+VE	1.21	1.20	1.19	1.18	1.17	1.16	1.15
	-VE	-0.96	-0.96	-0.95	-0.95	-0.94	-0.94	-0.94
α_{22} ($degrees$)	+VE	1.76	1.75	1.74	1.73	1.72	1.70	1.69
	-VE	-1.43	-1.43	-1.42	-1.42	-1.41	-1.40	-1.40
α_{23} ($degrees$)	+VE	2.34	2.33	2.31	2.30	2.28	2.26	2.24
	-VE	-1.92	-1.91	-1.90	-1.90	-1.89	-1.88	-1.88

The articulation damping influences not only the yaw and lateral response of the vehicle, but also the steer angles required to follow the prescribed lane-change path at a given forward speed. Figure 3.11 illustrates the time-history of the front wheel steer angle required to negotiate the path, at a speed of 100 km/h. The steer angle required to negotiate the lane-change increases only slightly when articulation damping is introduced. The damped articulation also causes a slightly longer correction phase as shown in the Figure.

The lateral damping force and yaw damping moment generated by the articulation dampers tend to reduce the magnitude of transient response of both the tractor and the semitrailer, as evident in Figures 3.11 to 3.17. The peak lateral acceleration response of the tractor and semitrailer decrease with increase in articulation damping, while the settling time remains almost unaffected, as shown in Figure 3.12. The peak value of lateral acceleration response just before the correction phase of the steering specifically reduces with increase in damping. While the lateral velocity response of the tractor reduces only slightly with increase in damping, the articulation damping suppresses the peak lateral velocity of the semitrailer considerably (approximately by 30%), as shown in Figure 3.13. The lateral oscillatory response of the semitrailer can thus be suppressed significantly through damped articulation. The yaw velocity response of the tractor and semitrailer of the damped vehicle are similarly lower than that of the conventional vehicle, as shown in Figure 3.14. The peak yaw velocities of the tractor and semitrailer of the damped vehicle (C_{SL} = C_{SR} = 1200 Ns/m) are 9.5% and 14% lower than those of the conventional vehicle.

Figure 3.15 illustrates the path followed by the c.g.'s of the tractor and semi-trailer's sprung weights for different values of articulation damping. The figure reveals that the damped vehicle tends to overshoot slightly more than the conventional vehicles. The increase in the overshoot for tractor and semitrailer (for C_{SL} = C_{SR} = 1200 Ns/m), however, is approximately 1%. While the conventional vehicle reverses its direction of

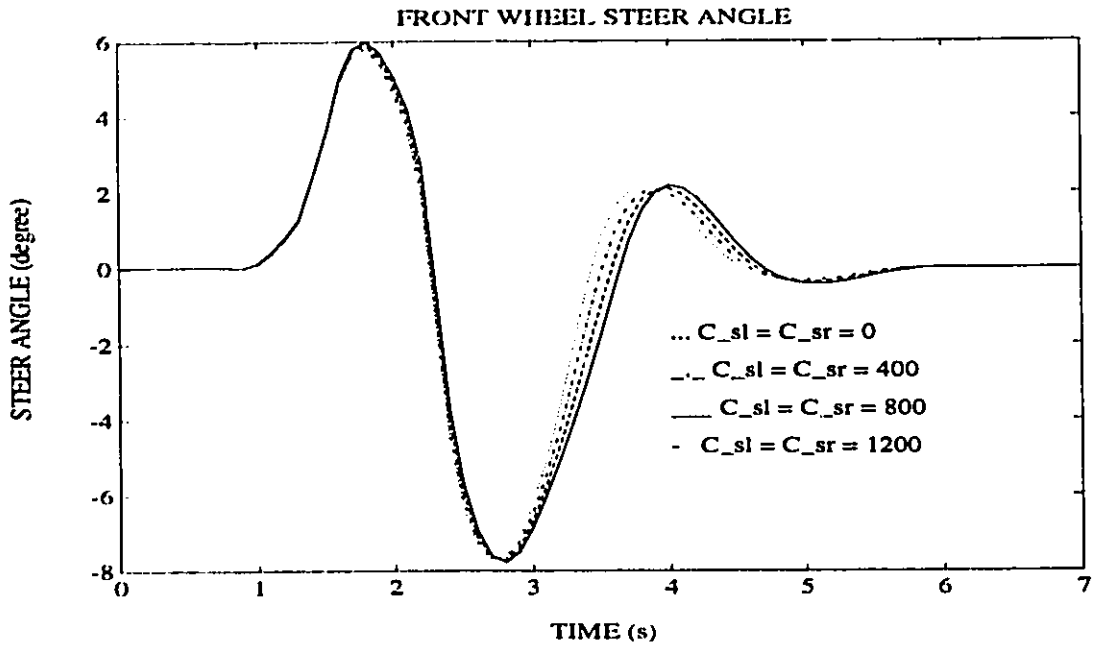

Figure 3.11: Front Wheel Steer Angle Required to negotiate a Lane-Change Maneuver at 100 km/h

travel slightly earlier than the damped vehicle, the overall settling times of both vehicles are quite similar. The increase in the overshoot and the delay in path reversal of the damped vehicle may be attributed to the decrease in articulation angle caused by the articulation dampers, as shown in Figure 3.16.

The side-slip angles of the tires also decrease with increase in damping as evidenced in Table 3.8. The influence of the articulation dampers on the side-slip angles of tires on the tractor axles, however, is relatively small. The peak side-slip angles of tires on all the semitrailer axles reduce considerably when articulation damping is increased, as shown in Figure 3.17.

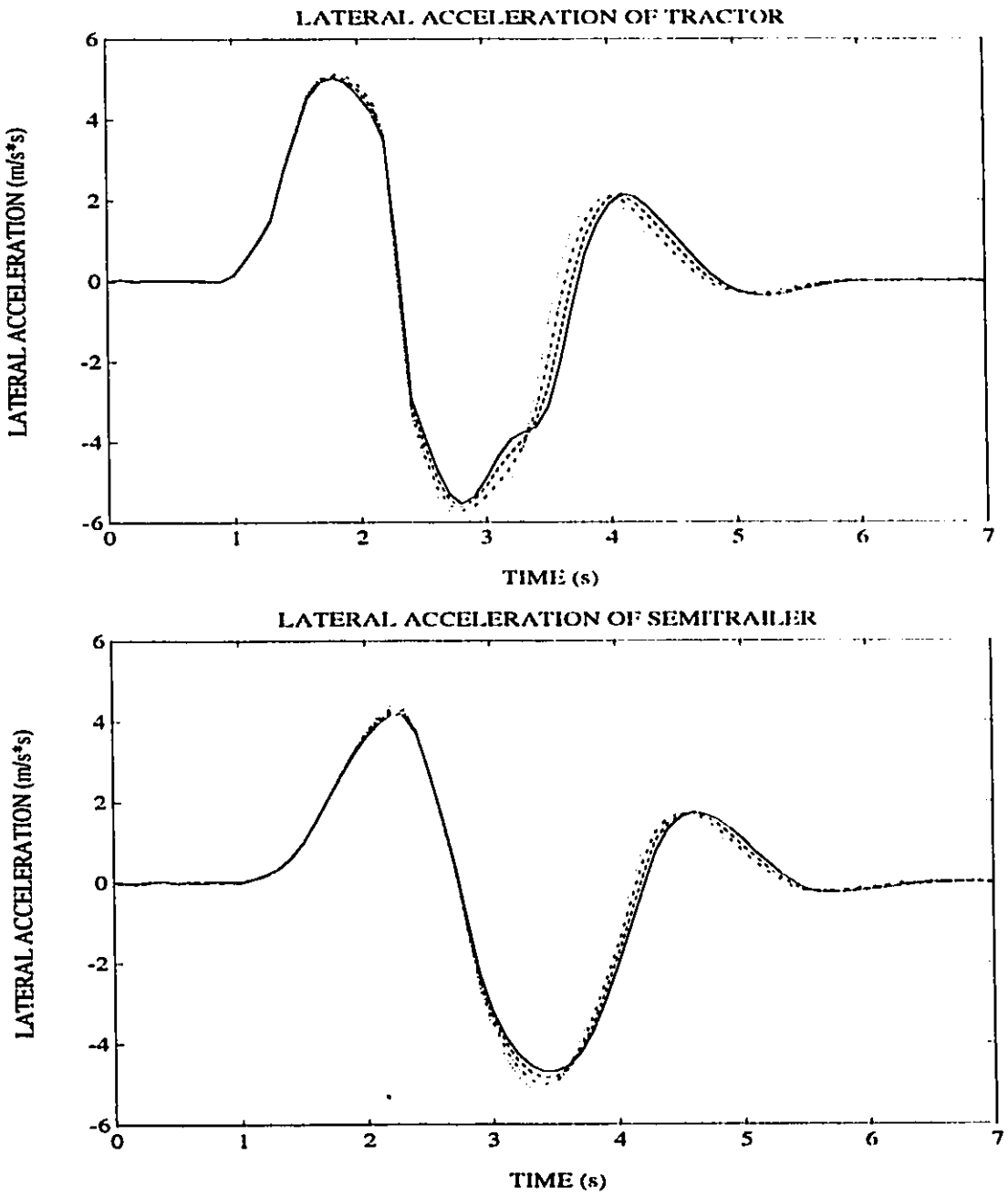

Figure 3.12: Lateral Acceleration Response of Tractor and Semitrailer for a Lane-Change Maneuver at 100 km/h

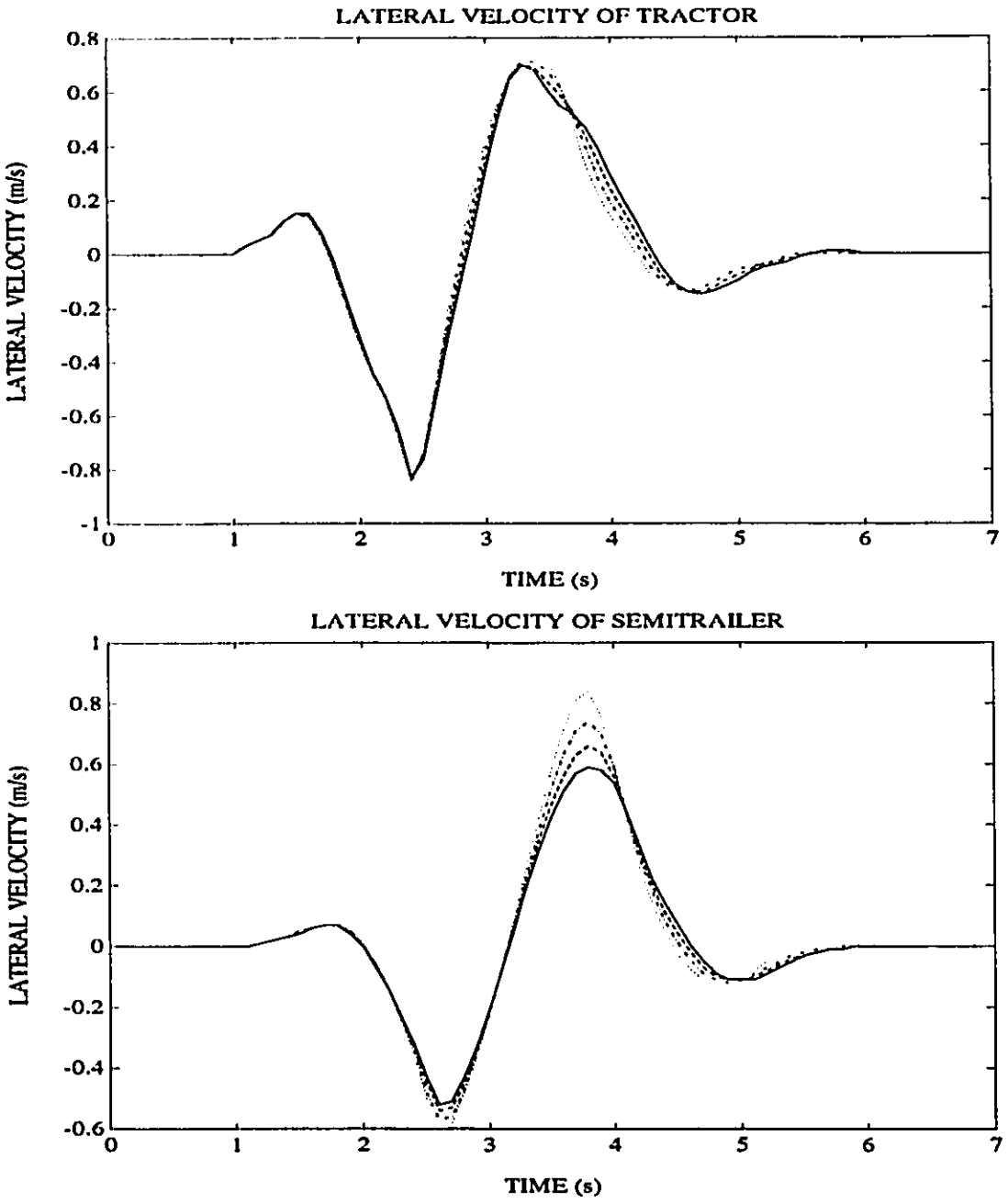

Figure 3.13: Lateral Velocity Response of Tractor and Semitrailer for a Lane-Change Maneuver at 100 km/h

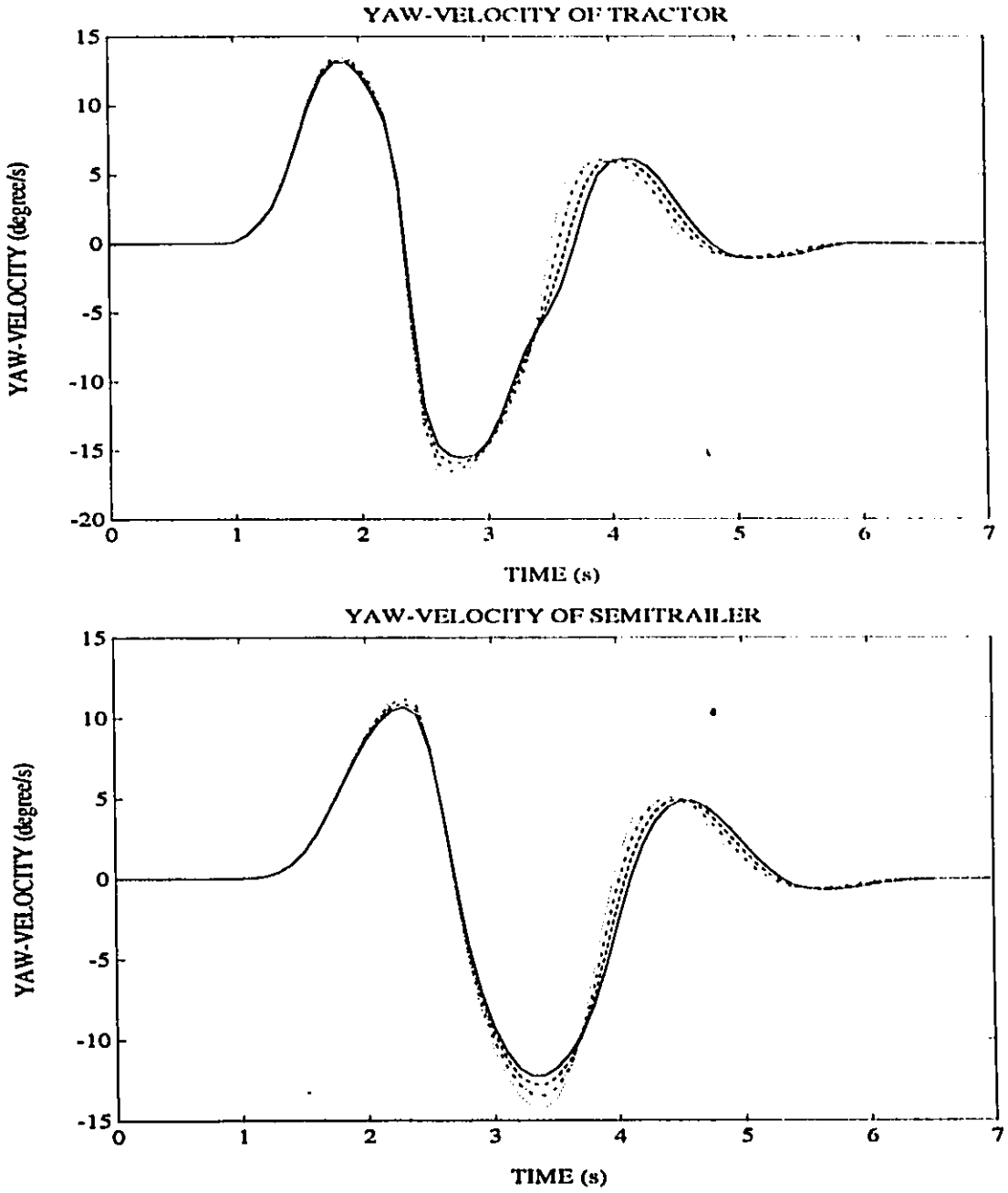

Figure 3.14: Yaw-Velocity Response of Tractor and Semitrailer for a Lane-Change Maneuver at 100 km/h

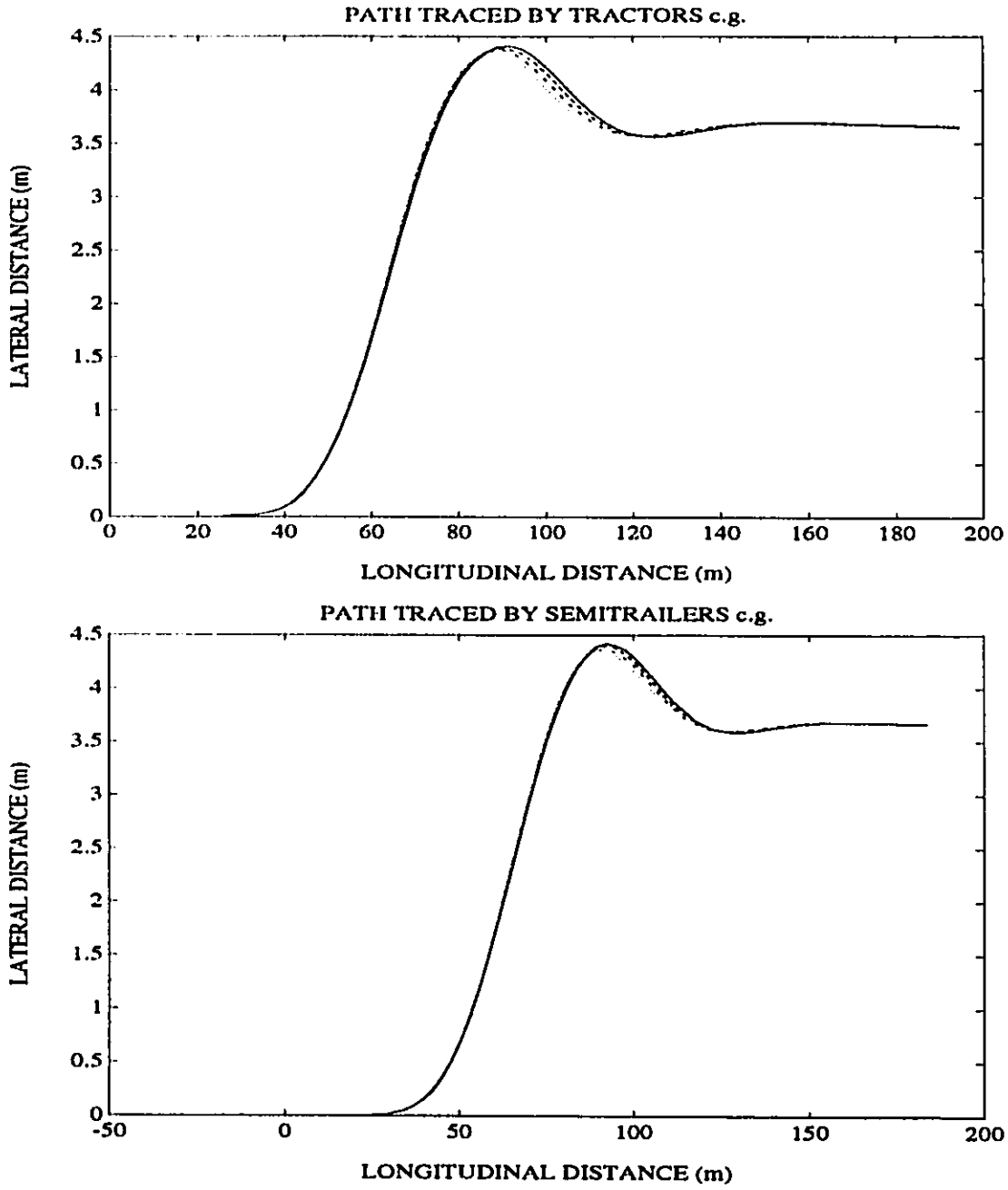

Figure 3.15: Path followed by the Tractor and Semitrailer c.g.s for a Lane-Change Maneuver at 100 km/h

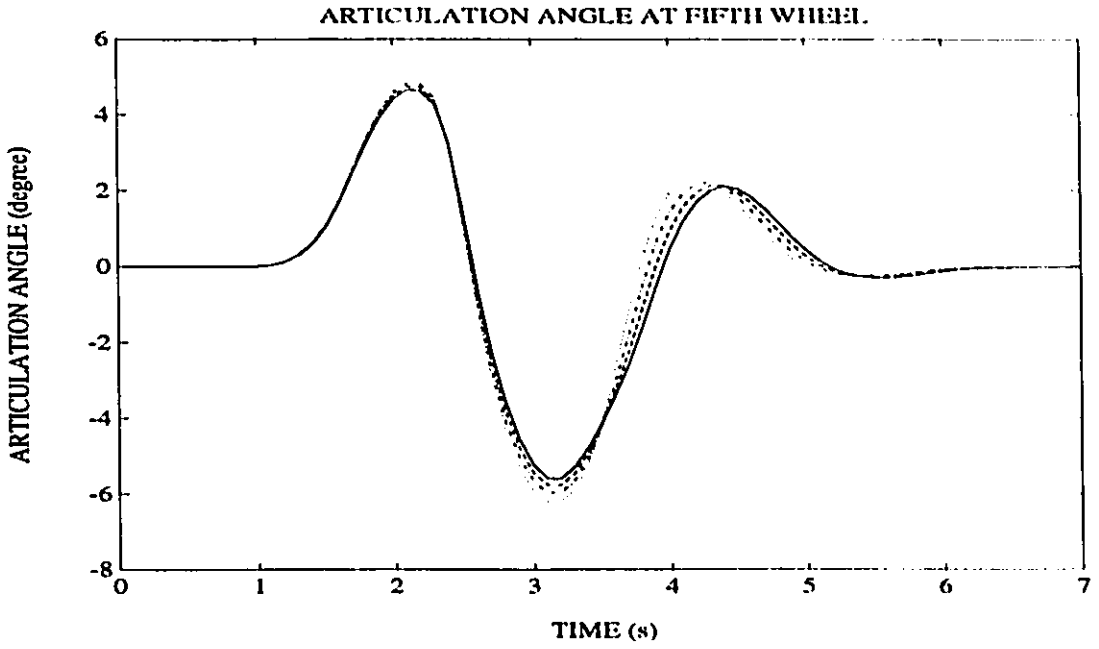

Figure 3.16: Articulation Angle Response of Vehicle for a Lane-Change Maneuver at 100 km/h

3.5 Vehicle Response to an Evasive Maneuver

The transient directional response characteristics of articulated vehicle are further derived for an evasive maneuver to investigate the influence of articulation dampers. The response characteristics are computed using the path follower model in conjunction with the path presented in Figure 3.2 at forward speeds of 80 km/h and 100 km/h. The peak values of directional response parameters and the rearward amplification factors of the vehicle subject to an evasive maneuver at 100 km/h are computed for three combinations of articulation damping and are summarized in Tables 3.12 to 3.14. Table 3.12 illustrates the peak values for the left-handed evasive maneuver when only the left-articulation damper is employed (Combination I). The peak values of lateral acceleration, lateral and yaw velocities, and articulation angle response of both tractor and semitrailer decrease considerably due to damping forces and moments generated by the left articulation dampers.

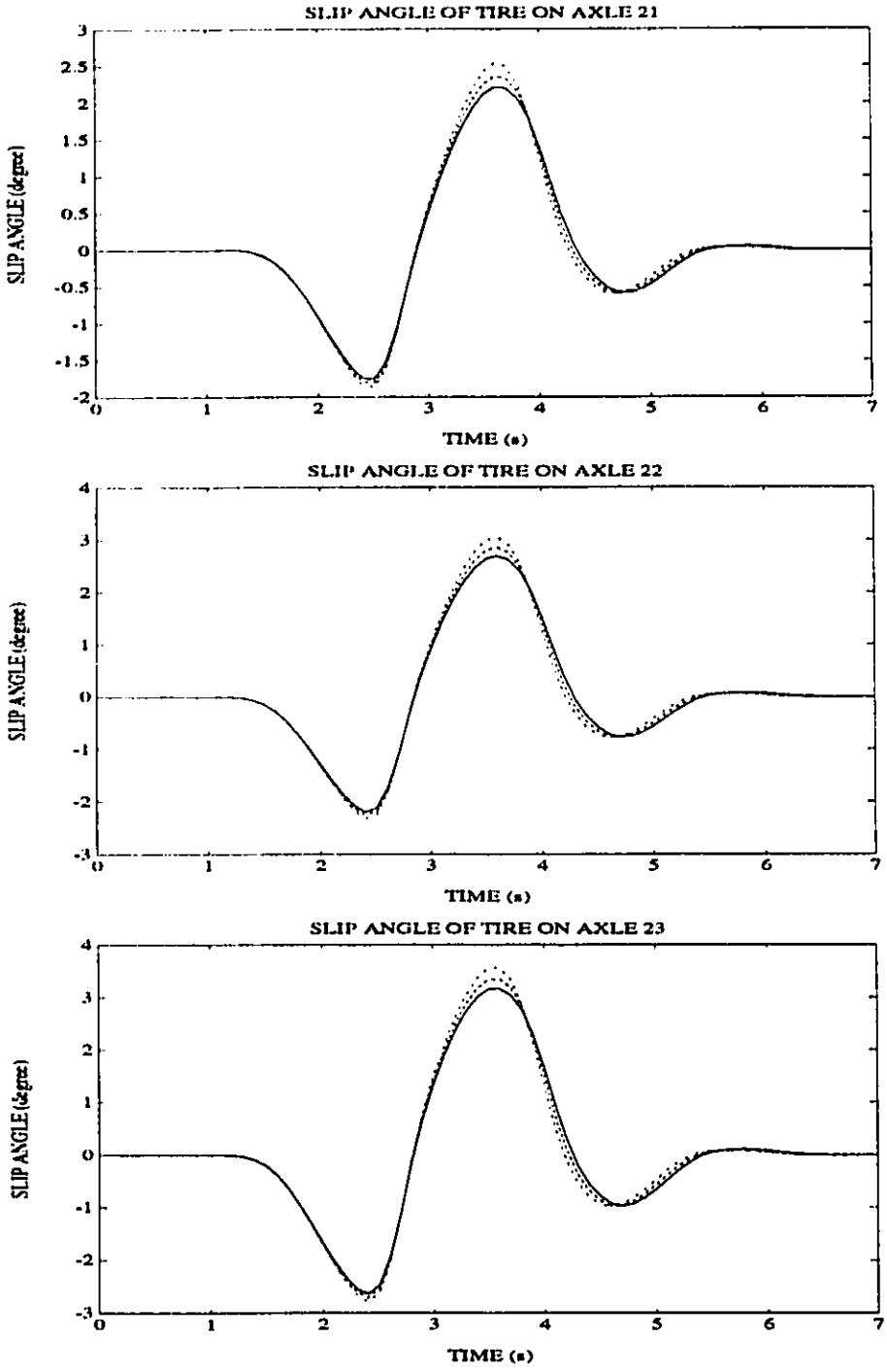

Figure 3.17: Side-Slip Angles of tires on Semitrailer during a a Lane-Change Maneuver at 100 km/h

The rearward amplification factors, α_a and α_ω, also decrease with an increase in the left-articulation damping coefficient (C_{SL}). A comparison of the peak response values of the damped vehicle to those of the conventional vehicle reveals that the yaw-velocity, and lateral acceleration rearward amplification factors reduce by 19% and 12.5% respectively, when the damping coefficient C_{SL} = 1200 Ns/m. The results of the study thus clearly illustrate that the articulation damping increases the directional control performance of the vehicle by reducing the amplitudes of yaw and lateral oscillation encountered.

The side-slip angles of tires on all the axles, except the tractor's front axle, reduce considerably with increase in the left-articulation damping. The peak magnitude of side-slip angles of tires on the tractor's rear and semitrailer axles of the vehicle with left-articulation damper (C_{SL} = 1200 Ns/m) are approximately 40% lower than those of the conventional vehicle. The side-slip angle of the tractor's front axle, however, increase with increase in the damping coefficient. The peak values of the tires on front axle of the damped vehicle (C_{SL} = 1200 Ns/m) is approximately 30% larger than that of the conventional vehicle. This increase in the side-slip angle of the front axle tires is primarily attributed to increase in the front wheel steer angle required to negotiate the prescribed maneuver, as shown in Figure 3.18. The peak front-wheel angle of the conventional vehicle, observed near 12 degrees, increases to approximately 17 degrees for C_{SL} = C_{SL} = 1200 Ns/m.

Table 3.14 summarizes the peak response values of the vehicle with only right-articulation damper (Combination II), while negotiating the left-hand evasive maneuver at 100 km/h. It is evident from the table that the influence of right-articulation damper on the peak values of directional response quantities is insignificant. The peak values of lateral acceleration, lateral and yaw velocities, articulation angle decrease only slightly when the damping coefficient C_{SR} is increased. The slip angles of tires on all the axles, except the tractor's front axle, also decrease by approximately 1%, when damping coefficient is increase to 1200 Ns/m. The side-slip angle of the front-axle tires increases by almost 4%

Table 3.11: Transient Response of the Vehicle with Left-Articulation Damping, Evasive Maneuver at 100 km/h

COMBINATION I: EVASIVE MANEUVER WITH DAMPING MECHANISM								
C_{SL} ($\frac{Ns}{m}$) = C_{SR} ($\frac{Ns}{m}$) =		000.00 0	200.00 0	400.00 0	600.00 0	800.00 0	1000.0 0	1200.0 0
Positive and Negative Peak Parametric Values at 100 km/h								
a_1 (m/s^2)	+VE	6.62	6.46	6.40	6.36	6.31	6.27	6.23
	-VE	-6.66	-6.56	-6.52	-6.49	-6.46	-6.44	-6.41
a_2 (m/s^2)	+VE	6.36	6.08	5.83	5.62	5.45	5.31	5.19
	-VE	-6.67	-6.39	-6.18	-6.01	-5.97	-5.74	-5.62
Rearward Amplification		1.002	0.974	0.948	0.926	0.924	0.891	0.877
r_1 ($degrees/s$)	+VE	20.42	19.48	19.41	19.40	19.22	19.12	18.76
	-VE	-18.18	-18.03	-17.92	-17.83	-17.76	-17.69	-17.64
r_2 ($degrees/s$)	+VE	18.56	17.28	16.29	15.50	14.85	14.29	13.82
	-VE	-17.19	-16.03	-15.25	-14.65	-14.16	-13.74	-13.38
Rearward Amplification		0.909	0.887	0.839	0.799	0.773	0.747	0.737
v_1 (m/s)	+VE	1.32	1.16	1.13	1.16	1.19	1.21	1.20
	-VE	-1.03	-1.00	-0.99	-0.98	-0.96	-0.95	-0.94
v_2 (m/s)	+VE	1.70	1.42	1.21	1.06	0.96	0.89	0.84
	-VE	-1.60	-1.33	-1.13	-0.98	-0.87	-0.78	-0.72
γ ($degrees$)	+VE	8.08	7.75	7.49	7.26	7.05	6.86	6.69
	-VE	-7.26	-6.99	-6.80	-6.64	-6.51	-6.39	-6.29
P-CG1 (m)		4.13	4.13	4.14	4.15	4.15	4.16	4.16
OS-CG1 (m)		-0.95	-0.95	-0.97	-0.99	-1.00	-1.01	-1.02
P-CG2 (m)		4.07	4.08	4.09	4.10	4.12	4.13	4.15
OS-CG2 (m)		-1.03	-1.03	-1.05	-1.06	-1.07	-1.08	-1.08
α_{11} ($degrees$)	+VE	14.75	15.43	16.25	17.13	17.98	18.76	19.45
	-VE	-9.23	-9.03	-8.95	-8.89	-8.85	-8.81	-8.86
α_{12} ($degrees$)	+VE	3.56	3.30	3.16	3.06	2.98	2.92	2.87
	-VE	-3.28	-3.23	-3.16	-3.08	-2.99	-2.91	-2.84
α_{13} ($degrees$)	+VE	4.36	4.09	3.94	3.82	3.74	3.67	3.61
	-VE	-4.06	-4.00	-3.91	-3.82	-3.71	-3.62	-3.53
α_{21} ($degrees$)	+VE	4.67	4.09	3.63	3.28	3.00	2.81	2.66
	-VE	-4.54	-3.98	-3.57	-3.24	-3.00	-2.80	-2.64
α_{22} ($degrees$)	+VE	5.33	4.71	4.21	3.83	3.54	3.33	3.18
	-VE	-5.19	-4.60	-4.15	-3.81	-3.54	-3.33	-3.15
α_{23} ($degrees$)	+VE	6.01	5.34	4.81	4.40	4.08	3.86	3.70
	-VE	-5.88	-5.25	-4.77	-4.40	-4.11	-3.87	-3.68

Table 3.12: Transient Response of the Vehicle with Right-Articulation Damping, Evasive Maneuver at 100 km/h

COMBINATION II: EVASIVE MANEUVER WITH DAMPING MECHANISM								
C_{SL} ($\frac{Ns}{m}$) = C_{SR} ($\frac{Ns}{m}$) =		0 000.00	0 200.00	0 400.00	0 600.00	0 800.00	0 1000.0	0 1200.0
Positive and Negative Peak Parametric Values at 100 km/h								
a_1 (m/s^2)	+VE	6.62	6.56	6.51	6.42	6.37	6.37	6.38
	-VE	-6.66	-6.65	-6.64	-6.64	-6.63	-6.63	-6.62
a_2 (m/s^2)	+VE	6.36	6.39	6.41	6.44	6.46	6.48	6.50
	-VE	-6.67	-6.67	-6.66	-6.66	-6.66	-6.66	-6.66
Rearward Amplification		1.002	1.003	1.003	1.003	1.005	1.005	1.006
r_1 ($degrees/s$)	+VE	20.42	20.23	20.05	19.88	19.72	19.56	19.41
	-VE	-18.18	-18.13	-18.07	-18.02	-17.98	-17.94	-17.91
r_2 ($degrees/s$)	+VE	18.56	18.54	18.53	18.50	18.45	18.39	18.32
	-VE	-17.19	-17.18	-17.16	-17.15	-17.14	-17.13	-17.11
Rearward Amplification		0.909	0.916	0.924	0.931	0.936	0940	0.944
v_1 (m/s)	+VE	1.32	1.31	1.30	1.29	1.29	1.28	1.28
	-VE	-1.03	-1.05	-1.06	-1.07	-1.08	-1.07	-1.07
v_2 (m/s)	+VE	1.70	1.69	1.68	1.67	1.66	1.66	1.65
	-VE	-1.60	-1.61	-1.61	-1.62	-1.62	-1.62	-1.62
γ ($degrees$)	+VE	8.08	8.09	8.09	8.07	8.04	8.00	7.95
	-VE	-7.26	-7.23	-7.20	-7.18	-7.15	-7.13	-7.11
P-CG1 (m)		4.13	4.14	4.14	4.15	4.15	4.16	4.16
OS-CG1 (m)		-0.95	-0.98	-1.00	-1.03	-1.05	-1.08	-1.11
P-CG2 (m)		4.07	4.07	4.08	4.08	4.09	4.09	4.10
OS-CG2 (m)		-1.03	-1.06	-1.08	-1.11	-1.13	-1.16	-1.18
α_{11} ($degrees$)	+VE	14.75	14.86	14.96	15.07	15.18	15.28	15.38
	-VE	-9.23	-9.40	-9.58	-9.76	-9.96	-10.16	-10.37
α_{12} ($degrees$)	+VE	3.56	3.54	3.52	3.50	3.49	3.48	3.47
	-VE	-3.28	-3.34	-3.39	-3.43	-3.46	-3.47	-3.49
α_{13} ($degrees$)	+VE	4.37	4.34	4.33	4.31	4.30	4.29	4.28
	-VE	-4.06	-4.13	-4.19	-4.24	-4.26	-4.28	-4.28
α_{21} ($degrees$)	+VE	4.67	4.65	4.64	4.63	4.62	4.61	4.60
	-VE	-4.54	-4.55	-4.57	-4.58	-4.58	-4.59	-4.59
α_{22} ($degrees$)	+VE	5.33	5.31	5.30	5.29	5.28	5.27	5.26
	-VE	-5.19	-5.21	-5.23	-5.24	-5.24	-5.25	-5.25
α_{23} ($degrees$)	+VE	6.01	6.00	5.99	5.98	5.96	5.95	5.94
	-VE	-5.88	-5.90	-5.92	-5.94	-5.94	-5.95	-5.95

Table 3.13: Transient Response of the Vehicle with both Left- and Right-Articulation Damping, Evasive Maneuver at 100 km/h

COMBINATION III: EVASIVE MANEUVER WITH DAMPING MECHANISM								
C_{SL} ($\frac{N_s}{m}$) =		000.00	200.00	400.00	600.00	800.00	1000.0	1200.0
C_{SR} ($\frac{N_s}{m}$) =		000.00	200.00	400.00	600.00	800.00	1000.0	1200.0
Positive and Negative Peak Parametric Values at 100 km/h								
a_1 (m/s^2)	+VE	6.62	6.40	6.31	6.24	6.19	6.14	6.09
	-VE	-6.66	-6.54	-6.50	-6.46	-6.42	-6.39	-6.36
a_2 (m/s^2)	+VE	6.36	6.09	5.85	5.65	5.49	5.36	5.25
	-VE	-6.67	-6.39	-6.19	-6.02	-5.88	-5.74	-5.62
Rearward Amplification		1.002	0.977	0.952	0.932	0.916	0.898	0.884
r_1 ($degrees/s$)	+VE	20.42	19.35	19.06	18.83	18.53	18.17	17.83
	-VE	-18.18	-17.98	-17.82	-17.68	-17.56	-17.56	-17.36
r_2 ($degrees/s$)	+VE	18.56	17.26	16.25	15.45	14.80	14.26	13.80
	-VE	-17.19	-16.00	-15.19	-14.57	-14.05	-13.62	-13.24
Rearward Amplification		0.909	0.892	0.853	0.821	0.799	0.785	0.774
v_1 (m/s)	+VE	1.32	1.15	1.12	1.12	1.12	1.12	1.10
	-VE	-1.03	-1.01	-1.00	-0.99	-0.98	-0.97	-0.96
v_2 (m/s)	+VE	1.70	1.41	1.21	1.06	0.96	0.88	0.83
	-VE	-1.60	-1.33	-1.13	-0.99	-0.88	-0.79	-0.73
γ ($degrees$)	+VE	8.08	7.75	7.48	7.23	7.02	6.83	6.66
	-VE	-7.26	-6.97	-6.75	-6.58	-6.43	-6.31	-6.20
P-CG1 (m)		4.13	4.14	4.15	4.16	4.17	4.18	4.19
OS-CG1 (m)		-0.95	-0.98	-1.00	-1.03	-1.06	-1.08	-1.10
P-CG2 (m)		4.07	4.08	4.10	4.12	4.13	4.15	4.17
OS-CG2 (m)		-1.03	-1.05	-1.08	-1.11	-1.13	-1.14	-1.16
α_{11} ($degrees$)	+VE	14.75	15.52	16.39	17.29	18.15	18.94	19.66
	-VE	-9.23	-9.18	-9.21	-9.25	-9.30	-9.38	-9.51
α_{12} ($degrees$)	+VE	3.56	3.29	3.14	3.03	2.94	2.88	2.82
	-VE	-3.28	-3.26	-3.20	-3.12	-3.05	-2.98	-2.92
α_{13} ($degrees$)	+VE	4.37	4.08	3.90	3.78	3.68	3.60	3.53
	-VE	-4.06	-4.03	-3.96	-3.86	-3.77	-3.69	-3.62
α_{21} ($degrees$)	+VE	4.67	4.09	3.64	3.31	3.05	2.84	2.69
	-VE	-4.54	-3.98	-3.57	-3.26	-3.02	-2.83	-2.67
α_{22} ($degrees$)	+VE	5.33	4.71	4.23	3.87	3.59	3.37	3.20
	-VE	-5.19	-4.60	-4.16	-3.83	-3.56	-3.36	-3.19
α_{23} ($degrees$)	+VE	6.02	5.34	4.83	4.43	4.13	3.90	3.72
	-VE	-5.88	-5.26	-4.79	-4.41	-4.13	-3.90	-3.72

Table 3.14: Transient Response of the Vehicle with Left-Articulation Damping, Evasive Maneuver at 80 km/h

COMBINATION I: EVASIVE MANEUVER WITH DAMPING MECHANISM								
C_{SL} ($\frac{Ns}{m}$) =		000.00	200.00	400.00	600.00	800.00	1000.0	1200.0
C_{SR} ($\frac{Ns}{m}$) =		0	0	0	0	0	0	0
Positive and Negative Peak Parametric Values at 80 km/h								
a_1 (m/s^2)	+VE	4.25	4.32	4.39	4.47	4.55	4.64	4.75
	-VE	-5.89	-5.87	-5.85	-5.84	-5.82	-5.82	-5.81
a_2 (m/s^2)	+VE	3.32	3.33	3.34	3.36	3.37	3.38	3.40
	-VE	-5.02	-4.97	-4.92	-4.86	-4.79	-4.73	-4.65
Rearward Amplification		0.852	0.847	0.841	0.832	0.823	0.813	0.800
r_1 ($degrees/s$)	+VE	12.88	13.05	13.25	13.46	13.71	13.97	14.26
	-VE	-17.21	-17.22	-17.24	-17.26	-17.29	-17.33	-17.37
r_2 ($degrees/s$)	+VE	9.71	9.75	9.79	9.84	9.89	9.95	10.03
	-VE	-14.75	-14.57	-14.38	-14.19	-13.99	-13.78	-13.58
Rearward Amplification		0.857	0.846	0.834	0.822	0.809	0.795	0.782
v_1 (m/s)	+VE	0.46	0.45	0.44	0.43	0.41	0.41	0.42
	-VE	-0.36	-0.36	-0.36	-0.36	-0.36	-0.37	-0.37
v_2 (m/s)	+VE	0.28	0.27	0.25	0.24	0.23	0.22	0.22
	-VE	-0.21	-0.21	-0.21	-0.21	-0.21	-0.21	-0.21
γ ($degrees$)	+VE	5.04	5.09	5.16	5.23	5.30	5.38	5.47
	-VE	-7.63	-7.60	-7.57	-7.53	-7.49	-7.46	-7.42
P-CG1 (m)		3.86	3.87	3.87	3.87	3.87	3.87	3.87
OS-CG1 (m)		-0.21	-0.21	-0.22	-0.22	-0.23	-0.23	-0.24
P-CG2 (m)		3.59	3.59	3.59	3.59	3.59	3.60	3.60
OS-CG2 (m)		-0.07	-0.08	-0.08	-0.09	-0.09	-0.10	-0.11
α_{11} ($degrees$)	+VE	7.85	7.87	7.89	7.92	7.94	7.96	7.99
	-VE	-3.59	-3.66	-3.73	-3.82	-3.92	-4.04	-4.16
α_{12} ($degrees$)	+VE	2.34	2.35	2.37	2.39	2.40	2.42	2.43
	-VE	-1.30	-1.33	-1.37	-1.41	-1.45	-1.50	-1.55
α_{13} ($degrees$)	+VE	3.42	3.43	3.44	3.45	3.46	3.47	3.47
	-VE	-2.11	-2.15	-2.19	-2.23	-2.28	-2.33	-2.39
α_{21} ($degrees$)	+VE	2.08	2.05	2.02	1.98	1.94	1.89	1.85
	-VE	-1.05	-1.06	-1.06	-1.06	-1.07	-1.07	-1.08
α_{22} ($degrees$)	+VE	2.83	2.79	2.75	2.71	2.66	2.60	2.55
	-VE	-1.55	-1.56	-1.56	-1.57	-1.58	-1.59	-1.60
α_{23} ($degrees$)	+VE	3.61	3.57	3.52	3.46	3.39	3.33	3.26
	-VE	-2.07	-2.08	-2.09	-2.09	-2.11	-2.12	-2.13

Table 3.15: Transient Response of the Vehicle with Right-Articulation Damping, Evasive Maneuver at 80 km/h

COMBINATION II: EVASIVE MANEUVER WITH DAMPING MECHANISM								
C_{SL} ($\frac{Ns}{m}$) = C_{SR} ($\frac{Ns}{m}$) =		0 000.00	0 200.00	0 400.00	0 600.00	0 800.00	0 1000.0	0 1200.0
Positive and Negative Peak Parametric Values at 80 km/h								
a_1 (m/s^2)	+VE	4.25	4.26	4.27	4.28	4.28	4.29	4.30
	-VE	-5.89	-5.91	-5.92	-5.94	-5.95	-5.97	-5.98
a_2 (m/s^2)	+VE	3.32	3.34	3.35	3.67	3.38	3.39	3.41
	-VE	-5.02	-5.02	-5.02	-5.03	-5.02	-5.03	-5.02
Rearward Amplification		0.852	0.849	0.848	0.847	0.844	0.843	0.839
r_1 ($degrees/s$)	+VE	12.88	12.34	12.99	13.06	13.13	13.20	13.28
	-VE	-17.21	-17.36	-17.54	-17.69	-17.86	-18.02	-18.18
r_2 ($degrees/s$)	+VE	9.71	9.75	9.79	9.84	9.88	9.93	9.97
	-VE	-14.74	-14.74	-14.74	-14.73	-14.72	-14.71	-14.69
Rearward Amplification		0.856	0.849	0.840	0.833	0.824	0.816	0.808
v_1 (m/s)	+VE	0.46	0.51	0.56	0.61	0.66	0.71	0.76
	-VE	-0.36	-0.36	-0.37	-0.36	-0.37	-0.37	-0.37
v_2 (m/s)	+VE	0.28	0.28	0.28	0.28	0.28	0.28	0.28
	-VE	-0.21	-0.21	-0.21	-0.21	-0.21	-0.21	-0.21
γ ($degrees$)	+VE	5.04	5.07	5.09	5.12	5.15	5.18	5.21
	-VE	-7.63	-7.74	-7.84	-7.95	-8.04	-8.14	-8.24
P-CG1 (m)		3.86	3.87	3.87	3.87	3.87	3.88	3.88
OS-CG1 (m)		-0.21	-0.22	-0.22	-0.23	-0.24	-0.24	-0.25
P-CG2 (m)		3.59	3.59	3.59	3.60	3.60	3.60	3.61
OS-CG2 (m)		-0.07	-0.08	-0.08	-0.09	-0.09	-0.10	-0.11
α_{11} ($degrees$)	+VE	7.85	7.89	7.92	7.96	7.99	8.03	8.06
	-VE	-3.59	-3.65	-3.72	-3.78	-3.85	-3.93	-4.00
α_{12} ($degrees$)	+VE	2.32	2.42	2.52	2.61	2.70	2.80	2.89
	-VE	-1.29	-1.31	-1.33	-1.34	-1.36	-1.38	-1.39
α_{13} ($degrees$)	+VE	3.42	3.51	3.60	3.69	3.79	3.87	3.97
	-VE	-2.11	-2.12	-2.14	-2.15	-2.17	-2.18	-2.20
α_{21} ($degrees$)	+VE	2.08	2.07	2.07	2.07	2.06	2.06	2.05
	-VE	-1.05	-1.06	-1.07	-1.09	-1.09	-1.10	-1.11
α_{22} ($degrees$)	+VE	2.83	2.83	2.83	2.83	2.82	2.82	2.81
	-VE	-1.55	-1.57	-1.58	-1.59	-1.60	-1.61	-1.11
α_{23} ($degrees$)	+VE	3.61	3.61	3.60	3.61	3.60	3.59	3.59
	-VE	-2.07	-2.08	-2.09	-2.11	-2.13	-2.14	-2.16

Table 3.16: Transient Response of the Vehicle with both Left- and Right-Articulation Damping, Evasive Maneuver at 80 km/h

COMBINATION III: EVASIVE MANEUVER WITH DAMPING MECHANISM								
C_{SL} ($\frac{Ns}{m}$) =		000.00	200.00	400.00	600.00	800.00	1000.0	1200.0
C_{SR} ($\frac{Ns}{m}$) =		000.00	200.00	400.00	600.00	800.00	1000.0	1200.0
Positive and Negative Peak Parametric Values at 80 km/h								
a_1 (m/s^2)	+VE	4.25	4.32	4.40	4.49	4.58	4.69	4.80
	-VE	-5.89	-5.88	-5.88	-5.89	-5.90	-5.91	-5.93
a_2 (m/s^2)	+VE	3.32	3.35	3.37	3.39	3.41	3.43	3.45
	-VE	-5.02	-4.97	-4.91	-4.83	-4.74	-4.64	-4.54
Rearward Amplification		0.852	0.845	0.835	0.820	0.803	0.785	0.766
r_1 ($degrees/s$)	+VE	12.88	13.10	13.34	13.61	13.91	14.24	14.59
	-VE	-17.21	-17.39	-17.55	-17.72	-17.88	-18.04	-18.20
r_2 ($degrees/s$)	+VE	9.71	9.79	9.86	9.93	10.01	10.08	10.17
	-VE	-14.74	-14.56	-14.33	-14.08	-13.80	-13.52	-13.24
Rearward Amplification		0.856	0.837	0.817	0.795	0.772	0.749	0.727
v_1 (m/s)	+VE	0.46	0.50	0.52	0.54	0.56	0.60	0.66
	-VE	-0.36	-0.36	-0.37	-0.37	-0.37	-0.37	-0.37
v_2 (m/s)	+VE	0.28	0.27	0.25	0.23	0.22	0.22	0.22
	-VE	-0.21	-0.21	-0.21	-0.21	-0.21	-0.21	-0.21
γ ($degrees$)	+VE	5.04	5.12	5.21	5.29	5.40	5.50	5.62
	-VE	-7.63	-7.70	-7.76	-7.79	-7.80	-7.80	-7.79
P-CG1 (m)		3.86	3.87	3.87	3.88	3.88	3.88	3.89
OS-CG1 (m)		-0.21	-0.22	-0.23	-0.24	-0.26	-0.27	-0.29
P-CG2 (m)		3.59	3.59	3.59	3.60	3.61	3.61	3.62
OS-CG2 (m)		-0.07	-0.08	-0.09	-0.10	-0.11	-0.13	-0.15
α_{11} ($degrees$)	+VE	7.85	7.91	7.96	8.02	8.07	8.12	8.17
	-VE	-3.59	-7.72	-3.86	-4.02	-4.21	-4.43	-4.67
α_{12} ($degrees$)	+VE	2.32	2.44	2.54	2.64	2.72	2.79	2.85
	-VE	-1.29	-1.35	-1.40	-1.45	-1.51	-1.58	-1.66
α_{13} ($degrees$)	+VE	3.42	2.52	3.61	3.68	3.75	3.80	3.84
	-VE	-2.11	-2.16	-2.21	-2.28	-2.34	-2.42	-2.50
α_{21} ($degrees$)	+VE	2.08	2.04	2.00	1.95	1.89	1.82	1.75
	-VE	-1.05	-1.06	-1.07	-1.08	-1.09	-1.11	-1.12
α_{22} ($degrees$)	+VE	2.83	2.79	2.74	2.68	2.60	2.52	2.44
	-VE	-1.55	-1.57	-1.58	-1.59	-1.61	-1.63	-1.64
α_{23} ($degrees$)	+VE	3.61	3.56	3.50	3.42	3.33	3.24	3.14
	-VE	-2.07	-2.09	-2.11	-2.12	-2.14	-2.16	-2.18

corresponding to C_{SR} = 1200 Ns/m, due to corresponding increase in the front-wheel steer angle.

A comparison of Tables 3.13 and 3.14 suggests that the left-articulation damping can yield considerable improvement in the directional control performance under a left-handed evasive maneuver. The peak values of the directional response parameters of the vehicle employing both articulation dampers (Combination III) are summarized in Table 3.14. From the table it is evident that an increase in articulation damping (C_{SR} and C_{SL}) yields considerably lower peak values of the directional response and thus improves directional performance. A comparison of Tables 3.13 and 3.15 shows the influence of two articulation dampers (Combination III) is quite similar to that of the left-damper (Combination I), while the implementation of both dampers yields slight further reduction in the peak values.

The peak values of directional response quantities of the conventional and damped vehicle, subject to an evasive maneuver at 80 km/h, also exhibit similar influence of the articulation damping. The peak values of the response parameters, however, are lower than those encountered during the evasive maneuver conducted at 100 km/h, as evident in Tables 3.16 to 3.18. The transient response characteristics of the articulated vehicle are thus presented and discussed for an evasive maneuver at 100 km/h.

The forces and moments developed by the articulation dampers affect the transient response of both tractor and semitrailer in a considerable manner, as illustrated in Figures 3.19 to 3.26. The influence of articulation damping on the lateral acceleration response of sprung weights of the tractor and semitrailer subjected to an evasive maneuver is demonstrated in Figure 3.19. The lateral acceleration response of the vehicle with damped articulation is similar to that with conventional articulation during the initial period of the maneuver (t < 2s). The low steer angle in this period yields lower side-slip angle, cornering force, and low velocities across the dampers. The resulting damping forces

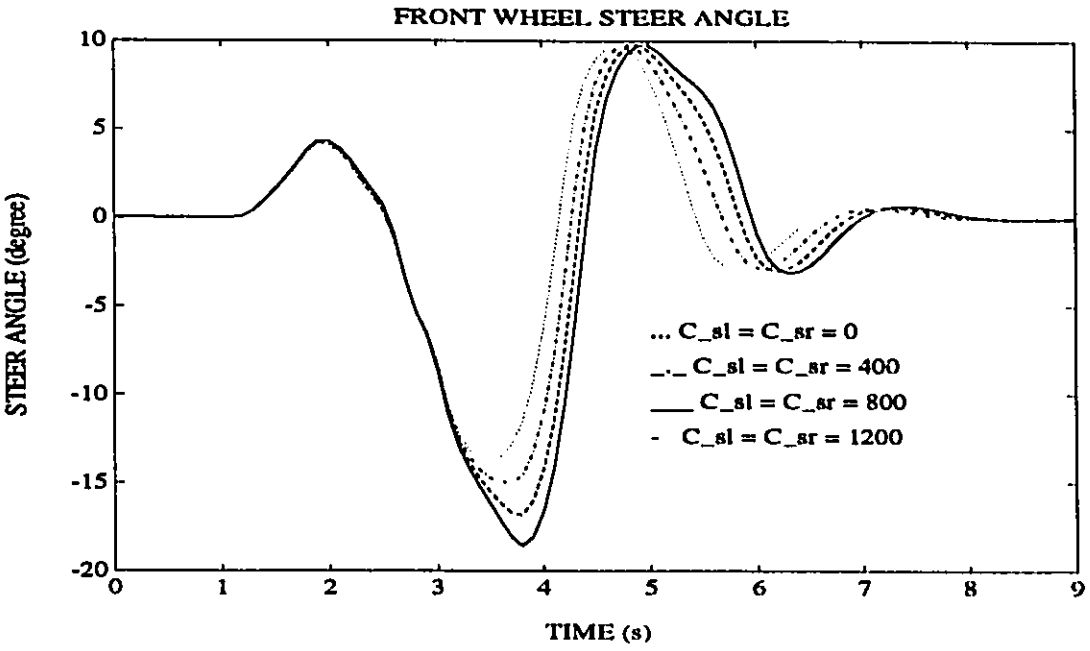

Figure 3.18: Front Wheel Steer Angle required to perform an Evasive Maneuver at 100 km/h

and moments are low and thus do not influence the vehicle lateral acceleration. The influence of articulation damping on lateral velocity, yaw velocity, articulation angle, vehicle path and side-slip angles is also insignificant during this intial period of the directional maneuver, as shown in Figures 3.20 to 3.26. As the front-wheel steer angle is increased, the corresponding increase in the velocities and thus the damping forces reduces the peak values of lateral acceleration, and yaw and lateral velocities. The corresponding side-slip angles of tires approach the nonlinear regime (> 4 degrees) as evident in Figures 3.24 to 3.26.

The peak values of the response parameters during both lane-change and evasive maneuvers decrease with increase in the articulation damping coefficients, while the settling time increases slightly. While the lateral acceleration of tractor and semitrailer of the vehicle with damped articulation are 8% and 16%, respectively, lower than those encountered by the vehicle with conventional articulation, the influence of articulation on

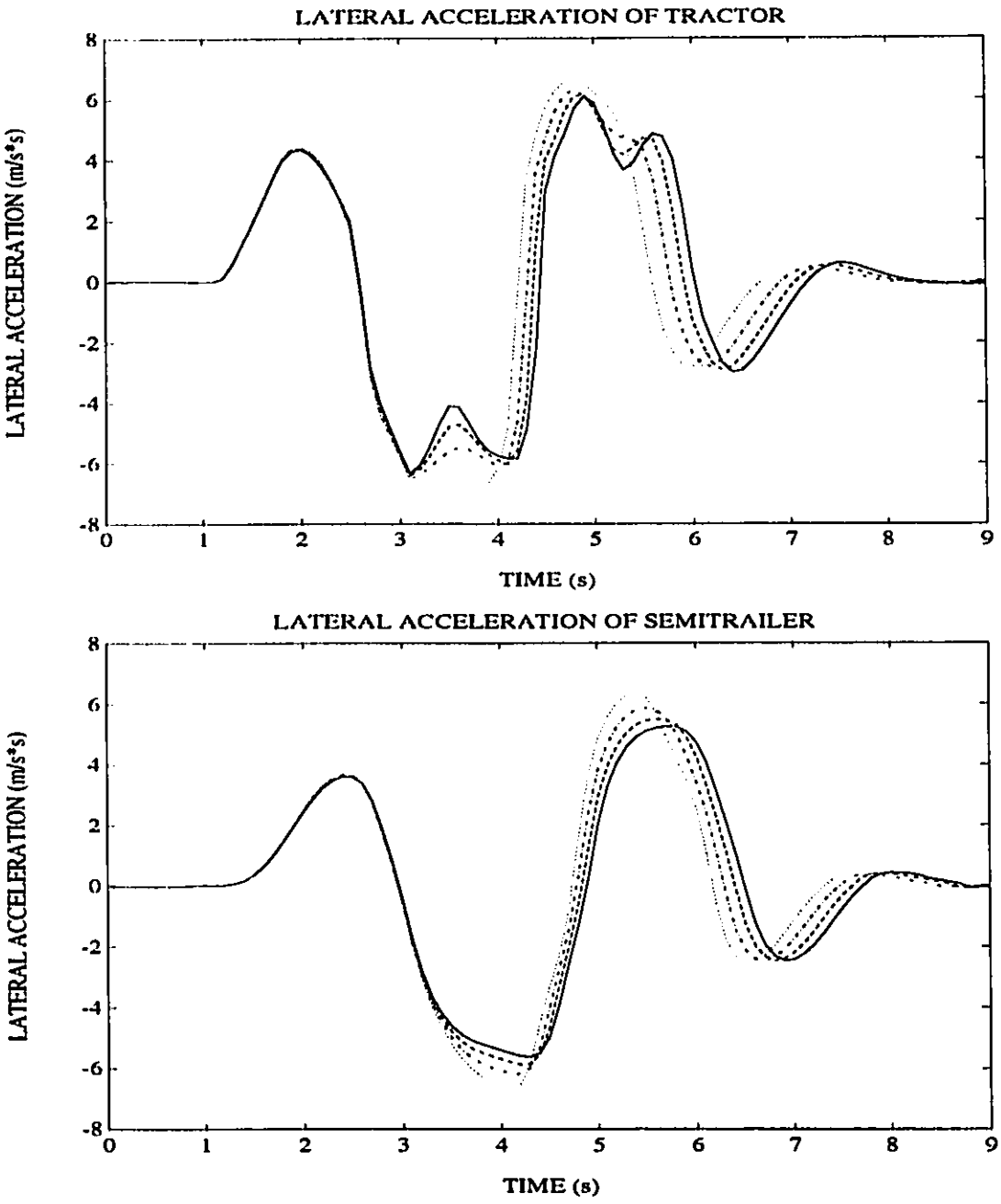

Figure 3.19: Lateral Acceleration Response of Tractor and Semitrailer for an Evasive Maneuver at 100 km/h

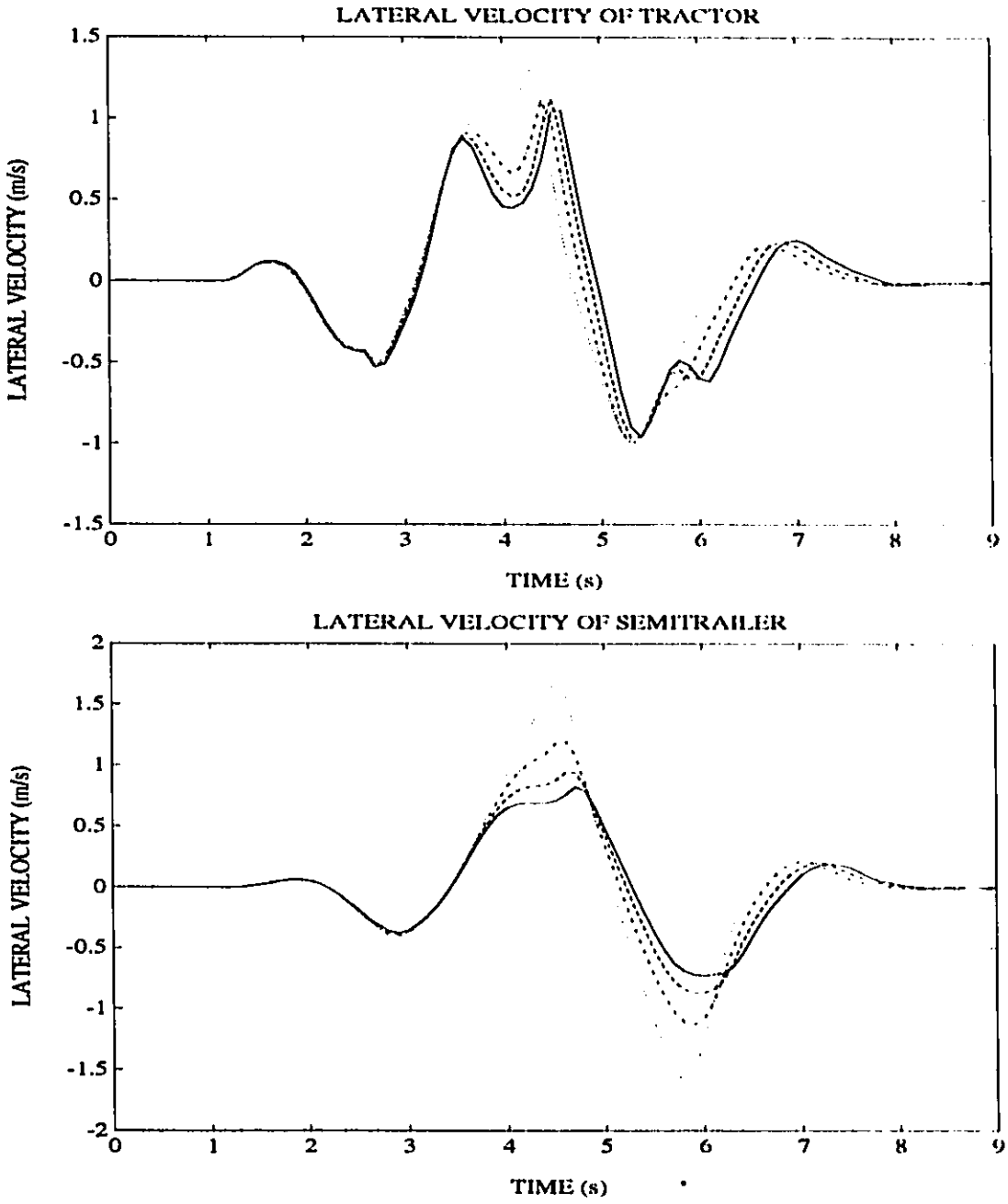

Figure 3.20: Lateral Velocity Response of Tractor and Semitrailer for an Evasive Maneuver at 100 km/h

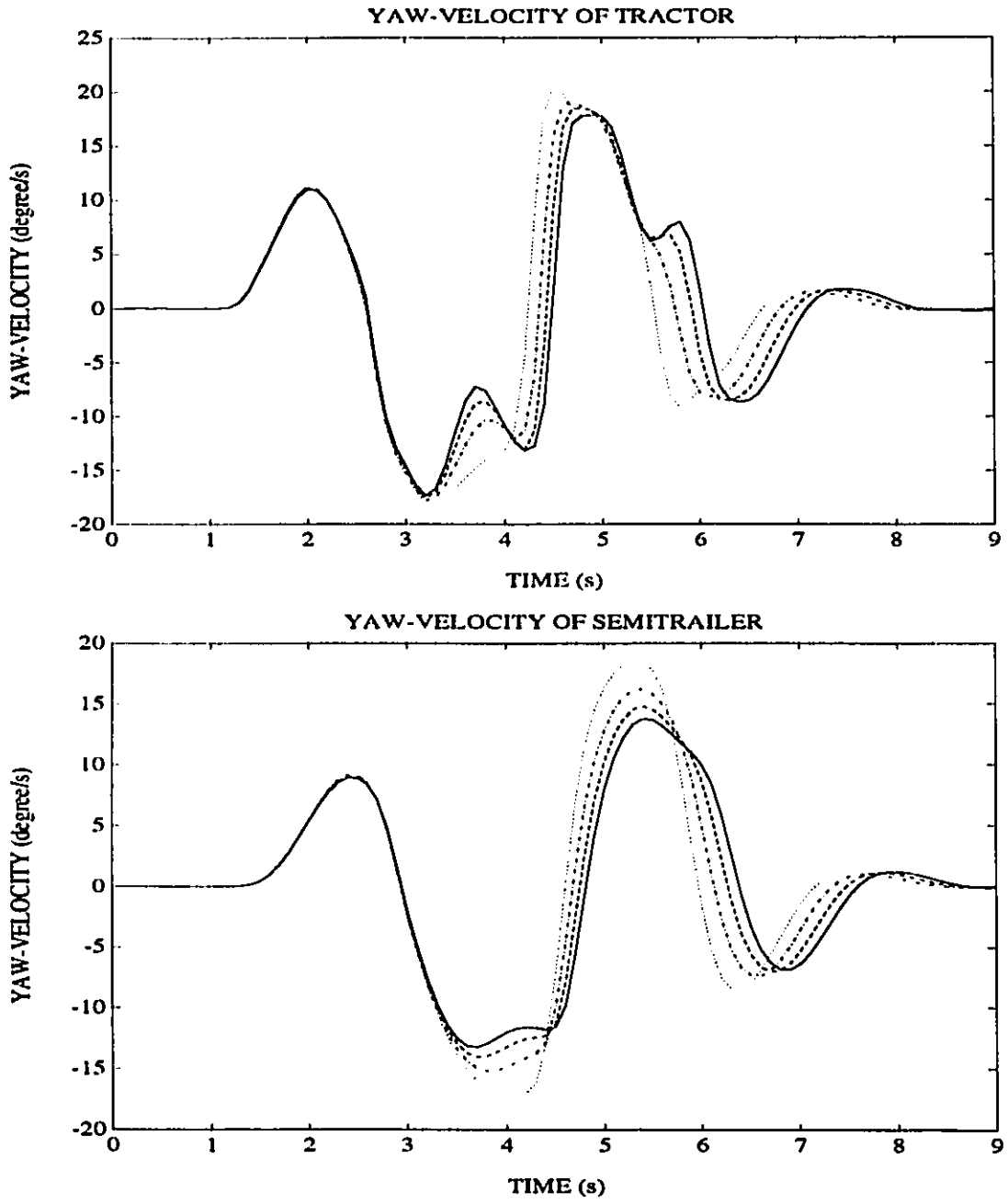

Figure 3.21: Yaw-Velocity Response of Tractor and Semitrailer for an Evasive Maneuver at 100 km/h

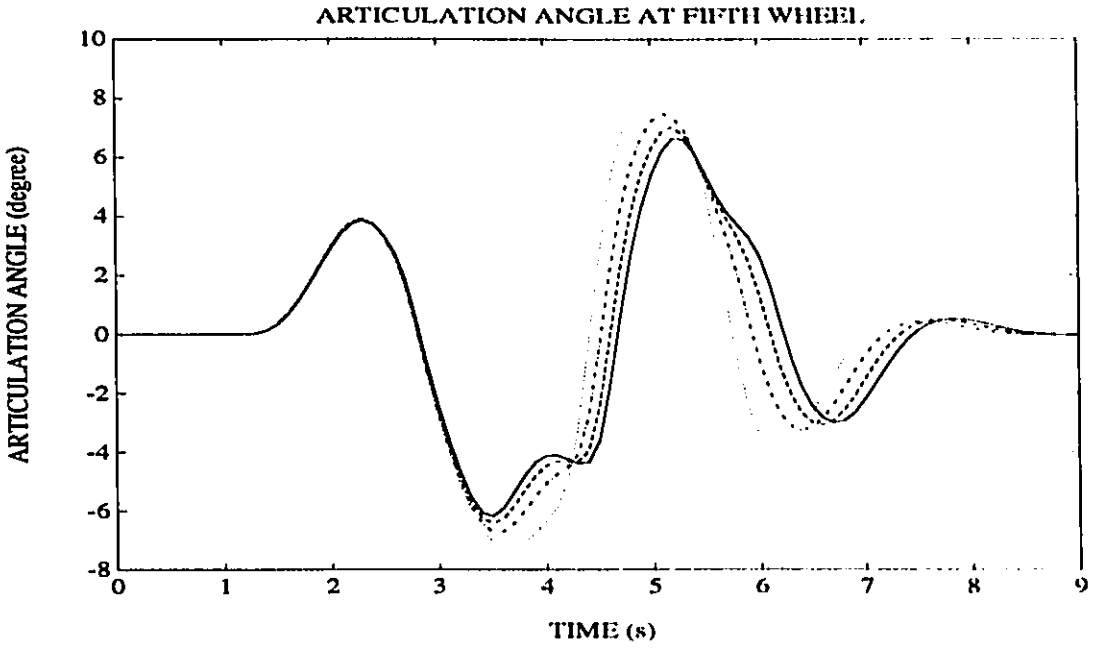

Figure 3.22: Articulation Angle Response of Vehicle for an Evasive Maneuver at 100 km/h

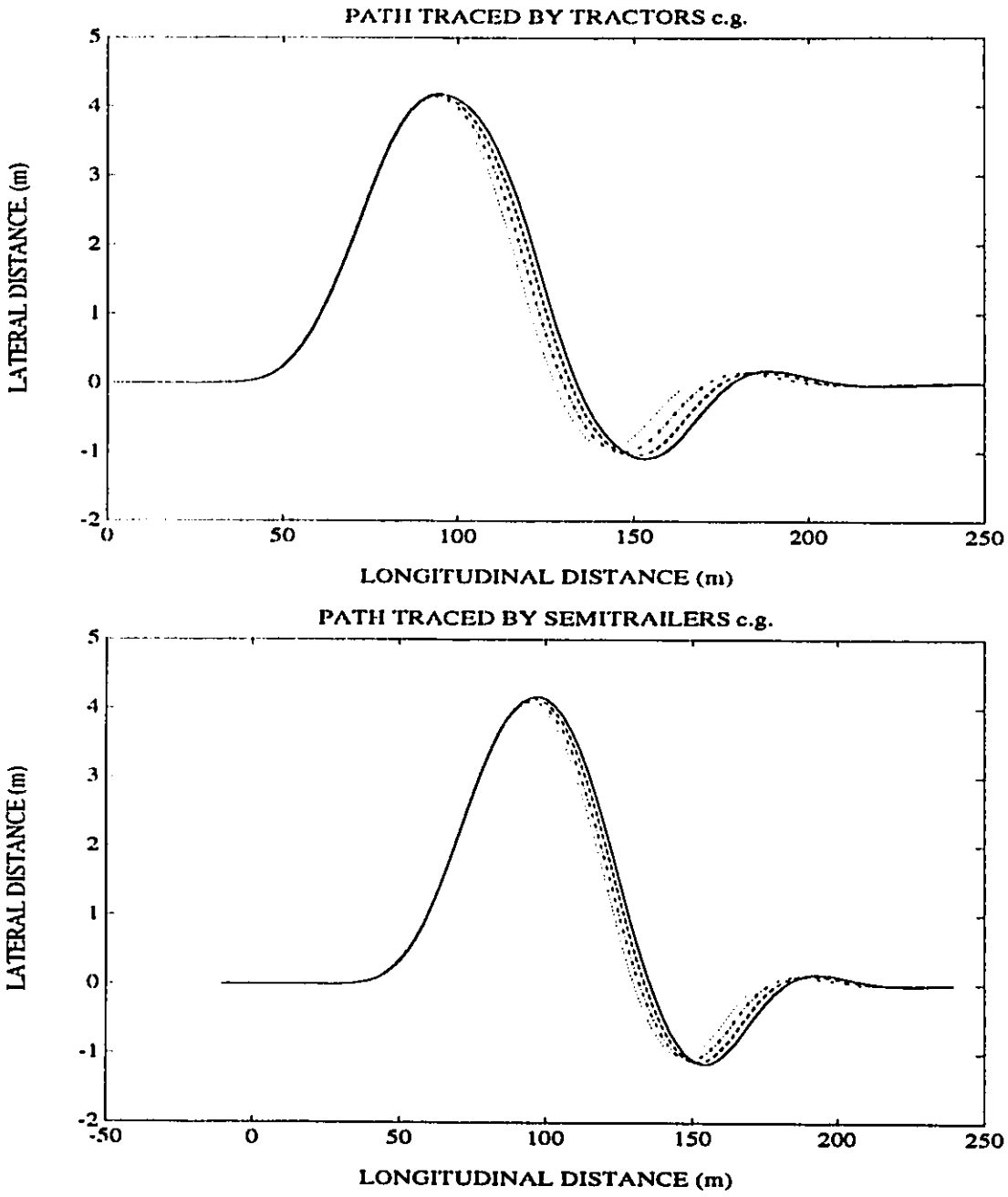

Figure 3.23: Path followed by the Tractor and Semitrailer for an Evasive Maneuver at 100 km/h

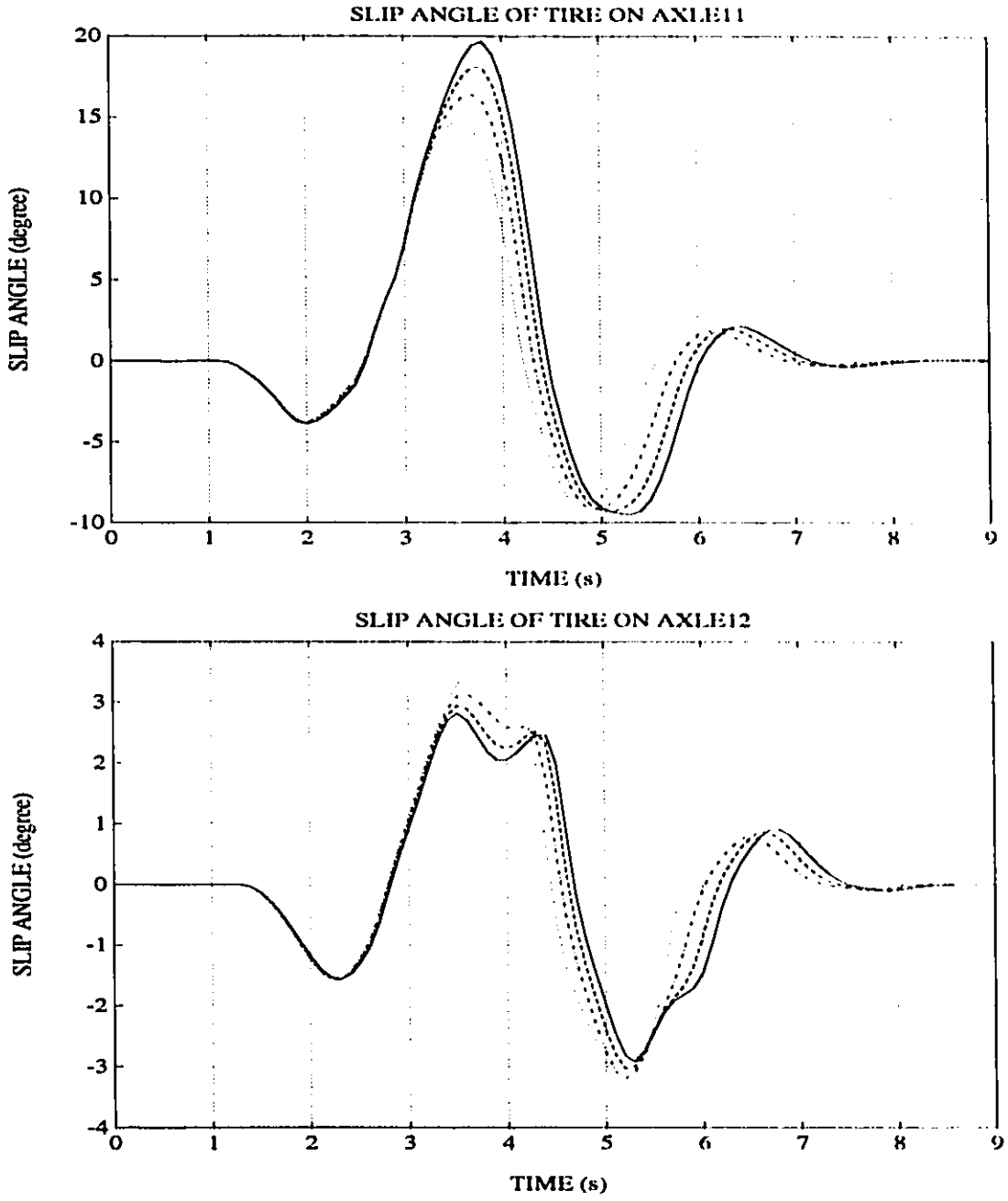

Figure 3.24: Side-Slip Angles of tires on Axles 11 and 12 of Articulated vehicle for an Evasive Maneuver at 100 km/h

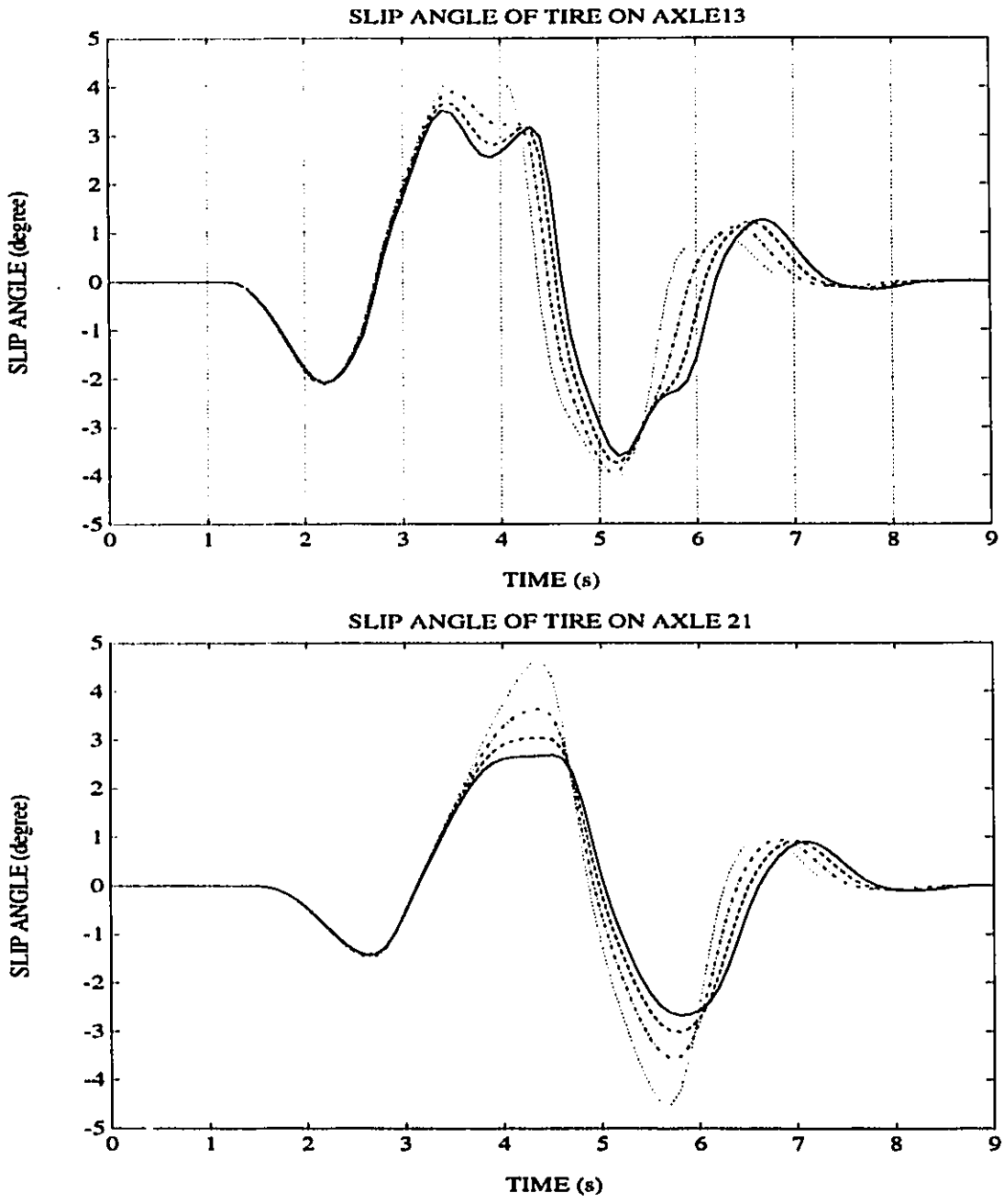

Figure 3.25: Side-Slip Angles of tires on Axles 13 and 21 of Articulated vehicle for an Evasive Maneuver at 100 km/h

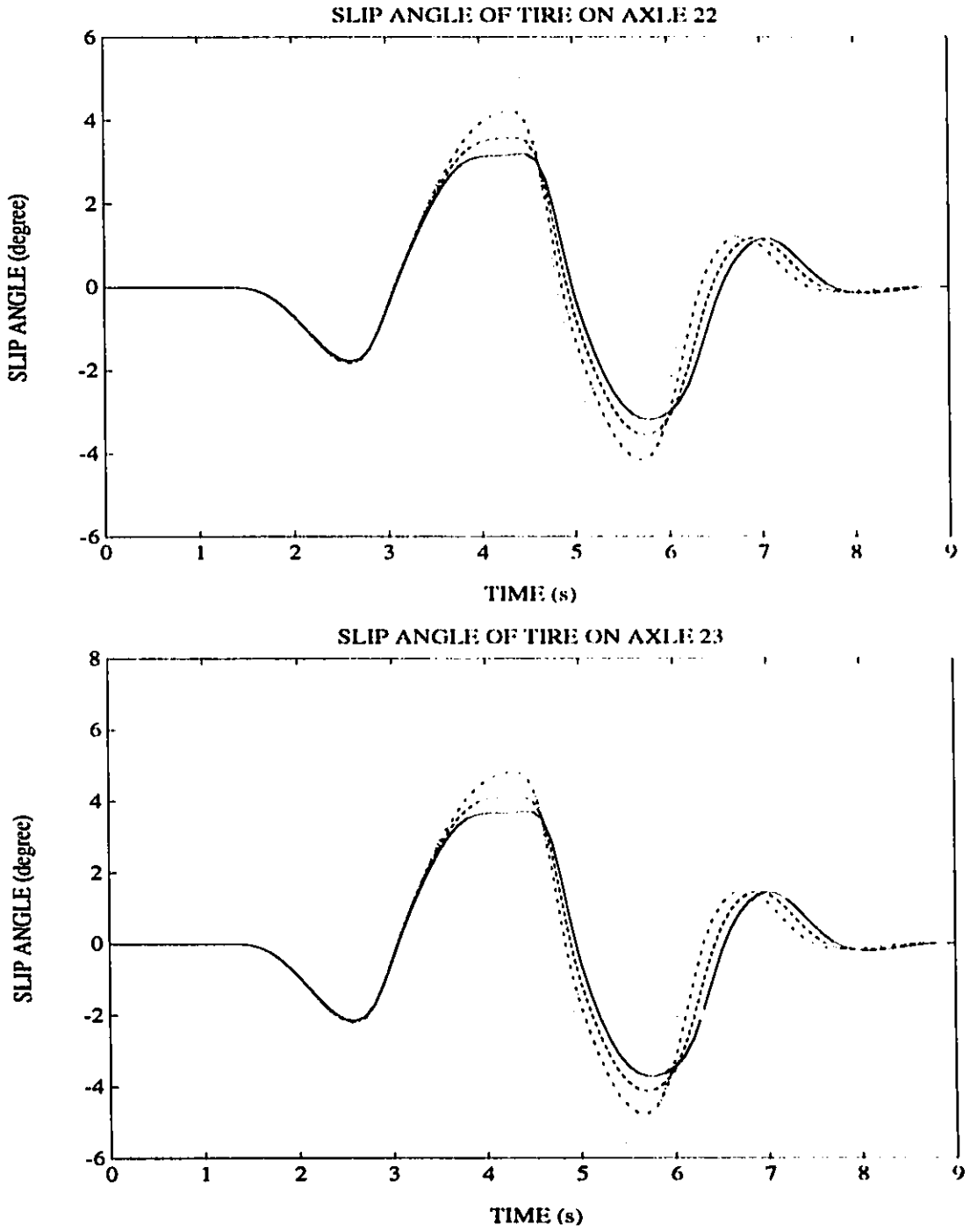

Figure 3.26: Side-Slip Angles of tires on Axles 22 and 23 of Articulated vehicle for an Evasive Maneuver at 100 km/h

the lateral and yaw velocity oscillations are far more significant, as shown in Figure 3.20 and 3.21, respectively. The magnitude of peak lateral velocity oscillation of the semitrailer of the vehicle with damped articulation (C_{SL} = C_{SR} = 1200 Ns/m) is approximately 51% lower than that of the vehicle with conventional articulation. The peak amplitude of yaw velocity oscillations of the damped vehicle is approximately 26% lower than the conventional vehicle, as shown in Figure 3.21. These figures suggest that the amplitudes of yaw and lateral oscillations of the semitrailer can be considerably reduced by the articulation damping.

An increase in articulation damping also reduces the peak amplitude of articulation angle response as shown in Figure 3.22. The vehicle thus experiences slightly larger overshoot, specifically during the correction phase of steering, as evident from the path prescribed by the tractor and semitrailer shown in Figure 3.23. The lateral overshoot distances of the tractor and semitrailer with articulation dampers (C_{SL} = C_{SR} = 1200 Ns/m) are observed to be 0.15 m and 0.13 m, respectively, higher than those of the conventional vehicle. The side-slip angles of the tires on axles of tractor and semitrailer decreases considerably with increase in the left- and right-articulation damping, except for the side-slip angle of tires on axle 11 as shown in Figures 3.24 to 3.26. The side-slip angle of the tires on the steered axle 11 increases with articulation damping, primarily, due to increased steer angle required to perform the maneuvers as shown in Figure 3.16.

3.6 Summary

The steady-state and transient directional response characteristics of the articulated vehicle with articulation dampers are investigated. The directional response characteristics of the vehicle are compared to those of a conventional vehicle to highlight the influence of articulation damping. The effect of articulation damping on the steady-state and transient directional response is investigated for constant steer, lane-change and evasive maneuvers

at different speeds. The results of the study showed that the lateral damping force and yaw damping moment generated by the articulation dampers help to reduce the transient lateral and yaw oscillations of the vehicle encountered during high speed directional maneuvers.

Chapter 4

Dynamic Response of the Vehicle with Forced-Steering Axle

4.1 General

The low-speed maneuverability and high-speed directional stability of freight vehicles have been adversely influenced by increased weights and dimension, and introduction of multi-axle semitrailers. Conventional articulated vehicles with steering at the tractor's front axle alone yield excessive offtracking, tire scrub and wear, strain on the suspension components and poor fuel economy. Air-lift axles have been used to improve the maneuverability and to reduce the rate of tire wear during cornering maneuvers. The increase in weight on the remaining axles caused by the lifted axle, however, yield premature damage to the pavement. Alternatively, self- or forced-steering axles have been proposed to increase the maneuverability limits and to reduce the rate of tire wear. While the self-steering axles provide improved maneuverability and eliminate the excessive road damage caused by drop axles, lower lateral cornering forces generated by these axles decreases the directional stability and control of the vehicle.

A number of force-steering algorithms relating the vehicle response quantities to

the angle of wheels of the steerable axle are formulated, and integrated to the nonlinear yaw-plane model of the vehicle, presented in Chapter 2. The influence of force-steering on both the low-speed maneuverability and high-speed directional control of the articulated vehicle is investigated for different algorithms. The results are discussed in view of the conflicting requirements corresponding to low- and high-speed maneuvers.

4.2 Control Schemes

Different forced-steering control schemes are formulated to study their performance potentials related to low-speed maneuverability and high-speed directional dynamics [39,41,42]. Assuming proportional control laws and negligible delays, the wheel angle of the forced-steered axle is related to one or more response quantities of the vehicle. The directional characteristics of the vehicle are first investigated using a single control variable feedback to establish the influence of independent variables. Articulated buses have employed forced-steered axles at the trailing unit, where the wheel angle is generated proportional to the articulation angle [39]. In light vehicles, the rear wheel angle is frequently generated in portion with the front wheel steer angle. The control schemes based on single variable control are thus formulated as a function of front wheel steer angle (δ), articulation angle (γ) and articulation rate ($\dot{\gamma}$):

$$\text{Scheme A: } \delta_{FSi} = K_{1i}\,\delta$$

$$\text{Scheme B: } \delta_{FSi} = K_{2i}\,\gamma$$

$$\text{Scheme C: } \delta_{FSi} = K_{3i}\,\dot{\gamma} \qquad (4.1)$$

Where, δ_{FSi} is the wheel angle of the forced-steering axle i, and i = 1, 2, 3 represent the axles 21,22 and 23 of the semitrailer, respectively. K_{1i}, K_{2i} and K_{3i} are the proportional front wheel steer, articulation and articulation rate gains, respectively. Few studies

reported on the performance characteristics of forced-steering axles have indicated conflicting requirements for low-speed maneuverability and high-speed directional dynamics. The angle of the wheels on the semitrailer axle needs to be in a direction opposite to the tractor's front wheel angle in order to achieve improved low-speed manoeuvrability, off-tracking and reduced rate of tire wear [41,42]. The semitrailer axle wheel angle at high-speeds, however, needs to be in the same direction as the tractor's front wheel in order to achieve improved directional stability limits [41,42]. The forced-steering control algorithms thus must be formulated as a function of vehicle speed, such that requirements at low as well as high-speeds may be realized.

The directional performance characteristics of the articulated vehicle with forced-steering axles are investigated for control schemes based on feedback from combination of response quantities and vehicle speed. Four different schemes are formulated to achieve the forced steering angle of the steered axle:

$$\text{Scheme I: } \delta_{FSi} = K_{1i}\,\delta + K_{2i}\,\gamma$$

$$\text{Scheme II: } \delta_{FSi} = K_{2i}\,\gamma + K_{5i}\,U\,\dot{\gamma}$$

$$\text{Scheme III: } \delta_{FSi} = K_{1i}\,\delta + K_{4i}\,U\,\gamma$$

$$\text{Scheme IV: } \delta_{FSi} = K_{2i}\,\gamma + K_{4i}\,U\,\gamma \qquad (4.2)$$

4.3 Performance Criteria

The parameters and dimension of the six-axle articulated vehicle considered in the study have been presented in Table 3.1. The nonlinear cornering properties of tires have been described in Section 2.3.1. The location of axle 21 is derived from the simulation results

discussed in Chapter 3. The axle 21 located 1.22 m ahead of axle 22, yields lowest amplitudes of yaw and lateral oscillation, and side-slip angles of tires on all the axles. This finding is further supported by the studies reported in the literature [41].

The directional response characteristics of the six-axle tractor-semitrailer, equipped with a forced steering axle, is investigated for steady and transient steer inputs. The directional response characteristics are assessed in terms of low- and medium-speed manoeuvrability, and medium- and high-speed directional dynamics. The low- and medium-speed maneuverability characteristics of the vehicle are investigated for a constant steer maneuvers (Figure 3.2) at forward speeds of 30 km/h and 50 km/h. The medium- and high-speed directional dynamics of the vehicle are investigated for evasive maneuvers (Figure 3.3) at forward speeds of 50 km/h, 80 km/h and 100 km/h using the path follower model. The low- and medium-speed maneuverability of the vehicle are assessed in terms of steady-state off-tracking, curve radius, side-slip angles, and articulation angle. The medium- and high-speed directional performance of the vehicle are assessed in terms of lateral acceleration, lateral and yaw velocities, articulation angle, path overshoot, and side-slip angles of tires of the semitrailer. A parametric study is carried out to determine the influence of various control gains, on the performance indicates described above.

4.4 Results and Discussion

The steady-state handling and directional dynamics of the articulated vehicle are investigated for a constant steer maneuver of 5^0 at forward speeds of 30 km/h and 50 km/h. The magnitude of the wheel angle (5^0) is selected to achieve a turn radius of approximately 70 m at 50 km/h. The transient directional response characteristics of the vehicle with forced-steering axles are computed for an evasive maneuvers performed at 50 km/h, 80 km/h and 100 km/h. The peak values of the response characteristics of the semitrailer with forced-steering are evaluated for different maneuvers and compared to those of a

conventional vehicle in order to highlight the influence of forced-steering axle.

4.4.1 SCHEME A: Front Wheel Steer Gain

The forced-steered axle angle is varied in proportion to the tractor's front wheel steer angle. The low-speed manoeuvrability and high-speed directional dynamics are evaluated for forced-steering axle replacing the conventional semitrailer axle 21 or 22 or 23. The influence of proportional control gains (K_{11} or K_{12} or K_{13}) on the performance characteristics is presented in terms of steady-state values of the vehicle response quantities. The directional response characteristics of the vehicle with a forced-steering axle are compared to those of the conventional vehicle to highlight the performance potentials of the forced-steering axle.

Figures 4.1 and 4.12 present the steady-state values of directional response quantities related to low-speed manoeuvrability (lateral acceleration, lateral and yaw velocities of the semitrailer, curve radius, off-tracking, and side-slip angles) as a function of the front wheel steer angle gain (K_{11}), when the axle 21 is replaced by a forced-steering axle. The peak lateral acceleration and yaw velocity of the semitrailer increase slightly when negative front wheel steer gain is selected, irrespective of the vehicle speed. The peak lateral velocity decreases with opposite steer control ($K_{11} < 0$). The peak lateral velocity, however, may approach high values for larger negative gains. Although the curve radius and vehicle off-tracking, both decrease, when negative front-wheel steer gain is selected, the corresponding magnitudes of side-slip angles of tires on semitrailer axles increase. This control scheme thus yields increased tire wear rate, decreased off-tracking and lateral oscillations corresponding to low- and medium-speed constant steer maneuvers.

The low- and medium-speed directional response characteristics of the articulated

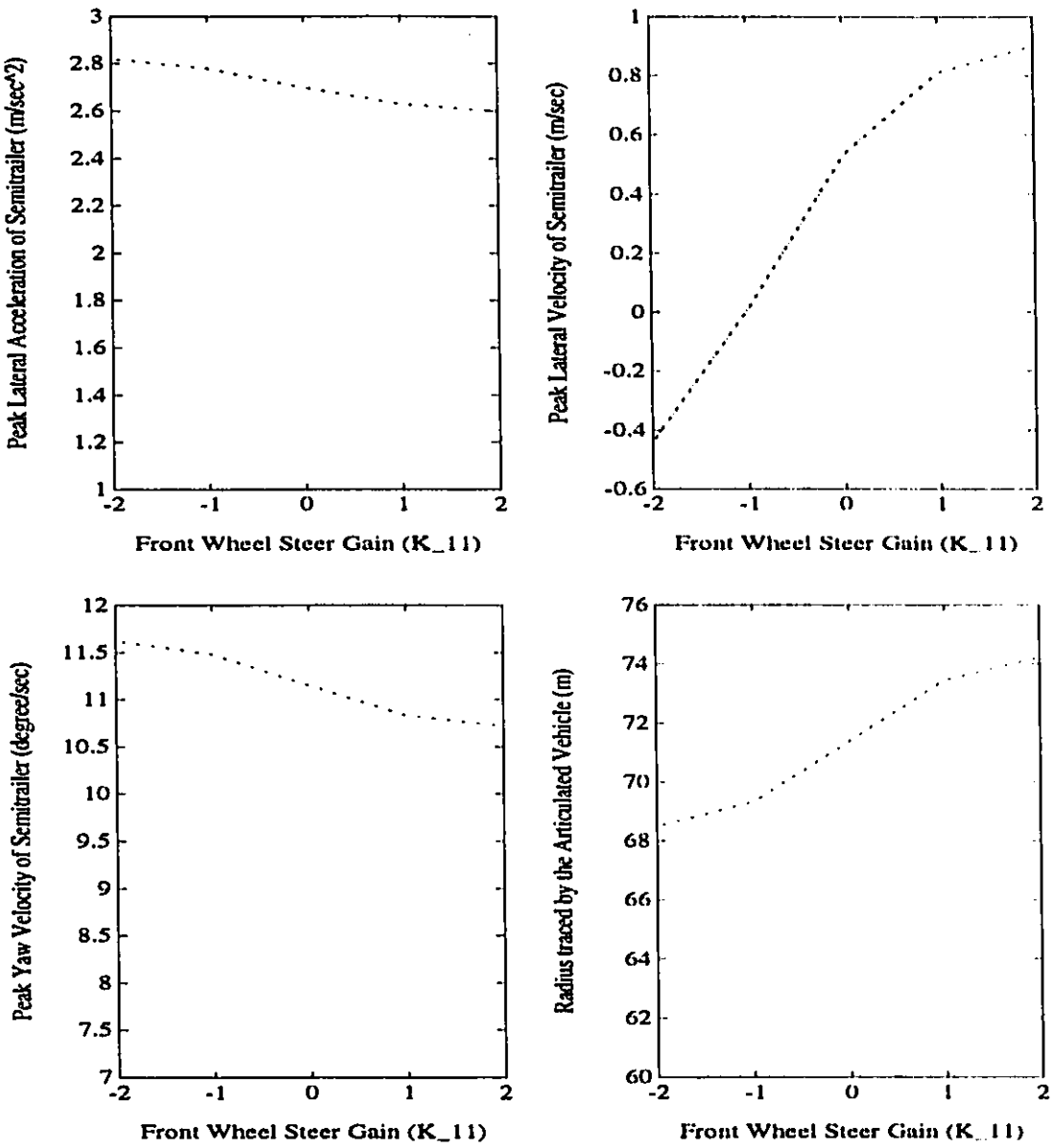

SCHEME A: FORCED-STEERING AXLE 21

Figure 4.1: Influence of front wheel steer gain on the steady-state response (..... 30 km/h; -.-.- 50 km/h)

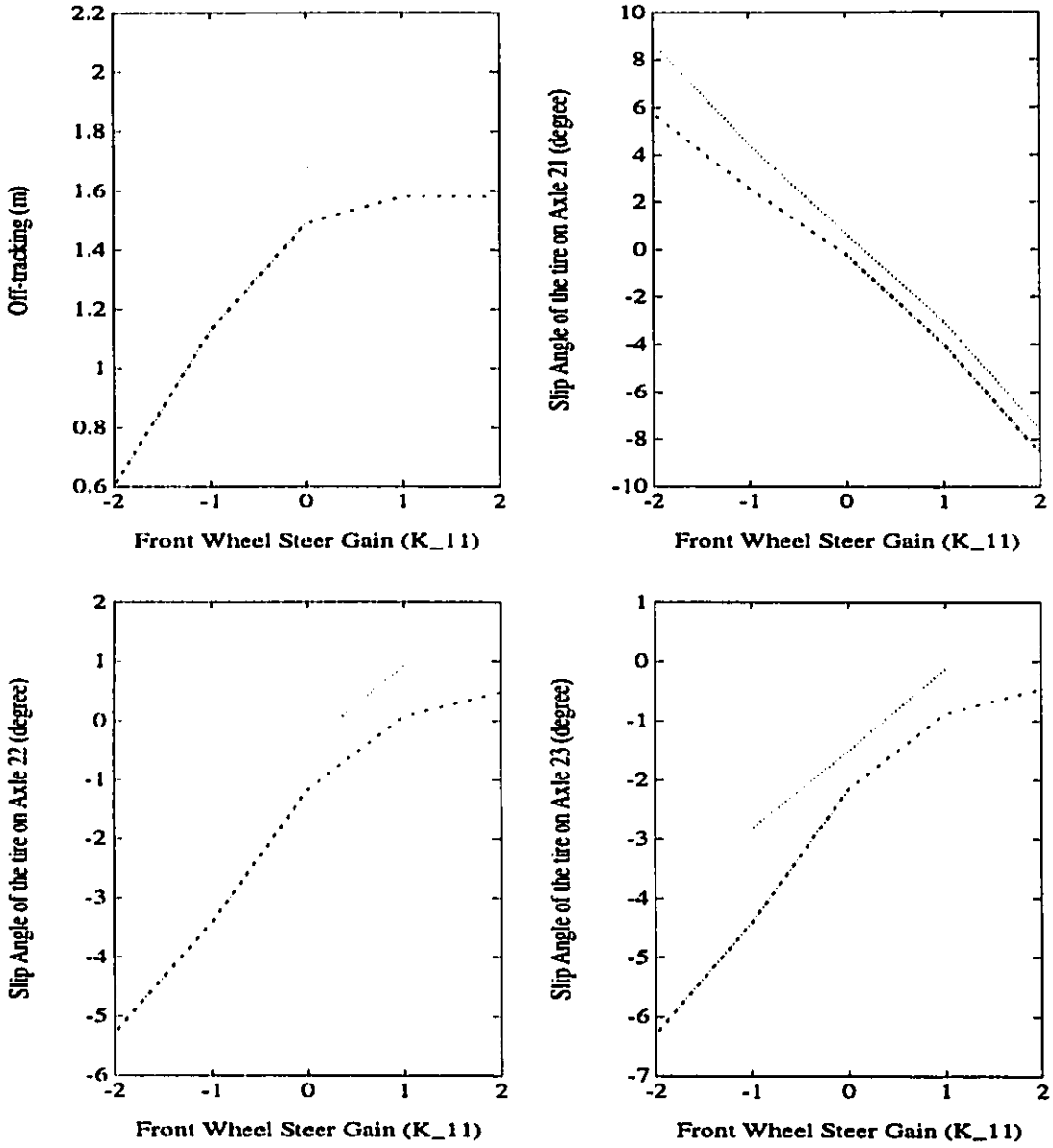

SCHEME A: FORCED-STEERING AXLE 21

Figure 4.2: Influence of front wheel steer gain on the steady-state response (..... 30 km/h; -.-.- 50 km/h)

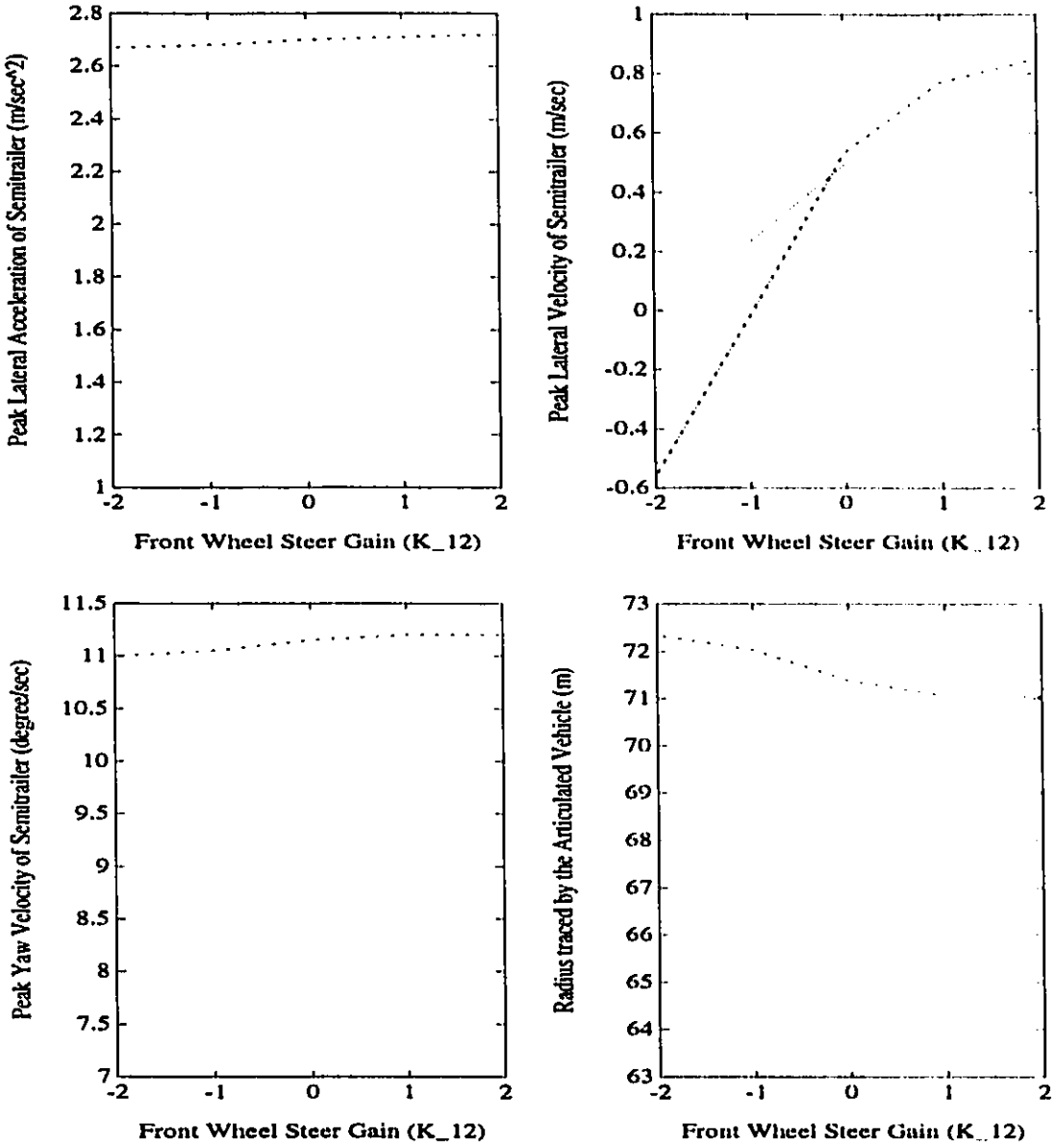

SCHEME A: FORCED-STEERING AXLE 22

Figure 4.3: Influence of front wheel steer gain on the steady-state response (..... 30 km/h; -.-.- 50 km/h)

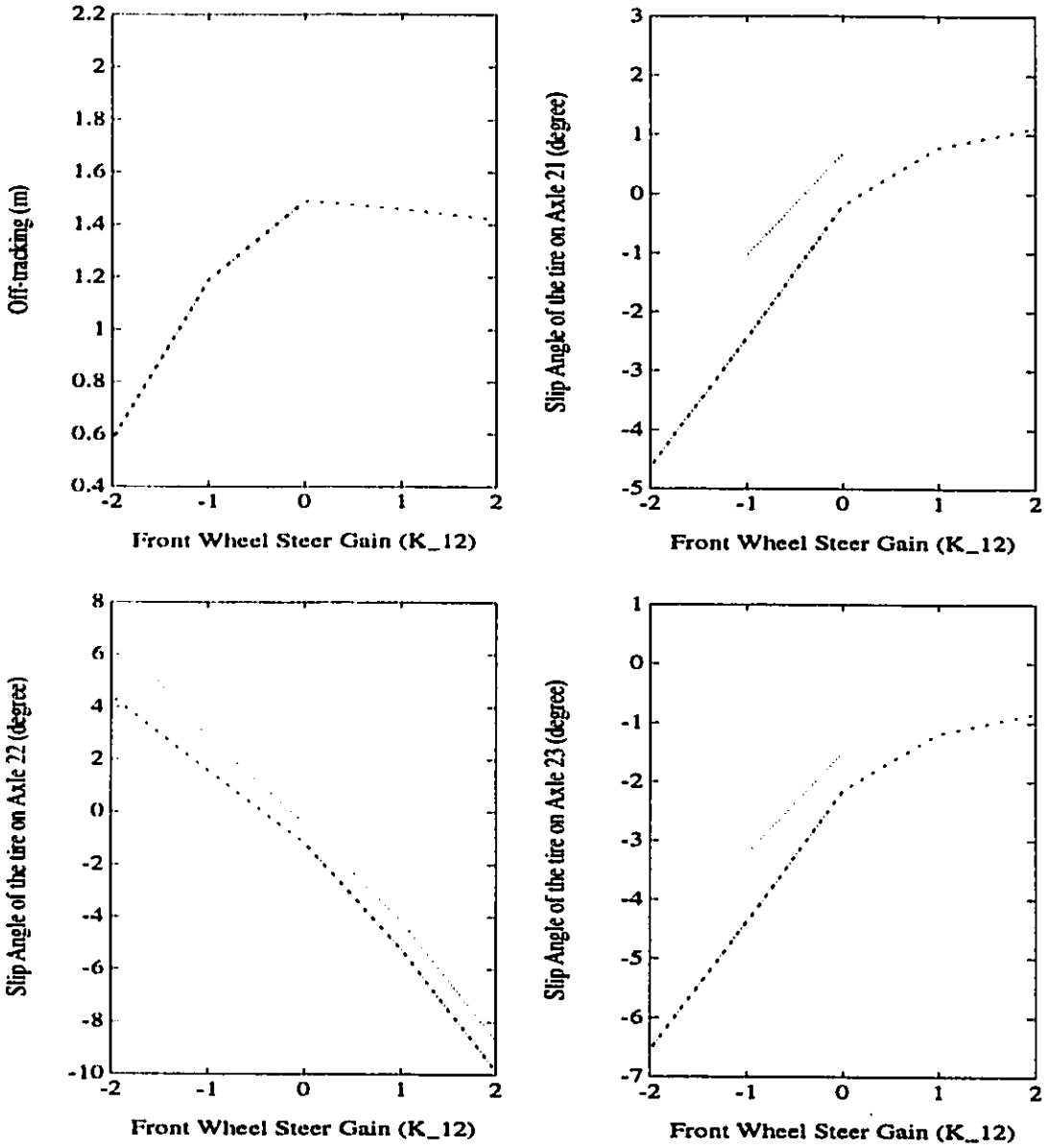

SCHEME A: FORCED-STEERING AXLE 22

Figure 4.4: Influence of front wheel steer gain on the steady-state response (..... 30 km/h; -.-.- 50 km/h)

vehicle with a force-steering axle located at 22 are summarized in Figures 4.3 and 4.4. The figures reveal that the lateral acceleration and yaw velocity of the semitrailer vary only slightly with variation in the control gain (K_{12}), irrespective of the vehicle speed. The lateral velocity response of the semitrailer decreases with negative values of the proportional gain. At forward speed of 50 km/h, the peak lateral velocity approaches high values for $K_{12} < -2$. The curve radius of the semitrailer, however, increases slightly for negative values of the gain K_{12}. Although, the negative gain values yield low off-tracking, the side-slip angles of tires on all the axles increase. A comparison of peak response values of vehicles with force-steering axle located at 21 (Figures 4.1 and 4.2) and 22 (Figures 4.3 and 4.4) reveals that the influence of forced-steering axle located at 22 is less significant than that located at 21. The force-steering axle located at 22 also yields larger turning radius of the semitrailer.

Figures 4.5 and 4.6 present the steady-state response parameters of the semitrailer under constant steer maneuvers when conventional axle 23 is replaced by the forced-steering axle. The peak response values vary with the control gain K_{13} in a similar manner, as discussed above. The variations in lateral acceleration and yaw velocity are observed to be small, as shown in Figure 4.5. The lateral velocity response of the semitrailer tends to decrease with negative gain values at vehicle speed 30 km/h. The lateral velocity response at 50 km/h also tends to decrease with negative values of gain K_{13}, provided the magnitude of the gain is low. The curve radius of the vehicle increases (approximately 4m) for negative values of front wheel steer gain K_{13}. Although the vehicle off-tracking decreases irrespective of the direction of the forced-steering axle, the reduction is more significant for negative steer gain.

The influence of front wheel steer gain (K_{1i}) and the location of the forced-steering axle on the directional response characteristics are further investigated for an evasive maneuver performed at 50 km/h, 80 km/h and 100 km/h. Figures 4.7 to 4.12 present the peak response values for different control gains and locations of the forced-

steering axle. The peak semitrailer lateral acceleration tends to decrease only slightly for positive steer gains (K_{1i}) irrespective of the vehicle speed and the location of the forced-steering axle. The negative front-wheel steer gains yield a considerable increase of the peak lateral acceleration, as shown in Figures 4.7, 4.9 and 4.11. The peak lateral acceleration approaches quite high values, well above the lateral acceleration threshold of the vehicle related its roll stability. The peak lateral velocity response of the semitrailer corresponding to high-speed maneuvers (80 km/h and 100 km/h) increases irrespective of the control gain and location of the forced-steering axle. The peak lateral velocity correspond to medium-speed maneuver, however, decreases slightly for negative values of steer gain. Corresponding to high-speed (100 km/h) evasive maneuvers, the peak yaw velocity response increases considerably with the negative values of steer gain, while the variations are insignificant for positive values of the gains. The peak yaw velocity at 50 km/h and 80 km/h also varies only slightly irrespective of the gain values and the location of forced-steering axle.

The maximum overshoot encountered at the completion of the maneuver is strongly related to the vehicle speed as shown in Figures 4.7, 4.9 and 4.11. A conventional vehicle exhibits only small overshoot at medium speeds, and excessively large overshoot at 100 km/h (approximately 1 m) due to increased lateral and yaw oscillations. A positive value of the front wheel steer gain tends to reduce the overshoot encountered at high-speeds, while the overshoot corresponding to medium-speed maneuvers remain almost unaffected. The side-slip angles of tires on all the axles, in general, increase with the front wheel steer gain irrespective of the vehicle speed, values of the control gain and location of the forced-steering axle. The peak values of side-slip angle of tires of the forced-steering axle, however, is observed to be larger than those of the non-steered axle.

The directional response characteristics presented in Figures 4.1 to 4.12 are examined to select the location of the forced-steering axle. The forced-steering axles located at axles 22 or 23 yield larger slip angles of tires, and the forced-steering axle located at

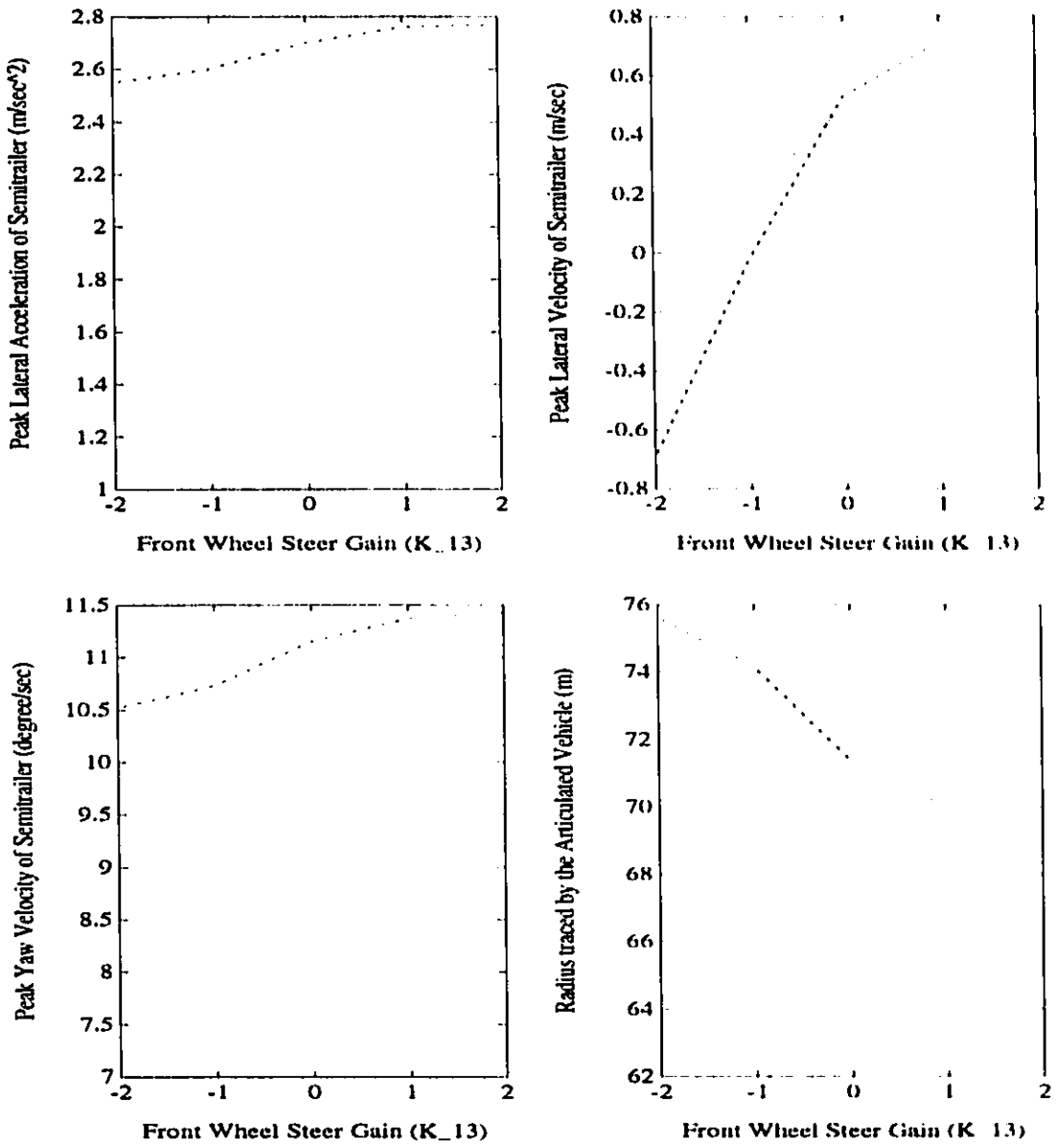

SCHEME A: FORCED-STEERING AXLE 23

Figure 4.5: Influence of front wheel steer gain on the steady-state response (..... 30 km/h; -.-.- 50 km/h)

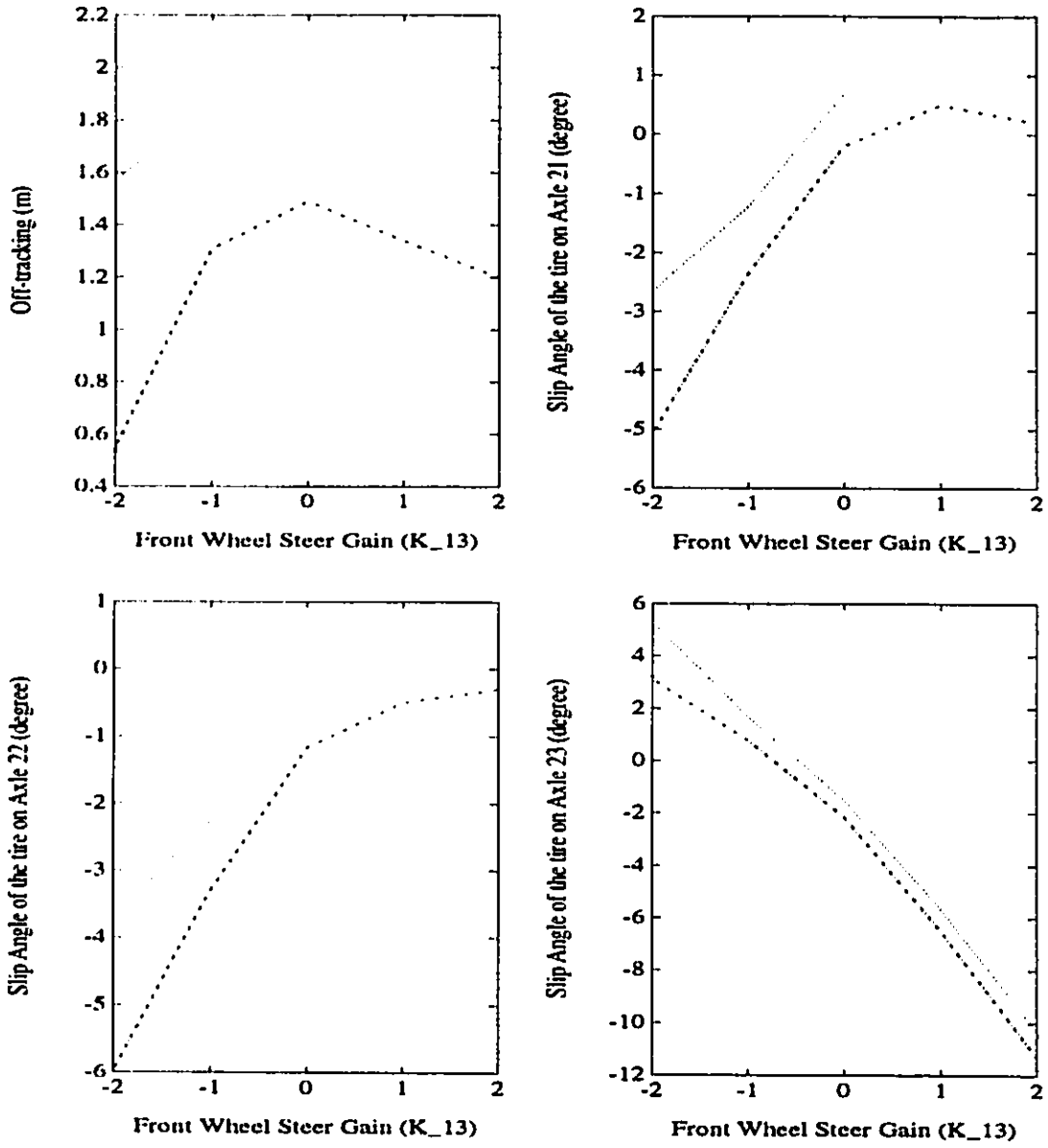

SCHEME A: FORCED-STEERING AXLE 23

Figure 4.6: Influence of front wheel steer gain on the steady-state response (..... 30 km/h; -.-.- 50 km/h)

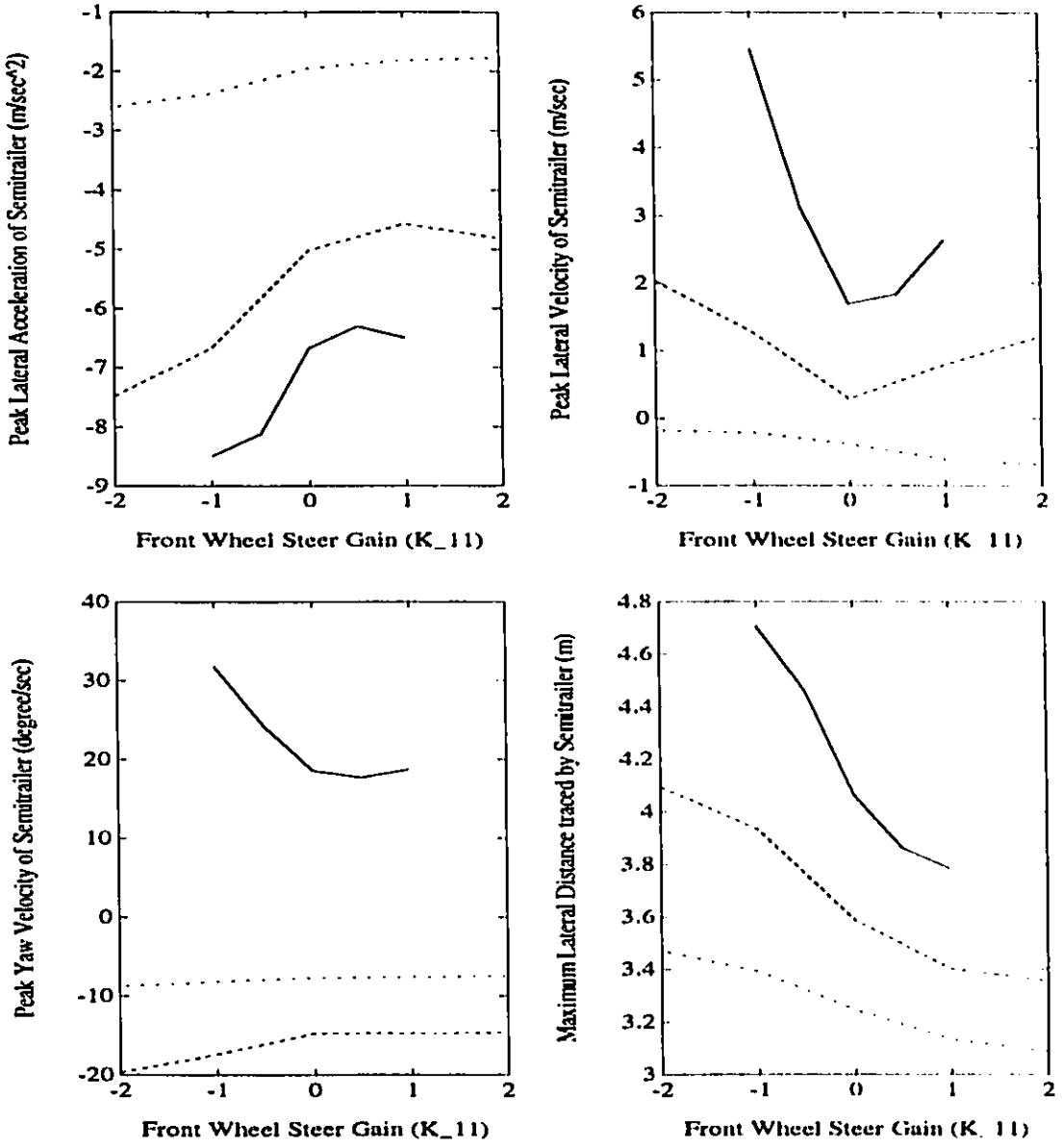

SCHEME A: FORCED-STEERING AXLE 21

Figure 4.7: Influence of front wheel steer gain on the transient response
(-.-.- 50 km/h; - - - 80 km/h; — 100 km/h)

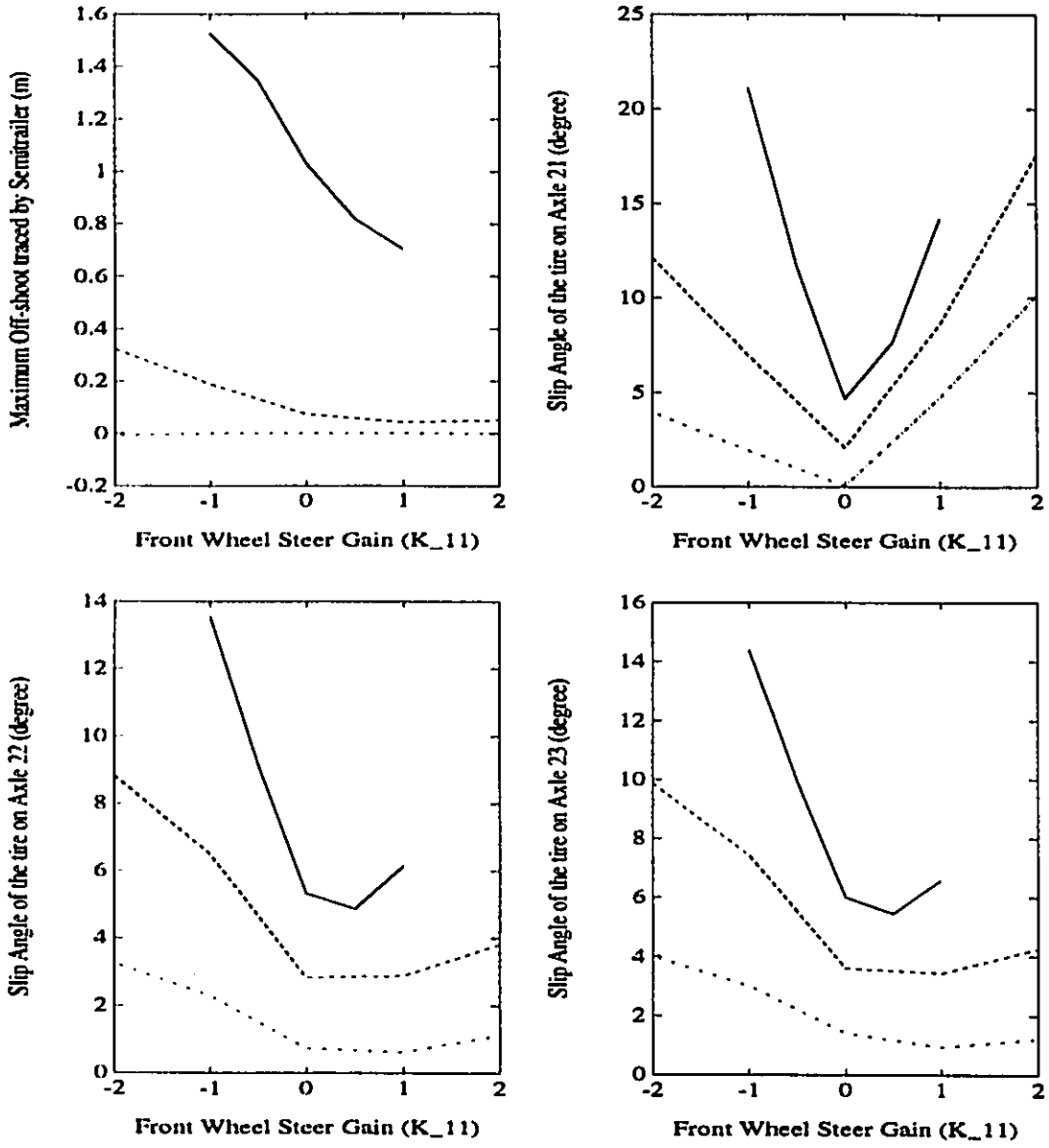

SCHEME A: FORCED-STEERING AXLE 21

Figure 4.8: Influence of front wheel steer gain on the transient response
(-.-.- 50 km/h; - - - 80 km/h; — 100 km/h)

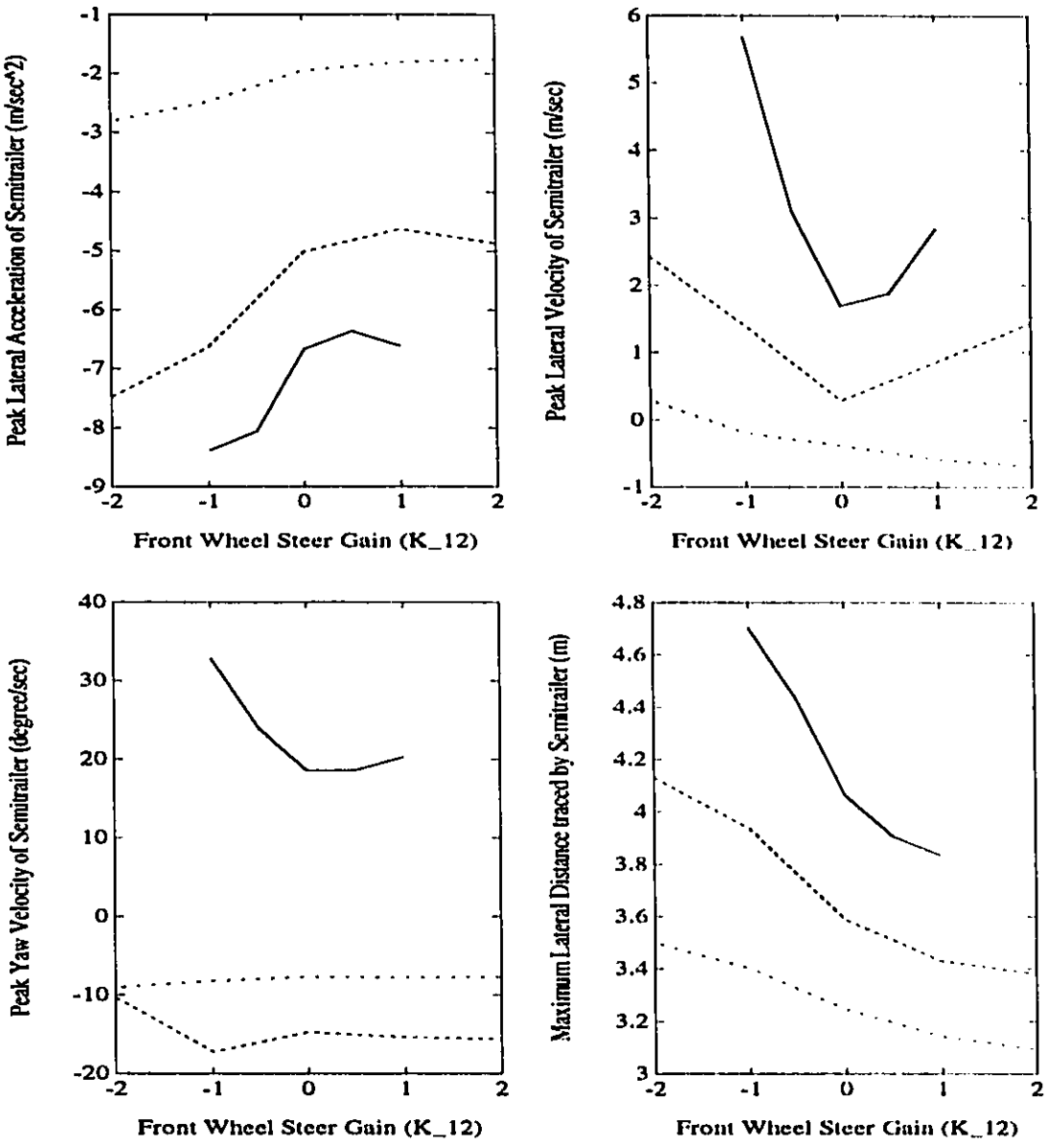

SCHEME A: FORCED-STEERING AXLE 22

Figure 4.9: Influence of front wheel steer gain on the transient response
(-.-.- 50 km/h; - - - 80 km/h; — 100 km/h)

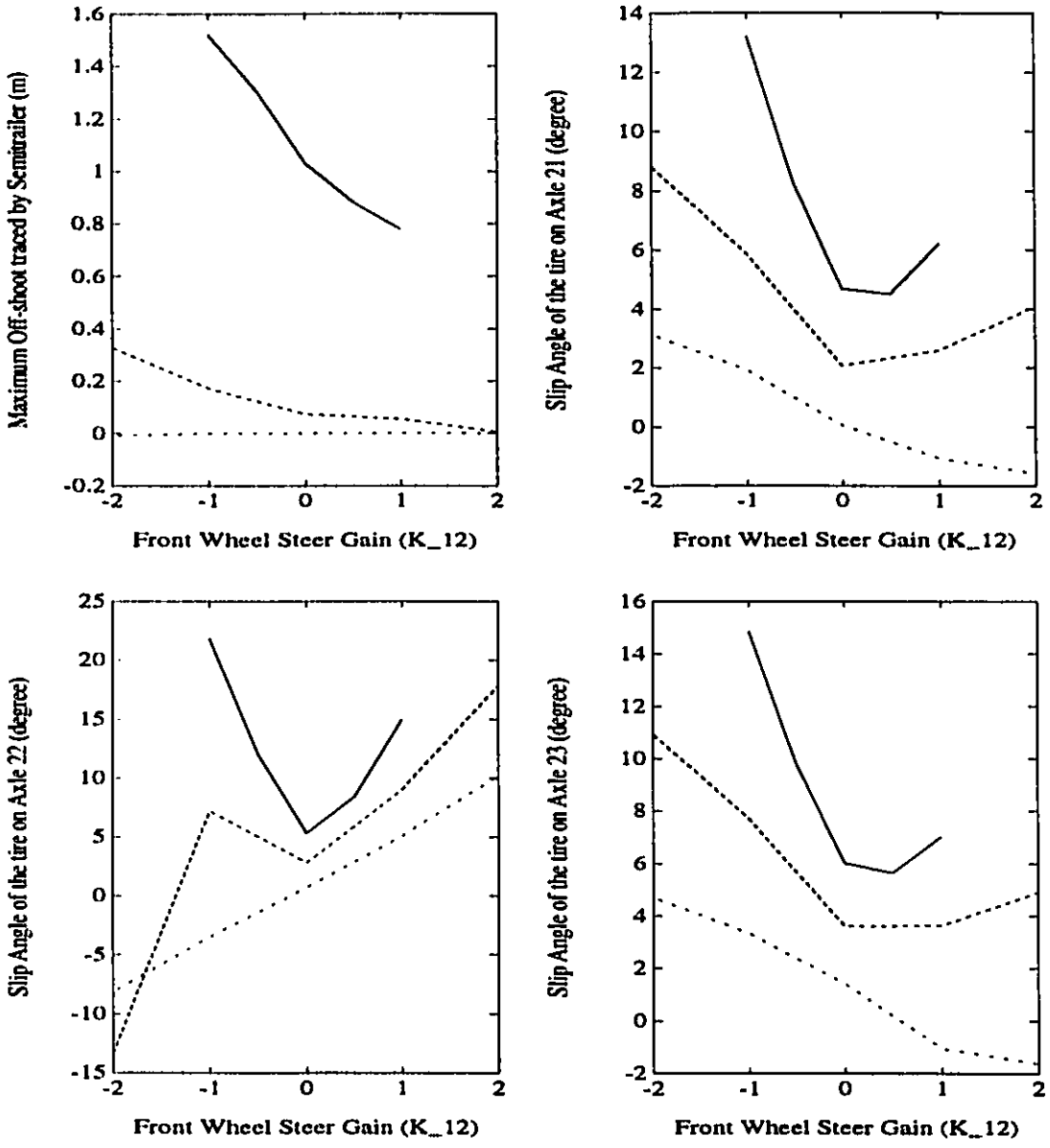

SCHEME A: FORCED-STEERING AXLE 22

Figure 4.10: Influence of front wheel steer gain on the transient response
(-.-.- 50 km/h; - - - 80 km/h; — 100 km/h)

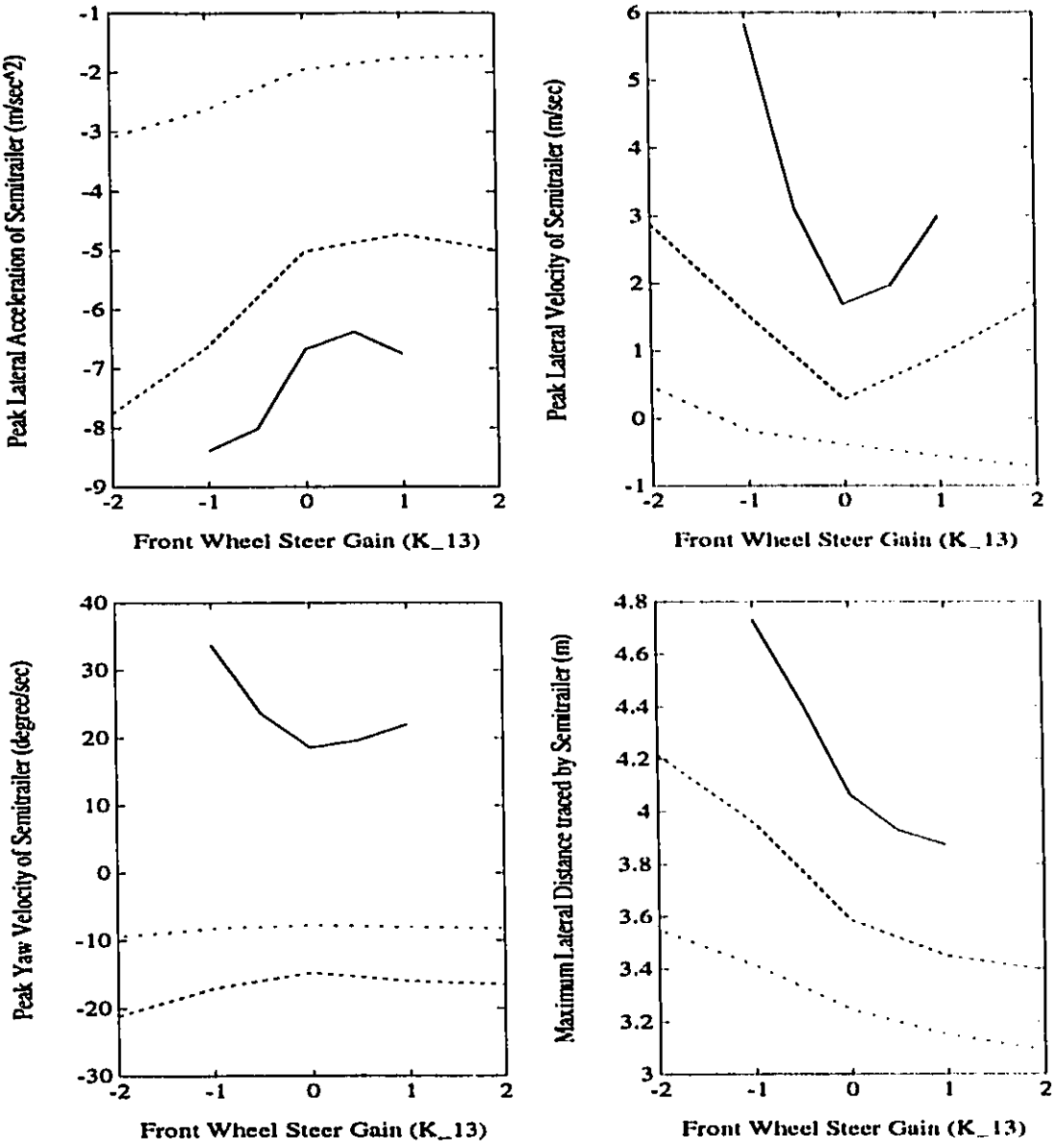

SCHEME A: FORCED-STEERING AXLE 23

Figure 4.11: Influence of front wheel steer gain on the transient response (-.-.- 50 km/h; - - - 80 km/h; — 100 km/h)

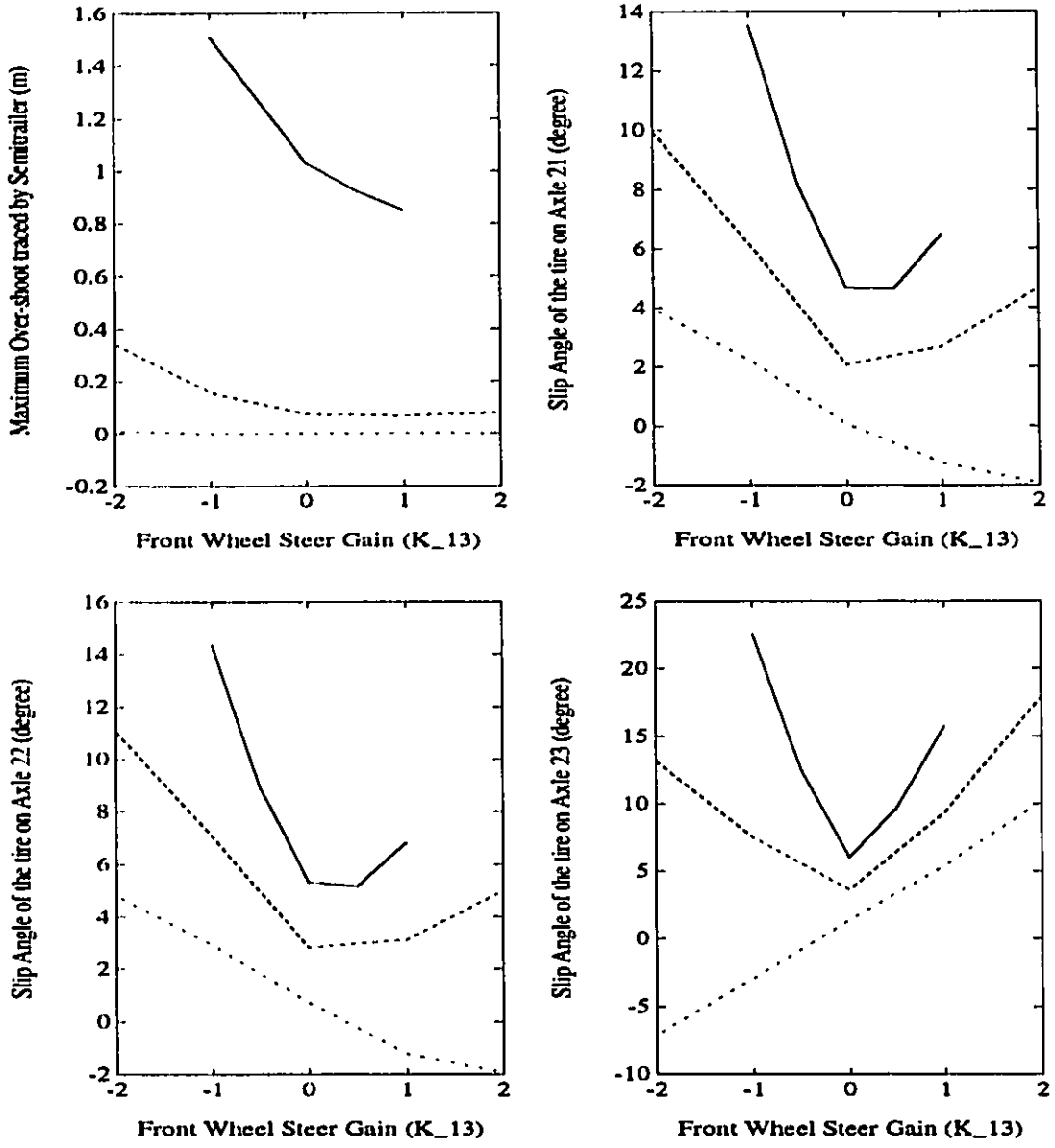

SCHEME A: FORCED-STEERING AXLE 23

Figure 4.12: Influence of front wheel steer gain on the transient response
(-.-.- 50 km/h; - - - 80 km/h; —— 100 km/h)

axle 22 influences the vehicle maneuverability only slightly. Further, the Quebec regulations do not permit installation of self- or forced-steering axles at the semitrailer's rearmost axle. The response characteristics of the forced-steering axle, located at axle 21 of the semitrailer, are thus further examined to derive the influence of front wheel steer gain on the low-speed manoeuvrability and the high-speed directional performance.

An examination of Figures 4.1 and 4.2 reveals that a negative front wheel steer gain (K_{11}) is desirable to reduce the vehicle off-tracking, curve radius and thus the tire wear rate at low-speed directional maneuvers. A positive front wheel steer gain, however, is needed to improve the high-speed directional dynamics as evident from the peak lateral acceleration and path overshoot response presented in Figures 4.7 and 4.8, respectively. The positive gain (parallel steer) further yields lower side-slip angles corresponding to high-speed directional maneuvers. The control scheme A, based upon feedback from the front wheel steer angle, thus cannot be used to achieve both improved low-speed maneuverability and high-speed directional performance.

4.4.2 SCHEME B: Articulation Gain

The low-speed maneuverability and high-speed directional performance characteristics of the vehicle with force-steering, based upon scheme B, are investigated for the maneuvers described in previous section. The wheel angle of the forced-steered axle is determined as a proportional function of the articulation angle (γ). The performance characteristics are investigated for different location of the forced-steering axle (axle 21,22 and 23). The dependence of response characteristics on the forced-steering axle location was observed to be similar to that obtained for the front wheel steer gain. The results are therefore discussed for the forced-steering axle located at axle 21 only.

Figures 4.13 and 4.14 illustrate the peak values of response of the vehicle with

a force-steering at axle 21 to constant steer maneuvers performed at forward speeds of 30 km/h and 50 km/h. A comparison of the peak response values of the forced-steered vehicle to those of the conventional vehicle reveals that the peak lateral acceleration and yaw velocity of the semitrailer increase slightly when the proportional control gain is selected to be positive ($K_{21}' > 0$). The peak lateral velocity response corresponding to directional maneuvers at 30 km/h reduces by approximately by 50%, when a negative articulation gain is selected. The lateral velocity response corresponding to 50 km/h also reduces considerably for low values of negative articulation gain, as shown in Figure 4.13. The turn radius of the vehicle decrease when forced-steering with negative articulation gain is introduced, irrespective of the speed. The reduction in the turn radius, however, is insignificant for articulation gain, $K_{21}' < -1$. The introduction of articulation dependent forced-steering axle affects the vehicle off-tracking in a significant manner similar to the front wheel steer gain. The vehicle off-tracking, corresponding to medium-speed maneuver, decreases considerably (approximately 1 m) for negative values of articulation gain. The off-tracking corresponding to low-speed maneuvers, however, reduces when the articulation gain is selected in the range $-1 < K_{21}' < 0$. The off-tracking at this speed tends to increase when the larger values of negative gains are selected ($K_{21}' < -1$). While the side-slip angles of tires on axles 22 and 23 reduce for low values of positive articulation gains. At low-speeds, the variations in side-slip angles are observed to be quite significant for the gain values ranging from -1 to 1.

The peak response values of the articulated vehicle with forced-steered axle 21 are evaluated for medium- and high-speed evasive maneuvers, and compared to those of the conventional vehicle, as shown in Figures 4.15 and 4.16. The peak lateral acceleration, lateral velocity and yaw velocity response of the semitrailer, in-general, decrease when forced steering with positive articulation gain is introduced. The peak lateral acceleration and lateral velocity, however, increase considerably with negative articulation gain. The influence of forced-steering axle on the vehicle response corresponding to the medium-

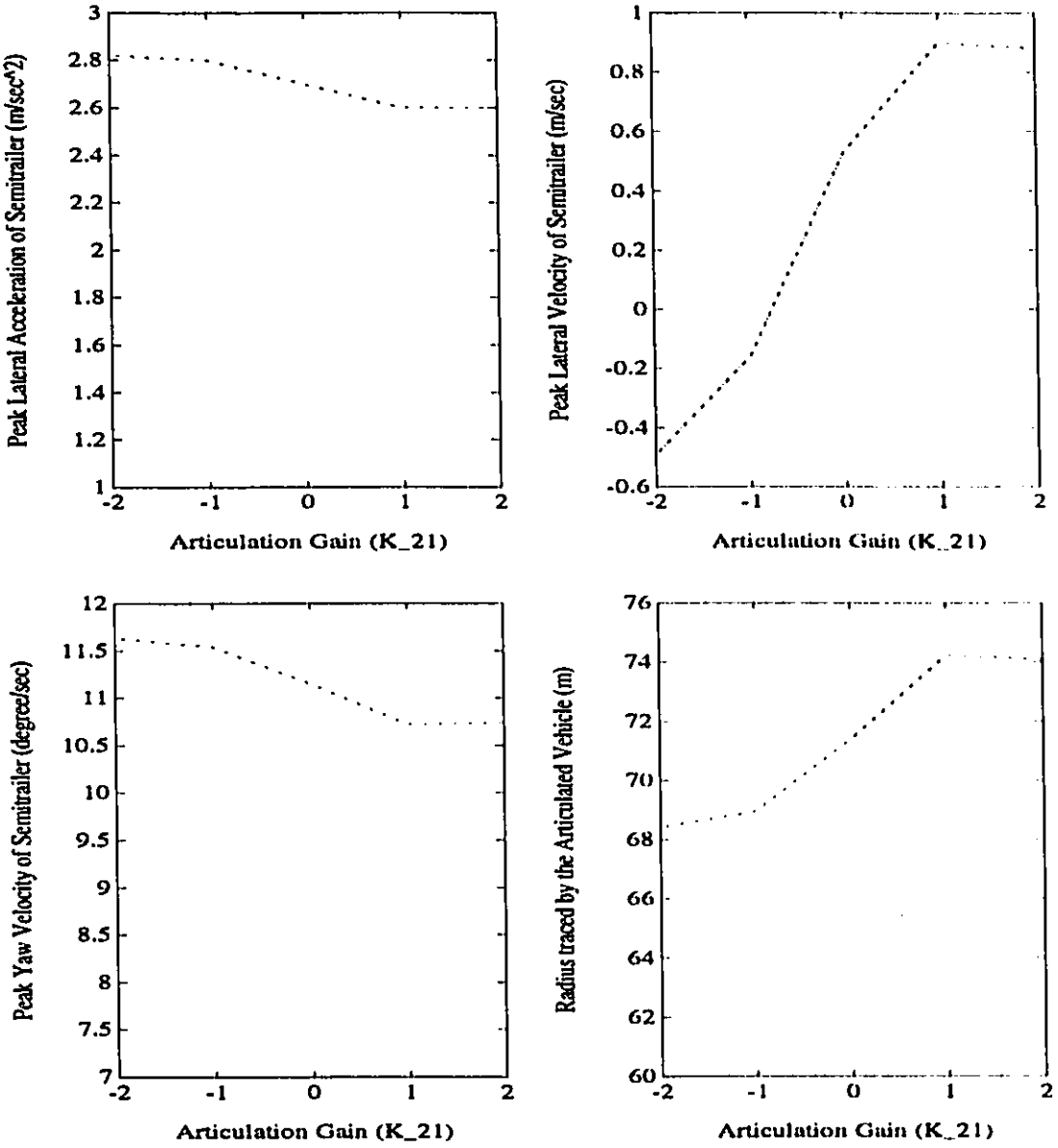

SCHEME B: FORCED-STEERING AXLE 21

Figure 4.13: Influence of articulation gain on the steady-state response (..... 30 km/h; -.-.- 50 km/h)

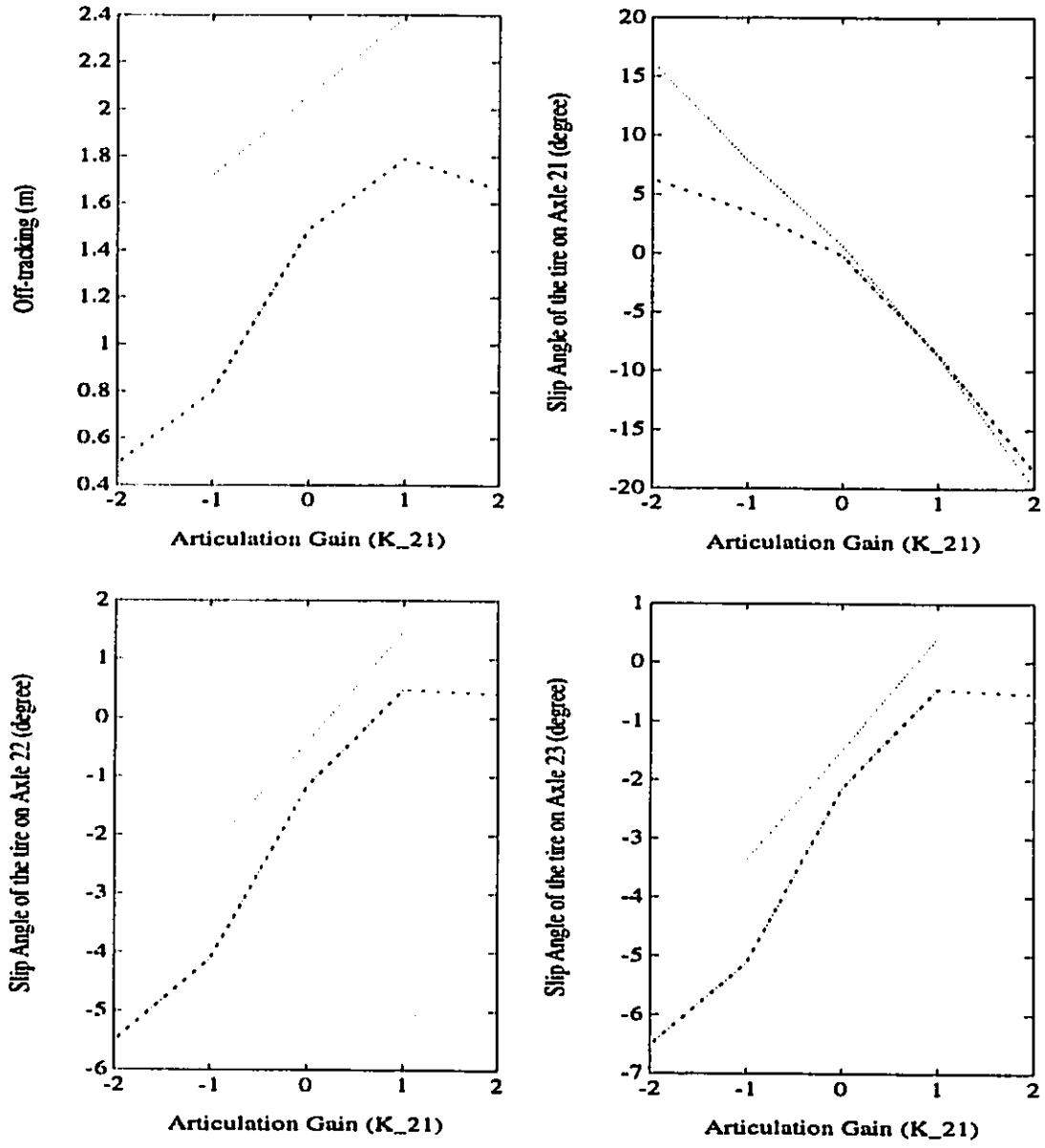

SCHEME B: FORCED-STEERING AXLE 21

Figure 4.14: Influence of articulation gain on the steady-state response (..... 30 km/h; -.-.- 50 km/h)

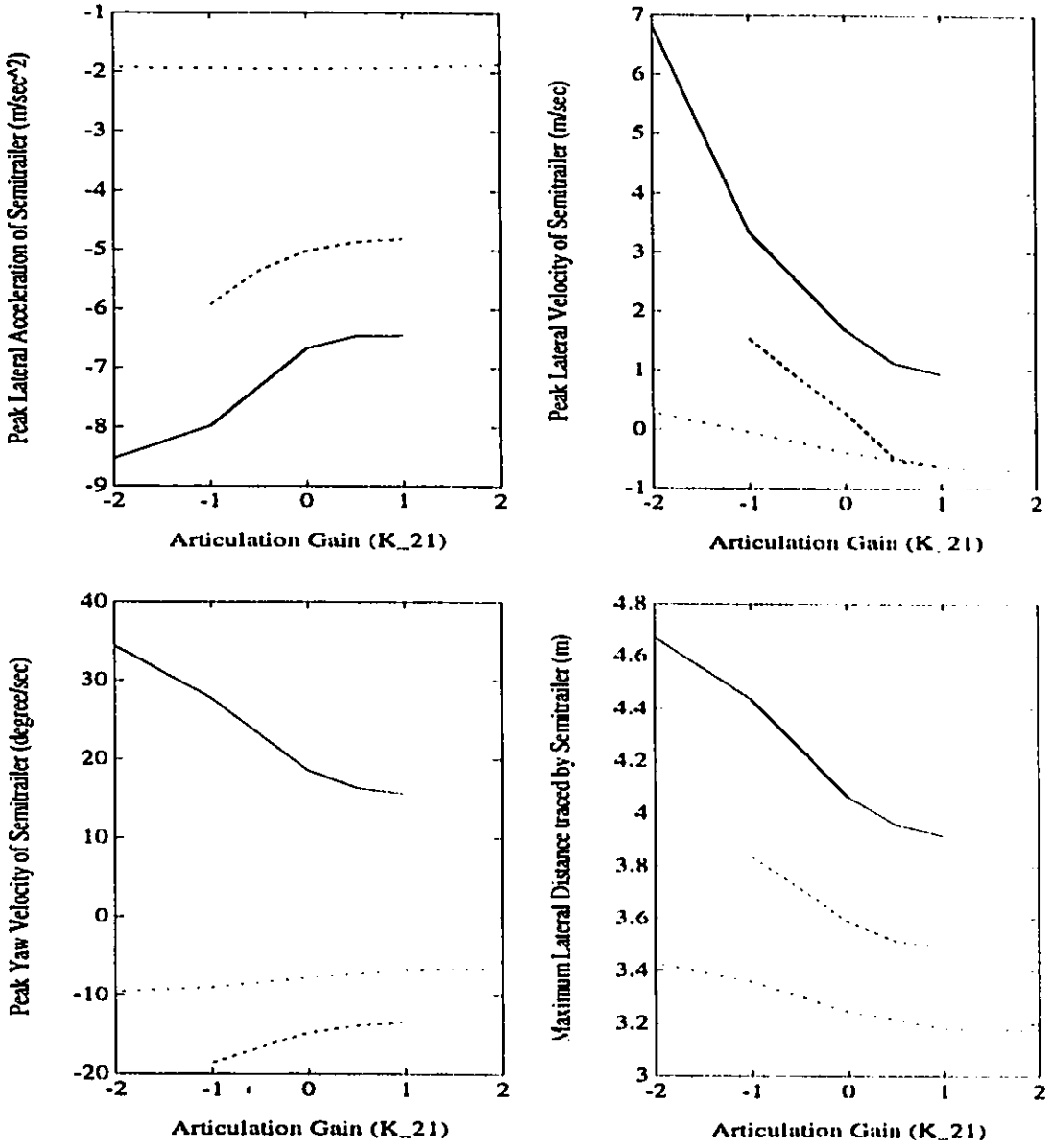

SCHEME B: FORCED-STEERING AXLE 21

Figure 4.15: Influence of articulation gain on the transient response
(-.-.- 50 km/h; - - - 80 km/h; — 100 km/h)

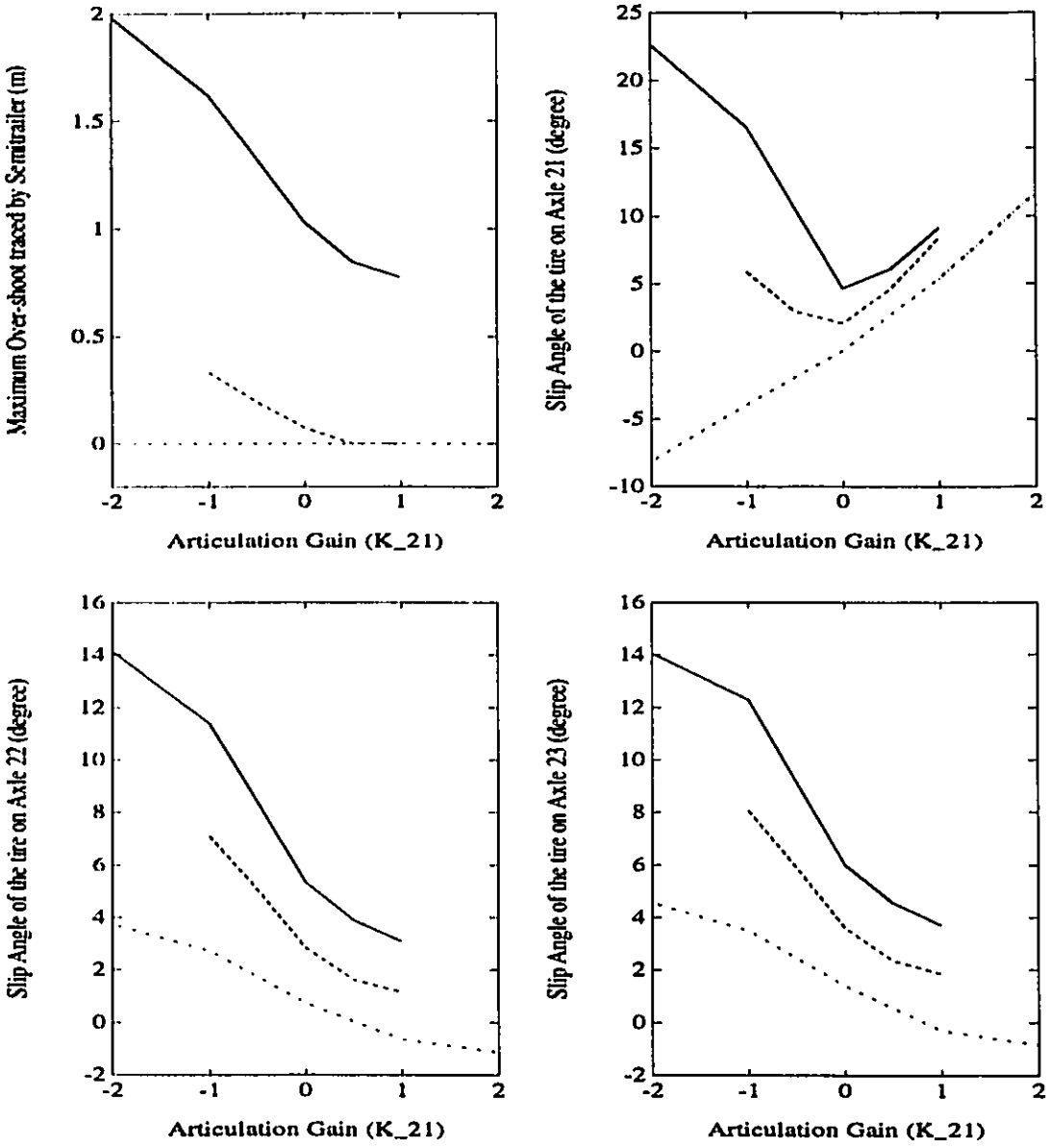

SCHEME B: FORCED-STEERING AXLE 21

Figure 4.16: Influence of articulation gain on the transient response
(-.-.- 50 km/h; - - - 80 km/h; —— 100 km/h)

speed (50 km/h) maneuver is relatively insignificant. The path overshoot of the vehicle, and the side-slip angles of tires on axle 22 and 23 also decrease by 40% to 80% for positive values of articulation gain. A comparison of results presented in Figures 4.13 to 4.15 indicate conflicting requirements on the articulation gain in view of the low-speed maneuverability and high-speed directional performance characteristics.

4.4.3 SCHEME C: Articulation Rate Gain

The low-speed maneuverability and high-speed directional performance characteristics of the vehicle with a forced-steering axle 21 are further investigated, where the wheel angle of the forced-steered axle is varied proportional to the rate of articulation. Figures 4.17 to 4.19 summarize the peak response values corresponding to constant steer and evasive maneuvers. The lateral acceleration, lateral and yaw velocities, curve radius and side-slip angle response characteristics of the vehicle under constant steer maneuvers were observed to be insensitive to the articulation rate gain. The vehicle off-tracking, however, reduces considerably for positive values of the articulation rate gain, as illustrated in Figure 4.17. The positive articulation rate gain, however, tends to considerably increase the peak lateral velocity, yaw velocity, path overshoot and side-slip angles of tires on axles 22 and 23, under high-speed evasive maneuvers, as shown in Figures 4.18 and 4.19. The peak lateral acceleration response reduces slightly when force-steering is generated using positive gain values. Figures 4.17 to 4.19 clearly illustrate the conflicting requirements on the articulation rate gain when both the low-speed maneuverability and high-speed directional control performance are considered. The forced-steering algorithms based upon single response variable control yield conflicting requirements on the control gains, when both low-speed and high-speed maneuvers are considered. The performance characteristics of the vehicle are thus investigated using forced-steering algorithms based upon combination of response variables. The low-speed and high-speed response characteristics of forced-steering employing control schemes I and IV, described

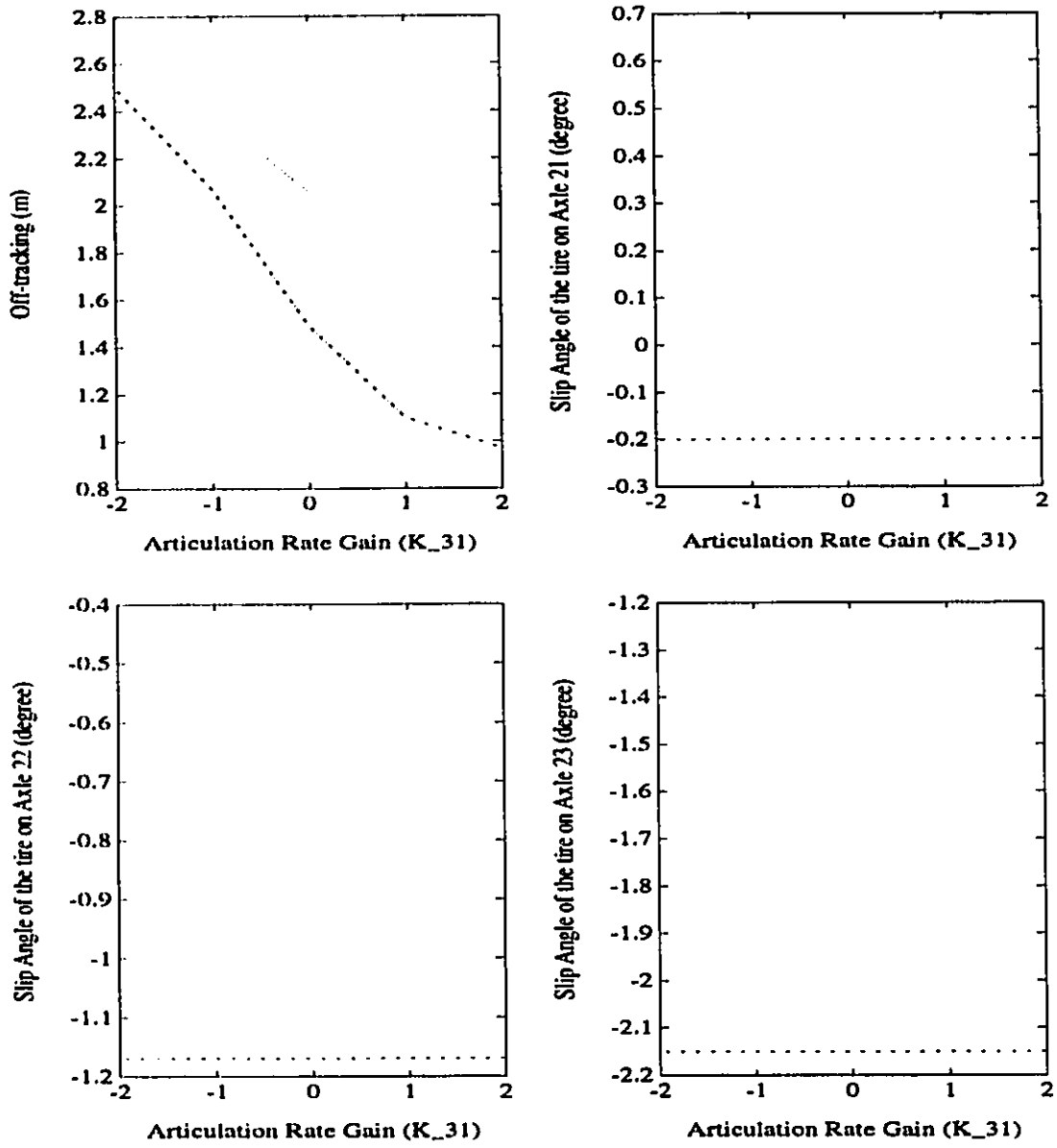

SCHEME C: FORCED-STEERING AXLE 21

Figure 4.17: Influence of articulation rate gain on the steady-state response (..... 30 km/h; -.-.- 50 km/h)

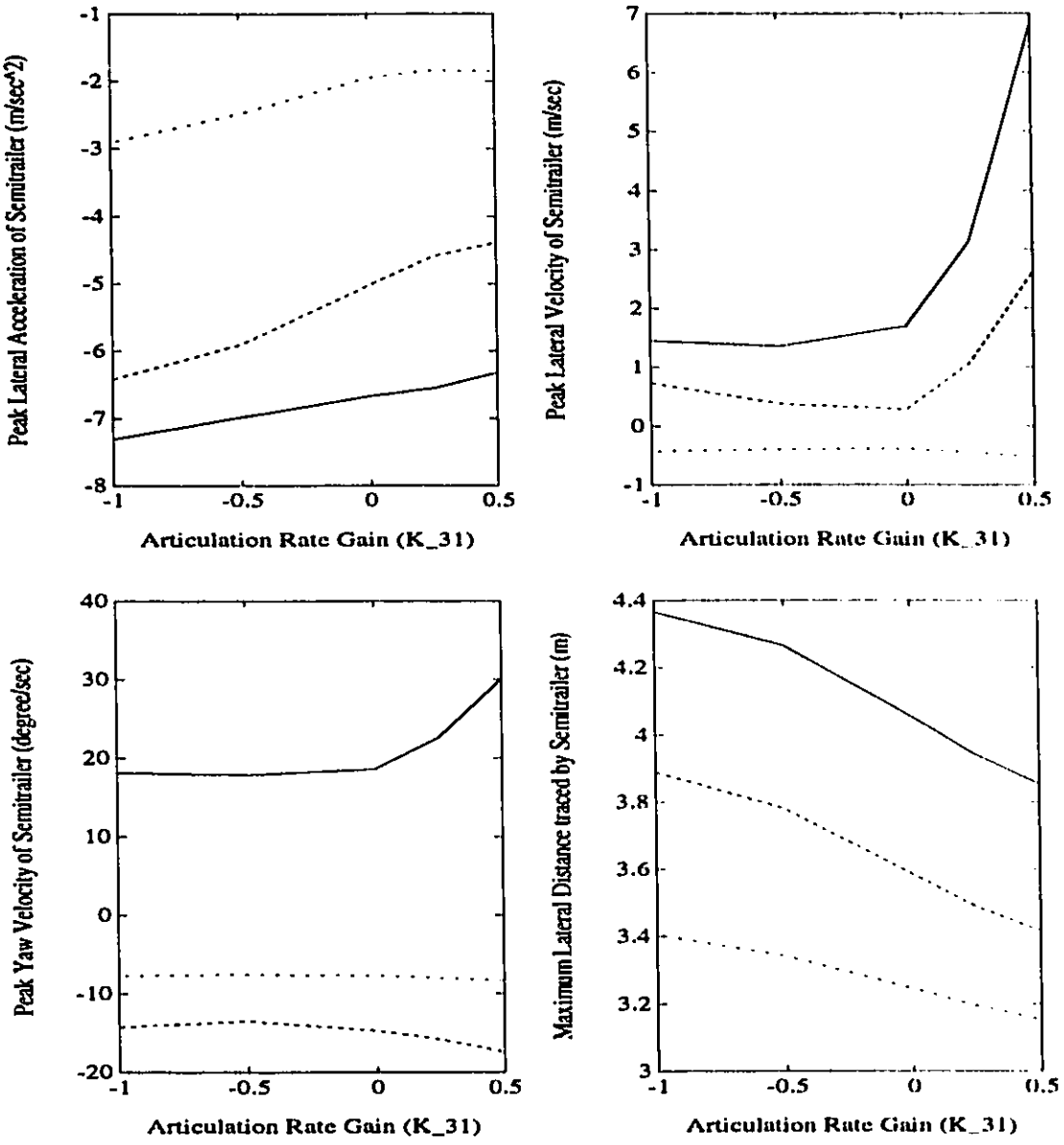

SCHEME C: FORCED-STEERING AXLE 21

Figure 4.18: Influence of articulation rate gain on the transient response
(-.-.- 50 km/h; - - - 80 km/h; — 100 km/h)

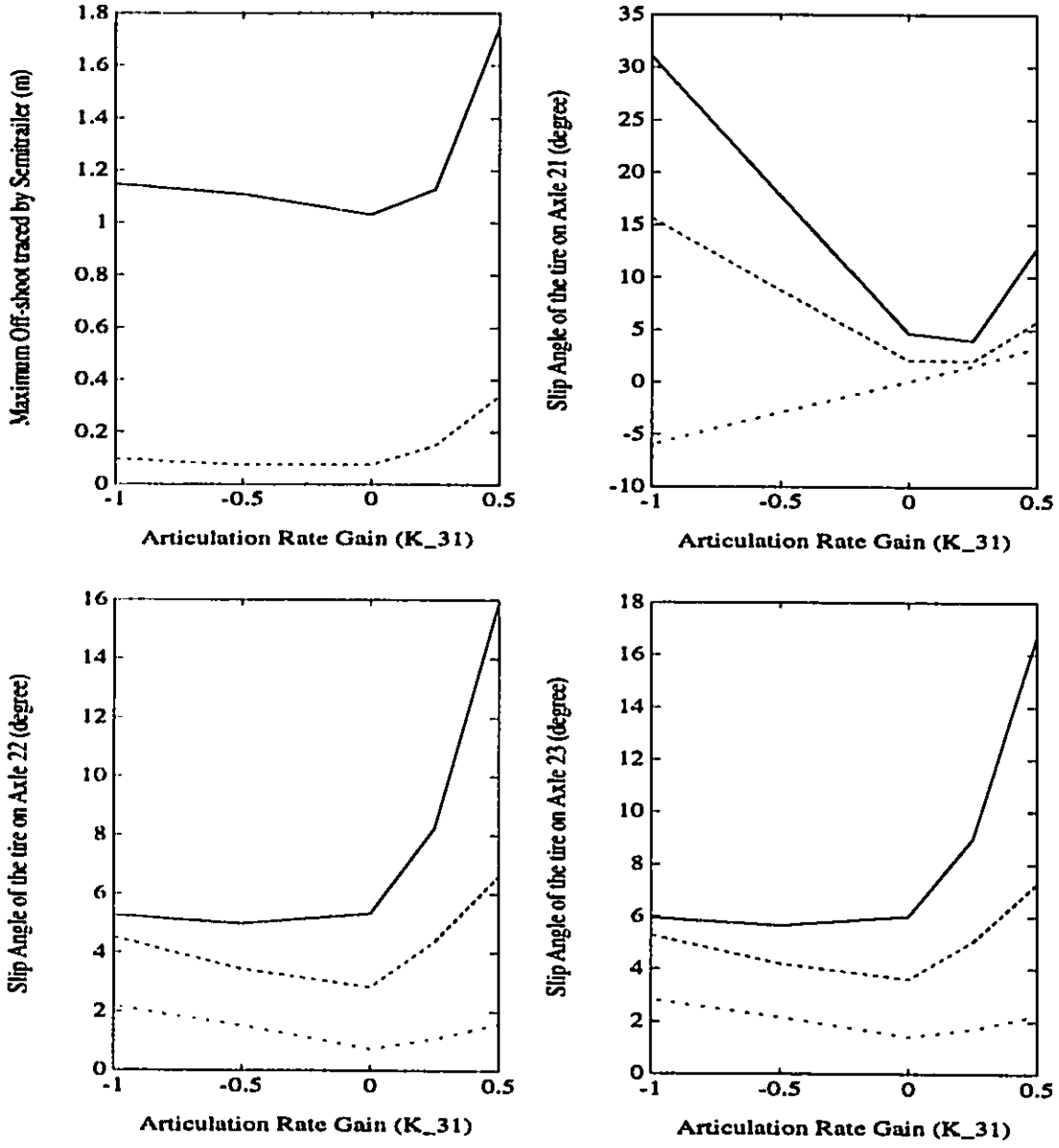

SCHEME C: FORCED-STEERING AXLE 21

Figure 4.19: Influence of articulation rate gain on the transient response
(-.-.- 50 km/h; - - - 80 km/h; —— 100 km/h)

in section 4.2 are investigated to deduce a desirable control algorithm.

4.4.4 SCHEME I: Front Wheel Steer and Articulation Combination Gains

Figures 4.20 and 4.21 illustrates the steady-state offtracking, lateral acceleration, lateral and yaw velocities, turn radius and side-slip angles response of the vehicle employing a forced-steering on axle 21 based on Scheme I, under constant steer maneuver at a speed of 30 km/h. It should be noted that the wheel angle of forced steer axle varies as a combined function of front wheel steer gain and articulation gain (K_{11}, K_{21}) values of (0,0). The figures clearly illustrate that the steady-state response of the vehicle is strongly related to both gain values. The steady-state lateral acceleration and yaw response are more strongly related to articulation gain. A positive value of articulation gain yields lowest lateral acceleration irrespective of the front wheel steer gain. The corresponding reductions in the lateral acceleration and yaw velocity, however, are small. The gain values (0,-1.25) and (-2,0) yield lowest steady-state lateral velocity response. The lowest value of off-tracking are realized using the gain combination of (3,-2), while the combinations (-2,0) and (1,-2) yield lowest turn radius. While the side-slip angles of the tires on forced-steered axle increase, the side-slip angle of tires on axle 23 are lowest for gain values of (3,2). Figures 4.22 and 4.23 illustrate the steady-state response of the vehicle to a medium-speed (50 km/h) constant steer maneuver as functions of the front wheel steer and articulation gains. The lowest off-tracking is realized for gain values (-2,-1.25), while the lowest turn radius is observed for (-1,-2). The side-slip angles of tires on axle 23 approach lowest values for gains (-2,2), while the lateral velocity approaches near the minimum for gain values of (-1,0).

Although the results presented in Figures 4.20 to 4.23 exhibit number of conflicting requirements for the control gains. A close examination of the results reveal that the

gain values of (2,-2) can yield considerable reduction in the off-tracking, turn radius, and articulation angle response, while the corresponding increase in lateral acceleration, lateral velocity and yaw velocity is observed to be below 4%. This combination of gain values may thus be considered to realized improved maneuverability at low and medium-speeds. The peak lateral acceleration, lateral velocity, yaw velocity and the path overshoot of the vehicle subject to an evasive maneuver at 100 km/h are illustrated in Figure 4.24 for different values of control gains. The peak side-slip angles of tires on the semitrailer axles are not discussed due to their highly transient nature, and they occur only for an extremely short duration. It is evident from the figure that the peak lateral acceleration, and lateral yaw velocity are observed to be lowest when the gain values are selected as (-0.5,2). The figure further reveals that the peak lateral acceleration, lateral velocity and yaw velocity response of the vehicle with a forced-steering axle employing these gain values are 5%, 57% and 18%, respectively, lower than those of the conventional vehicle. The path overshoot is observed to be considerably lower for gain values of $0 \leq K_{11}^{'} \leq 2$ and $0 \leq K_{21}^{'} \leq 2$; and for $1 \leq K_{11}^{'} \leq 2$ and $-1.25 \leq K_{21}^{'} \leq 2$.

An examination of Figures 4.20 to 4.24 also indicates conflicting requirements on the combined front wheel steer and articulation gains in view of low-, medium- and high-speed maneuvers.

4.4.5 SCHEME II: Articulation and Speed Sensitive Articulation Rate Gains

The results presented in sections 4.4.1 to 4.4.4 clearly illustrate the conflicting requirement on the forced-steering control gains. While a negative gain yields improved off-tracking and low-speed maneuverability, the positive gains are needed to achieve improved directional dynamics.

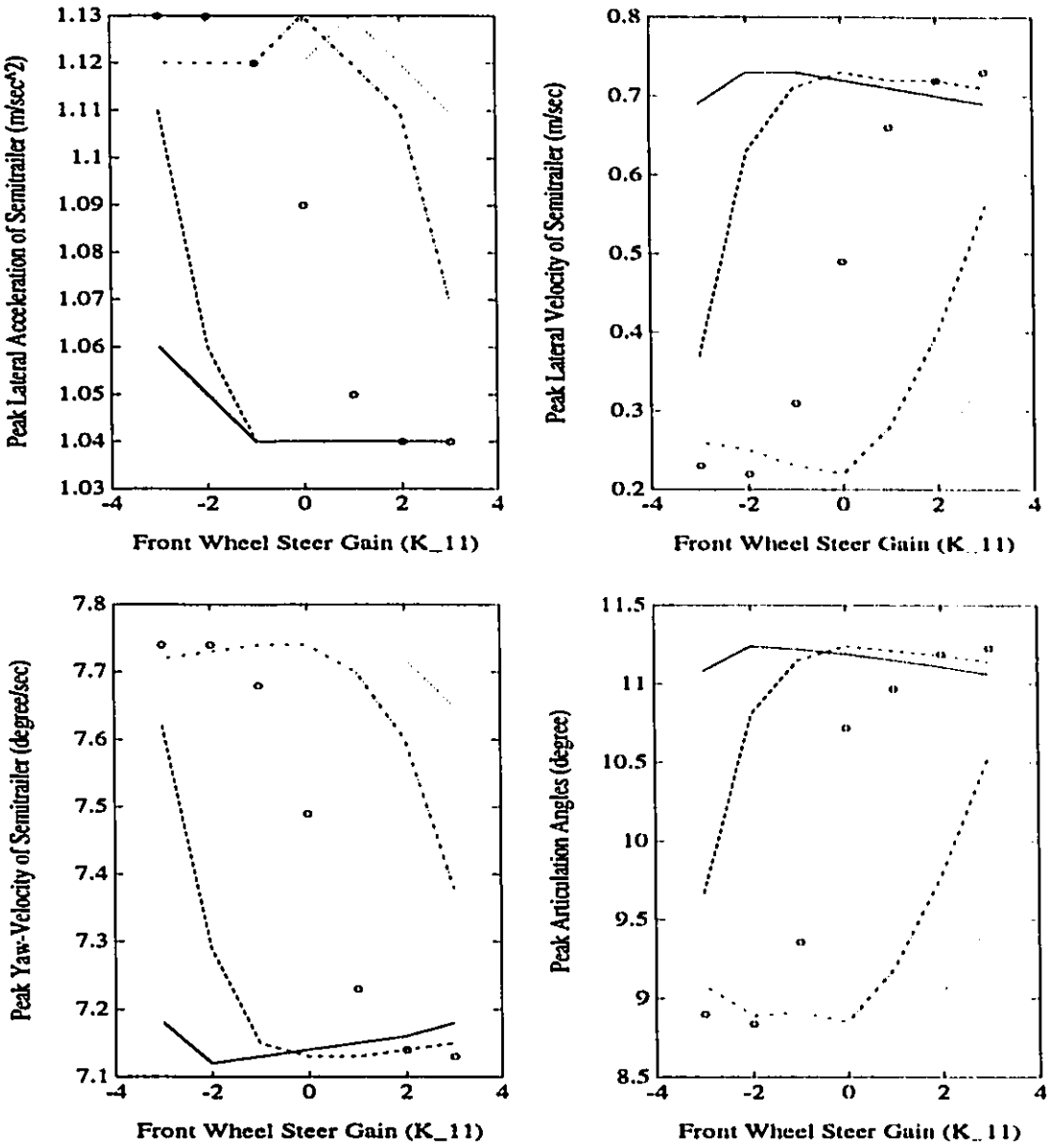

SCHEME I: FORCED-STEERING AXLE 21

Figure 4.20: Influence of front wheel steer gain and articulation gain on steady-state response at 30 km/h
(— K_{21} = 2; - - - K_{21} = 1.25; ooo K_{21} = 0; -.-.- K_{21} = -1.25; ..... K_{21} = -2;)

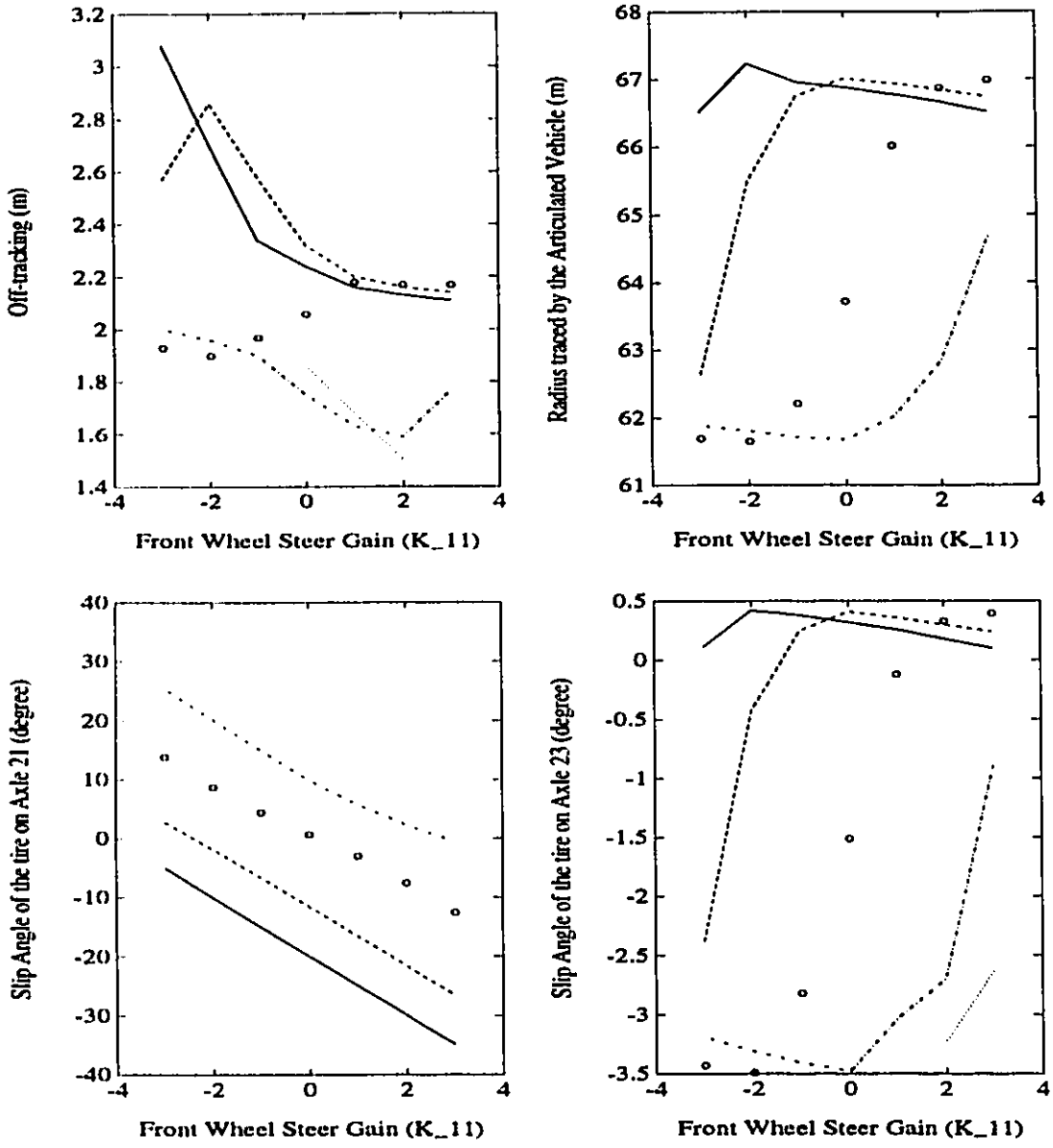

SCHEME I: FORCED-STEERING AXLE 21

Figure 4.21: Influence of front wheel steer gain and articulation gain on steady-state response at 30 km/h
(—— K_{21} = 2; - - - K_{21} = 1.25; ooo K_{21} = 0; -.-.- K_{21} = -1.25; ..... K_{21} = -2;)

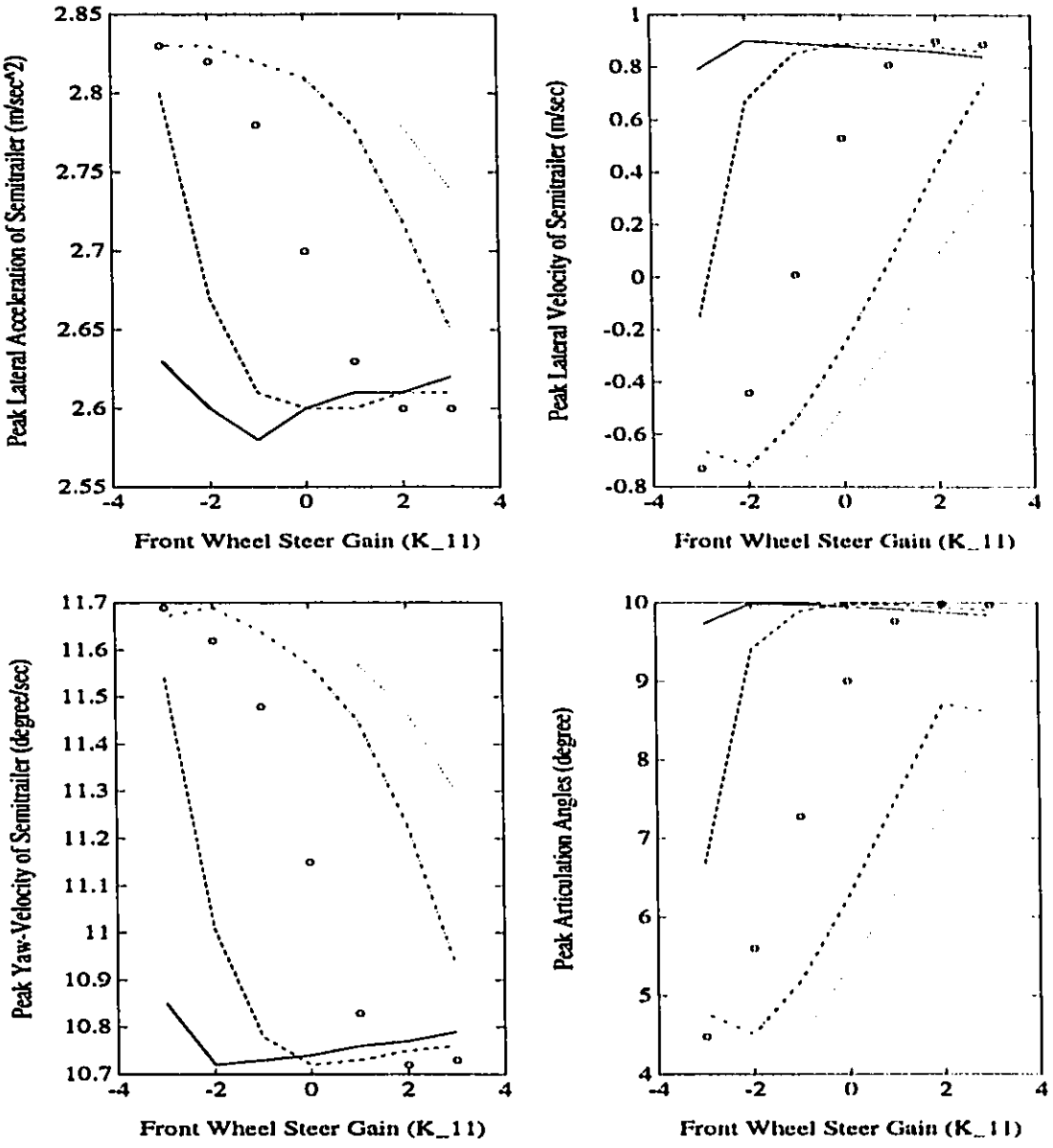

SCHEME I: FORCED-STEERING AXLE 21

Figure 4.22: Influence of front wheel steer gain and articulation gain on steady-state response at 50 km/h
(— K_{21} = 2; - - - K_{21} = 1.25; ooo K_{21} = 0; -.-.- K_{21} = -1.25; ..... K_{21} = -2;)

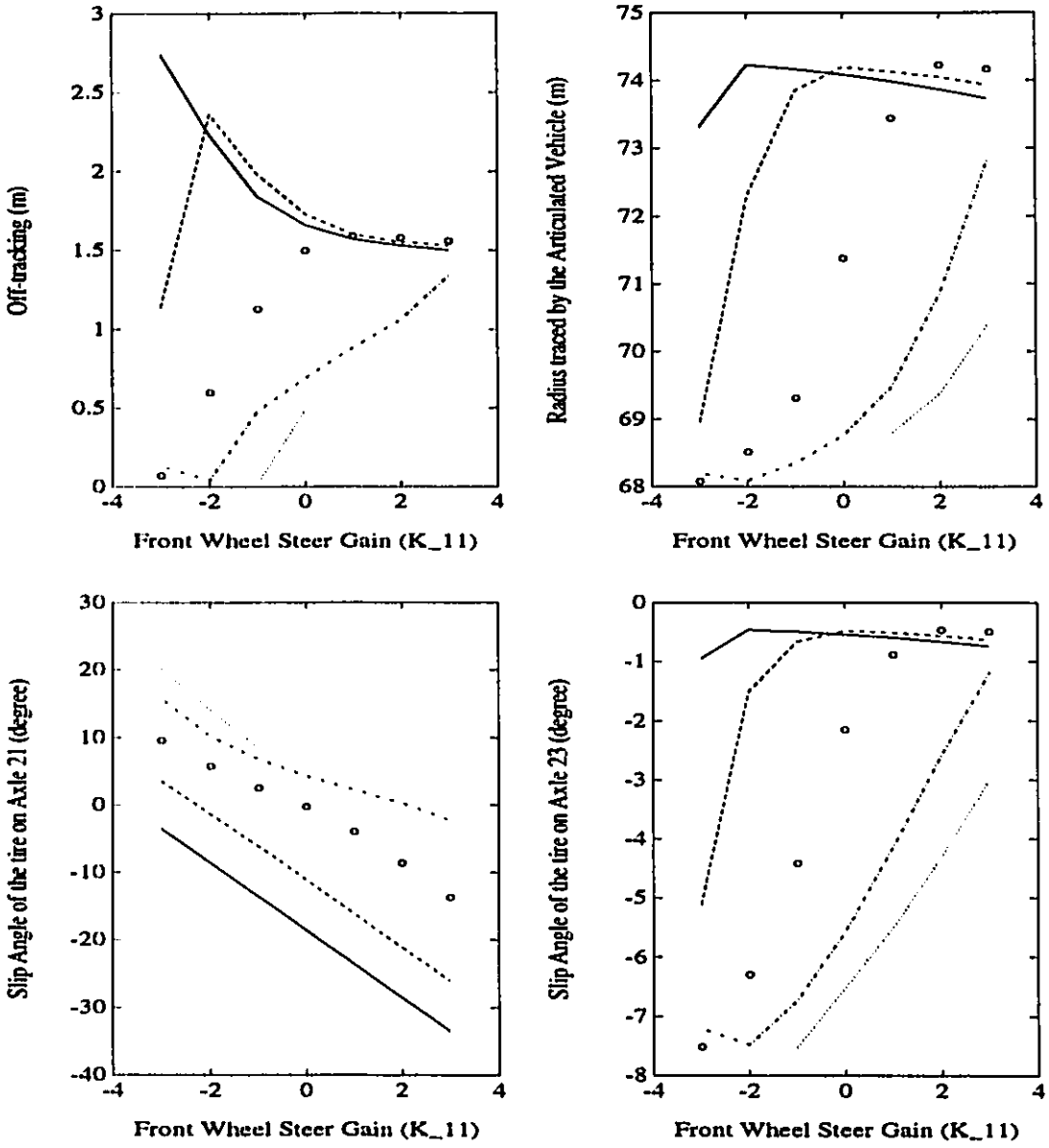

SCHEME I: FORCED-STEERING AXLE 21

Figure 4.23: Influence of front wheel steer gain and articulation gain on steady-state response at 50 km/h
(— K_{21}^{*} = 2; - - - K_{21}^{*} = 1.25; ooo K_{21}^{*} = 0; -.-.- K_{21}^{*} = -1.25; ..... K_{21}^{*} = -2;)

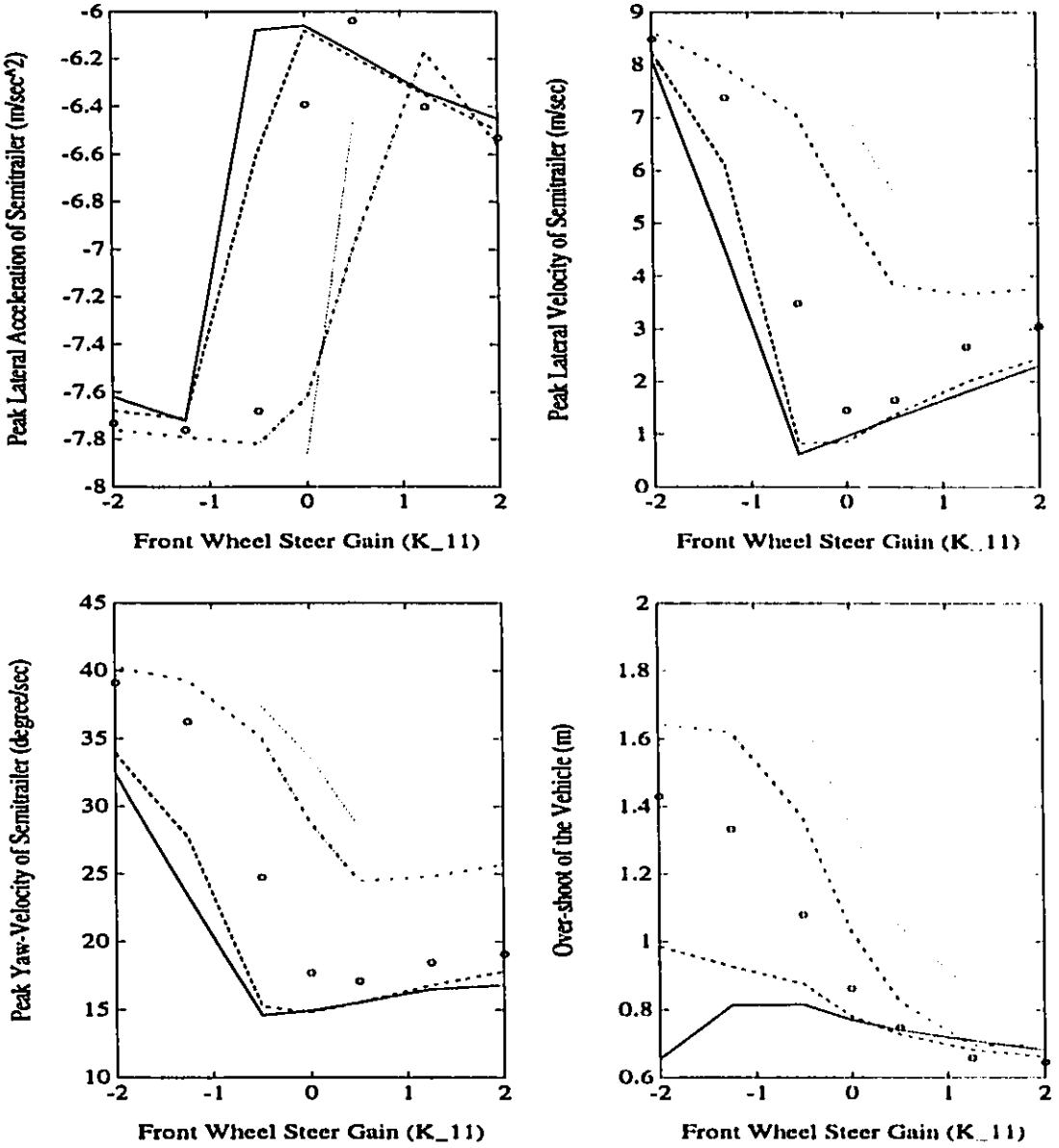

SCHEME I: FORCED-STEERING AXLE 21

Figure 4.24: Influence of front wheel steer gain and articulation gain on transient response at 100 km/h

(— K_{21} = 2; - - - K_{21} = 1.25; ooo K_{21} = 0; -.-.- K_{21} = -1.25; ..... K_{21} = -2;)

This force steering control algorithm generates the wheel axle of axle 21 as a function of the articulation gain (K_{21}), articulation rate gain (K_{51}) and speed. The low- and medium-speed maneuverability characteristics of the vehicle with force steering axle 21, employing this control algorithm, are investigated for constant steer maneuvers performed at 30 km/h and 50 km/h, respectively. Since the steady state articulation rate approaches 0, the low- and medium-speed dynamics are observed to insensitive to the articulation rate, as shown in Figures 4.25 and 4.26. Although the lateral acceleration varies only slightly with variations in the articulation gain (K_{21}), a negative values of K_{21} yields lower lateral velocity, turn radius and off-tracking. The low- and medium-speed manoeuvrability of the vehicle is similar to that achieved using scheme B, presented in Figures 4.13 and 4.14. The force-steering axle based on this control scheme affects the high-speed directional dynamics of the vehicle in a significant manner as shown in Figure 4.3. The figure clearly illustrates that a positive articulation gain (K_{21} = 1) and negative articulation rate gain (K_{51} = -0.005 h/km) yield low values of peak lateral acceleration, lateral velocity, yaw velocity and path overshoot. A comparison of Figures 4.25 and 4.26 shows conflicting requirements of the control gains corresponding to low- and high-speed maneuvers.

4.4.6 SCHEME III: Front Wheel Steer and Speed Sensitive Articulation Gains

In this control scheme the wheel angle of axle 21 is generated as a function of the front wheel steer angle gain (K_{11}), speed sensitive articulation gain (K_{41}) and forward speed. Figures 4.28 and 4.29 illustrate the steady state response to constant steer maneuvers at 30 km/h and 50 km/h, respectively, for different values of control gains. A comparison of the steady state response of the vehicle with forced-steering axle to that of a conventional vehicle shows that the low- and medium-speed maneuverability can be considerably improved by selecting K_{11} = -0.6 and K_{41} = -0.015. These gain values yield wheel angle

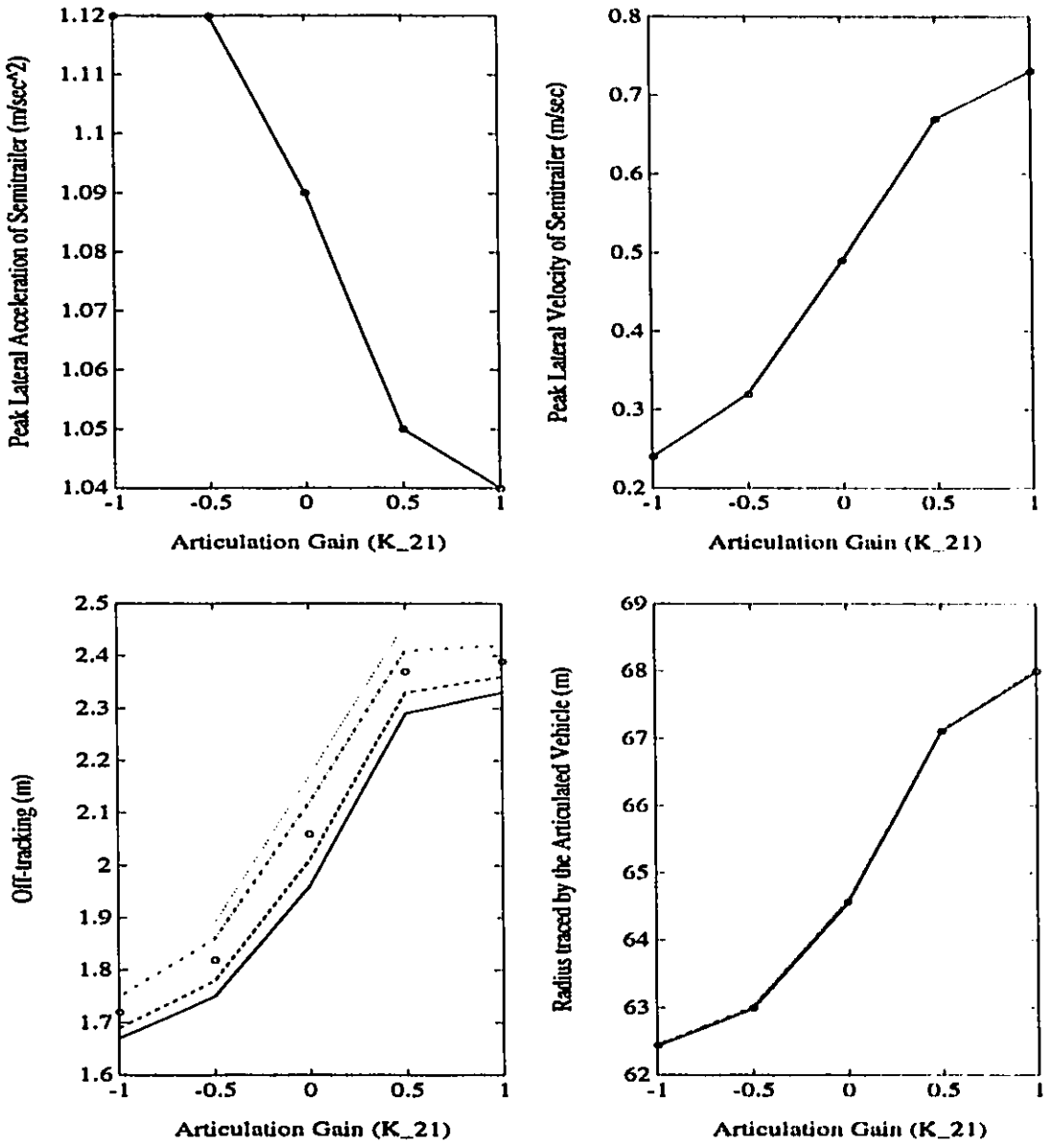

SCHEME II: FORCED-STEERING AXLE 21

Figure 4.25: Influence of articulation gain and speed sensitive articulation rate gain on steady-state response at 30 km/h
(— K_{51} = 0.01 h/km; - - - K_{51} = 0.005 h/km; ooo K_{51} = 0 h/km; -.-.- K_{51} = -0.005 h/km; ..... K_{51} = -0.01 h/km;)

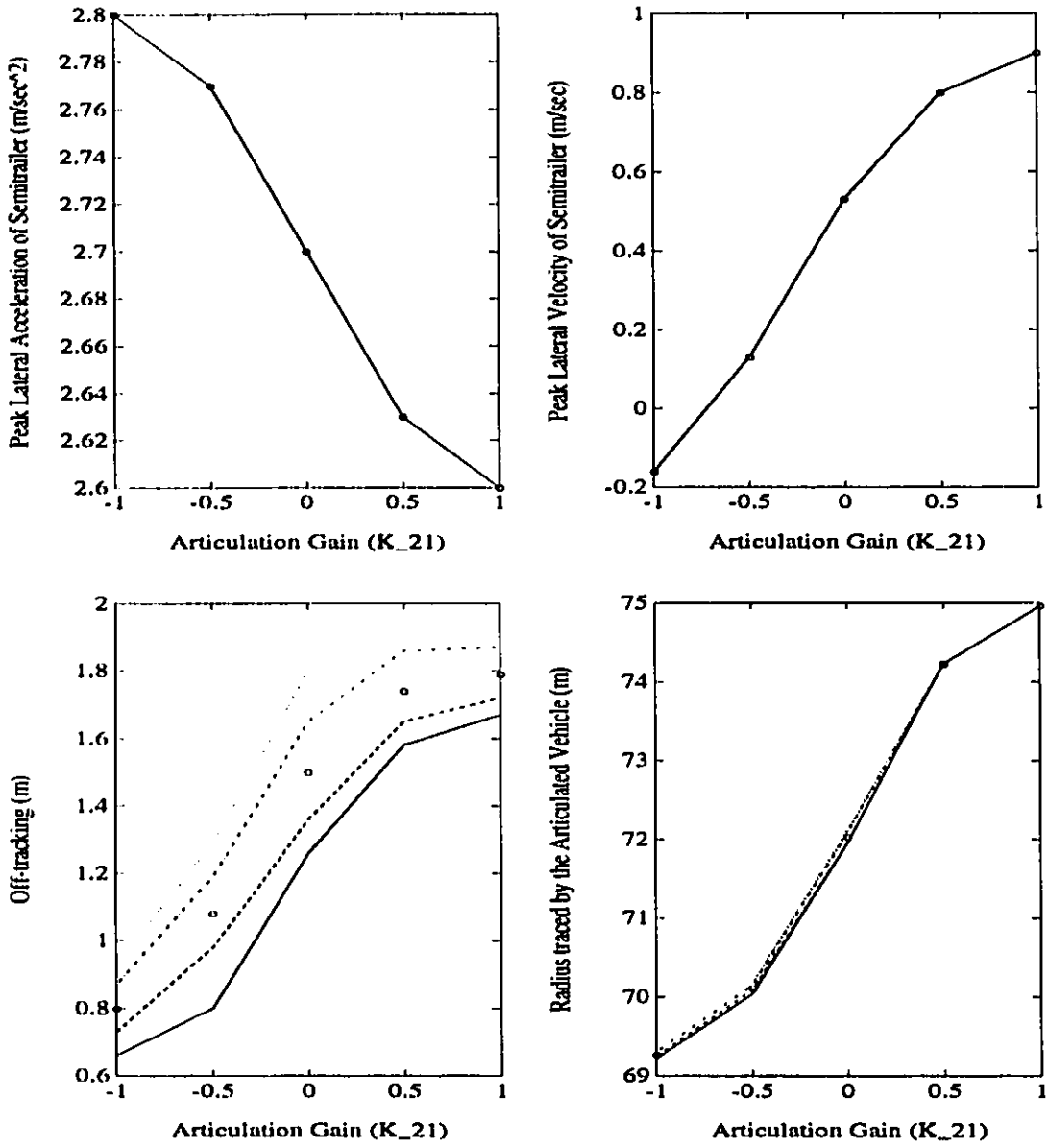

SCHEME II: FORCED-STEERING AXLE 21

Figure 4.26: Influence of articulation gain and speed sensitive articulation rate gain on steady-state response at 50 km/h
(— K_{51} = 0.01 h/km; - - - K_{51} = 0.005 h/km; ooo K_{51} = 0 h/km; -.-.- K_{51} = -0.005 h/km; ..... K_{51} = -0.01 h/km;)

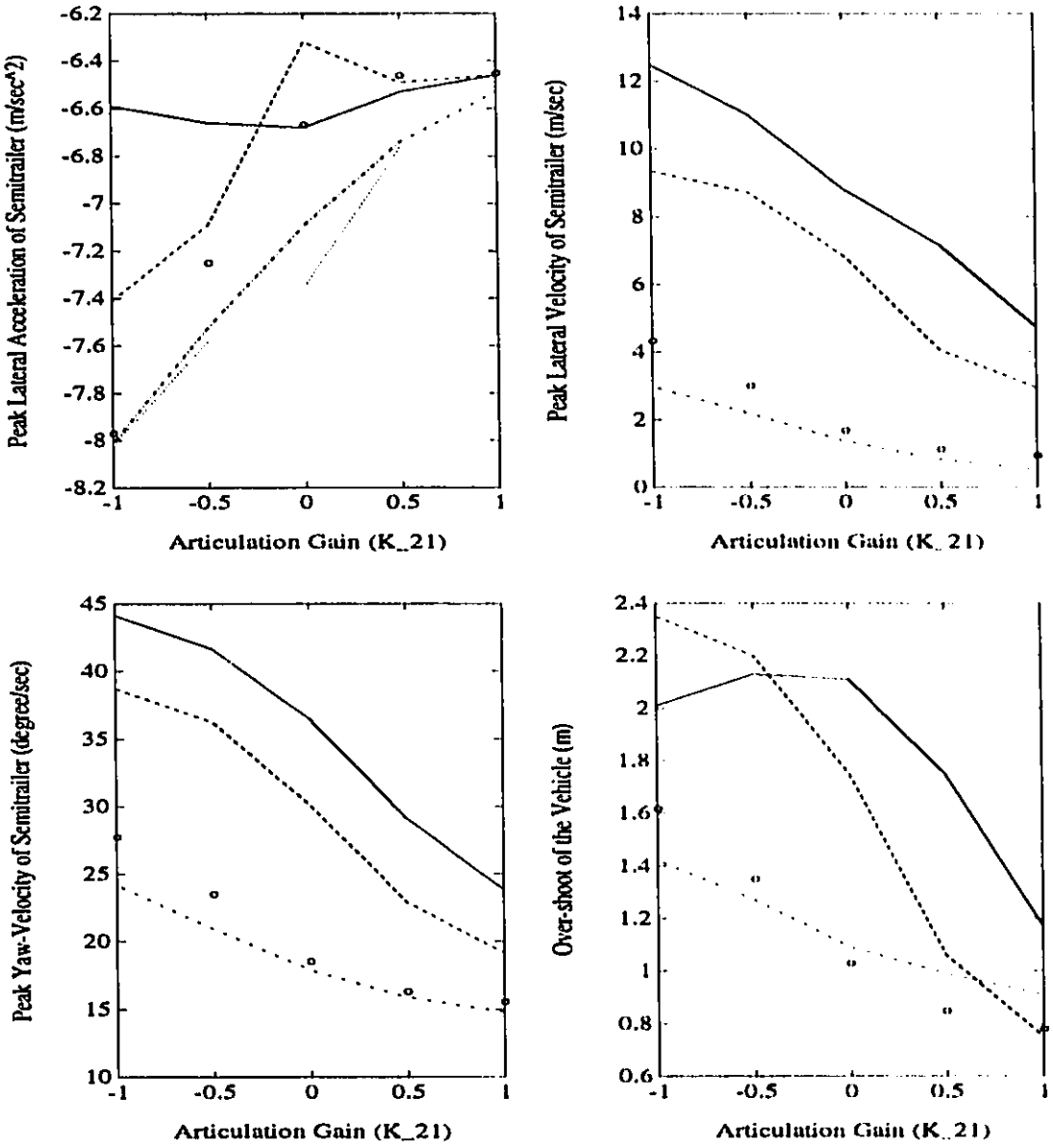

SCHEME II: FORCED-STEERING AXLE 21

Figure 4.27: Influence of articulation gain and speed sensitive articulation rate gain on transient response at 100 km/h
(—— K_{51} = 0.01 h/km; - - - K_{51} = 0.005 h/km; ooo K_{51} = 0 h/km; -.-.- K_{51} = -0.005 h/km; ..... K_{51} = -0.01 h/km;)

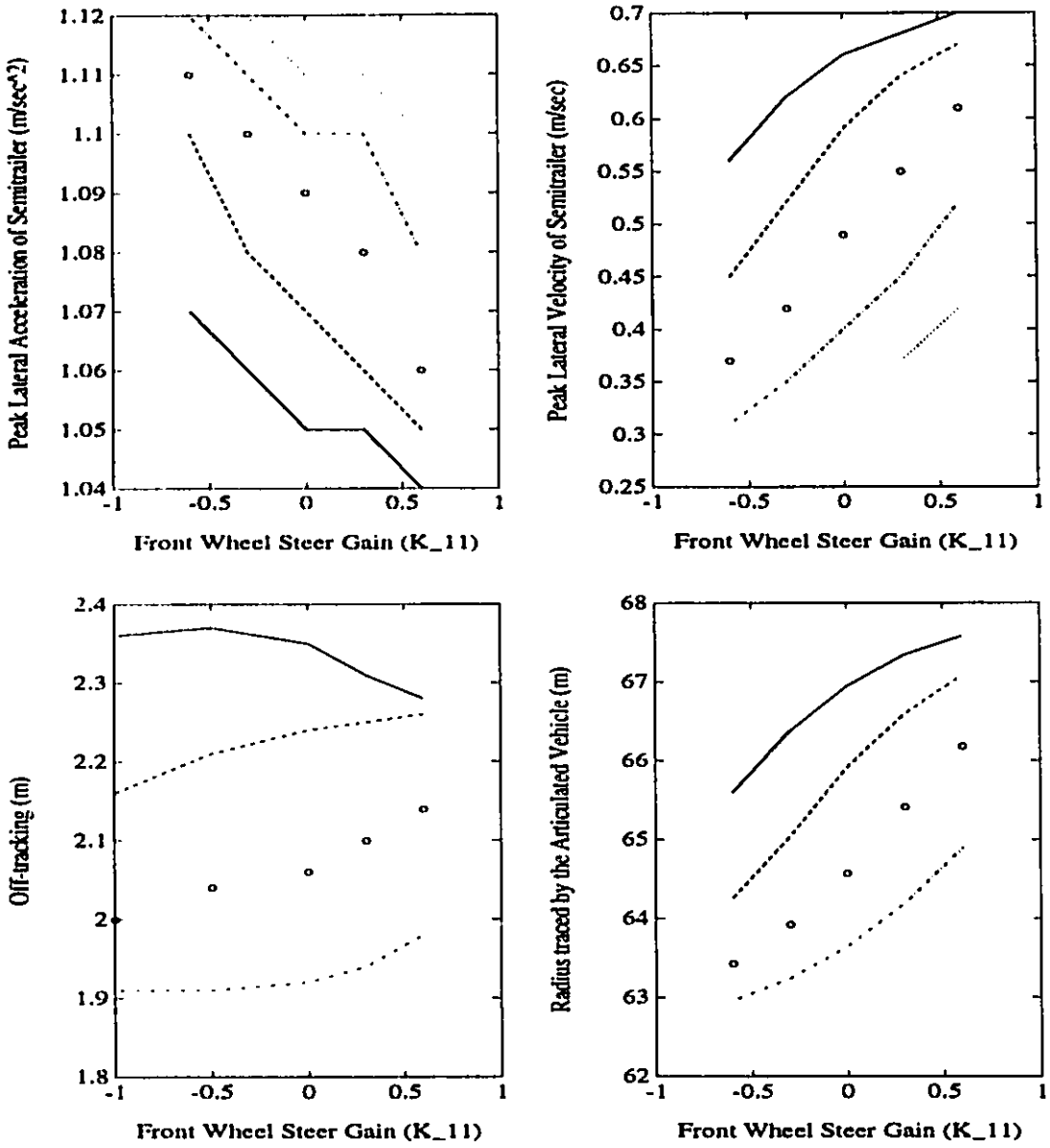

SCHEME III: FORCED-STEERING AXLE 21

Figure 4.28: Influence of front wheel steer gain and articulation gain on steady-state response at 30 km/h
(— K_{41} = 0.015 h/km; - - - K_{41} = 0.0075 h/km; ooo K_{41} = 0 h/km; -.-.- K_{41} = -0.0075 h/km; ..... K_{41} = -0.015 h/km;)

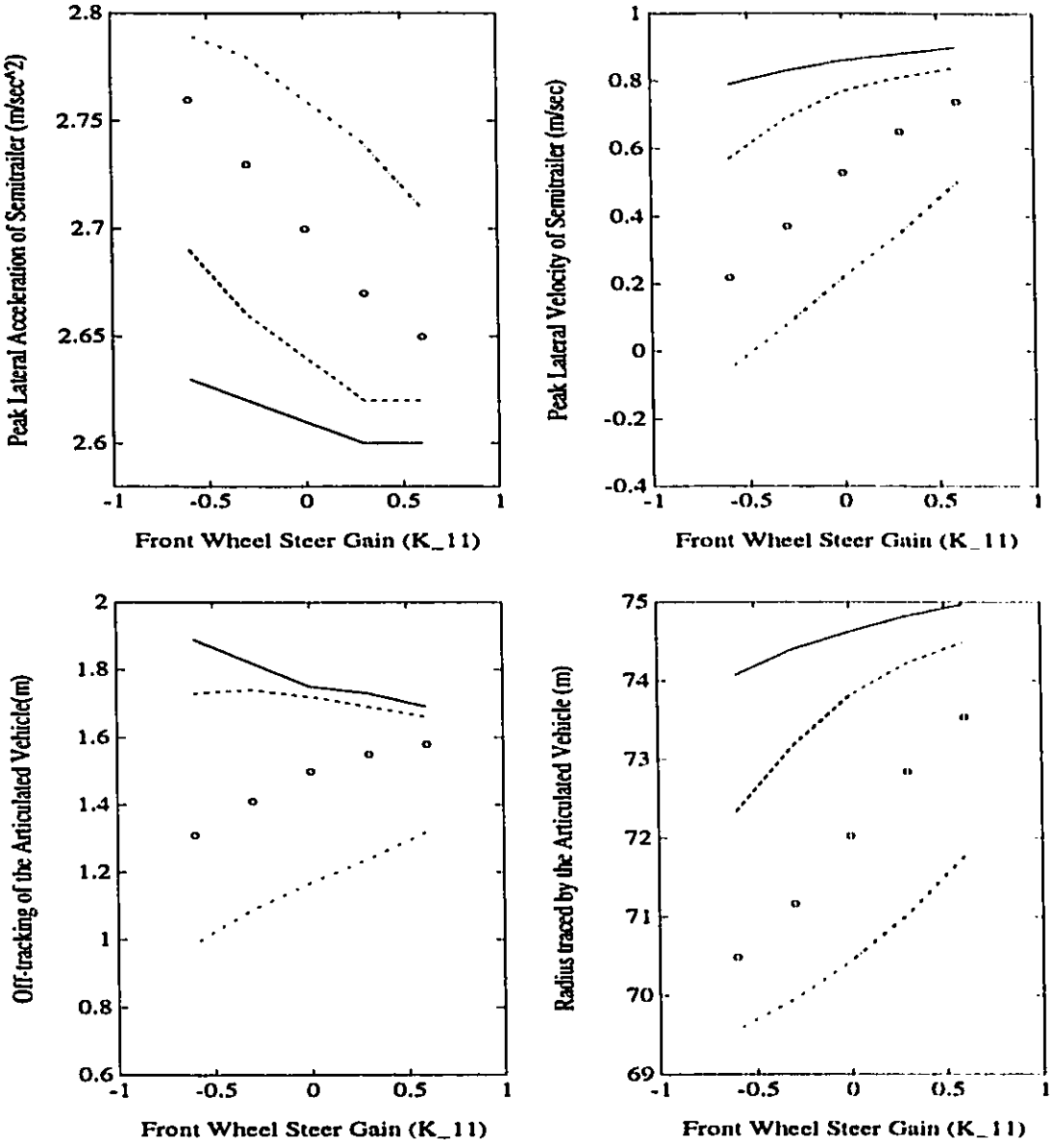

SCHEME III: FORCED-STEERING AXLE 21

Figure 4.29: Influence of front wheel steer gain and articulation gain on steady-state response at 50 km/h
(— K_{41} = 0.015 h/km; - - - K_{41} = 0.0075 h/km; ooo K_{41} = 0 h/km; -.-.- K_{41} = -0.0075 h/km; ..... K_{41} = -0.015 h/km;)

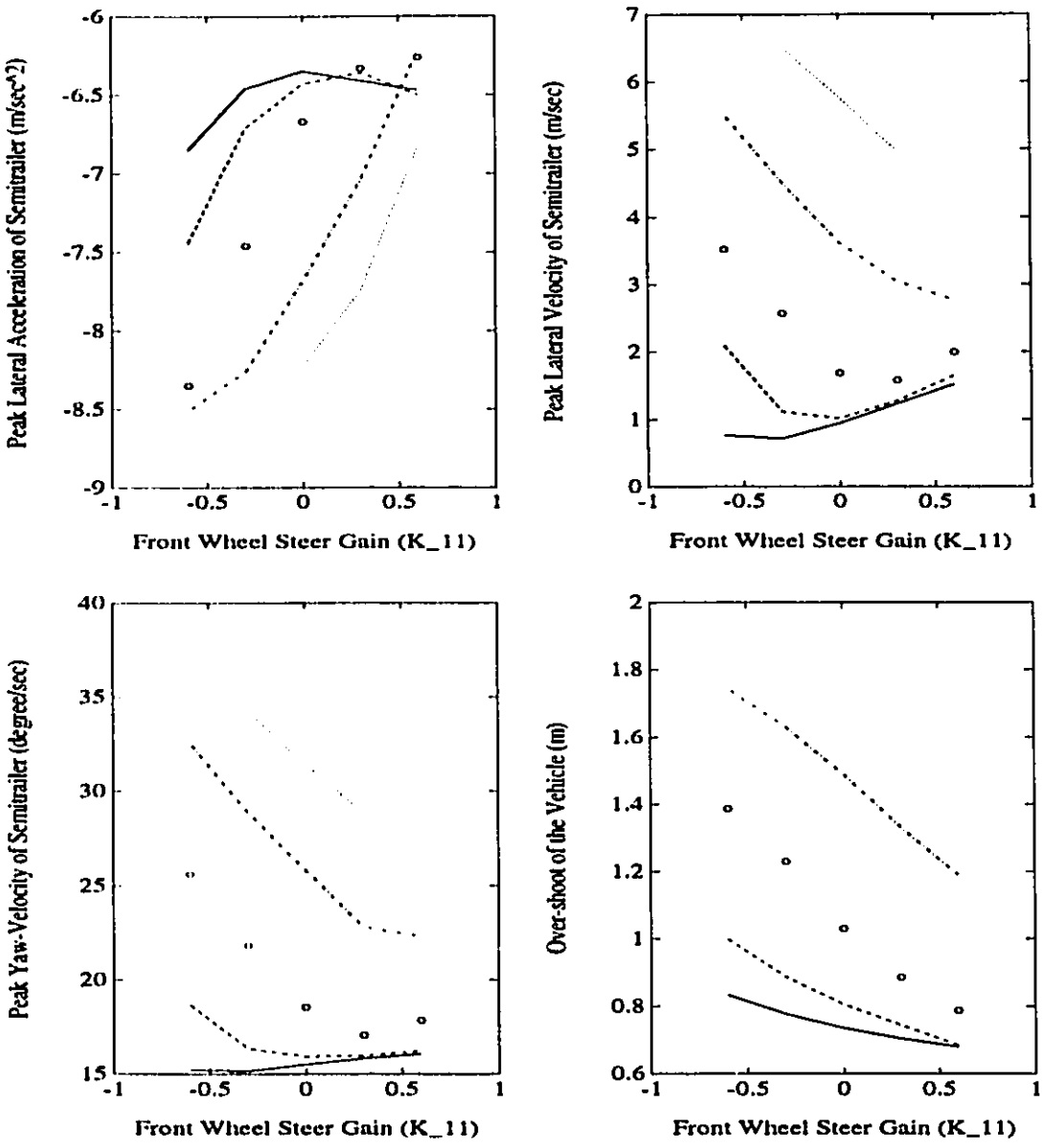

SCHEME III: FORCED-STEERING AXLE 21

Figure 4.30: Influence of front wheel steer gain and articulation gain on transient response at 100 km/h
(— K_{41} = 0.015 h/km; - - - K_{41} = 0.0075 h/km; ooo K_{41} = 0 h/km; -.-.- K_{41} = -0.0075 h/km; ..... K_{41} = -0.015 h/km;)

of the forced steering axle 21 opposite to the front wheel angle resulting in considerable reduction in turn radius, off-tracking and steady state lateral velocity of the vehicle. The lateral acceleration of the vehicle with forced-steering axle, however, is slightly larger then that with the conventional axle. The increase in lateral acceleration is 2.5% and 3.7% respectively, for 30 km/h and 50 km/h constant steer maneuvers.

The combination of control gains, however, deteriorates the high-speed directional dynamics indicating the conflicting requirements as evident for schemes I and II. Figures 4.30 illustrates the peak lateral acceleration lateral and yaw velocities, and path overshoot response of the vehicle subject to an evasive maneuver at 100 km/h. The figure clearly shows that for the gain values, selected to achieve improved low- and medium-speed manoeuvrability, the peak values of lateral acceleration, lateral velocity, yaw velocity and path overshoot of the vehicle with forced-steering are considerably larger then those of the vehicle with the conventional axles. The high-speed directional performance, however, can be improved by selecting a positive values of the articulation gain (K_{41}).

4.4.7 SCHEME IV: Articulation and Speed Sensitive Articulation Gains

The forced-steering algorithm comprising an articulation gain (K_{21}) and speed sensitive articulation gain (K_{41}) is formulated to achieve opposite and parallel steering of the leading axle of semitrailer at low- and high-speeds, respectively. The steady-state lateral acceleration, lateral velocity, yaw velocity, turn radius, offtracking and side-slip angle of tires on the semitrailer axle 23 are evaluated as functions of the control gains K_{21} and K_{41}. Figures 4.31 to Figures 4.34 illustrate the response characteristics for constant steer maneuver at low- (30 km/h) and medium (50 km/h) forward speeds. The lateral acceleration and yaw velocity response of semitrailer vary only slightly with changes in the control gains, irrespective of the speed. A combination of negative articulation gain (-0.5 to -1.0) and positive speed sensitive articulation gain (0.015 to 0.03 h/km)

yield lowest values of lateral acceleration and yaw velocity. This combination provides opposite steer at low- and medium-speeds resulting in lower side-slip angle, turn radius and offtracking, as shown in Figures 4.32 and 4.34. While this combination yields lower steady-state lateral velocity at 30 km/h, the response at 50 km/h is relatively higher.

The peak lateral acceleration, yaw velocity and lateral velocity, and path overshoot response of the semitrailer corresponding to an evasive maneuver performed at a speed of 100 km/h are presented in Figure 4.35. The figure clearly shows that the peak directional response of the semitrailer decreases considerably when $K_{21}^{*} < 0$ and $K_{41}^{*} > 0$. The lowest values of peak lateral acceleration, lateral and yaw velocities and path overshoot are attained when $K_{21}^{*} = -1$ and $K_{41}^{*} = 0.03$. This combination of gains yields the desired parallel steer of the forced-steering axle corresponding to high-speed maneuvers. An examination of Figures 4.31 to 4.35 shows that this control algorithm can provide both improved low-speed maneuverability and high-speed directional control for control gains, $K_{21}^{*} = -0.5$ to -1.0 and $K_{41}^{*} = 0.015$ to 0.03.

Transient Response Analysis of Scheme IV

Articulation and speed sensitive articulation gain scheme shows the desired dual behaviour, improved low-speed maneuverability and high-speed directional control. For a better understanding, a study on transient behaviour of the vehicle is made. Figures 4.36 to 4.38, shows the transient response of the articulated vehicle for an evasive maneuver at 100 km/h, equipped with forced-steering axle at 21 and for gain values of $K_{21}^{*} = -1$ and $K_{41}^{*} = 0.03$ h/km. In these figures, the peak values of directional response of lateral acceleration, lateral and yaw velocities, and side-slip angles decreases considerably. The correction phase peak values and settling time of the response also show a remarkable decrease. The magnitude of the peak lateral acceleration and velocity response values decrease by 6% and 40%, respectively, as shown in Figure 4.36. The peak amplitude of yaw velocity oscillation of the damped vehicle is approximately 17% lower than the

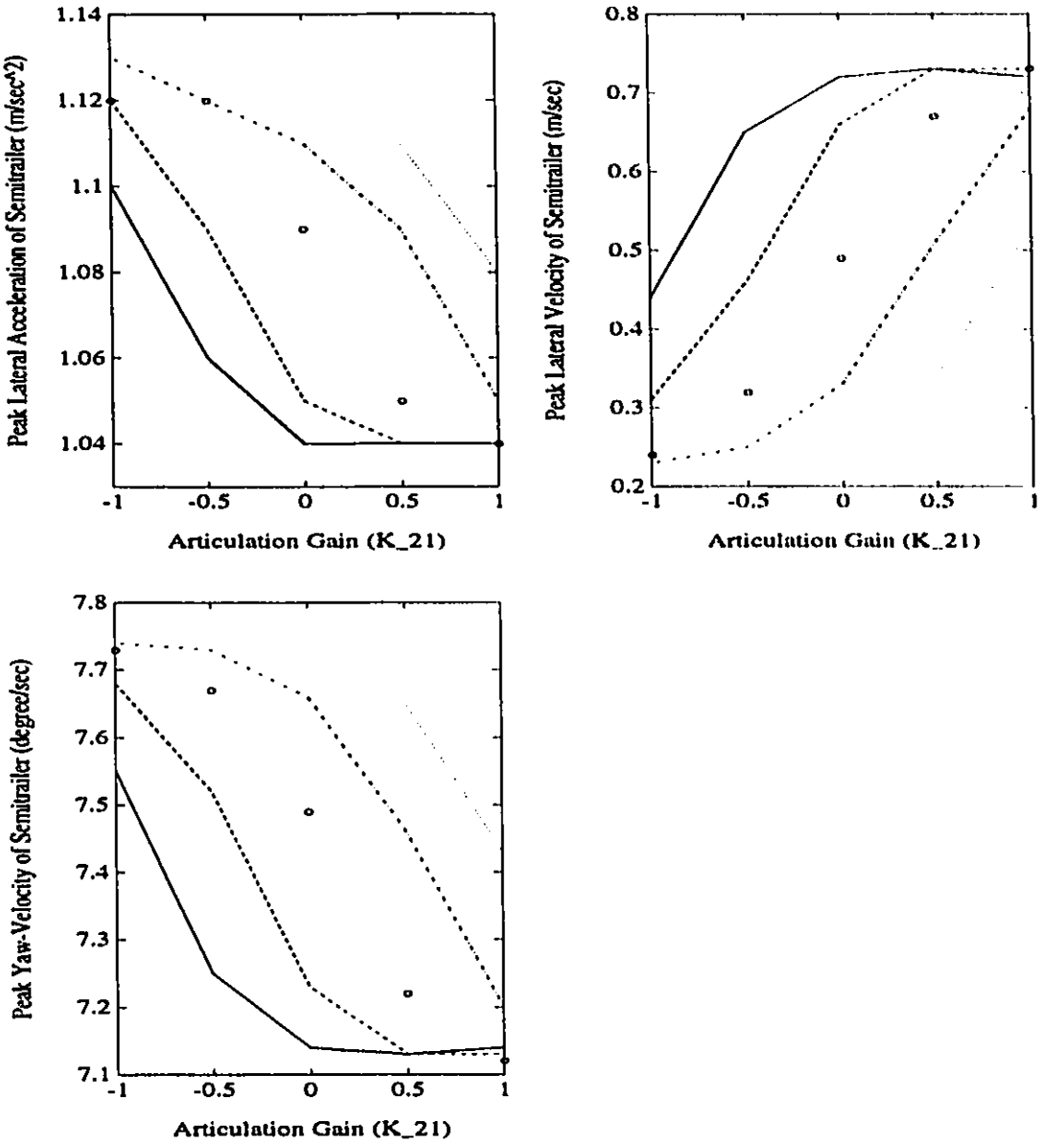

SCHEME IV: FORCED-STEERING AXLE 21

Figure 4.31: Influence of articulation gain and speed sensitive articulation gain on steady-state response at 30 km/h
(— K_{41} = 0.03 h/km; - - - K_{41} = 0.015 h/km; ooo K_{41} = 0 h/km; -.-.- K_{41} = -0.015 h/km; ..... K_{41} = -0.03 h/km;)

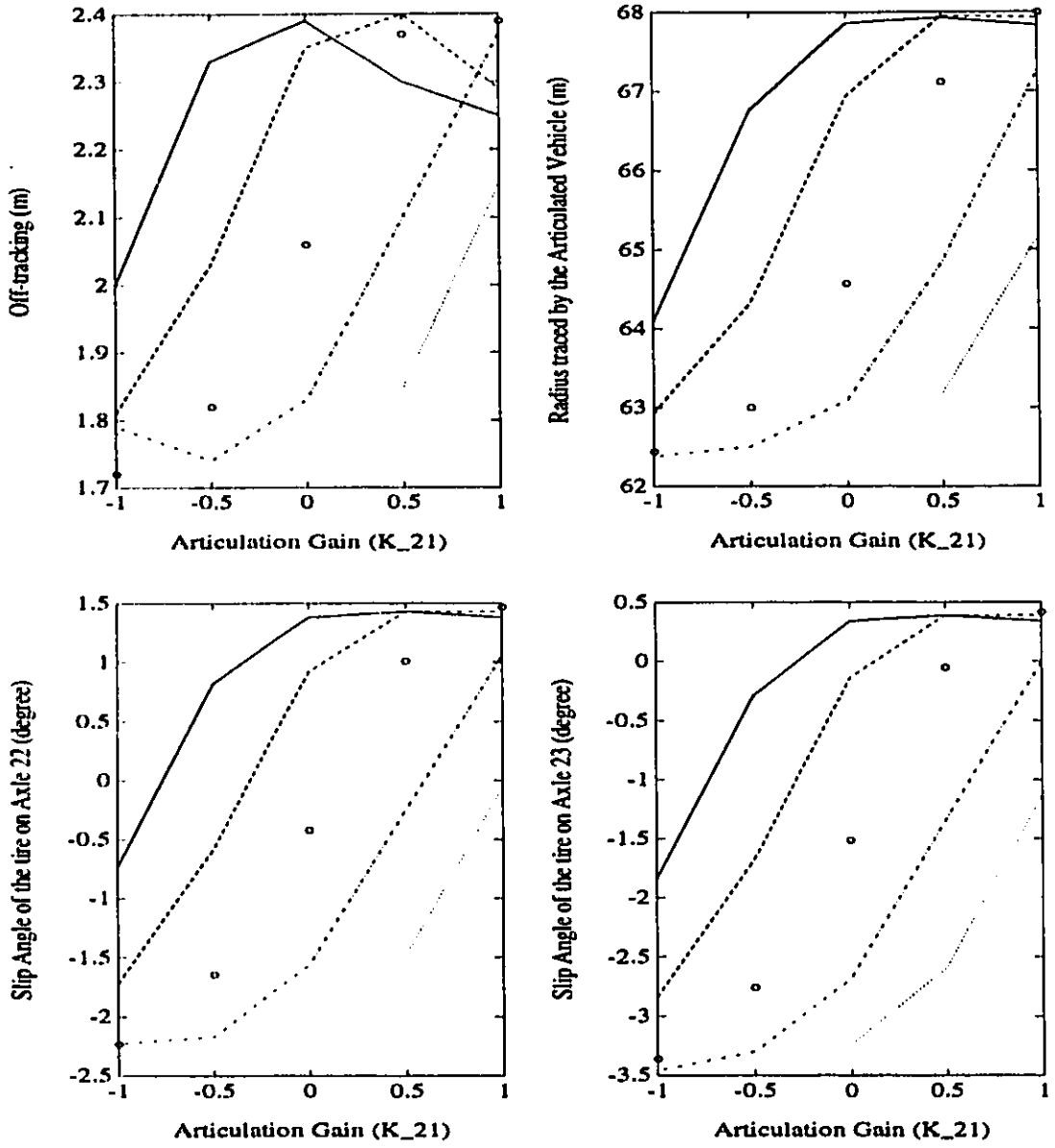

SCHEME IV: FORCED-STEERING AXLE 21

Figure 4.32: Influence of articulation gain and speed sensitive articulation gain on steady-state response at 30 km/h
(— K_{41} = 0.03 h/km; - - - K_{41} = 0.015 h/km; ooo K_{41} = 0 h/km; -.-.- K_{41} = -0.015 h/km; ..... K_{41} = -0.03 h/km;)

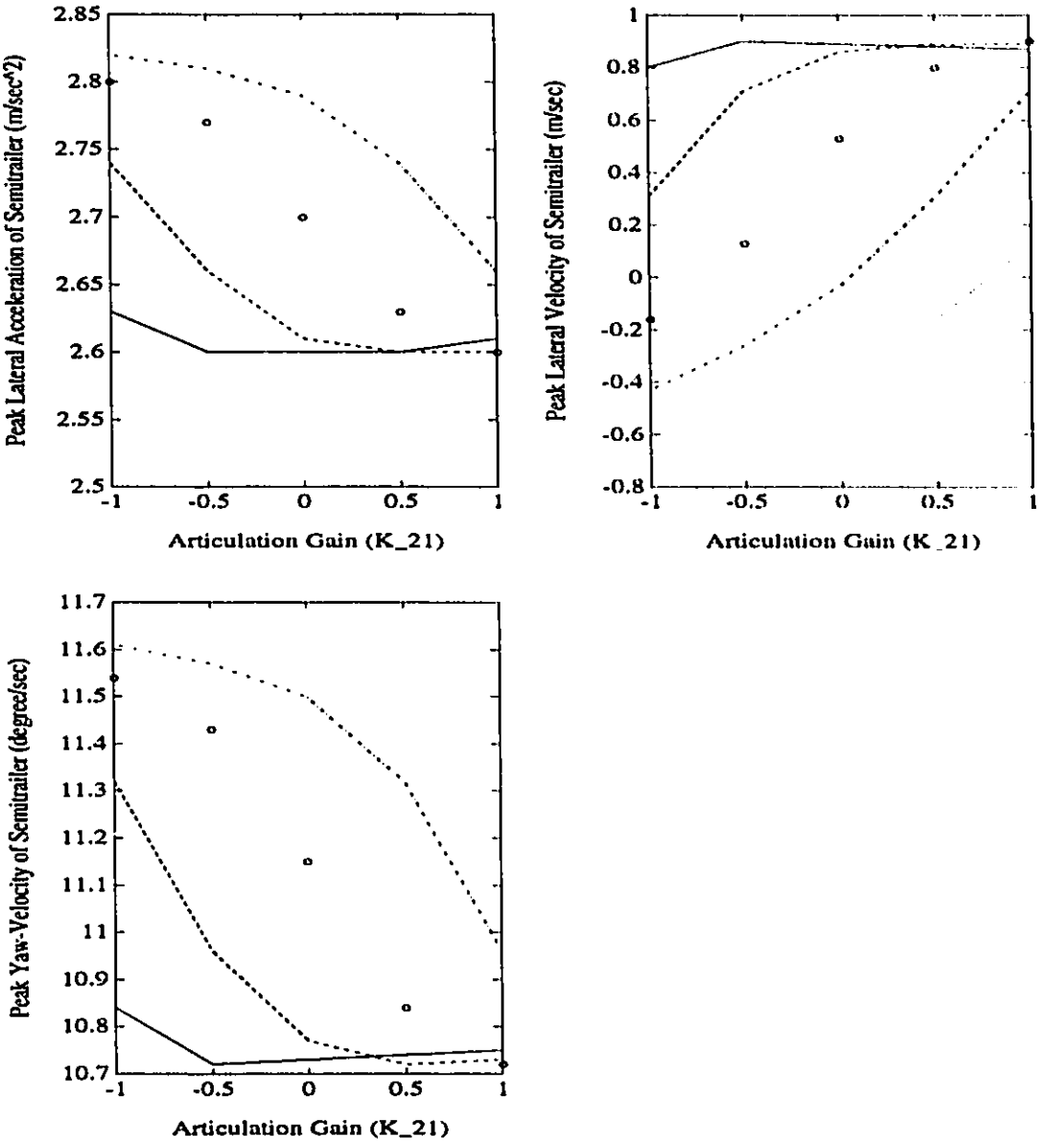

SCHEME IV: FORCED-STEERING AXLE 21

Figure 4.33: Influence of articulation gain and speed sensitive articulation gain on steady-state response at 50 km/h

(—— K_{41} = 0.03 h/km; - - - K_{41} = 0.015 h/km; ooo K_{41} = 0 h/km; -.-.- K_{41} = -0.015 h/km; ..... K_{41} = -0.03 h/km;)

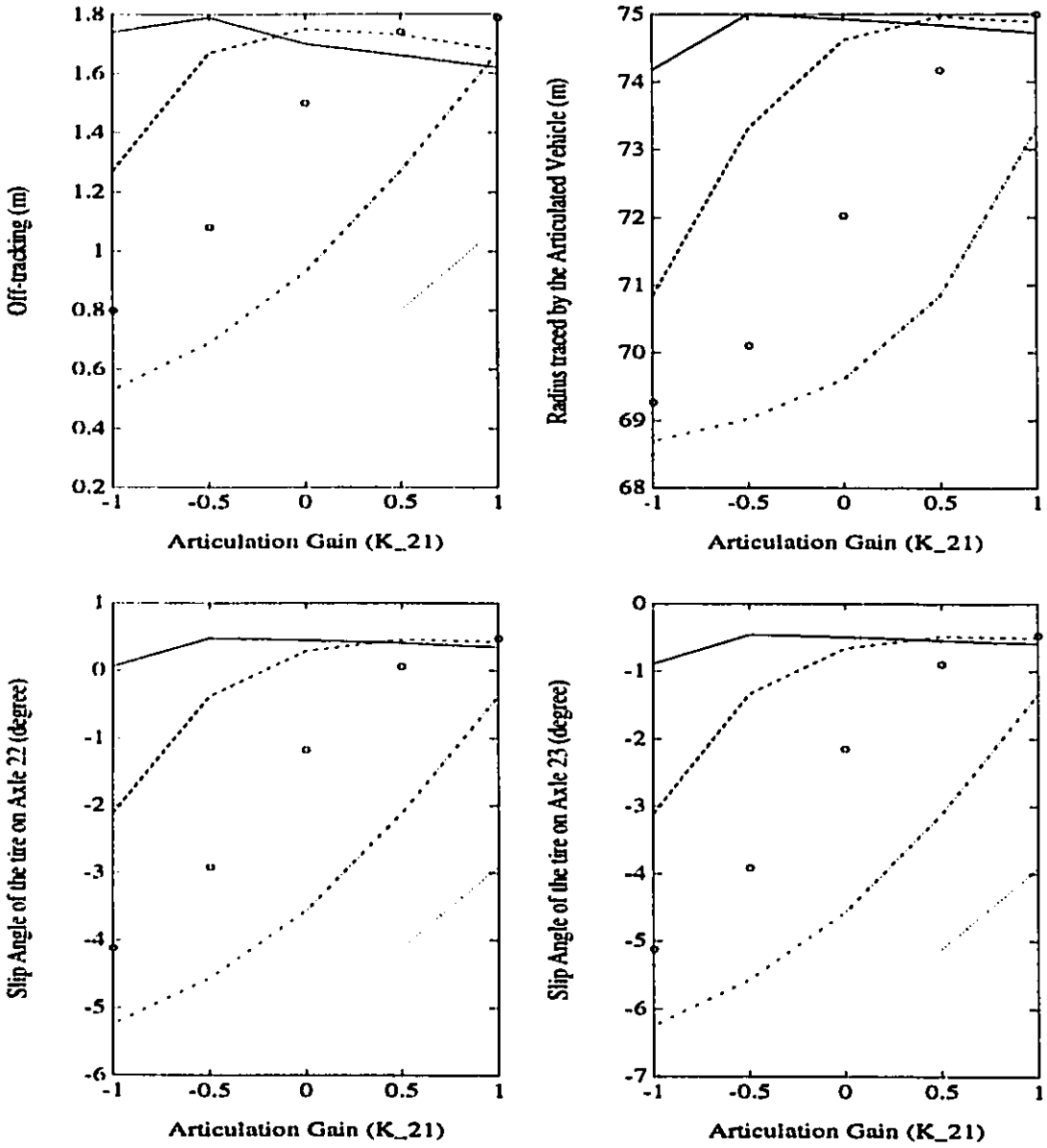

SCHEME IV: FORCED-STEERING AXLE 21

Figure 4.34: Influence of articulation gain and speed sensitive articulation gain on steady-state response at 50 km/h
(—— K_{41} = 0.03 h/km; - - - K_{41} = 0.015 h/km; ooo K_{41} = 0 h/km; -.-.- K_{41} = -0.015 h/km; ..... K_{41} = -0.03 h/km;)

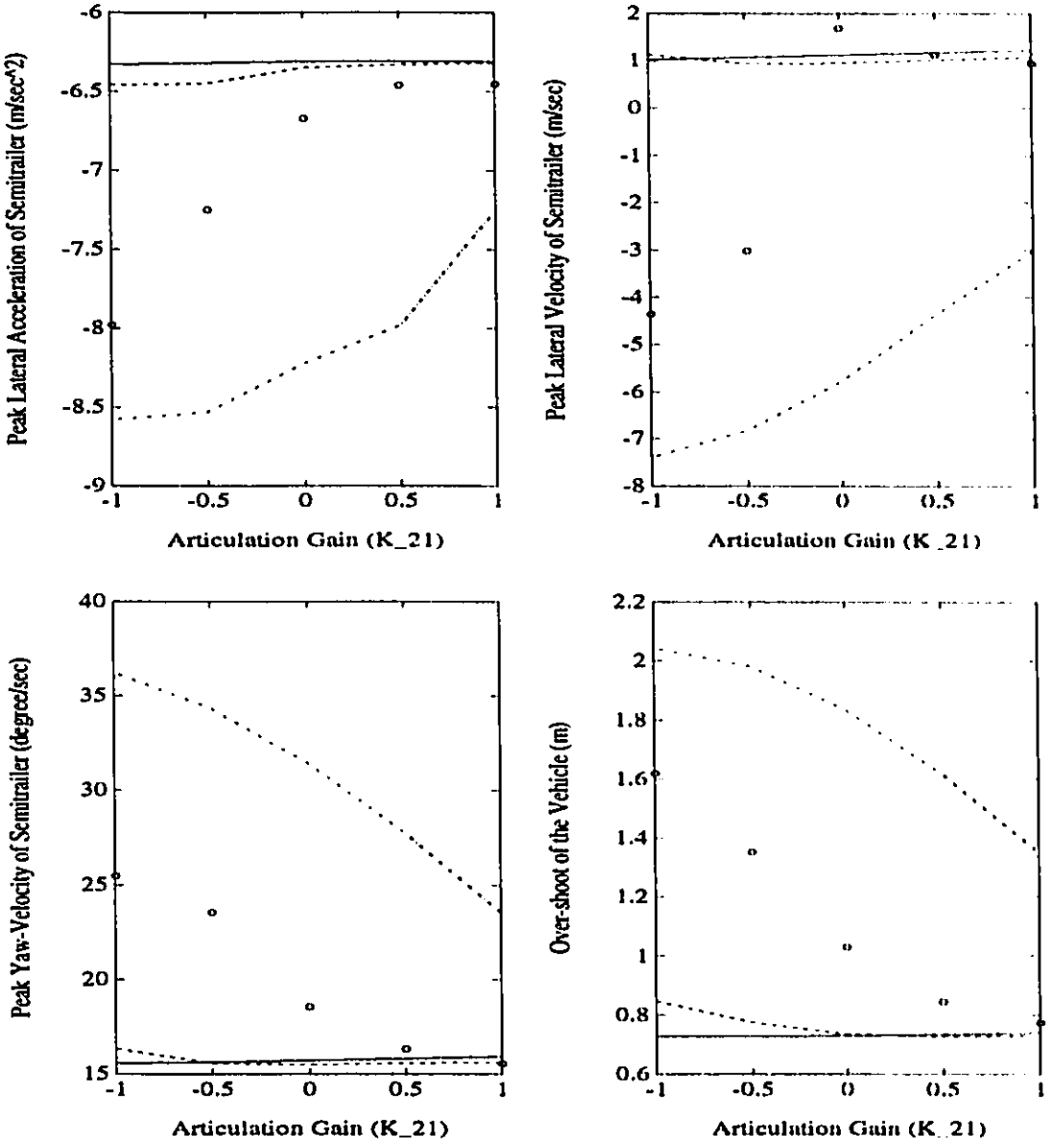

SCHEME IV: FORCED-STEERING AXLE 21

Figure 4.35: Influence of articulation gain and speed sensitive articulation gain on transient response at 100 km/h
(— K_{41} = 0.03 h/km; - - - K_{41} = 0.015 h/km; ooo K_{41} = 0 h/km; -.-.- K_{41} = -0.015 h/km; ..... K_{41} = -0.03 h/km;)

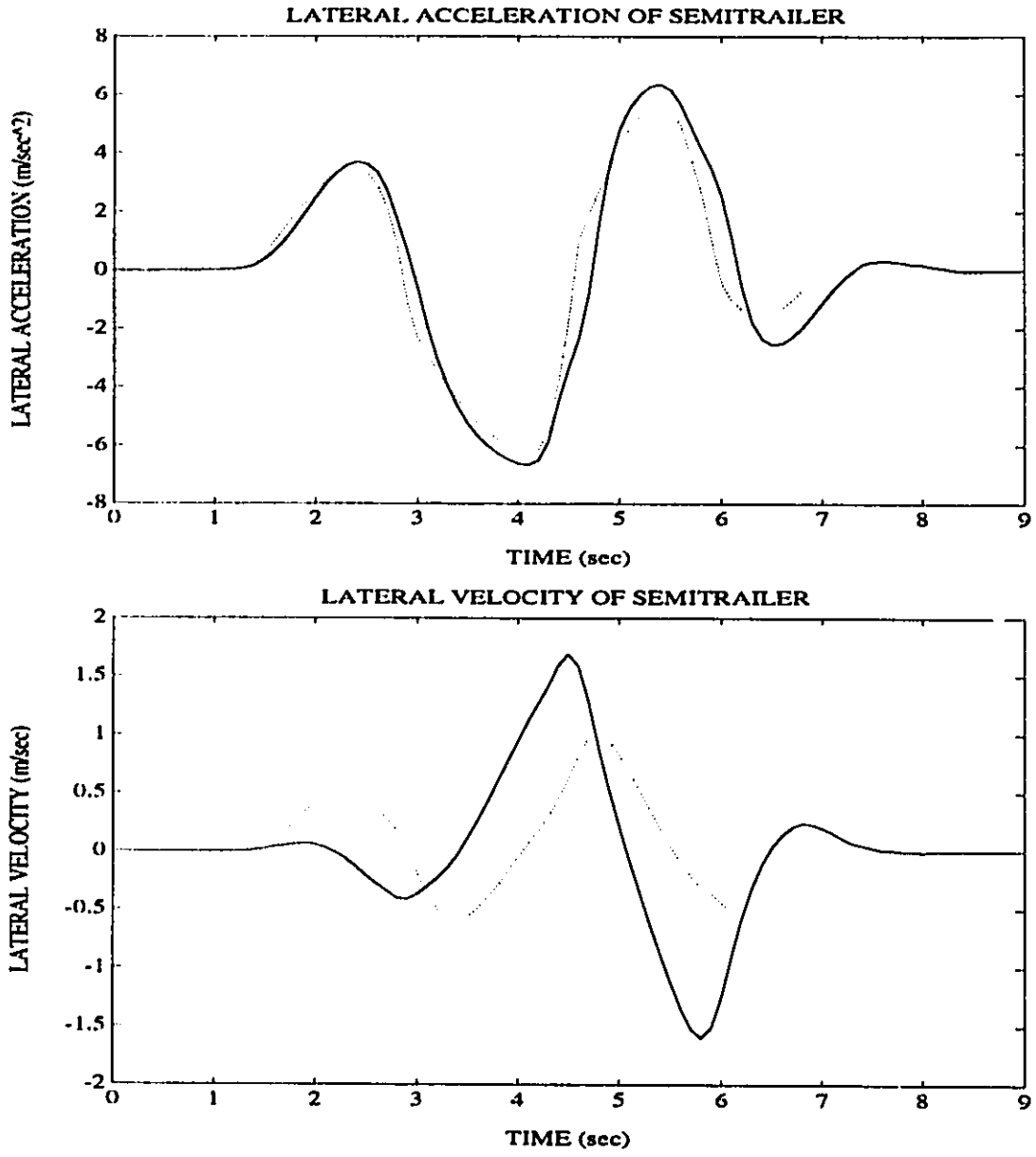

Figure 4.36: SCHEME IV: Transient Response of lateral acceleration and Lateral Velocity of Semitrailer for an Evasive Maneuver at 100 km/h
(— K_{21} = 0, K_{41} = 0; .....K_{21} = -1, K_{41} = 0.03 h/km)

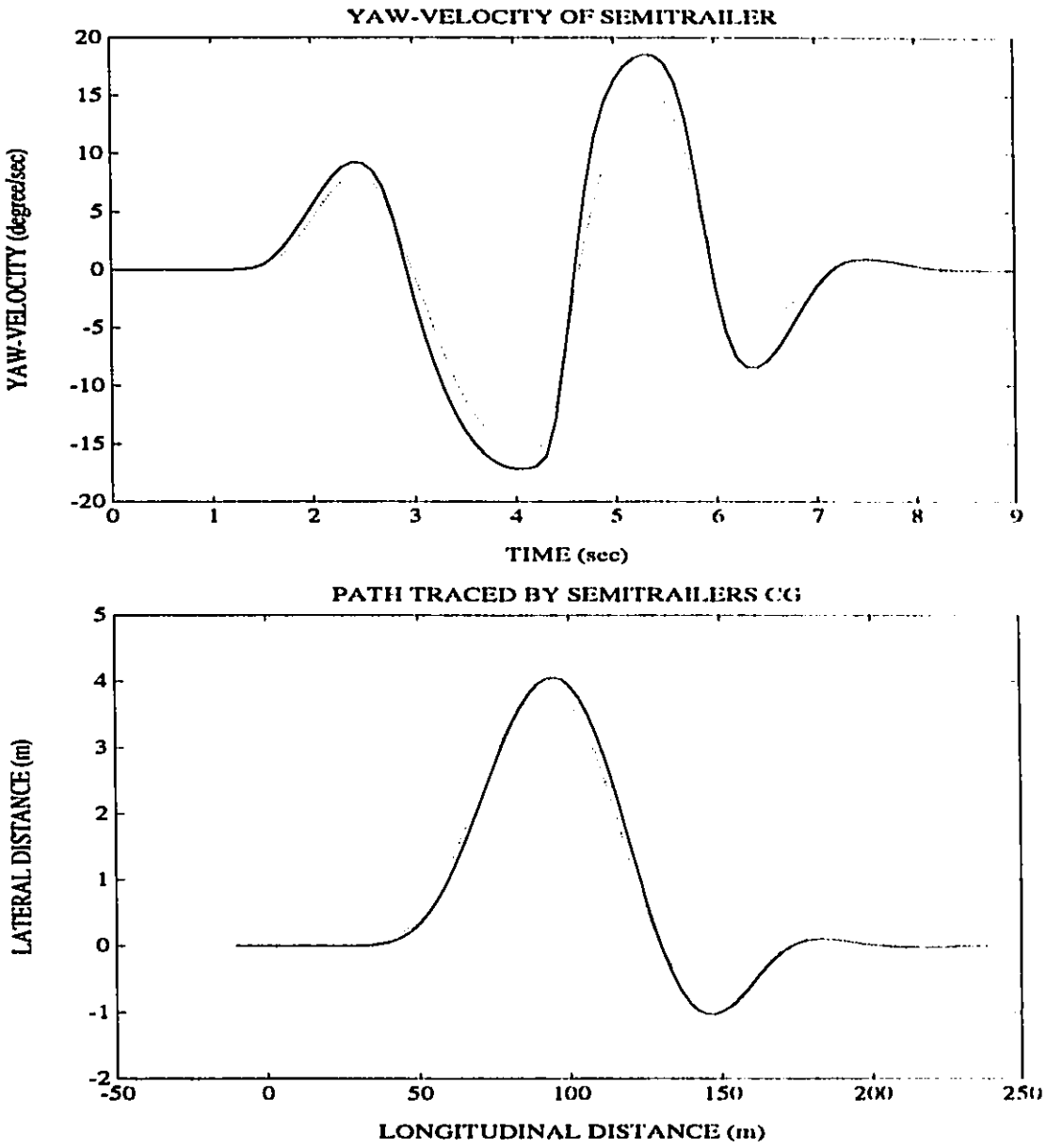

Figure 4.37: SCHEME IV: Transient Response of Yaw-Velocity and path and over-shoot made by Semitrailer for an Evasive Maneuver at 100 km/h
(—— K_{21} = 0, K_{41} = 0; .....K_{21} = -1, K_{41} = 0.03 h/km)

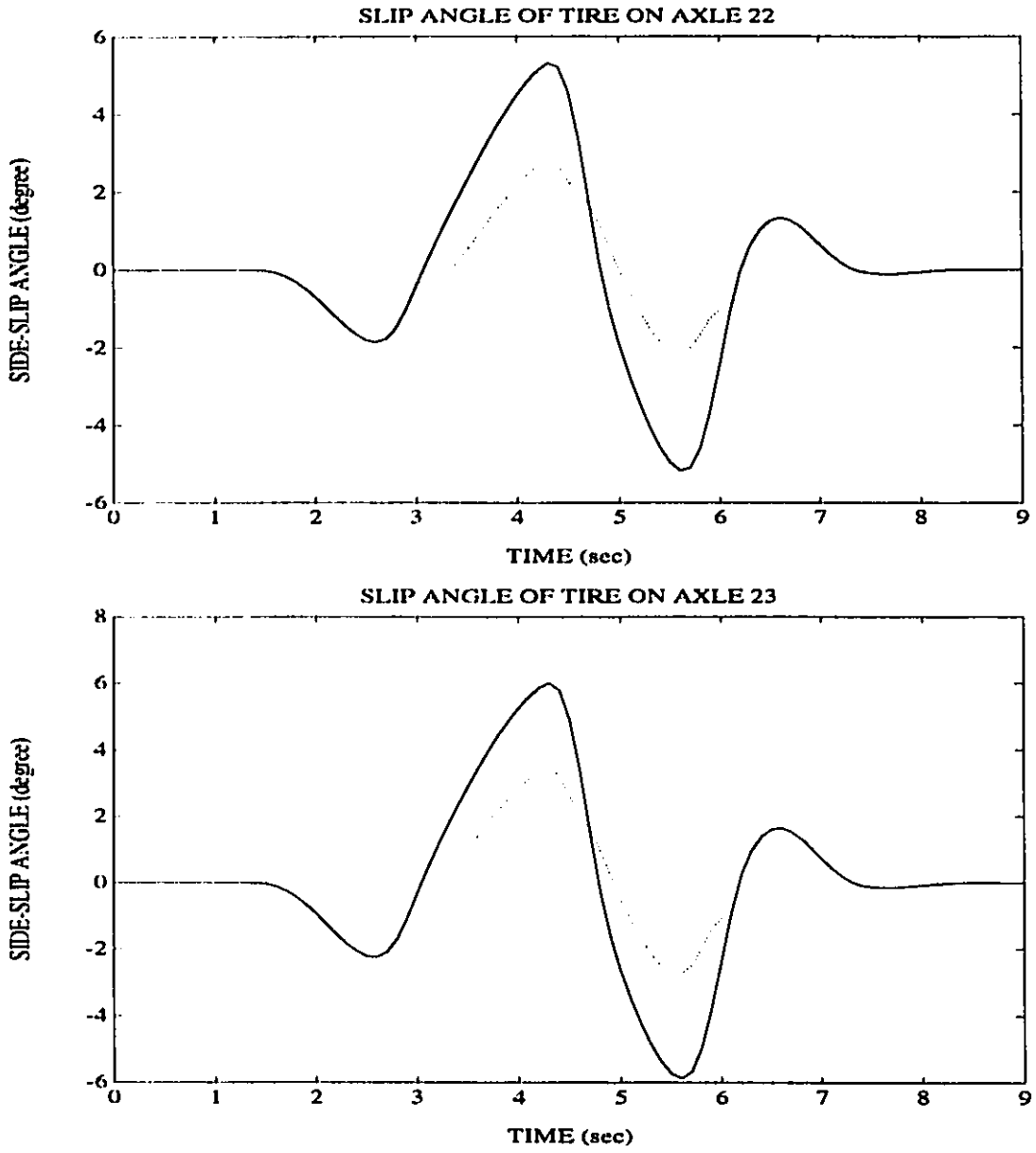

Figure 4.38: SCHEME IV: Transient Response of side-slip angles of tires on axles 22 and 23 of Semitrailer for an Evasive Maneuver at 100 km/h
(— K_{21}^{*} = 0, K_{41}^{*} = 0; .....K_{21}^{*} = -1, K_{41}^{*} = 0.03 h/km)

conventional vehicle as evident from Figure 4.37. These figures suggest that the amplitudes of yaw and lateral oscillations can be effectively suppressed for gains K_{21} = -1 and K_{41} = 0.03 h/km. The reduction is oscillations of semitrailer brings stability in the vehicle and reduction in overshoot of the semitrailer. The overshoot of the semitrailer decreases by 0.63 m as shown in Figure 4.37. The side-slip angles of tires on axle 22 and 23 decreases considerably, as illustrated in Figure 4.38. The side-slip angles decrease by 47% and 40%, respectively, for tires on axle 22 and 23, in process increases the life of tire by reducing tire scrub and wear.

4.5 Summary

The steady-state and transient directional response characteristics of the articulated vehicle with forced steering equipped on one of the axle on semitrailer are investigated. Single and combined control feedback algorithms are used to generate the force-steer angle. The response characteristics of the articulated vehicle for low- and medium-speed constant steer, and high-speed evasive maneuvers are compared to that of the conventional vehicle to highlight the influence of forced-steering. The conclusions made from the investigation are the force-steering integrated within the lead-axle of the semitrailer yields better performance than that integrated to the rear axles. The force steering algorithms based on single variable controls yield conflicting requirements for low-speed maneuverability and high-speed directional performance. The steady-state directional performance is insensitive to force-steering based on articulation rate control. The forced-steering algorithm based on combined articulation gain and speed sensitive articulation gain can provide both improved low-speed manoeuvrability and high-speed directional performance.

Chapter 5

Conclusions and Suggestions for Future Research

5.1 General

With the relaxation of weights and dimensions regulations, the population of articulated vehicles with multiple axle trailers has been increasing steadily. The handling and directional control characteristics of articulated freight and passenger vehicles are adversely influenced by the increased weights and dimensions. The lateral and yaw motions associated with side-sway of the articulated vehicles, during a directional maneuvers, specifically pose a severe threat to the highway safety due to excessively high inertia of the heavy vehicle. Articulated vehicles equipped with multiple-axle semitrailer and steering at the tractor's front axle yield excessive swept path and off-tracking during a turning maneuver. The excessive off-tracking of the vehicles cause rapid tire scrub and wear, poor fuel economy, and increased fatigue. Self- and forced-steering axles have been proposed to achieve improved low speed maneuverability with reduced off-tracking and rate of tire wear. While the self-steering axles provide improved maneuverability and eliminate the excessive road damage caused by drop axles semitrailers, considerably low lateral cornering forces generated by these axles affect the directional stability and control

in an adverse manner.

The overall objective of this dissertation research was to investigate the performance potentials of articulation dampers and forced-steering axles in realizing improved low speed maneuverability, and reduced amplitude of yaw and lateral oscillations encountered during high speed directional maneuvers.

5.2 Highlights of the Investigations

The steady-state and transient directional dynamics of an articulated vehicle with a multiple axle semitrailer are investigated through simulation of a nonlinear analytical model. A nonlinear model of the vehicle in the yaw-plane is developed to study its lateral and yaw directional dynamics. The cornering forces and aligning moments of the radial tires are characterized by a nonlinear describing function in side-slip angles and normal loads. The directional dynamics analysis of the vehicle with varying axle loads can thus be carried out using the nonlinear model. The steady-state directional analysis is carried out for constant speed maneuvers at low and medium speeds. The transient directional analysis of the vehicle is performed for highway speed lane-change and evasive maneuvers using a simple path-follower model.

5.2.1 Articulation Damping Mechanism

An articulation damping mechanism compresses of two dampers, arranged in a V-shaped manner on either side of the articulation point, is configured. The damping forces and moments imposed on the tractor and the semitrailer units are derived from the kinematics analysis of the damper links, damping coefficients and dynamic response of the vehicle. The damping forces incorporating geometric nonlinearities due to dampers links are in-

tegrated to the nonlinear yaw-plane model of the tractor-semitrailer vehicle comprising nonlinear cornering properties of the tires. The yaw and lateral dynamics of the vehicle with articulation dampers subject to constant steer, lane-change and evasive directional maneuvers.

5.2.2 Forced-Steering

A number of force-steering algorithms relating the vehicle response quantities to the wheel angle of the steerable axle are formulated, and integrated to the nonlinear yaw-plane model of the vehicle. Different forced-steering control schemes are formulated to study their performance potentials related to low-speed maneuverability and high-speed directional dynamics. Assuming potential control laws and negligible delays, the wheel angle of the forced-steered axle is related to one or more response quantities of the vehicle including front wheel steer angle, articulation angle, articulation rate and forward speed.

The performance potentials af the forced-steering axles are investigated in terms of: (i) steady-state off-tracking and turn radius corresponding to low- and medium-speed maneuvers; (ii) peak magnitudes of lateral acceleration, lateral velocity, yaw velocity and path overshoot corresponding to high-speed evasive maneuvers. The forced-steering algorithm, based on single variable control, are first investigated to establish the influence of feedback variables and control gains on the low speed maneuverability and high speed directional performance. The influence of location of forced-steering axle is further investigated using the single variable control. A force-steering algorithms, based upon combined control variables, are then formulated to achieve improved performance for low as well as high speed maneuvers.

5.3 Conclusions

Following conclusions are drawn from the results of the study:

- The yaw and lateral dynamics of an articulated vehicle can be effectively represented through a yaw-plane model.
- The directional dynamics of a heavy vehicle is strongly related to the cornering properties of tires, nonlinear function of side-slip angles and normal load.
- The nonlinear cornering force of a radial tire can be accurately characterized by a describing function in side-slip angle and normal load.
- The nonlinear aligning moment due to pneumatic trail can be expressed using the describing function and the pneumatic trail.
- The steady-state and transient directional response characteristics derived from the analytical model with linear tire properties correlated very well with those derived from the linear yaw-plane software.
- The magnitude of yaw and lateral oscillations experienced during highway speed maneuvers can be effectively reduced through articulation dampers.
- In a left-turn constant steer maneuver, the articulation mechanism comprising either the left damper or both dampers, results in increased steady-state lateral acceleration, lateral and yaw velocity, side-slip angles, and articulation. The turn radius, however, decreases by approximately 29%.
- The inclusion of right damper alone yields lower steady state response with increased turn radius.
- The articulation dampers affect the high-speed directional dynamics in a significant manner. The reduction in magnitudes of yaw and lateral oscillations encountered

during an evasive maneuver is for more significant than that achieved for lane-change maneuvers.

- The articulation damping mechanism comprising both dampers yields maximum reduction in the yaw and lateral oscillation of the semitrailer.
- The lateral acceleration and yaw velocity rearward amplification of the vehicle are reduced considerably by the articulation dampers.
- The peak side-slip angles of the semitrailer axle tires reduces by approximately 40% corresponding to high-speed directional maneuvers.
- The force-steering integrated within the lead-axle of the semitrailer yields better performance than that integrated to the rear axles.
- The force steering algorithms based on single variable controls yield conflicting requirements for low-speed manoeuvrability and high-speed directional performance.
- Negative control gains (opposite steer) are desirable to achieve improved off-tracking and turn radius for low speed maneuvers, while positive control gains (parallel steer) are needed to achieve improved high-speed directional performance.
- The steady-state directional performance is insensitive to force-steering based on articulation rate control.
- The forced-steering algorithm based on combined articulation gain and speed sensitive articulation gain can provide both improved low speed manoeuvrability and high-speed directional performance.

5.4 Suggestions for Future Research

In view of the considerable performance potentials of articulation dampers illustrated in this study, it is recommended to further investigate the directional dynamics of the vehicle articulation dampers. A comprehensive directional dynamics analysis should be carried using a three-dimensional vehicle model comprising the yaw, roll and lateral dynamics of the suspension and unsprung masses. The performance potentials should be further investigated for combined braking and steering maneuvers, which induce large magnitudes of lateral and yaw oscillation. Road tests must be performed to validate the analytical model, and an optimization study may be undertaken to derive optimal damping coefficients for typical directional maneuvers. A damper, in-general, generates the damping forces which is a nonlinear function of the relative velocity. The damping forces developed by either a single- or multiple-stage orifice dampers may be derived using the shock absorber models reported in the literature. The vehicle model comprising the nonlinear damping force and moment may be analyzed to determine the performance potentials of a realistic damping mechanism. The forced-steering algorithms should be developed using the delays caused by measurements, signal processing and generator dynamics. The control schemes based on integral control may also be explored to derive a forced-steering algorithm that satisfies the requirements for low and high-speed maneuvers. The performance characteristics of forced-steering axles should be further investigated using the three-dimensional vehicle models in conjunction with the dynamics of the hydraulic system generating the forced-steering.

Bibliography

[1] Vlk,F. 'Lateral Dynamics of Commercial Vehicle Combinations - a Literature Survey', Vehicle Systems Dynamics, vol. 11, no. 6, pp. 305-324, 1982.

[2] Huber, L. and Dietz, O. 'Pendelbewegungen Von Lastkraftwagen - Anhangern und iher Vereidung', VDI-Zeitschrift, vol.81, no. 16, pp. 459-463, 1937.

[3] Dietz, O. 'Pendelerscheinungen an Strassen-Anhangerzugen', DKF, Heft 16, 1938.

[4] Dietz, O. 'Uber das Spuren und Pendeln von Lastkraftwagen-Anhangern', ATZ, vol. 41. no. 15, 1939.

[5] Ziegler, H. 'Die Querschwingungen von Kraftwagenanhagern', Ing.- Archiv, vol. 9, no. 2, pp. 96-108, 1938.

[6] Ziegler, H. 'Der Einfluss von Bremsung und Steigung auf die Querschwingungen von Kraftwagenanhangern', Ing,- Archiv, vol. 9, no. 4, pp.241-243, 1938.

[7] Laurien, F. 'Untersuchung der Anhangerseitenschwingungen in Strassinzugen', Dissertation, TH, Hannocer, 1955.

[8] Paslay, P.R. and Slibar, A. 'Uber Quersvhwingungen von gelenkten Anhangern', Ing.-Archiv, vol. 26, no. 6, pp. 383-386, 1958.

[9] Zakin, J.C. 'Causes of the Origin of trailer Oscillations' (in Russian), Avtomob.promyshlennost, vol. 26, no. 11, pp. 9-12, 1959.

[10] Zakin, J.C. 'Lateral Stability of Trailer Movement' (in Russian), Avtomob. promyshlemmost , vol. 26, no. 2, pp. 27-31, 1960.

[11] Zakin, J.C. 'Applied Theory of Trailer Movement Stability', Transport, Moscow, (in Russian), 1967.

[12] Morozov, B.I. et al 'Research of the full Trailer Oscillations' (in Russian). Works NAMI, Moscow, no, 48, pp, 29-39, 1962.

[13] Meyer, J. 'Zur Prage der Querschwingungen eine Zweiachsigen I.Kw.Anhangers', Techn. Mitteilungen Krupp, Forsch.-Berichte, vol. 21, no. 1, pp. 34-36, 1963.

[14] Schmid, I. 'Das Fahrstabilitatsverhalten zwei - und dreigliedriger Fahrzeugketten', Dissertation TH, Stuttgart, 1964.

[15] Jindra, F. 'Off-tracking of tractor-trailer Combinations', Automobile Engineer, vol. 53, no. 3, pp. 96-101, 1963.

[16] Gerlach, R. 'Untersuchung der Querschwingungen von Lastzugen auf Analogrechnern', 8. Kraftfahrzeugtechnische Tagung, Karl-Marx-Stadt, Vortrag A9, Kammer der Technik, Fachverband Fahrzeugbau und Verkehr IZV Automobilbau, 1968.

[17] Nordstrom, O., Magnusson, G. and Strandberg, L. 'The Dynamic Stability of Heavy Vehicle Combinations' (in Swedish), VTI Rapport No. 9, Statens vag-och trafikinstitut, Stockholm, 1972.

[18] Nordstrom, O. and Strandberg, L. 'The Dynamic Stability of Heavy Vehicle Combinations', International Conference of Vehicle System Dynamics, Blacksburg, Virginia, Report no. 67A. Statens vag-och trafikinstitut, linkoping, 1975.

[19] Nordstrom, O. and Nordmark, S.,'Test procedures for the Evaluation of the Lateral Dynamics of Commercial Vehicle combinations', Automobile-Industrie, vol 23, no.2, pp. 63-69, 1978

[20] Bakhmutskii, M. M. and Ganesburg, I. I.,'Relation of Road Train Steering responses and Handling Performance within System Articulated Vehicle-Driver', (in Russian), Avtomob.promyshiennnost, vol. 39, no. 2, pp 32-33, 1973.

[21] Mallikarjunarao, C. and Fancher, P. 'Analysis of the Directional Response Characteristics of Double Tanker', Society of Automotive Engineers, Paper no 781064, pp. 4007-4026, 1979.

[22] Vlk, F. 'Stability Control of the Commercial Vehicle Combinations - a Digital Simulation' (in Czech), Dept. of Automob. Eng., Report no. VO1/82, Techn. University of Brno, Czechoslovakia, 1982.

[23] Robert, D. Ervin. 'Influence of Size and Weight Variables on the Stability and Control Properties of Heavy Trucks', Report UMTRI-83-10-2, University of Michigan Transportation Research Institute, 1982.

[24] Johnson, D.B. and Huston, J.C, 'Nonlinear Lateral Stability Analysis of Road Vehicles Using Liapunov's Second Method', SAE, paper no. 841507, 1984.

[25] Susemihl, E.A. and Kranter, A.I., 'Automatic Stabilization of Tractor Jackknife in Tractor- Semitrailer Trucks', SAE, Paper no 740138, 1974.

[26] Wong, J.Y. and El-Gindy, M., 'Computer Simulation of Heavy Vehicle Dynamic Behavior - User Guide to UMTRI Models', no. 3, Road and Transport Association of Canada, 1985.

[27] El-Gindy, M. and Wong, J.Y., 'A Comparison of Various Computer Simulation Models for Predicting the Directional Responses of Articulated Vehicles', Vehicle System Dynamics, 16, pp. 249-268, 1987.

[28] Leucht, P.M., 'The Directional Dynamics of the Commercial Tractor - Semitrailer Vehicle during Braking', Society of Automatic Engineers paper no. 700371, 1970.

[29] Gillespie, T.D. and Winkler,C.B., 'On the Directional Response Characteristics of Heavy Vehicles'.

[30] Paul S.Fancher, 'Directional Dynamics Considerations for Multi- Articulated, Multi-Axled Heavy Vehicles', Society of Automotive Engineers, paper no. 892499, 1989.

[31] Winkler, C.B., 'Innovative Dollies:Improving the Dynamic Performance of Multi-Trailer Vehicles'.

[32] Woodrooffe, J. et al., Development of Design and Operational Guidelines for the C - Converter Dolly'.

[33] Sweatman, P.Z., 'A Study of Dynamic Wheel Forces in Axle - Group Suspensions of Heavy Vehicles', Australian Road Research Board, Special Report, SR NO. 27.

[34] Grandbois, J. and Richard, M. J., "Fleet test program for self-steering axles ," Proceedings of CSME Forum 1992, JUne 1992, Montreal.

[35] LeBlanc, P. A. et al., "Self-Steering axles : Theory and Practise," Society of Automotive Engineers, Paper number 891633, 1989.

[36] Woodrooffe, J., LeBlanc, P. and El-Gindy, M., "Self steering and the commercial vehicle," The third International IRTENZ seminar, Christ Church, New Zealand, August 1989.

[37] Billing, A. M., "Tests of Self-Steering Trailer Axles", Ontario ministry of Transportation and communications, report cvos 79-02.

[38] Billing, J. R. et al., "Development of regulating principles for Multi-Axles semi-trailer", Second International Symposium of Heavy Vehicle Weights and Dimensions, Kelowna, British Columbia, June 18-22, 1989.

[39] Vlk, F., "A linear study of the transient and steady turning behaviour of articulated buses", International Journal of Vehicle Design, Vol. 5, No. 1/2, pp. 171-196.

[40] Dulac, Alain, "Articulation damping of Prevost car buses", Personal Communication, 1992.

[41] Aurell, J. and Edlund, S., "The influence of steered axles on the dynamic stability of heavy vehicles", Society of Automotive Engineers, paper no. 892498 , Journal of Commercial vehicles, 1989.

[42] Sankar, S., Rakheja, S. and Alain Piche, "Directional Dynamics of a Tractor - semitrailer with self- and forced-steering axles", SAE, paper no. 912686, 1991.

[43] Rakheja, S. and Sankar, S.," Vibration and Shock Isolation Performance of a Semi-Active 'on-off' Damper", ASME Journal of Vibration, Acoustics, Stress and Reliability in Design, Vol.107, 1985, pp. 398-403.

[44] Winkler, C. B., Mallikarjunarao, C. and MacAdam, C. C., "Analytical test plan : Part I - description of Simulated models", Parametric Analysis of Heavy Truck dynamic stability, Contract no. DTNH22-80-C-07344, The University of Michigan Transportation Research Institute, April 1981.

[45] Barbara F. Ryan, Brain L. Joiner and Thomas A. Ryan, Jr.,"Minitab Handbook", Second Edition, PWS-KENT Publishing Company, Boston, 1985.

[46] Robert, D. E. and Yoram Guy,' The influence of Weights and Dimensions on the Stability and Control of Heavy Duty Trucks in Canada', The University of Michigan Transportation Research Institute. 1986.

[47] Sireteanu, T., "The Effect of Sequential Damping on Ride Comfort Improvement", Vehicle Noise and Vibration, IMechE Conference, London, June, 1984, pp 77-83.